A TRANSCRIPTIONAL PROGRAM REMODELS GABAERGIC SYNAPSES IN *C. ELEGANS*

By

Sarah Catherine Petersen

Dissertation

Submitted to the Faculty of the

Graduate School of Vanderbilt University

in partial fulfillment of the requirements

for the degree of

DOCTOR OF PHILOSOPHY

in

Cell and Developmental Biology

December, 2011

Nashville, Tennessee

Approved:

David M. Miller, III

Christopher V. E. Wright

Joshua T. Gamse

Donna J. Webb

ACKNOWLEDGEMENTS

First and foremost, I want to thank my thesis advisor, David Miller, for the opportunity to work on this project as a brand-new graduate student, straight out of college. Looking back, I am a little amazed that he allowed a green, naïve student to take on such a promising, but new and challenging project! I am especially grateful that he recognized some glimmer of tenacity in me and invested his time and energy to help me make this project successful. Because of David's mentorship, I have learned how asking simple questions can answer complex problems. This foundational skill has shaped my success as a scientist, my writing style, and my ability to communicate clearly while speaking or teaching. I am also grateful to David for working to secure the funds to support my training and this project. The work in this dissertation was made possible with financial support from the NIH: David's awards (R21 MH077302 and R01 NS26115), the Cellular, Molecular, and Biochemical Science training program organized by Jim Patton (T32 GM08554), and my NRSA (1F31 NS063669).

I also want to thank the community here at Vanderbilt in the Department of Cell and Developmental Biology and the Program in Developmental Biology for providing a stellar training environment. In particular, I want to thank Chris Wright for leading our top-notch developmental biology program and personally for all his thoughtful mentoring as my committee chair, Josh Gamse, Donna Webb, Daniela Drummond-Barbosa, and Bruce Appel for serving on my thesis committee (past and present), Kim Kane and Elaine Caine for their unfailing

willingness to help, and Susan Wente for building a great department in her time as Department Chair. To all those who have made it possible to do great science here in a collaborative, supportive, *happy* atmosphere, I am grateful.

I've been fortunate to have labmates that, in addition to being talented scientists, have also become great friends. Steve, Becca, Joseph, and Clay were invaluable for teaching me how to do the microarray experiments and answering my constant stream of questions. Jud and Rachel were always willing to help me craft the ideal genetics scheme, and Rachel also provided much-needed microscope room chats to break the monotony of scoring! I owe everything I know about confocal microscopy to Cody, who with Kathie, also taught me how to clone successfully (*finally!*). Mallory was always willing to share the latest GABA reagent she built with all its accompanying paperwork. Tim and Becky, along with Kathie, keep our lab running, and we'd be lost without them. And Tyne, I'm so glad that you love this project as much I do, enough to devote your graduate career studying it, too. I know you'll do great things with it.

Finally, I am endlessly grateful for the support of my dear friends I made as a first-year in IGP, and to my family: to my late father, who encouraged me as a child to strive for perfection; to my stepfather, who has offered constant support throughout my upper-level education; to my mother, who was the first person to teach me how to explore, ask questions, and think for myself, and whose love and support are a cornerstone for my life; and to my husband David, who was willing to hold my hand throughout this journey and to keep holding it for the journey to come.

TABLE OF CONTENTS

LIST OF TABLES

LIST OF FIGURES

CHAPTER I

GENETIC MECHANISMS THAT GOVERN SYNAPTIC ASSEMBLY AND ELIMINATION DURING DEVELOPMENT

Introduction

Information flow in nervous systems depends on the asymmetric polarity of the neurons that comprise the circuit. Maintenance of the postsynaptic domain allows for reception of stimuli from the environment or from other neurons, whereas the axonal domain emits a signal from the presynaptic apparatus to the next partner in the circuit. Because postsynaptic and presynaptic domains are specifically defined by the molecular components responsible for these functions, intracellular rearrangement of these molecules is sufficient to redirect information flow (Craig and Banker, 1994). The exquisite ability of axonal and dendritic specializations to remodel during development or injury is conserved throughout phylogeny, from simple eumetazoans such as *C. elegans* and *Aplysia* to more recently derived primates, including humans. However, the genetic mechanisms that govern synaptic remodeling during development are not well understood.

Metamorphic animals undergo extensive changes in the body plan during development, which includes reorganization of the nervous system and musculature. The architectural changes that occur in the nervous system during metamorphosis are well-documented for crustaceans, nematodes, and multiple insect species (White et al., 1978; Atwood, 1992; Consoulas et al., 2000; Tissot

and Stocker, 2000). These structural remodeling events are genetically controlled and may be triggered by hormones or other diffusible cues that are released during metamorphosis (Consoulas et al., 2005; Brown and Truman, 2009). In addition to gross metamorphic changes in neuronal architecture, synapses are also selectively strengthened or eliminated via activity-dependent mechanisms. This type of neuronal remodeling may be coupled to the structural changes observed during metamorphosis or may be in response to environmental stimuli and form the basis for learning and memory (Griffith and Budnik, 2006; Bailey and Kandel, 2008; Giles and Rankin, 2009).

Investigations of the plasticity of mammalian neurons were initiated with the goal of understanding how neurons respond to injury. For example, axotomy of cultured hippocampal neurons often results in the transformation of a residual neurite into a new axon (Dotti and Banker, 1987). The mechanisms that reorganize circuits post-injury are likely similar to those that function in development. Noninvasive imaging techniques such as fMRI (functional magnetic resonance imaging) demonstrate that the motor cortex reorganizes following injury and also during normal learning (Butefisch, 2004; Gomis-Ruth et al., 2008). These results are certainly suggestive of the rewiring of the individual neurons within the affected circuit, but this interpretation requires validation through direct observation of single neurons. These analyses have relied upon fixed and stained tissue slices collected at developmental timepoints. With this methodology, however, it is categorically not possible to analyze the same animal throughout its development, and therefore dynamic events that may drive

synaptic plasticity cannot be observed. Finally, although much has been learned from cultures of primary neurons, this approach necessarily excludes the potential of detecting plasticity mechanisms that depend on contextual cues derived from developmental programs or experience (Ajay and Bhalla, 2006; Yu and Zuo, 2011).

Recent developments in multi-photon imaging are allowing the field to move toward visualizing synaptic rearrangement as it occurs in living mammalian brains (Chklovskii et al., 2004; Holtmaat and Svoboda, 2009). For instance, the stability and maintenance of individual fluorescently-labeled dendritic spines has been monitored *in vivo* throughout the post-natal life of a rodent (Trachtenberg et al., 2002). These powerful technologies now allow investigation into mammalian synaptic remodeling at a depth that was previously limited to simpler model organisms. Therefore, although the conservation of plasticity justifies the continued use of invertebrate models to investigate the molecular mechanisms of synaptic plasticity, these powerful new tools should allow scientists to validate conservation of these remodeling pathways in the mammalian brain (Yu and Zuo, 2011).

Synaptic remodeling events across species may be simplified into three steps: disassembly of the existing specialized domain, proper trafficking of molecular components to the nascent synaptic domain, and re-establishment of a functional synapse at the new connection site (Ho et al., 2011). The mechanisms that govern each of these processes have been extensively studied in the context of neurodevelopment. In this chapter, I will broadly discuss our current

understanding of how synaptic domains are established, disassembled, and then reconstituted in models of development and plasticity. Part 1 describes the mechanisms that create a polarized neuron with distinct presynaptic and postsynaptic domains, and how these same processes may be re-used to generate new synapses during remodeling. Part 2 discusses synaptic architecture and the current understanding of how local mechanisms can alter synaptic stability. Part 3 will introduce how transcription governs synaptic plasticity. This section features examples of how transcription factors may be exploited to uncover downstream genes that are directly involved in synaptic remodeling and how this approach relates to our study of a transcriptionally regulated program that regulates GABAergic synaptic plasticity in *C. elegans*.

Part 1: Creating a polarized neuron

Initial establishment of neuronal polarity

Cultured hippocampal neurons have provided a useful model for studies of neuronal polarity (Craig and Banker, 1994; Barnes and Polleux, 2009). Because hippocampal neurons can establish and maintain polarized structures *in vitro*, the mechanisms that govern neuronal polarity are likely to function as cell-intrinsic processes (Craig and Banker, 1994). Key events in hippocampal neuron polarization have been classified in five successive stages in which an immature neuron extends filopodia that ultimately adopt axonal or dendritic identities and form synapses (**Figure 1.1A**) (Dotti et al., 1988). Studies of these dynamic

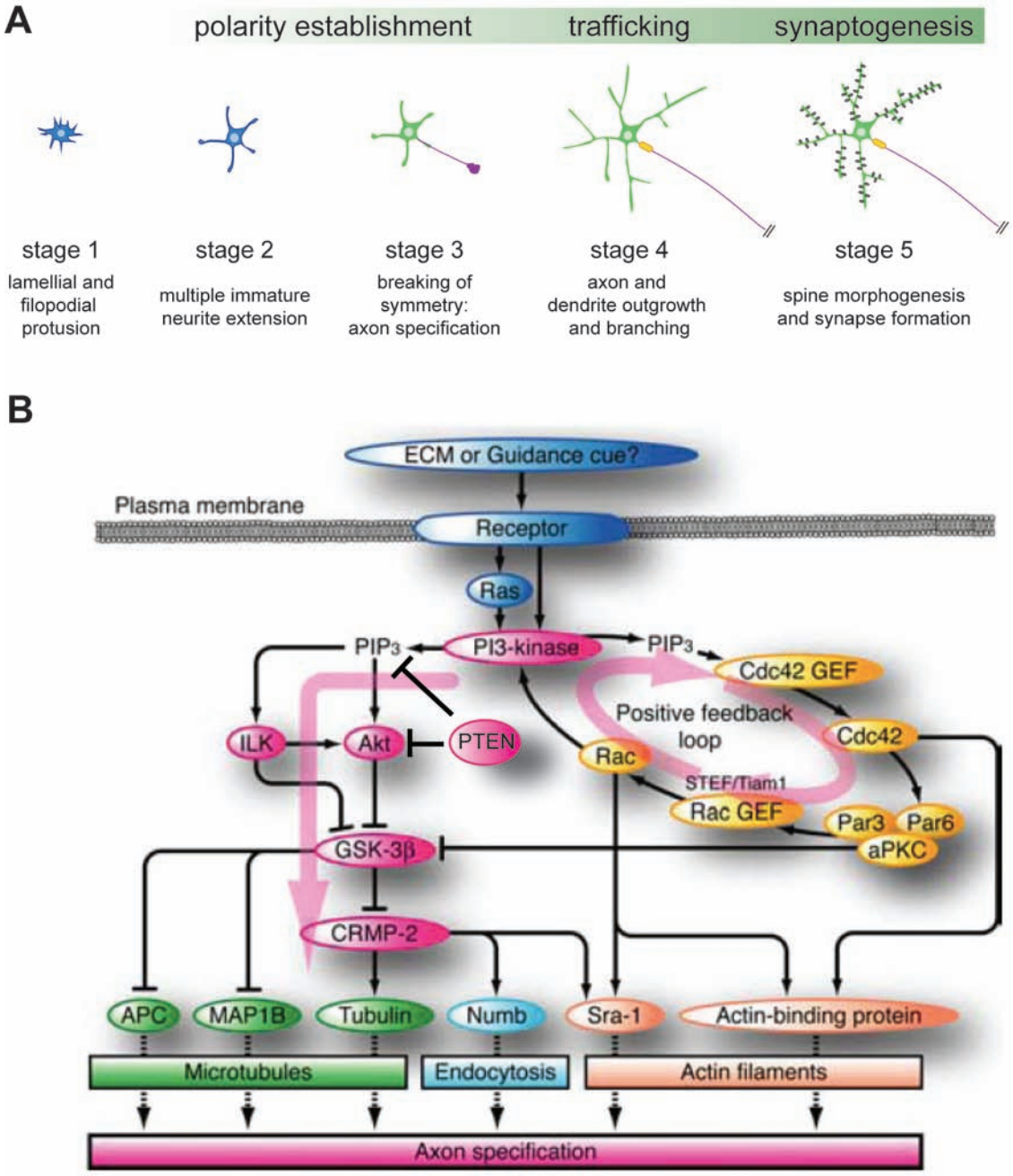

Figure 1.1. Establishment of neuronal polarity in hippocampal neurons. (A) Stages of hippocampal neuron development in culture as defined by Dotti et. al., 1988. Adapted from Barnes and Polleux, 2009. **(B)** PI3K directs both a phospho-Akt/GSK-3β/CRMP-2 pathway (left), which promotes microtubule outgrowth, and a GTPase/Par pathway (right), which destabilizes the actin cytoskeleton. Note intersection of the pathways via GSK-3β regulation. Originally published in Yoshimura et. al., 2006.

processes have revealed two major, interconnected signaling pathways that drive the emergence of polarity, GSK-3β/CRMP2 and Par/GTPase.

GSK-3β activation specifies the site of axonal outgrowth

The distal accumulation of phosphatidylinositol 3,4,5-triphosphate (PIP_3) and phosphorylated Akt (Akt-P) near the tip of a neuronal filopodia marks the single neurite destined to become an axon (Shi et al., 2003; Jiang et al., 2005) (**Figure 1.1B**, pathway denoted with left pink arrow). PIP_3 is locally produced by phosphoinositide-3-kinase (PI3K), which in turn recruits Akt to be phosphorylated by phosphoinositide-dependent protein kinases. This key role of PI3K is evident in experiments that alter the activity of PTEN (phosphatase and tensin homologue deleted on chromosome 10). Normally, PTEN dephosphorylates PIP_3 which results in depletion of local Akt-P; thus PTEN inactivates the ability of PIP_3 and Akt-P to promote axonogenesis. Overexpression of PTEN in cultured hippocampal neurons inhibits axon formation, whereas knockdown of PTEN results in outgrowth of multiple axons (Jiang et al., 2005). These results have been recapitulated *in vivo* in *Pten* mutant mice which show neurons with multiple axons (in addition to other defects) and in *C. elegans* egg-laying neurons which require *age-1/PI3K* for the asymmetric distribution of cytoplasmic determinants that drive axon extension (Adler et al., 2006; van Diepen and Eickholt, 2008).

In cultured hippocampal neurons, both PIP_3 and Akt-P function to inhibit GSK-3β. As in the experiments with PTEN misexpression, constitutive activation of GSK-3β blocks axonogenesis whereas knockdown of GSK-3β results in multiple axons (Jiang et al., 2005; Yoshimura et al., 2005). PIP_3 and Akt-P-

dependent inactivation of GSK-3β releases CRMP-2 (collapsin response mediator protein-2) to interact with tubulin dimers and promote microtubule assembly. CRMP-2 also promotes endocytosis of adhesion molecules such as Numb to allow for axon outgrowth and transports presynaptic proteins to the nascent axons via interaction with kinesin-1 (Inagaki et al., 2001; Fukata et al., 2002; Nishimura et al., 2003). This crucial role of CRMP-2 in axon establishment and subsequent outgrowth is evolutionarily conserved; in *C. elegans*, proper localization of UNC-33/CRMP in neurites is required for axon establishment, whereas loss of *unc-33/CRMP* results in severe axonal abnormalities and uncoordinated locomotion (Hedgecock et al., 1985; Tsuboi et al., 2005).

An additional study, however, indicates that this pathway may be more complex than a simple on-off switch for axon outgrowth. In *C. elegans* interneurons, DAF-18/PTEN appears to promote neurite extension, as loss-of-function *daf-18* axons extend more slowly. This may represent a novel function of PTEN in establishing polarity. Alternatively, these defects may be due to global misregulation of PIP_3 within the neuron, as *age-1/PI3K* mutations suppress the *daf-18* defect (Christensen et al., 2011). Nevertheless, this apparently contradictory result highlights the importance of regulation of PIP_3 and Akt-P within neuronal polarity.

Small GTPases activate Par proteins to induce axonogenesis

A second polarity establishment pathway is also initiated by PI3K. In this mechanism, a positive feedback loop with small Rho-family GTPases and PAR (partitioning-defective) proteins reorganizes the actin cytoskeleton in the nascent

axon (Yoshimura et al., 2006) (**Figure 1.1B**, denoted with right pink arrow). In this case, PI3K recruits the small GTPase Cdc42 (cell division cycle 42) to the tip of a nascent axon. Here, Cdc42 is activated by its GEF (guanine nucleotide exchange factor) and destabilizes the actin cytoskeleton (Shi et al., 2003). Local and regulated destabilization of the actin cytoskeleton is key for axonal development. This can be demonstrated by pharmacological treatment of hippocampal neurons with actin destabilizers which results in outgrowth of multiple axons (Bradke and Dotti, 1999). Activated Cdc42-GTP also binds Par6 to localize the Par complex [Par3, Par6, and atypical protein kinase C (aPKC)] to the nascent axon. There, the Par complex amplifies PI3K signaling through the small GTPase Rac, which is also implicated in actin dynamics. Notably, Par3/Par6/aPKC can also inhibit GSK3β activity. This intersection of the two polarity pathways results in stabilized microtubules coupled to destabilized actin, a hallmark of axon selection (Macara, 2004; Goldstein and Macara, 2007; Zhang and Macara, 2008). Again, this pathway appears to have some conservation in *C. elegans* neurodevelopment with related Par proteins. The PAR-1-related serine-threonine kinase *sad-1* is necessary for exclusive establishment of the presynaptic domain, and *par-4/LKB1* promotes dendritic growth (Crump et al., 2001; Biernat et al., 2002; Barnes et al., 2007; Kim et al., 2010; Teichmann and Shen, 2010).

Thus, these pathways (**Figure 1.1B**) function together to initiate neuronal polarity via regulation of the cytoskeleton and to promote outgrowth of a single axon in hippocampal neurons. However, not all neurons exhibit these distinctive

morphological features (i.e. long axonal process, short protrusive dendrites) that are correlated with the spatial segregation of presynaptic and postsynaptic components. For example, most *C. elegans* neurons display a single, unbranched process that contain adjacent but partially segregated presynaptic and postsynaptic domains (White et al., 1976). Are the same mechanisms that drive hippocampal neuron polarity also utilized to establish separate domains within this simple architecture? PI3K-GSK3β and PAR-GTPase dependent signaling pathways are certainly utilized to establish asymmetric molecular domains that are not correlated with prominent differences in local morphology. For instance, epithelial cells, newly fertilized eggs, and migrating cells depend on the asymmetric distribution of PIP_3 and PAR proteins to reorganize the cytoskeleton into discrete structural and functional domains (Goldstein and Macara, 2007; Bryant and Mostov, 2008). It is conceivable, therefore, that these same mechanisms function to establish polarity in neurons with simpler architecture, and furthermore, can potentially re-direct polarity within intact neurons during synaptic remodeling. A few studies are consistent with this idea (Crump et al., 2001; Hung et al., 2007; Christensen et al., 2011), but the mechanism is not understood.

Axonogenesis and outgrowth

Polarized structures arising from symmetry-breaking events in hippocampal neuron polarity are maintained during axonogenesis. In this process, an axon may extend long distances relative to the size of the neuron

soma to reach its synaptic partner and establish a functional circuit. The navigational apparatus that promotes growth at the tip of the axon, termed the growth cone, is a highly specialized structure with a dynamic cytoskeleton and is capable of sensing and responding to the extracellular environment. The morphogens that guide axonal growth, the extracellular matrix through which growth cones navigate, and cytoskeletal components that drive axonal growth have all been extensively reviewed (Lee and Van Vactor, 2003; Lowery and Van Vactor, 2009). Here, I will broadly highlight some key molecules in axon guidance and early synaptogenesis that also have roles in synaptic remodeling.

Cytoskeletal regulation during growth cone development

After determining the site of axonogenesis via the symmetry-breaking events described above, the cytoskeleton then promotes axonal outgrowth in multiple ways: first, microtubules and actin microfilaments form the shape of the neurite; second, the cytoskeletal meshwork serves as a scaffold for intracellular signaling in the growth cone; and third, the microtubule bundles within the neurite function as tracks for transport of organelles and synaptic molecules out to the synapse (Lowery and Van Vactor, 2009; Stiess and Bradke, 2011) (**Figure 1.2A**). The growth cone displays dynamic microtubule polymerization and depolymerization, surrounded by “treadmilling” F-actin filaments that drive filopodial protrusions. Extension of the growth cone requires instability of the actin cytoskeleton to allow polymerization of microtubules into the end of the growth cone (Conde and Caceres, 2009).

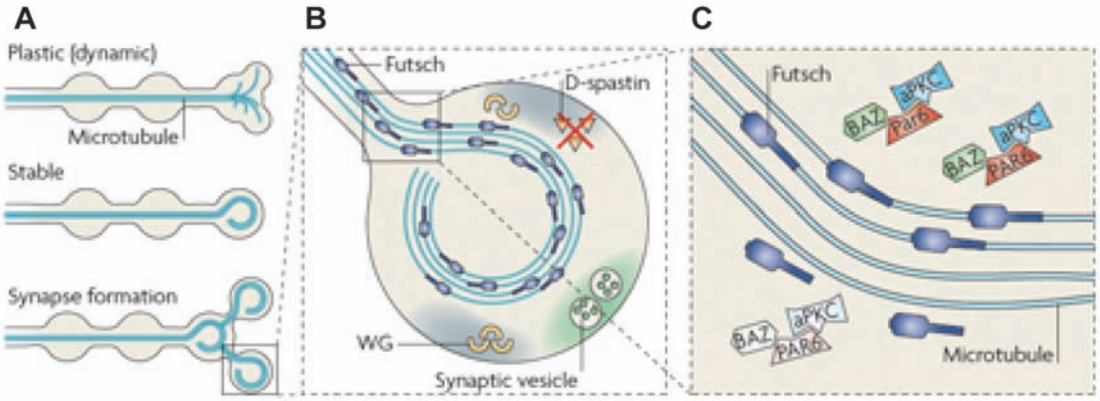

Figure 1.2. Regulation of the synaptic microtubule cytoskeleton. (A) Microtubules in advancing growth cones are stabilized within the neurite shaft but remain dynamic in the growth cone prior to formation of a synaptic bouton at *Drosophila* NMJs. **(B)** Futsch/MAP1B associates with stable microtubules in the neurite as well as the microtubule loop within the bouton. Synaptic stability is also mediated by D-spastin and Wingless/Wnt (WG). **(C)** Bazooka/Par3, in a complex with Par6 and aPKC, promotes association of Futsch with microtubules. Adapted from Conde and Caceres, 2009.

Rho family GTPases regulate the actin dynamics in the growth cone that drive translocation, while Rac GTPases control microtubule elongation. Rho GTPases cycle between an inactive, GDP-bound state and an active, GTP-bound state, aided by the action of GEFs (which induce the GTP-bound state) and GAPs (which promote the GDP-bound state) (Jaffe and Hall, 2005). In the growth cone, Cdc42 and Rac generally drive rearrangements of the actin cytoskeleton. Cdc42 is a critical regulator for axon outgrowth via its effector Wiskott-Aldrich syndrome protein (WASP), which promotes actin polymerization and filopodial outgrowth. The WASP-interacting Arp2/3 complex also promotes cytoskeletal rearrangement in the growth cone via increased actin branching; however, recent data suggest that Arp2/3 negatively regulates axon outgrowth, in contrast to its active role in lamellipodial protrusion (Korey and Van Vactor, 2000; Strasser et al., 2004; Hall and Lalli, 2011). Ras-family GTPases, in contrast to Rho-family GTPases, promote PI3K signal transduction to extend microtubules. However, there is evidence that Rac (a Rho-family GTPase) also stimulates PI3K, and thus indirectly stimulates microtubule elongation via CRMP (Yoshimura et al., 2006; Hall and Lalli, 2011). Thus, these small GTPases, their regulators, and their effectors exercise multiple roles in regulating the cytoskeleton to establish axon architecture and control growth cone outgrowth.

In contrast to the dynamic growth cone, the lengthening neurite has a central and densely arranged bundle of microtubules. Stabilization of microtubules within the neurite requires microtubule-associated proteins (MAPs). MAP1B and its homologue Futsch in *Drosophila* function as critical regulators of

this architectural feature (Pedrotti and Islam, 1995; Roos et al., 2000; Gogel et al., 2006; Riederer, 2007) (**Figure 1.2B-C**). All microtubules within the neurite are uniformly oriented with plus-ends directed toward the growth cone. This feature is unique to axons; dendritic microtubules show mixed orientations. Given that plus-end directed kinesin and minus-end directed dyenin motors are essential for trafficking axonal proteins (see below), the polarized orientation of microtubule bundles within axons is critically important for the efficient distribution of synaptic proteins in the growing axon (Baas and Lin, 2011).

The extracellular matrix during growth cone guidance and synaptogenesis

Neurons and their surrounding support cells secrete a variety of proteoglycans, including laminin, fibronectin, and collagens, to generate the extracellular matrix (ECM). The ECM forms a semi-rigid structure upon which growth cones migrate in response to growth factors that may be embedded within the ECM (Hynes, 2009). Collagens, which were originally viewed as providing basic structural support for tissue, are now understood to provide a wide array of specialized functions including the promotion of axon outgrowth. For example, genetic ablation of type XV/XVIII collagens disrupts axon guidance in *C. elegans* and *Drosophila* (Ackley et al., 2001; Ackley et al., 2003; Meyer and Moussian, 2009). In zebrafish, Collagen XVIII serves as a cue to direct motor axons into the periphery at the appropriate exit point (Schneider and Granato, 2006). This growing body of work suggests that collagens are a permissive substrate for migration as well as cues for accurate pathfinding and targeting.

Degradation and restructuring of the ECM is required for axonal guidance to its target location and forming a synapse with its partner. Matrix metalloproteases (MMPs) are expressed in developing axons of *Drosophila* (MMP1) and mouse (BMP-1/Tolloid, TIMP-2, MMP2, MMP 9), and MMP inhibition causes axon guidance and patterning defects in *Xenopus*. Emerging evidence suggests that different MMPs are required for cleaving particular ligands that the axon encounters along its path (Llano et al., 2000; Webber et al., 2002; VanSaun and Matrisian, 2006; Myers et al., 2011). MMPs are also necessary in later circuit formation by promoting synaptogenesis. For instance, MMP3 degrades the proteoglycan Agrin at the neuromuscular junction (NMJ) (Werle and VanSaun, 2003) (see discussion of Agrin below). Thus, MMPs appear to fulfill multiple roles of altering the ECM to allow simple mechanical outgrowth, directing the migration of the growth cone to the target, and promoting connectivity with synaptic partners.

Parallel mechanisms direct polarized trafficking of membrane proteins in epithelial cells and neurons

Polarized epithelial cells are defined by distribution of different integral membrane proteins to separate apical or basolateral domains. These membrane proteins are sorted for shipment to these specific destinations on the basis of intrinsic signal sequences embedded in each protein. Related mechanisms are employed in neurons for protein sorting to either axonal or dendritic domains (Winckler and Mellman, 1999). For example, viral glycoproteins expressed in

either cultured MDCK epithelial cells or hippocampal neurons are sorted to corresponding apical and axonal domains. Similarly, proteins that are normally sorted to the basolateral domain in epithelial cells are also trafficked to the somatodendritic region of neurons (Dotti and Simons, 1990). Based on the evident similarity of these sorting mechanisms, the wealth of research in epithelial cells has been very useful for revealing key elements of polarized trafficking in neurons.

Basolateral signal sequences in epithelial membrane proteins are typically located in the cytoplasmic tail. As these proteins traverse the trans-Golgi network, these signal sequences interact with μ subunits of AP-1 or AP-2 adaptor complexes for sorting into targeted clathrin-coated vesicles (Mellman, 1996; Winckler and Mellman, 1999). This mechanism appears to be conserved in a pathway that directs specific neurotransmitter receptors to the dendritic domain of *C. elegans* neurons. A mutation that removes the UNC-101/AP-1 subunit μ1 results in the mislocalization of glutamate and acetylcholine receptors and ROR-type receptor tyrosine kinases to axons. These results indicate that UNC-101 is required for receptor trafficking to the dendritic domain. Although these AP-1 adaptor proteins may perform parallel roles in both epithelial and neuronal trafficking, the molecular mechanisms are likely to include tissue-specific features. For example, AP-1 adaptor proteins function primarily in the Golgi in epithelial cells, but UNC-101 is largely restricted to the axon. This key difference predicts that membrane receptors may be targeted in *C. elegans* neurons by a transcytosis mechanism in which dendritic proteins are initially broadly directed to

the membrane and then endocytosed for trafficking to more specific destinations (Dwyer et al., 2001; Margeta et al., 2009).

Mechanisms that direct trafficking of axonal proteins are less well-understood in part because of differences in apical sorting in epithelial cells compared to axonal targeting in neurons (Silverman et al., 2001). One potential explanation for this disparity is the endocytosis/transcytosis mechanism mentioned above, which may also be utilized for axonal trafficking. For example, β-APP (amyloid precursor protein) is initially targeted to the neuronal cell soma membrane. From there, it is endocytosed and trafficked to an axonal destination (Winckler and Mellman, 1999). The signals that direct this transcytosis pathway and whether they are provided by the axonal protein remain unknown (Brunholz et al., 2011).

The Arf family of small GTPases are important regulators for sorting membrane proteins in epithelial cells and neurons. Arf proteins were originally identified as regulators of clathrin coat assembly in the trans-Golgi network where membrane protein sorting occurs. In addition, Arf GTPase activating proteins (ArfGAPs) have been shown to interact with vesicle cargo as well as coat proteins, suggesting that Arfs and ArfGAPs are directly involved in a sorting mechanism at the trans-Golgi. Arfs also localize to the plasma membrane where they can regulate PI3K signaling. These dual roles suggest the possibility that Arf activity can mediate “early” sorting at the trans-Golgi as well as “later” sorting during transcytosis (Nie and Randazzo, 2006; Myers and Casanova, 2008). Evidence that Arfs regulate neuronal polarity via vesicle sorting comes from a

recent study in *C. elegans* revealing that the Arf-related protein ARL-8 is necessary for synaptic vesicle (SV) trafficking to the axonal domain. In this case, ARL-8 protein travels with SV precursors to prevent “clumping” of presynaptic components that might indicate premature synaptogenesis (Klassen et al., 2010). Taken together, these data implicate Arf in multiple steps of vesicular sorting in polarized cells and predict that Arf signaling is required for accurate delivery of axonal proteins to their target domains.

Delivery of synaptic vesicles to axonal domains

Because of the central role of SVs in neurotransmitter release, the translocation of these signaling organelles to the axonal domain is critically important to neuronal function. Following establishment of neuronal polarity, “packets” of SV precursors are moved in an anterograde direction along microtubules by KIF1A kinesins (*unc-104* in *C. elegans*) (Hall and Hedgecock, 1991; Ahmari et al., 2000). SV trafficking is mediated by adaptor proteins that bind kinesins, such as the small GTPase Rab3. Rab3 is an SV vesicle component that mediates SV trafficking by cycling through GTP- and GDP-bound states. Although Rab3 is a key regulator of SV trafficking, additional mechanisms can also traffic SVs to axons in the absence of Rab3 (Pfeffer and Aivazian, 2004; Schluter et al., 2004).

SVs can also move in a retrograde direction along microtubule tracks via the minus-end directed transporter dyenin. Regulation of dyenin activity is important for SV delivery to axons (Schlager and Hoogenraad, 2009). For

example, recent work in *C. elegans* identified two cyclin-dependent kinases, CDK-5 and PCT-1, as well as the cyclin CYY-1, that promote SV targeting by inhibiting dyenin-regulated retrograde transport (Ou et al., 2010). As noted below, this work also linked these components to a remodeling mechanism in which SVs are relocated to a new synaptic domain (Park et al., 2011). The delivery of axonal proteins and SVs constitutes an ongoing area of research.

Examples of polarity factors in synaptic remodeling

In the preceding sections, I have broadly reviewed the establishment of polarity and axonogenesis via signal transduction cascades, cytoskeletal regulators, and extracellular interactions. Current studies are demonstrating that many of the same proteins required for the initial establishment of neuronal polarity early in development are also required later for modifying these structures in synaptic remodeling mechanisms. Below, I will detail several published examples in which neurodevelopment proteins (*e. g.* MAP1B, Par complex, GSK-3β, trafficking regulators, etc.) are required for synaptic remodeling. Later chapters will feature additional proteins (Arp2/3, collagens, MMPs, ArfGAPs) that our findings have suggested are actively involved in synaptic remodeling.

Par complex and GSK-3β regulate presynaptic domains in the *Drosophila* NMJ

The *Drosophila* NMJ is composed of an axon with multiple synaptic terminals or “boutons”. These synaptic boutons are highly enriched in

microtubules, which enter the flattened portion of the nerve terminal around the periphery of the bouton and then re-enter the neurite (Tsui et al., 1984). During larval metamorphosis, new synaptic boutons form from division of existing boutons; thus, both the development and remodeling of these synapses requires extensive regulation of the microtubule cytoskeleton. One such regulator is novel microtubule-associated protein, *futsch*, which is required for synaptic growth and bouton division (Hummel et al., 2000; Roos et al., 2000) (**Figure 1.2A-B**). The nearest vertebrate homologue is MAP1B, a key regulator of neuronal polarity, with high N- and C-terminal sequence similarity to *futsch*. *Drosophila futsch* appears to be positively regulated by *bazooka*, the Par3 homologue in *Drosophila*. A role for the Par3/Par6/aPKC complex (**Figure 1.2C**) is suggested by the finding that a dominant-negative aPKC mutation causes a phenotype similar to that observed in *futsch* mutants (Ruiz-Canada et al., 2004). Both *futsch* and MAP1B are also regulated by GSK-3β, which functions in a second major pathway of axonal specification in early neuronal polarity. Thus, regulation of microtubules by MAPs, Par proteins, and GSK-3β is important for initial polarity establishment, axonal outgrowth, and later synaptic remodeling (Budnik and Salinas, 2011).

Par3 and Par6 can alter dendritic specializations

A central role for the Par3/Par6/aPKC complex in cell polarity is well-documented for a variety of cell types (Macara, 2004; Mellman and Nelson, 2008). Recent work indicates that these key proteins also control maturation of postsynaptic specializations termed dendritic spines in mammalian neurons. In

contrast to the regulation of microtubule stability in the presynaptic boutons of *Drosophila* NMJs, Par proteins in dendrites control actin dynamics to regulate dendritic spine morphogenesis. In this setting, Par3 sequesters a Rac GEF (Tiam) in order to prevent ectopic Rac activation and stabilize F-actin. When Par3 is knocked down, filopodial protrusions do not mature into actin-rich spines (Zhang and Macara, 2006). Further study revealed that Par-6 and aPKC also participate in the formation of dendritic spines via regulation of Rho GTPase activity (Zhang and Macara, 2008). Further evidence from *Drosophila* NMJ postsynaptic domains (in contrast to presynaptic boutons described above) demonstrate that Par3/Bazooka localization and actin structure depend on aPKC phosphorylation; when the phosphorylation site of Par3/Bazooka is genetically disrupted, F-actin is destabilized and receptors are mislocalized (Ramachandran et al., 2009). Because of the necessity for remodeling the *Drosophila* NMJ during metamorphosis (described above), these results suggest that Par mediation of GTPase activity could be a mechanism for the reorganization of actin in dendritic maturation and plasticity.

A cyclin and cyclin-dependent kinase control anterograde transport to relocate synapses

C. elegans GABAergic motor neurons undergo synaptic remodeling program during larval development (discussed at length later in this chapter). During this remodeling event, GABAergic synapses are removed from one neurite which innervates ventral muscle and reconstituted with dorsal muscle (White et al., 1978). The rearrangement accommodates the addition of larval

GABAergic motor neurons that synapse onto ventral muscles. Interestingly, this process appears to involve a cyclin-dependent kinase-regulated pathway that also directs polarized trafficking in differentiating neurons. In this case, the cyclin-box containing protein CYY-1 appears to drive the removal of existing synapses, whereas CDK-5 is responsible for trafficking SVs to the new location. In this case, however, CDK-5 utilizes the anterograde kinesin *unc-104* (Park et al., 2011) rather than dyenin which is employed for initial SV trafficking (Ou et al., 2010).

Studies in mice have also detected roles for CDK-5 in synaptic remodeling, although the mechanism of its function differs. For example, a conditional *cdk-5* knockout was shown to enhance glutamate receptor turnover (a method of remodeling discussed in the following section). Additional evidence, however, points to roles for CDK-5 in the SV cycle which could potentially include functions that are also active in remodeling *C. elegans* neurons (Angelo et al., 2006; Hawasli et al., 2007).

Part 2: Presynaptic and postsynaptic mechanisms of plasticity

Neurons communicate with their targets via chemical synapses composed of specialized presynaptic and postsynaptic domains. The presynaptic domain may be positioned exclusively at the end of the axon, termed "*terminaux*", as in *Drosophila* NMJs, or alternatively *en passant* ("in passing") along the length of a neurite, as in *C. elegans* and in the mammalian brain (Shen and Scheiffele, 2010; Budnik and Salinas, 2011). In both cases, the presynaptic specialization

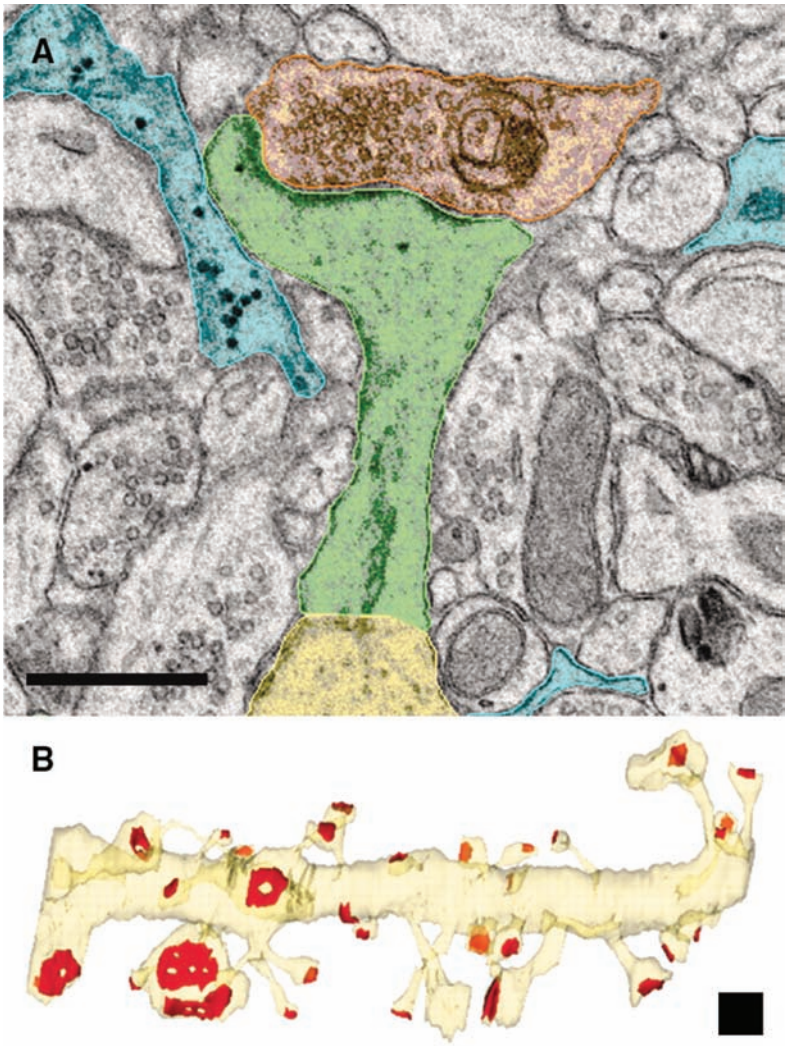

Figure 1.3. Ultrastructure of chemical synapses. (A) Electron micrograph from adult rat hippocampus. The dendritic shaft is colorized in yellow, the spine neck and head in green, the presynaptic terminal in orange, and astroglial processes in blue. Scale bar, 0.5 μm. **(B)** Three-dimensional reconstruction of an 8.5-μm-long dendrite (yellow) with the postsynaptic densities labeled in red. Scale cube, 0.5 μm^3. Originally published in Ho et. al., 2011.

is composed of an electron-dense matrix of scaffolding proteins, specific cytoskeletal elements, and synaptic vesicles (**Figure 1.3A**). The postsynaptic domain contains the neurotransmitter receptors, ion channels, and components of signal transduction pathways that propagate the synaptic signals throughout the circuit. In mammalian excitatory synapses, postsynaptic domains are located in actin-rich protrusions termed dendritic spines that are readily observable (**Figure 1.3B**). Although postsynaptic domains in *C. elegans* are not visible in electron micrographs, key molecular components of the postsynaptic region are conserved (Ho et al., 2011). Before discussing the known mechanisms that reorganize these domains during remodeling, I will briefly summarize what is known about the establishment of these domains with an emphasis on *C. elegans* neurodevelopment.

Assembly of presynaptic specializations

The ultrastructural appearance of the presynaptic domain is similar in *C. elegans* and vertebrate central nervous systems, and several proteins that function in synaptogenesis in other nervous systems were first identified in *C. elegans* neurons (**Figure 1.4A**). One such example is SYD-1, so named for its synaptic-defective phenotype. SYD-1 was originally discovered as a key determinant of neuronal polarity in developing GABAergic motor neurons. In *syd-1* mutants, SV markers appear diffuse and accumulate in neurites that normally do not have axonal components, indicating mis-specification of the presynaptic domain (Hallam et al., 2002). Accumulation of SYD-1 at synapses is partially

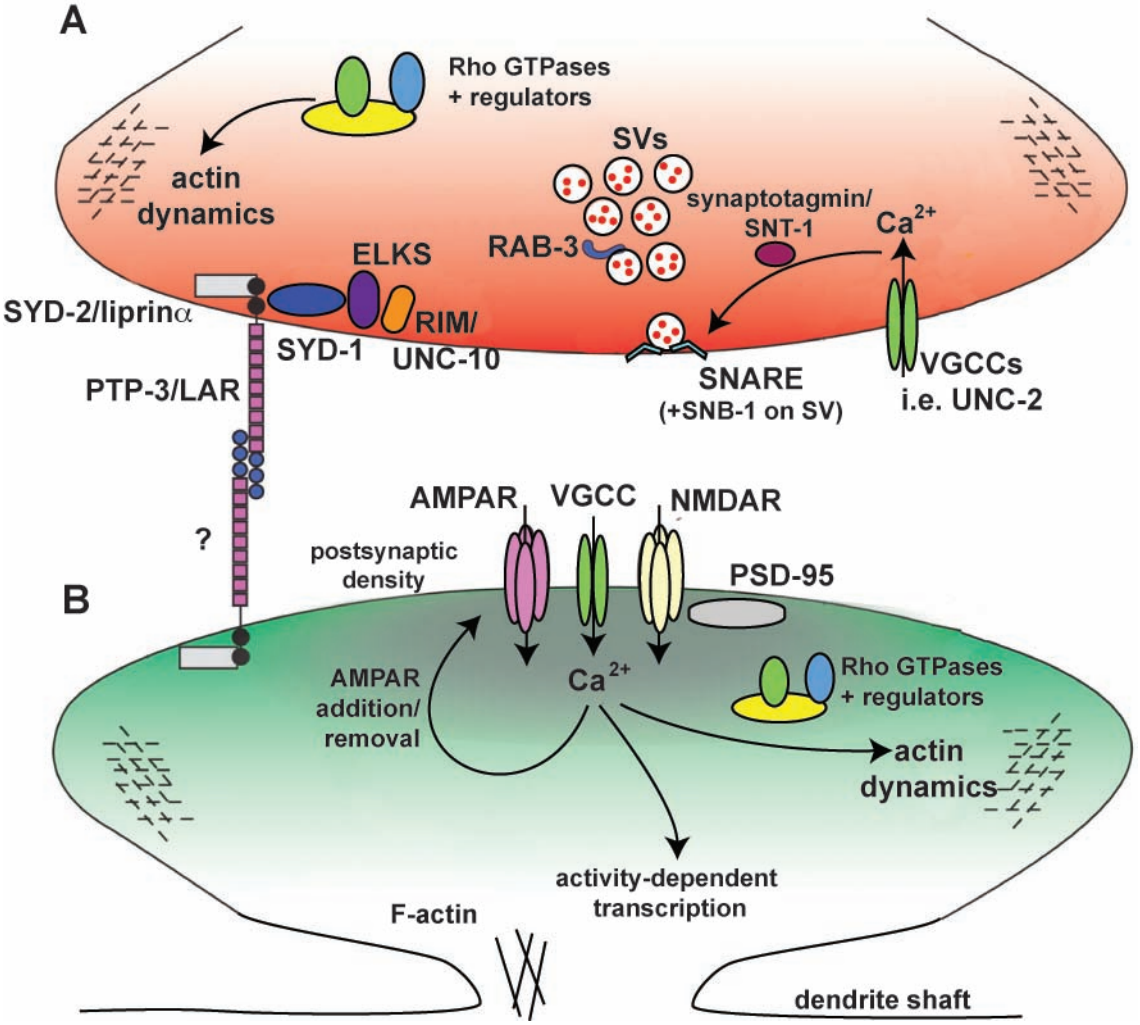

Figure 1.4. Key molecules that function within presynaptic and postsynaptic densities. (A) The presynaptic density is organized by SYD-1, ELKS, SYD-2, PTP-3, and UNC-10 in *C. elegans.* Together these molecules recruit RAB-3 and SNB-1 containing synaptic vesicles, which are released following calcium ion influx by voltage-gated calcium channels (VGCCs, such as UNC-2) and sending of calcium increase by SNT-1. Actin dynamics at the presynaptic density are regulated by RhoGTPases during outgrowth which may mediate actin at presynaptic densities following maturation. **(B)** Postsynaptic densities in the dendritic spine are opposed to presynaptic densities by the interaction of membrane spanning proteins (LAR in mammals, but not *C. elegans*) and PSD-95 functions to cluster postsynaptic proteins. AMPA and NMDA receptors, which sense glutamate, allow influx of calcium (UNC-49 sense GABA and cause Cl^- influx, and AChRs sense acetylcholine, not depicted here). Influx of calcium via glutamate receptors and/or VGCCs can cause changes in AMPA receptor trafficking, actin dynamics, and gene transcription. Adapted from Giagtzoglou et. al., 2009.

required for the recruitment of additional “downstream” presynaptic proteins (Patel et al., 2006). SYD-1 contains a RhoGAP domain, leading to speculation that it might interact with and/or mediate cytoskeletal dynamics; however, based on analysis of *syd-1* mutations that perturb this domain, it appears that GAP domain function is not necessary for SYD-1-dependent synaptogenesis (Hallam et al., 2002). Thus, SYD-1 is currently proposed to function primarily as a scaffold for assembly of active zone proteins. This role of SYD-1 seems particularly important considering that SYD-1-interacting proteins are not trafficked to synapses via the same UNC-104/KIF1A mechanism as SVs (see earlier section) and suggests that SYD-1 arrives at the membrane earlier via dense-core vesicles enriched in active zone proteins (Shapira et al., 2003).

ELKS (glutamine, leucine, lysine, and serine-rich) family proteins, including *Piccolo*, *Bassoon*, and *Bruchpilot* in *Drosophila*, are presynaptic active zone proteins that interact with SYD-1 (**Figure 1.4A**) The recruitment of ELKS-1 to *C. elegans* synapses depends upon SYD-1 (Patel et al., 2006). In *Drosophila,* the synaptic localization of ELKS family member Bruchpilot also depends on the *syd-1* homologue, *DSyd-1*; ELKS in turn recruits Liprin-α (discussed below) (Fouquet et al., 2009; Owald et al., 2010). In *Drosophila* and vertebrates, ELKS appears also localizes RIM (Rab3a-interacting molecule) to the active zone which then recruits synaptic vesicles. However, this role for ELKS may be dispensable in *C. elegans*. In all cases, ELKS appears to promote synaptic transmission via recruitment of calcium channel subunits (Deken et al., 2005; Patel et al., 2006; Saheki and Bargmann, 2009).

As noted above, Liprin-α, named SYD-2 in *C. elegans* and *Dliprin-α* in *Drosophila*, is recruited to the active zone by the early synaptic organizer SYD-1 in *C. elegans* and by ELKS in *Drosophila* (**Figure 1.4A**) (Zhen and Jin, 1999; Yeh et al., 2005; Patel et al., 2006). Liprin-α was originally identified via its interaction with transmembrane LAR tyrosine kinase (PTP-3 in *C. elegans*) in a yeast two-hybrid screen (Ackley et al., 2005; Stryker and Johnson, 2007). Mutations in *syd-2* in *C. elegans* and *Drosophila*, as well as defective *ptp-3* in *C. elegans*, cause reduced active zone complexity (Zhen and Jin, 1999; Ackley et al., 2005). This result is perhaps not surprising, given the myriad of interactions of Liprin-α with other synaptic proteins. For instance, Liprin-α forms a complex with RIM and ELKS that, in turn, interacts with UNC-13, a component for regulated synaptic vesicle release. Liprin-α also interacts with the MALS/Vel-Calsk-Mint1 complex, which is required for synaptic vesicle release (Stryker and Johnson, 2007). LAR, in contrast, appears to integrate signals from the ECM to regulate active zone stability. For instance, PTP-3/LAR has been shown to interact with the large glycoprotein Nidogen, encoded by *nid-1* in *C. elegans* (Ackley et al., 2003), and *Drosophila* LAR interacts with two extracellular heparin sulfate proteoglycans, Syndecan and Dallylike (Stryker and Johnson, 2007). While SYD-2/Liprin-α and its interacting proteins appear to function at the nexus of the developing synapse, SYD-2 single mutants and mutants of other synaptic proteins have differing phenotypes with varying severity, suggesting that the interactions between these proteins are complex and not fully understood (Giagtzoglou et al., 2009).

The localization of the PAR-1-related serine/threonine kinase SAD-1 at the synapse depends on SYD-1 and SYD-2. As noted earlier, synaptic vesicles are mislocalized to dendritic domains in *sad-1* mutant GABAergic motor neurons. This polarity defect is markedly similar to that of *syd-1* mutants and suggests that both proteins regulate SV localization (Crump et al., 2001; Hung et al., 2007). Hippocampal neurons that lack SAD kinases also display this characteristic phenotype (Kishi et al., 2005). SAD-1 also exercises additional roles in synaptic morphology and function (Crump et al., 2001; Inoue et al., 2006; Patel et al., 2006)

Role of calcium in SV release

Synaptic vesicle exocytosis involves docking, priming, and fusion steps, followed by endocytosis to complete the synaptic vesicle cycle (Murthy and Stevens, 1999; Harris et al., 2001). The synaptic localization of components that execute these processes is not fully understood, but in some cases, appears to depend on SYD-1, SYD-2, and ELKS as described above (**Figure 1.4A**) (Murthy and De Camilli, 2003; Patel et al., 2006). A discussion of each component of the exocytic and endocytic machinery is outside the scope of a chapter devoted to neuronal polarity and remodeling. I will instead focus on the role of intracellular calcium in exocytosis because of evidence of a necessary role for neuronal activity in synaptic plasticity (presented later in this chapter and in **Chapter V**).

Synaptic vesicle fusion depends on a local increase in calcium via voltage-gated calcium channels (VGCCs) (**Figure 1.4A**). Three distinct L-type calcium channel subunits are required for this process in *C. elegans*: UNC-2, EGL-19,

and CCA-1 (Richmond et al., 2001; Saheki and Bargmann, 2009; Gao and Zhen, 2011). Additional necessary components include an auxiliary subunit of UNC-2, UNC-36, and two novel channel subunits, NCA-1 and NCA-2 (Schafer et al., 1996; Yeh et al., 2008). The localization of UNC-2 at the synapse is dependent upon UNC-36 as well as a novel endoplasmic reticulum transmembrane protein encoded by CALF-1 (Saheki and Bargmann, 2009). The synaptotagmin homologues in *C. elegans* (*e.g.* SNT-1) and *Drosophila* integrate the rise in intracellular calcium from these channels to trigger synaptic vesicle release (**Figure 1.4A**) (Littleton et al., 1993; Nonet et al., 1993). When calcium levels rise, synaptotagmin associates with the active zone protein RIM, which in turn binds GTP-bound Rab3 on SVs. RIM also binds SNAP-25 to promote docking and release of SVs. Current models suggest that RIM functions as a scaffold to assemble a calcium-sensitive SV release complex (Coppola et al., 2001; Sudhof, 2004). Many of these presynaptic proteins are also required for synaptic plasticity. For instance, RAB-3 and RIM are both necessary for long-term synaptic plasticity (Lledo et al., 1993; Tsetsenis et al., 2011).

Assembly of postsynaptic specializations

A functional dendrite must include postsynaptic domains with the proper complement of neurotransmitter receptors and signal transduction proteins (Bruneau et al., 2009). In the mammalian central nervous system, excitatory transmission is largely directed through actin-rich protrusions termed dendritic spines (**Figure 1.3B**). Formation of these structures depends on localized

regulation of the actin cytoskeleton. These dendritic spines are established and maintained by the Rho family of small GTPases and the downstream actin-binding proteins that they regulate (**Figure 1.4B**) (Wegner et al., 2008; Lin and Webb, 2009; Svitkina et al., 2011). However, in contrast to the largely activity-independent filopodial protrusions of the axonal growth cone, the cytoskeletal reorganization that drives spine formation is stimulated by signaling activity from presynaptic partners (Portera-Cailliau et al., 2003; Calabrese et al., 2006).

Dendritic spines are highly enriched in AMPA (α-amino-3-hydroxy-5-methyl-4-isoxazole propionic acid)-type glutamate receptors (AMPARs), which are the main transducer for excitatory input in the mammalian central nervous system. These receptors are composed of heteromeric glutamate receptor subunits (*i.e.* GluR2/GluR1 or GluR2/GluR3 subunits), and the functional properties of the channel depend upon this subunit composition (Derkach et al., 2007). Another type of ionotropic receptor, N-methyl-D-aspartate receptor (NMDAR), also functions at glutamatergic synapses (**Figure 1.4B**). NMDARs are ligand-gated, requiring co-activation by glutamate and glycine, and also voltage-gated. This dual-sensing function of NMDARs and subsequent calcium influx is utilized in synaptic plasticity (see below) (Yashiro and Philpot, 2008).

The postsynaptic density protein PSD-95 interacts with glutamate receptors at the postsynaptic membrane (Rutter and Stephenson, 2000; Chetkovich et al., 2002). PSD-95 contains a PDZ domain and is a member of the membrane-associated guanylate kinase (MAGUK) family of postsynaptic signaling proteins (Xu, 2011). While overexpression of PSD-95 promotes

NMDAR clustering, it is not clear that PSD-95 is necessary to recruit glutamate receptors to the synapse, as time-lapse imaging reveals that receptors appear at postsynaptic densities prior to the arrival of PSD-95. Nevertheless, PSD-95 still appears to be a central organizer of the postsynaptic domain with many interacting proteins (Han and Kim, 2008). In *C. elegans*, the apparent PSD-95 homologue DLG-1 is required for epithelial junction formation, but it is not necessary for postsynaptic assembly (Firestein and Rongo, 2001). Instead, glutamate receptor localization appears to be driven by a different PDZ-domain containing protein, LIN-10/Mint, and a type II calcium/calmodulin-dependent protein kinase (CaMKII), UNC-43 (Rongo and Kaplan, 1999; Stricker and Huganir, 2003).

Whereas glutamate mediates excitatory synapses in the mammalian central nervous system, GABA and glycine are the predominant inhibitory neurotransmitters. Initiation and maintenance of postsynaptic clustering of GABA A-type and glycine receptors is driven by multiple proteins including a tubulin-associated protein, Gephyrin, a ubiquitin-like protein GABARAP, a dystrophin-glycoprotein complex, and other associated proteins involved in scaffolding and trafficking (Bruneau et al., 2009). In *C. elegans*, GABA inhibitory signaling has been extensively studied at NMJs in the ventral cord motor circuit. The ionotropic GABA receptor expressed in muscle is encoded by the *unc-49* locus. Alternative splice forms of UNC-49 yield UNC-49A, B, and C; however, UNC-49A is barely detectable and UNC-49B and C apparently form the GABA-gated chloride channel. The pharmacological properties of the UNC-49B-C heteromeric

receptors are similar to the vertebrate GABA-A receptor (Schuske et al., 2004). UNC-49 clusters in postsynaptic NMJs are directed by GABAergic innervation from motor neurons; in cases where presynaptic domains are misplaced by axon guidance defects or removal of SV trafficking machinery, UNC-49 clusters adjacent to misplaced presynaptic domains, indicating that the presynaptic domain is sufficient to drive clustering. Interestingly, UNC-49 clustering does not require GABA but does depend on SV function. The molecular identity of the presynaptically-derived UNC-49 clustering signal is currently unknown (Gally and Bessereau, 2003).

In the mammalian peripheral nervous system, the cholinergic NMJ has been well studied to identify factors that cluster acetylcholine receptors (AChR). The heparin sulfate proteoglycan Agrin functions as a key organizing signal. Agrin is secreted by motor neurons to promote neurotransmitter receptor clustering via activation of muscle-specific kinase (MuSK) (Magill-Solc and McMahan, 1988; Glass et al., 1996). However, this induction of AChR clustering by Agrin does not appear to be conserved in *C. elegans*; instead, AChRs are clustered at NMJs in a different mechanism by a transmembrane protein with multiple CUB domains, LEV-10 (Gally et al., 2004; Hrus et al., 2007). The downstream effector for Agrin, Rapsyn, does appear to be conserved and functions in a similar way in both *C. elegans* and vertebrates. Rapsyn is a membrane-targeted protein that anchors AChRs to the underlying postsynaptic cytoskeleton via Dystrophin and Utrophin (Banks et al., 2003; Nam et al., 2009). In *Drosophila,* cholinergic *Drosophila* NMJs undergo remodeling during

metamorphosis, suggesting that addition or removal of AChRs at the membrane could take place in a synaptic remodeling program. However, outside of MuSK and PSD-95, no other key factors have been identified that function in AChR remodeling (Hesser et al., 2006; Bruneau and Akaaboune, 2010; Drever et al., 2011).

Disassembly of synapses in pruning

Synapse elimination is an important mechanism required for both maturation and remodeling of neuronal networks. In some cases, synaptic elimination is accompanied by axonal retraction, as in the maturation of the vertebrate NMJ (Luo and O'Leary, 2005; Shen and Scheiffele, 2010). In the newborn mouse, individual muscle fibers are innervated by axons from multiple motor neuron partners. Individual NMJs are eliminated in an activity-dependent competition during development until a single axon innervates each muscle fiber. High-resolution studies have demonstrated that active synapses “win” over inactive synapses; however, the molecular cues that govern the pruning mechanism are unknown (Sanes and Lichtman, 1999; Lichtman and Colman, 2000).

Other instances of synaptic elimination coupled with retraction have been observed for neurons in both the hippocampus and visual cortex. In these cases, elimination is triggered by interaction of axon-guidance regulators PlexinA3 (in the neurons) and Semaphorin 3F (in the target). In PlexinA3-knockout mice, hippocampal synapses continue to mature at the transient target site, suggesting

that elimination of the synapse is the cue for retraction of the neurite. However, the downstream mediators of Semaphorin signaling, and how they contribute to synapse removal and axon retraction, are unknown (Yaron et al., 2005; Low et al., 2008; Shen and Scheiffele, 2010).

A different mechanism for synaptic pruning has been demonstrated in *C. elegans* (Miller, 2007). In the immature egg-laying circuit, HSN neurons form presynaptic specifications along vulval muscle. Normally, a subset of these synapses is removed at a later developmental stage. However, in either *syg-1* or *syg-2* mutant animals, these synapses persist into adulthood (Shen et al., 2004). SYG-1 and SYG-2 encode IgSF membrane proteins. SYG-2 is expressed in guidepost cells and interacts with SYG-1 in the neighboring HSN axon to position SYG-1 near the target egg-laying musculature. SYG-1 functions in this location to prevent degradation of a nascent presynaptic zone (**Figure 1.5**). The mechanism of this effect depends the local disruption of E3 ubiquitin ligase activity by SYG-1. Nascent synapses at distal locations in the HSN axon, however, are not protected and are ultimately removed by proteolytic activity (Ding et al., 2007).

Activity-dependent mechanisms at the synapse

In addition to synapse removal and establishment of entirely new pre- and postsynaptic domains, existing domains can be modulated by increasing or decreasing synaptic strength in response to stimulation. In the two examples described below, postsynaptic domains are altered by changing calcium influx, neurotransmitter receptor enrichment, and cytoskeletal specializations. Here, I

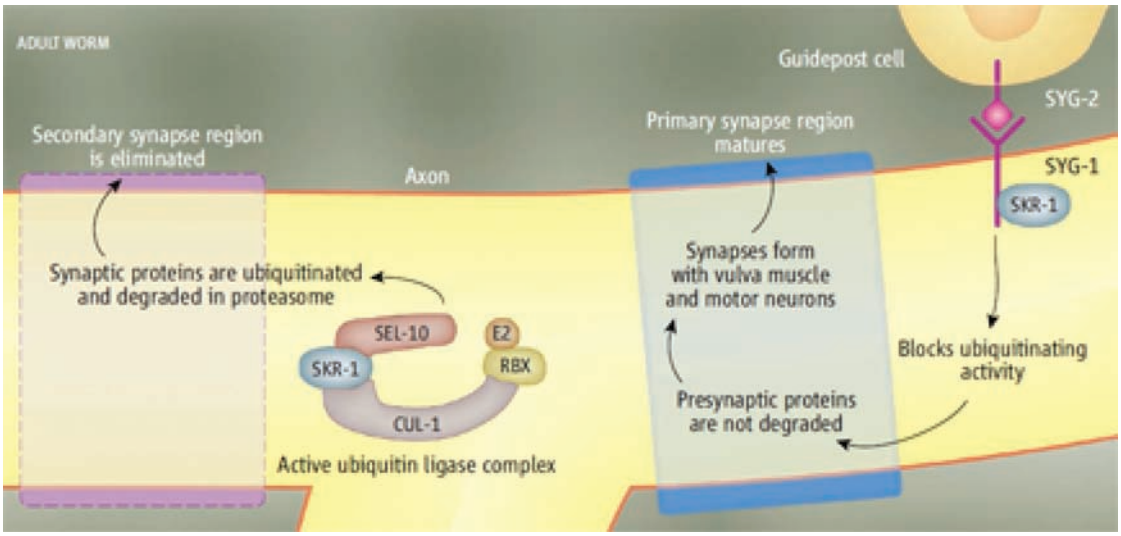

Figure 1.5. Localized ubiquitin-proteasome function eliminates immature synapses. The protein SYG-1, in HSN egg-laying neurons in *C. elegans*, is localized by SYG-2 in guidepost cells. SYG-1 blocks proteolysis of synaptic proteins at primary synapses by binding and inactivating SKR-1, but allows destruction of secondary synapses by the SKP-Cullin-F-box complex. E2, E2 ubiquitin conjugating enzyme; RBX, Ring finger protein. Originally published in Miller, 2007.

will focus on local changes at the synapse; in the following section (**Part 3**), I will describe how these synaptic alterations can interact with gene expression.

cAMP-dependent short term plasticity in *Aplysia*

Seminal work from Eric Kandel's group in the sea slug *Aplysia* revealed that short-term synaptic changes depend on a cyclic AMP (cAMP) second-messenger system to strengthen synapses and can occur in the absence of protein synthesis. These experiments showed that neural stimulation elevates cAMP at *Aplysia* synapses by activating adenylyl cyclase. In turn, the local increase in cAMP levels enhances synaptic activity (Brunelli et al., 1976). In this mechanism, cAMP activates cAMP-dependent protein kinase A (PKA) which downregulates K^+ channel activity. The resultant decrease in K^+ current enhances Ca^{2+} influx which increases neurotransmitter release (Klein and Kandel, 1978; Bacskai et al., 1993; Braha et al., 1993; Kandel, 2001).

AMPAR and spine plasticity induced by local calcium changes

The glutamate receptors on the dendritic spines of hippocampal neurons undergo activity-dependent remodeling. Because NMDA receptors are both ligand-gated as well as voltage-gated, they are considered "coincidence detectors" that are selectively activated with of frequent stimulation (Rutter and Stephenson, 2000; Yashiro and Philpot, 2008; Ho et al., 2011). The resultant Ca^{2+} influx initiates a signal transduction cascade involving protein kinase activation (including PKA and CaMKII) that promotes phosphorylation and trafficking of AMPA receptors. Net effects include either long-term potentiation (LTP), in which AMPAR concentration at the membrane increases, or long-term

depression (LTD), in which AMPARS are removed from the plasma membrane (**Figure 1.4B**) (Malenka and Bear, 2004; Jiang et al., 2006; Derkach et al., 2007; Shepherd and Huganir, 2007; Fu and Zuo, 2011). The induction of LTP in favor of LTD, or vice versa, appears to depend on the magnitude and frequency of the calcium ion influx; one large calcium increase stimulates LTP, whereas a prolonged rise of calcium over multiple stimulations results in LTD (Yang et al., 1999; Newpher and Ehlers, 2008).

The addition or removal of AMPA receptors from the dendritic membrane is correlated with increased or decreased F-actin within the spine, respectively (Okamoto et al., 2004). Even in stable spines, actin is rapidly turned over via cofilin (which promotes addition of new actin monomers via prevention of actin capping), indicating a homeostatic, dynamic actin cytoskeleton within spines (Morgan et al., 1993; Star et al., 2002). Thus, the actin cytoskeleton is readily remodeled in response to changes in synaptic strength by the action of Rho-family GTPases. The effectors of these GTPases are actin-binding proteins that can promote actin filament extension and larger spines (downstream of Rho) or actin destabilization and smaller spines (downstream of Rac). GTPases can also stimulate PIP_2 signaling, which promotes actin polymerization (Calabrese et al., 2006). Note here the recapitulation of the earlier theme of cytoskeletal rearrangements via GTPases and PI3K signaling; these mechanisms underlie both the establishment of neuronal domains as well as later remodeling events.

Part 3: Regulation of gene expression to remodel synapses

The examples of synaptic remodeling described above are regulated by temporal changes in neural activity. Synaptic plasticity can also occur by the activation of transcription factors that regulate expression of proteins that promote plasticity. The production of new proteins in developmental synaptic remodeling programs typically results in long-term changes to synaptic patterning. Synaptic activity can also stimulate transcription factor activity, and this activity-dependent transcription can function in concert with developmentally-programmed plasticity (Kania et al., 2000; Polleux et al., 2007; Barbosa et al., 2008; Lai et al., 2008; Boulanger et al., 2010; de la Torre-Ubieta and Bonni, 2011). Below, I will present examples of well-characterized transcriptional pathways that regulate synaptic remodeling.

Activity-dependent gene expression in *Aplysia*

Long-term memory depends on the upregulation of protein synthesis by synaptic activity. As summarized in the previous section, a local rise in cAMP levels at synapses enhances synaptic activity in the short term by promoting neurotransmitter release. However, cAMP also functions in long term plasticity (termed long-term facilitation, LTF) by regulating gene expression. Persistent activation of PKA by cAMP recruits mitogen-activated protein kinase (MAPK) to the synapse. Both PKA and MAPK then translocate to the nucleus, where they activate transcription of a specific suite of genes. These co-regulated genes are activated by the cAMP response element protein CREB-1 through a CREB

binding enhancer site. These “immediate response” genes then trigger a transcriptional cascade that activates additional downstream genes to strengthen synaptic connections (Kaang et al., 1993; Martin et al., 1997; Bartsch et al., 1998). Net effects include increased size and number of active zones as well as enhancement of the synaptic vesicle pool (Bailey and Kandel, 2008).

Intriguingly, this mechanism can also strengthen a specific synapse by selective transport of mRNA to the target synapse for local protein synthesis. This process offers a solution to the long-standing conundrum of how a global increase in transcription can strengthen a single synapse (Steward, 1997; Kandel, 2001). Another key to understanding local synapse strengthening is the evidence that persistent PKA activation results in the transcription of a deubiquitinating (DUB) enzyme that can recycle ubiquitin and promote degradation of existing synaptic proteins (Hegde et al., 1997; Bingol and Sheng, 2011). Given the role of spatially-localized E3-ligase function via SYG-1/SYG-2 interactions in *C. elegans* (**Figure 1.5**), the transcriptional activation of this DUB in *Aplysia* suggests another connection between transcriptional and spatial mechanisms of plasticity.

Regulation of excitatory synapse plasticity by calcium-dependent transcription

The influx of calcium in dendritic spines, as described earlier, is capable of altering synaptic efficacy, but it can also induce changes in gene transcription. Interestingly, differential gene expression can be induced based on the way

calcium enters the cell. For instance, transcription of brain-derived neurotrophic factor (BDNF) is greatly increased when intracellular calcium rises via VGCCs (voltage gated calcium channels), but less so when calcium enters via NMDA receptors, despite the fact that both channels cause comparable calcium spikes (Bading et al., 1993; Greer and Greenberg, 2008). Although this mechanism is not understood, it is possible that the method of calcium entry results in different spatial pools of calcium and activation of different effectors such as calcium/calmodulin-dependent protein kinases (*i.e.* CaMKII CaMKI, CaMKIV), MAP kinases, and the phosphatase calcineurin (**Figure 1.6**) (Ginty, 1997; Greer and Greenberg, 2008).

CREB functions as of one the major calcium-activated transcription factors in vertebrate neurons. CREB activation induces expression of *bdnf* (*brain-derived neurotrophic factor*), *c-fos*, and other genes that induce plasticity (Ho et al., 2011). Activation of CREB generally occurs via phosphorylation by calcium/calmodulin-dependent protein kinases and results in an increase in synapse number (**Figure 1.6A**). In contrast, another important transcriptional regulator of plasticity, MEF2 (myocyte enhancer factor 2), is activated by calcineurin-dependent dephosphorylation and reduces excitatory synapse number (**Figure 1.6B**) (Flavell et al., 2006). This MEF2-dependent effect is mediated by downstream genes, including a synaptic RasGAP (*synGAP*) and activity-regulated cytoskeletal-associated protein (*arc*) (Flavell et al., 2006; Flavell et al., 2008). synGAP and Arc both negatively regulate synapse development by inhibiting Ras, which in turn results in internalization of

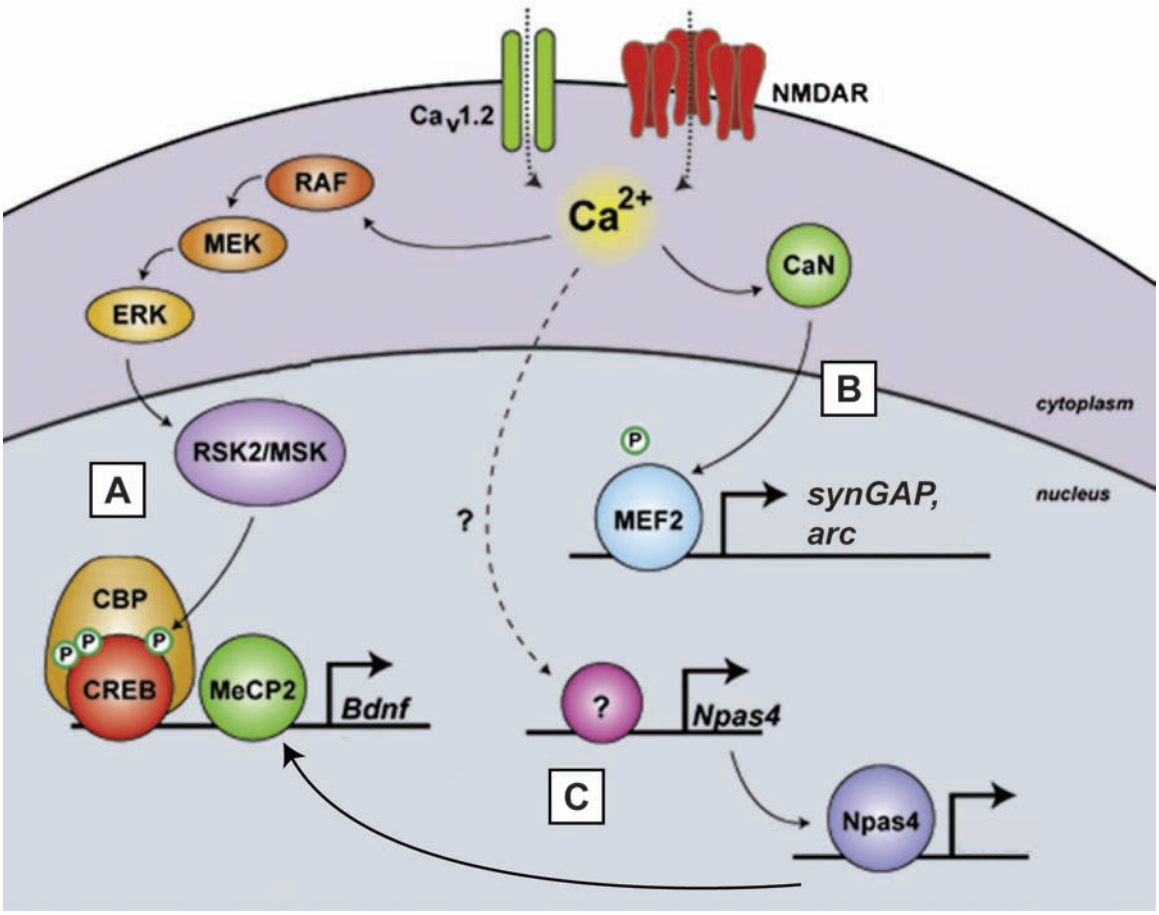

Figure 1.6. Components of activity-dependent gene expression pathways. Influx of calcium via glutamate receptors (NMDAR) and VGCCs ($Ca_v1.2$ shown in figure) cause activation of transcriptional pathways based on different calcium signaling effectors. **(A)** MAP kinase signaling (RAF, MEK, ERK in figure) cause activation of CREB and transcription of *bdnf*. **(B)** MEF2 activation by calcineurin causes transcription of *synGAP* and *arc*. **(C)** Npas4 transcription is activated by calcium influx, though the effector is not clear. Npas4 then activates the transcription of *bdnf* and other LTP effectors. Adapted from Greer and Greenberg, 2008.

glutamate receptors (Vazquez et al., 2004; Shepherd and Bear, 2011). Additional candidate MEF2 targets have been revealed by mRNA profiling studies, in which MEF2 was mis-expressed (gain-of-function or knockdown) to identify transcripts with altered expression. This study revealed over one hundred genes with potential roles in synaptic maturation and destabilization (including *arc*). The roles of individual genes from this list remain to be validated (Flavell et al., 2008). Together, the CREB and MEF2 activity-dependent transcriptional pathways demonstrate that changes in gene expression can promote or inhibit synaptogenesis.

Activity-dependent transcription mediates GABAergic synapse development

Although the regulation of excitatory synapse number and function by calcium-dependent transcription has been well-characterized, less is known about the activity-dependent regulation of inhibitory GABAergic synapses. The recent discovery that the bHLH-PAS family transcription factor controls GABAergic synaptic assembly in the mouse brain offers a useful opportunity to define a transcriptional mechanism for activity-dependent regulation of inhibitory synaptic assembly. Npas4 was identified in a microarray screen for genes that are transcribed in mouse cortical neurons in response to excitatory stimulation (**Figure 1.6C**) (Shamloo et al., 2006; Lin et al., 2008). When Npas4 activity is knocked down, GABAergic synapse number is reduced but excitatory synapses are not affected. Among the activity-dependent transcription factors, Npas4

seems to be unique in that it is activated by VGCC, NMDA and AMPA calcium transients, but not forskolin (which activates PKA) or growth factors that drive expression of other activity-dependent transcription factors. A microarray profiling experiment to identify Npas4 target genes uncovered the neurotrophin *bdnf*, a known regulator of synaptic plasticity. RNAi knockdown of BDNF confirmed its role in Npas4-dependent regulation of inhibitory synaptic assembly. This experiment also suggested that additional Npas4-regulated transcripts identified in the microarray experiment are also likely to contribute to this Npas4 function. These genes include additional transcription factors, ion channels, G-protein signaling components, and trafficking and endocytosis factors. The validation of these genes, as well as further investigation into the mechanism of Npas4 activation, will help guide our understanding of how inhibitory synapses are modified by activity-dependent transcription (Lin et al., 2008).

Opposing nuclear hormone receptors regulate *Drosophila* mushroom body remodeling during development

As described above, synaptic remodeling can be executed by transcriptional programs that depend on temporal changes in neuronal activity. Below I describe two examples of plasticity that depend on transcriptional pathways regulated by developmental cues.

The mushroom bodies in *Drosophila,* which function in olfactory learning and memory, are comprised of two vertical (α and α') and three medial (β, β', and γ) lobes. Initially, the larval-born γ neurons extend processes into both dorsal and

medial lobes. As the fly undergoes later metamorphic stages, the larval-specific dorsal neurites are selectively pruned such that in the adult stage, γ neurons only have processes in the medial lobe. The γ neuron remodeling program is coordinated with other developmental events by ecdysone, a steroid hormone that cues molting. In mushroom bodies, a heterodimeric nuclear receptor formed by the interaction of the ecdysone receptor (ECR) and a protein encoded by *ultraspiracle* (USP) regulates transcription in response to ecdysone to promote γ neuron pruning (Technau and Heisenberg, 1982; Lee et al., 2000; Williams and Truman, 2005).

A recent study has identified two additional nuclear hormone receptors that regulate ECR activity. In loss-of-function mutants for the transcription factor *ftz-f1*, γ neurons retain their larval branching patterns into the adult stage; overexpression of a similar nuclear hormone receptor, *Hr39*, results in a similar phenotype. Epistasis experiments revealed that both *ftz-f1* and *Hr39* regulate ECR-B1 in an antagonistic fashion. Whereas *Hr39* normally prevents pruning, *ftz-f1* promotes pruning in two ways: first, by transcriptionally preventing *Hr39* expression, and second, by promoting expressing of ECR-B1. The impact of this pruning event on learning and memory has not yet been studied; however, *Hr39*-overexpressing animals are viable and present an opportunity to uncover the behavioral consequence of mushroom body overgrowth as well as the downstream effectors of this transcriptional network (Boulanger et al., 2010).

A transcriptional program regulates remodeling in *C. elegans*

The *C. elegans* motor circuit undergoes a major expansion at the end of the first larval stage (the L1-L2 transition) to yield nineteen GABAergic motor neurons. As in other metamorphic animals, this expansion requires significant remodeling of the existing embryonic circuit to accommodate the additional neurons (White et al., 1976; Von Stetina et al., 2005). A mutation that disables the activity of a nuclear hormone receptor, *unc-55*, dysregulates remodeling in the GABAergic motor circuit and suggests that this key event is regulated by a transcriptional mechanism. Here, I introduce the *C. elegans* motor circuit, the larval reorganization of the GABAergic motor circuit during synaptic remodeling, and the transcriptional program that we have exploited to identify key components of this pathway.

Structure and function of the GABAergic motor circuit in *C. elegans*

Six GABAergic ventral nerve cord motor neurons are generated in the *C. elegans* embryo. Thirteen additional GABAergic motor neurons are added to the circuit during early larval development (**Figure 1.7A**). The cell soma for each of these “D-class” GABAergic motor neurons extends an anteriorly-directed ventral process with a circumferential commissure that projects a posteriorly-directed process in the dorsal nerve cord. D-class neurons form inhibitory synapses with dorsal and ventral body wall muscle cells (Schuske et al., 2004). Like mammalian GABAergic interneurons, D-class motor neurons are specified by the homeodomain-containing transcription factor *unc-30/Pitx2*, which drives expression of glutamic acid decarboxylase (*unc-25/GAD*) to synthesize GABA

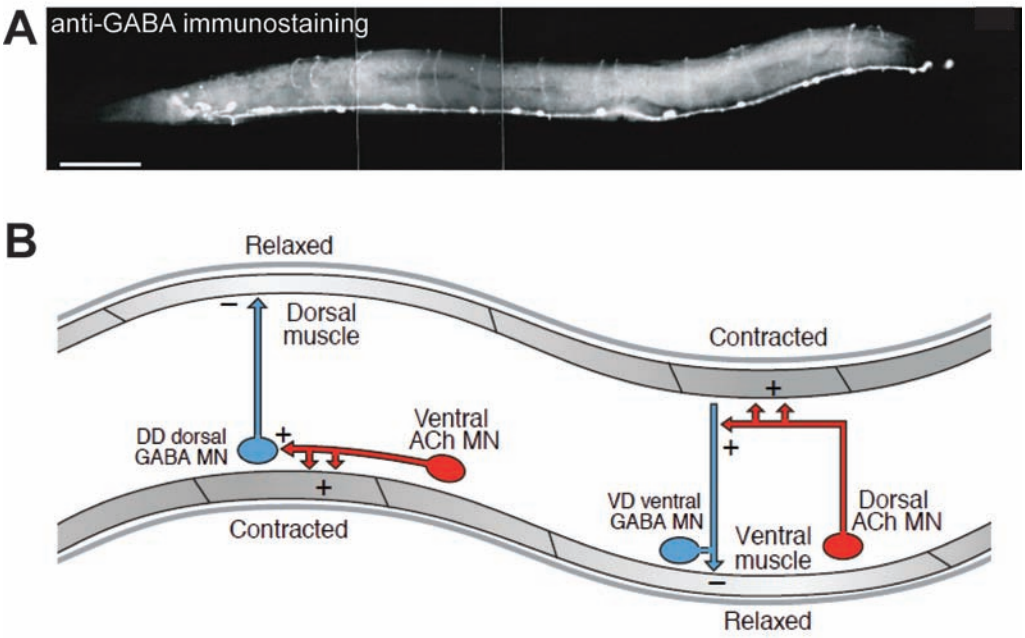

Figure 1.7. The adult GABAergic motor circuit. In both panels, anterior is to the right and dorsal is up. **(A)** anti-GABA immunostaining of an adult wild-type *C. elegans* hermaphrodite. There are 26 neurons that stain for GABA; nineteen of these are located in the ventral nerve cord and comprise the GABAergic motor circuit. Scale bar, 100 um. **(B)** Cross-inhibition in the motor circuit promotes coordinated locomotion. DD and VD GABAergic motor neurons (blue) synapse to the dorsal and ventral body muscles, respectively. Cholinergic motor neurons (red) send inputs to the ventral and dorsal body muscles, as well as to the GABA motor neurons. Release of acetylcholine leads to contraction of the body wall muscle on one side and stimulates GABA release onto muscles on the opposite side. This stimulation and contralateral inhibition causes the body to bend and leads to coordinated locomotion. Adapted from Schuske et. al. 2004

and the GABA synaptic vesicle transporter (*unc-47/VGAT*) which loads GABA into synaptic vesicles (Eastman et al., 1999; Westmoreland et al., 2001; Martin et al., 2002). Loss of *unc-30* abrogates anti-GABA staining and causes a movement phenotype consistent with the loss of functional GABAergic inhibitory NMJs (McIntire et al., 1993).

The characteristic architecture of the GABAergic motor circuit has suggested a model to explain the role of GABAergic signaling in locomotion. Dorsal D (DD) motor neurons provide output to dorsal muscle, whereas Ventral D (VD) motor neurons exhibit only ventral NMJs. Thus, DD and VD motor neurons establish separate inhibitory synapses on opposing muscle groups. When a cholinergic motor neuron stimulates muscle contraction and a resultant body-bend on one side of the animal, muscles on the opposite side are inhibited by GABA signaling (Schuske et al., 2004). This “cross-inhibition” model of *C. elegans* movement presumes dyadic cholinergic synapses on both muscle and D-class processes (**Figure 1.7B**). In this configuration, GABA motor neurons are activated on one side adjacent to the contracting muscle to then release an inhibitory signal that relaxes muscle on the opposite side. This model is consistent with the “shrinker” phenotype of GABA-deficient animals in which both dorsal and ventral muscles contract simultaneously with cholinergic stimulation (White et al., 1976; Schuske et al., 2004; Von Stetina et al., 2005). It is not clear, however, how GABAergic motor neurons are stimulated by cholinergic signals because the postsynaptic components that would mediate this response in GABAergic motor neurons have never been identified or visualized *in vivo*.

Development and remodeling in the GABAergic motor circuit

As noted above, GABAergic motor neuron differentiation occurs in two waves. First, six DD motor neurons are born in the embryo, and later, thirteen VD motor neurons are added during a postembryonic expansion of the motor circuit at the L1-L2 transition. In the embryo, DD motor neurons initially establish NMJs with ventral body wall muscle (**Figure 1.8A**). This synaptic arrangement can be observed by expression of fluorescently-tagged synaptobrevin (*e.g.* SNB-1::GFP), which labels synaptic vesicles, in GABAergic motor neurons. The resultant bright GFP puncta, corresponding to clusters of synaptic vesicles, are observed exclusively on the ventral side of the newly hatched L1 larvae (**Figure 1.8B**). SNB-1::GFP is also observed in cell bodies of DD motor neurons due to overexpression of the transgene.

DD motor neurons undergo a stereotypical change in this synaptic pattern during the L1-L2 larval transition (**Figure 1.8C-D**, dorsal puncta). During this period, DD ventral NMJs are removed and then re-established on the dorsal side. This change in synaptic location is accomplished with no evident alteration in DD neurite morphology (White et al., 1978). As noted in an earlier section, a recent study demonstrated that the synaptic trafficking regulators CYY-1 and CDK-5 function in this process; CYY-1 removes ventral presynaptic proteins, and CDK-5 facilitates trafficking to nascent dorsal synapses (Park et al., 2011). Additionally, the timing of the remodeling event depends on the heterochronic gene, *lin-14*. LIN-14 protein is localized to the nucleus and functions in a variety of cell types to promote L1-stage-specific features; in the case of DD motor neurons, LIN-14

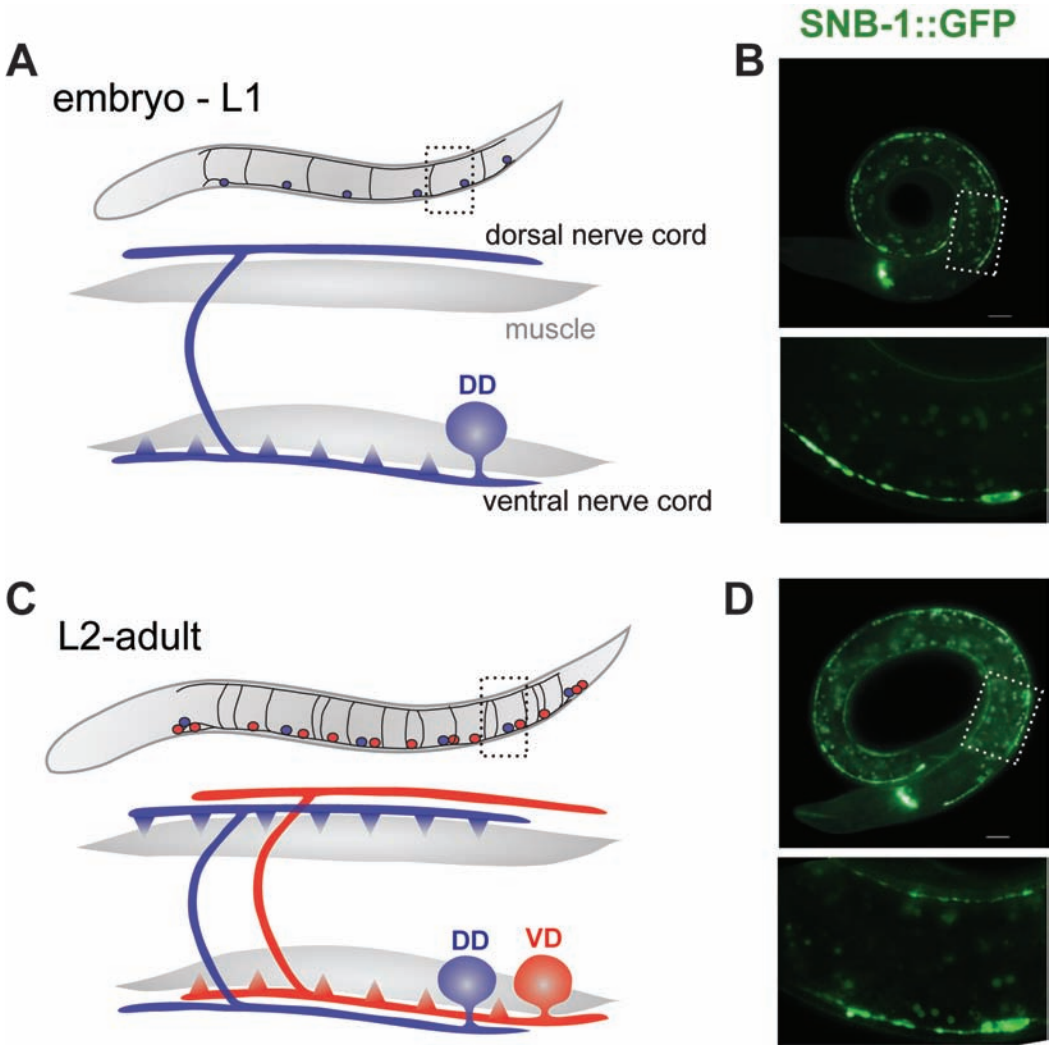

Figure 1.8. DD motor neurons undergo a stereotyped synaptic remodeling event during development. In all panels, anterior is to the right and dorsal is up. **(A)** Embryonic DD motor neurons (blue) extend an anterior ventral process and commissure to the dorsal nerve cord. NMJs are established with ventral muscles and are maintained throughout most of the first larval stage (L1). **(B)** GABAergic NMJs can be labeled with SNB-1::GFP. In the L1 animal, NMJs are formed by DDs exclusively within the ventral neurite. **(C)** Toward the end of the L1 larval period, ventral DD motor neuron NMJs are removed and new NMJs are assembled in the dorsal DD process. Postembryonic VD motor neurons (red) are born during this stage and adopt ventral NMJs. **(D)** Synaptic arrangement of L2 GABAergic motor neurons marked with SNB-1::GFP. Note small puncta on both the dorsal and ventral sides of the animal (fluorescent granules in the middle of the animal represent gut autofluorescence, inset panels have been enhanced to show synapses).

maintains the DD L1 synaptic pattern until the L1-L2 transition. In *lin-14* mutants, DDs remodel precociously. The mechanism by which LIN-14 prevents precocious remodeling is unknown (Hallam and Jin, 1998).

One interesting facet of the DD remodeling program is the ability to correct polarity or synaptogenic defects in immature DD motor neurons. In *syd-1* and *sad-1* mutants, axonal SNB-1::GFP-labeled vesicles distribute evenly in dorsal and ventral DD neurites in the L1 stage instead of the exclusively ventral location of SVs in wild-type DD motor neurons. Interestingly, however, remodeled DD motor neurons do not show these defects in *syd-1* or *sad-1* mutants, but display synapses of normal morphology exclusively localized to the dorsal nerve cord (Hallam et al., 2002; Hung et al., 2007; Kim et al., 2010) These results indicate that SYD-1 and SAD-1 are dispensable for the establishment of correctly located synapses in mature DD motor neurons and therefore indicate that an alternative set of factors must govern the polarized placement of synapses during the remodeling event.

As mentioned above, VD motor neurons are born at the end of the L1 stage and normally do not remodel (Walthall and Plunkett, 1995; Zhou and Walthall, 1998; Shan et al., 2005). Ventral VD synapses are established during the L2 larval stage and persist in the adult in this location (**Figure 1.8C-D**). This exclusively ventral pattern of VD synapses is disrupted in *syd-1* and *sad-1* mutants which show dorsal as well as ventral clusters of presynaptic markers (*e.g.* SNB-1::GFP) in the VD neurites (Hallam et al., 2002; Hung et al., 2007).

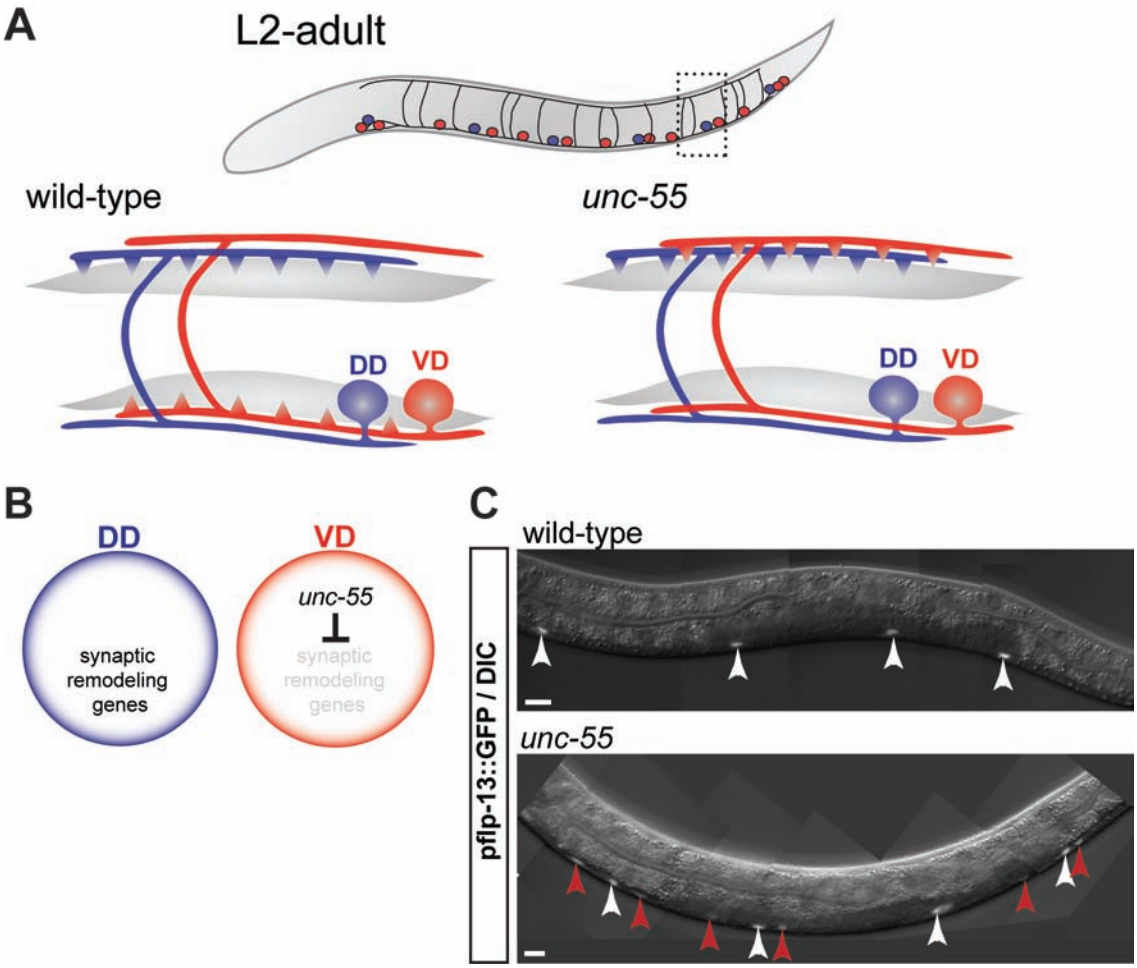

Figure 1.9 UNC-55 transcriptionally prevents synaptic remodeling of VD motor neurons. In all panels, anterior is to the right and dorsal is up. **(A)** Wild-type VD motor neurons form ventral NMJs (left) but VD motor neurons remodel ectopically in *unc-55* mutants and adopt dorsal NMJs (right). **(B)** UNC-55 is selectively expressed in VD motor neurons to prevent ectopic synaptic remodeling. **(C)** *flp-13* is repressed by UNC-55 in VD motor neurons. In wild-type (top), *pflp-13::GFP* is expressed in DD motor neurons (white arrowheads), but GFP is de-repressed in VDs in *unc-55* mutants (bottom panel, red arrowheads).

In *unc-55/COUP-TF* mutants, VD ventral synapses are removed and established instead in the dorsal nerve cord, similar to the synaptic pattern observed in DD motor neurons (**Figure 1.9A**). UNC-55 is selectively expressed in VD motor neurons in the ventral nerve cord and thus, UNC-55 is predicted to function cell-autonomously to prevent synaptic remodeling (**Figure 1.9B**).

The Walthall laboratory has identified one target of *unc-55,* the neuropeptide FLP-13. In wild-type animals, *flp-13* expression (observed with *pflp-13::GFP*) is restricted to DD motor neurons. In *unc-55* mutants, *pflp-13::GFP* is expressed in both DD and VD motor neurons (**Figure 1.9C**), indicating de-repression of the *flp-13* promoter in the absence of UNC-55. Furthermore, removal of a canonical COUP-TF binding site in the transgenic *flp-13* promoter resulted in GFP expression in wild-type VD motor neurons that contain functional UNC-55. These results predict that UNC-55 normally functions as a transcriptional repressor in VD motor neurons (Shan et al., 2005). However, FLP-13 does not appear to be required for execution of the synaptic remodeling program observed in *unc-55* mutant VD motor neurons (W. Walthall, personal communication).

Because UNC-55 functions as a repressor in VD motor neurons, and loss of *unc-55* results in VD remodeling, *unc-55* is proposed to function as a developmental switch that prevents VD motor neurons from activating a remodeling program that is otherwise exclusively active in DD motor neurons (**Figure 1.9B)**. This model is consistent with the finding that ectopic expression of UNC-55 in DD motor neurons blocks the relocation of DD synapses to the dorsal

nerve cord, similar to the synaptic pattern of wild-type VD motor neurons (Shan et al., 2005). Together, these results suggest that *unc-55* targets function in a transcriptional program that remodels GABAergic motor neurons. Thus, we chose to identify these target genes that are de-repressed in *unc-55* VD motor neurons and examine these candidate genes for roles in synaptic remodeling.

In the following chapters, I describe our characterization of the role of *unc-55* in synaptic remodeling and the strategy that we used to identify its downstream targets. Based on the high conservation between *C. elegans* and mammals in factors required for neuronal polarity, synaptogenesis, and remodeling, we expect that the suite of downstream genes that we have uncovered should provide a rich resource for future studies of the mechanism of synaptic plasticity.

CHAPTER II

THE UNC-55/COUP-TF TRANSCRIPTION FACTOR BLOCKS A SYNAPTIC REMODELING PROGRAM IN GABAERGIC MOTOR NEURONS

Introduction

The importance of transcription factors in synaptic remodeling is well-established, but the downstream targets that carry out the remodeling program are less understood (Barbosa et al., 2008; Flavell and Greenberg, 2008; Tian et al., 2010). In *C. elegans*, the single COUP-TF orphan nuclear receptor has been shown to control synaptic remodeling in the GABAergic motor neuron circuit (Zhou and Walthall, 1998). During normal development, embryonically-born Dorsal D (DD) motor neurons initially establish synaptic output to ventral muscles. After hatching in the L1 larval stage, ventral DD synapses are re-localized to the dorsal nerve cord. This rearrangement occurs within the intact neuron and without any gross changes in neurite morphology. VD motor neurons, which arise at the end of the L1 larval stage, innervate ventral muscles (White et al., 1978). The isolation of a mutant in the *unc-55* locus revealed that the COUP-TF transcription factor is expressed in VD motor neurons to prevent the adoption of dorsal synaptic outputs (Zhou and Walthall, 1998).

Members of the COUP-TF family comprise one of the largest orphan nuclear hormone receptor subgroups. Although some evidence indicates that retinoic acid interacts with the ligand-binding domain of COUP-TF proteins, the

ligands that regulate this family *in vivo* are unclear (Pereira et al., 2000; Kruse et al., 2008). In addition to determining a variety of tissue types during development of other model systems (*i.e.* adipocytes, kidney), COUP-TF is an important regulator of neurodifferentiation and migration (Pereira et al., 2000; Park et al., 2003). In the mammalian forebrain, COUP-TF is expressed in GABAergic interneurons, where it induces early-born cell division and directed cell migration from the telencephalon to the cortex during embryogenesis (Tripodi et al., 2004; Naka et al., 2008). Thalamocortical projections from serotonergic sensory areas in the cortex rely upon COUP-TF expression for proper neuron differentiation and targeting (Zhou et al., 1999; Armentano et al., 2007). Cerebellar neuron expansion and patterning also depends upon COUP-TF (Kim et al., 2009). Although some COUP-TF targets have been identified, the specific targets that execute cell division, differentiation, migration, and axonal targeting functions in the above cases are unknown (Pereira et al., 2000; Montemayor et al., 2010).

The COUP-TF homologue in *Drosophila, seven-up* (*svp*), specifies photoreceptor subtype by regulating a transcriptional cascade within the developing eye. The neuroblasts that ultimately comprise the compound eye are temporally defined by early-born cells that express the transcription factors *hunchback* and *Kruppel*, and later-born cells that express only *Kruppel* or neither of these transcription factors. *seven-up* functions to repress *hunchback* expression to prevent an expansion of early-born neuroblasts at the expense of late-born neuroblasts (Mlodzik et al., 1990; Hiromi et al., 1993; Kruse et al., 2008). Unpublished results suggest that *hbl-1/hunchback* in *C. elegans* is also

regulated by *unc-55/COUP-TF* (K. Thompson-Peer and J. Kaplan, personal communication).

Because of the conserved role of *COUP-TF* in neurodevelopment in other organisms, we hypothesized that we could use the ectopic remodeling phenotype in *unc-55* mutants to identify conserved synaptic remodeling genes (as detailed in subsequent chapters). However, we first required a set of molecular tools that could be used to monitor the synaptic remodeling program that is regulated by *unc-55*.

Author Contributions

Identification of the lesions in the *unc-55* locus was undertaken by the Walthall laboratory at Georgia State University. Kathie Watkins in the Miller laboratory assisted in construction of the *unc-55(gf)* strain by microinjecting the pSA6 plasmid into *dpy-20* mutants. All other experiments in this chapter were performed by Sarah Petersen.

Methods

Strains and genetics: Nematode strains were maintained at 20-25°C with standard culture techniques (Brenner, 1974). All animals used in this study were hermaphrodites. Animals were genotyped for the presence of the *e1170* lesion with primers e1170_for (5’ CCC AAG AAG AAA AGA GAG GT 3’) and e1170_rev (5’ TAA GGA CTA CAC GGA TCC TG 3’). These primers yield an 854-bp product that may be sequenced via Sanger sequencing to identify *e1170*.

Strain list:

note: *unc-119*(+) refers to *unc-119*-rescuing minigene from MM051 (Maduro and Pilgrim, 1995) (see details of strain construction)

CZ333 *juIs1[punc-25::SNB-1::GFP; lin-15+]*

CB402 *unc-55(e402)* >10x outcrossed

CB1170 *unc-55(e1170)* >10x outcrossed

VC1736 *unc-55;F55D12.6(gk818)*

NC1851 *unc-55(e1170); juIs1[punc-25::SNB-1::GFP; lin-15+]*

EG1653 *oxIs22 [punc-49::UNC-49::GFP; lin-15(+)]*

NC2122 *unc-55; oxIs22 [punc-49::UNC-49::GFP; lin-15(+)]*

ZM54 *hpIs3[punc-25::SYD-2::GFP; lin-15(+)]*

NC1849 *unc-55(e1170); hpIs3[punc-25::SYD-2::GFP; lin-15(+)]*

NC1551 *dpy-20; wdEx603(pC04G2.1::unc-55a::gfp; dpy-20+)*

NC1639 *wdIs49(pttr-39::unc-55a::gfp; dpy-20+)* III

NC2078 *unc-119; wdIs75[pttr-39::unc-38::GFP; unc-119+]*

NC2167 *unc-38; unc-119; wdIs75[pttr-39::unc-38::GFP; unc-119+]*

NC2191 *unc-38 unc-55; unc-119; wdIs75[pttr-39::unc-38::GFP; unc-119+]*

NC2231 *unc-119; wdEx703[punc-25::DYS-1::YFP; unc-119+]*

NC2267 *unc-119; wdEx729[punc-25::F35D2.3::YFP; unc-119+]*

Microscopy and synapse scoring: SNB-1::GFP assays were performed with the transgene *juIs1[punc-25::SNB-1::GFP; lin-15+]* (Hallam and Jin, 1998), SYD-2::GFP assays used *hpIs3[punc-25::SYD-2::GFP; lin-15+]* (Yeh et al., 2005),

and UNC-49::GFP assays used *oxIs22 [punc-49::UNC-49::GFP; lin-15+]* (Bamber et al., 1999). Animals were anesthetized with 0.1% tricaine/tetramisole, mounted on a 2% agarose pad, and imaged with a Zeiss Axiovert microscope using Metamorph software or a Leica TCS-SP5 confocal using LAS-AF software.

Movement assays: Animals were first tapped on the tail to ensure that they were capable of forward locomotion, then tapped on the head to assess ability to execute backward locomotion. Animals were binned into the following categories: "severe Unc" (coil ventrally immediately upon tapping), "moderate Unc" (coil ventrally while attempting backward locomotion), and "wild-type" (sustain backward locomotion with at least two body bends). To present the data in **Figure 2.3**, all "severe" and "moderate" Unc worms were grouped into a single "uncoordinated" category.

Construction of *unc-55(gf)* strain

The 891-bp *ttr39* promoter was cloned into a pGEM vector containing *unc-55a* cDNA (kindly provided by Bill Walthall) to create pSA3. The *pttr-39::unc-55a* cassette was then cloned into pPD117.01 in-frame with GFP to create pSA6. This construct (25 ng) was co-injected with *dpy-20* rescuing plasmid (25 ng) into *dpy-20(e1282)* animals to yield NC1551. Gamma irradiation of the transgenic line and outcrossing *dpy-20* yielded NC1639 containing *wdIs49[pttr-39::unc-55a::gfp; dpy-20+]* III.

Construction of *unc-38::GFP* strain

The pJL29 plasmid with genomic *unc-38* containing GFP inserted between the M3 and M4 transmembrane domains was kindly provided by Jean-Louis Bessareau (Rowland et al., 2006). The UNC-38::GFP construct was PCR-amplified and cloned into pCR2.1 to yield pSA27, then cloned into a derivative of *pitr-1::DYS-1::YFP* (kindly provided by Kang Shen) (Poon et al., 2008) with the *pitr-1* promoter replaced with the *pttr-39* promoter (Earls et al., 2010) to yield pSA30. The *unc-119* minigene [originally from MM051 (Maduro and Pilgrim, 1995)] was then cloned into the backbone to yield pSA33. This construct was linearized and transformed into *unc-119* worms via microparticle bombardment (Praitis et al., 2001) to yield a spontaneous integrated transgene, *wdIs75*. However, GFP is not visible via light microscopy with this transgene in either wild-type or *unc-38* mutant backgrounds. Consequently, we immunostained with mouse anti-XFP antibodies (Roche) and goat anti-mouse IgG Cy3 (each 1:1000 dilution) to detect expression of UNC-38::GFP (Finney and Ruvkun, 1990). Animals were co-stained with DAPI, mounted on a 2% agarose pad, and imaged on a Zeiss Axioplan compound microscope.

Construction of *DYS-1::YFP* and *F35D2.3::YFP* strains

The *pitr-1::DYS-1::YFP* and *pitr-1::F35D2.3::YFP* plasmids were kindly provided by Kang Shen (Poon et al., 2008). The *pitr-1* promoter was replaced with *punc-25* (Earls et al., 2010) to yield pSA57 (DYS-1) and pSA58 (F35D2.1). The *unc-119* minigene [originally from MM051 (Maduro and Pilgrim, 1995)] was then

cloned into the backbone to yield pSA59 (DYS-1) and pSA60 (F35D2.1). Both constructs were linearized and transformed into *unc-119* worms via microparticle bombardment (Praitis et al., 2001) to yield *wdEx703[punc-25::DYS-1::YFP; unc-119+]* and *wdEx729[punc-25::F35D2.3::YFP; unc-119+]* in NC2231 and NC2267, respectively.

Results

The *e1170* allele is a genetic null allele of *unc-55*

The *unc-55* locus encodes a nuclear hormone receptor family member with a DNA binding domain (DBD) and a downstream ligand binding domain (LBD) with a canonical ligand binding signature (**Figure 2.1**). The DBD contains two zinc fingers, termed P-box (proximal) and D-box (distal), for binding the canonical TGACCT half-site recognition sequence within the promoter of target genes, typically called the hormone response element. The LBD of *unc-55* contains a signature motif typically used for dimerization and binding of the ligand to activate the transcriptional response function of nuclear hormone receptors (Renaud and Moras, 2000). However, *unc-55* and the COUP-TF family of transcription factors are classified as orphan nuclear hormone receptors, with no confirmed ligand for the ligand-binding domain (Pereira et al., 2000), although retinoic acid is a candidate (Kruse et al., 2008)

Two *unc-55* point-mutation alleles, *e402* and *e1170*, were isolated in a screen by Sydney Brenner (Brenner, 1974) (**Figure 2.1**). For our studies, we have primarily used the *e1170* allele. The *e1170* allele contains an insertion

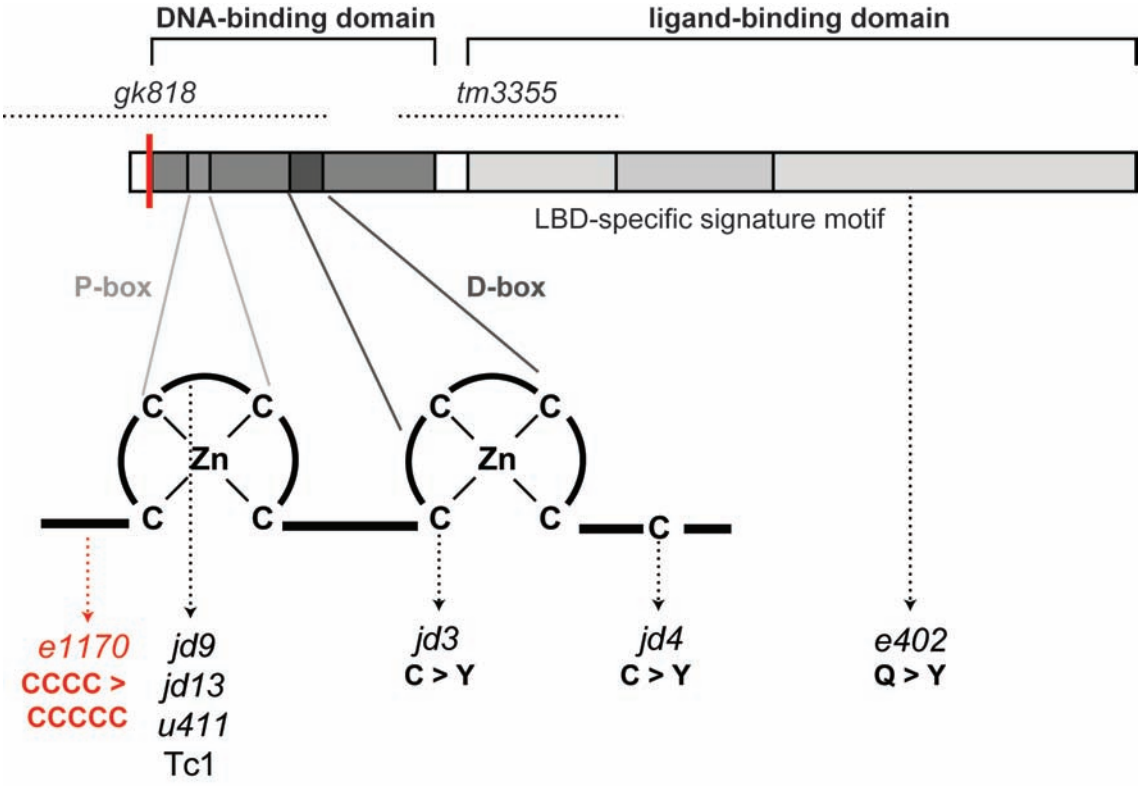

Figure 2.1. Genetic features and mutations in UNC-55. The *unc-55* locus encodes a nuclear hormone receptor with a DNA-binding domain, containing two zinc fingers termed P-box and D-box, and a ligand-binding domain. Point mutations in the *unc-55* locus, their location, and the nucleotide change are denoted with dotted arrows. The *e1170* frameshift mutation is marked in red. Dotted lines for *gk818* and *tm3355* denote deleted regions.

(CCCC → CCCCC) in the DNA binding domain which results in premature termination of the protein at amino acid 26 due to a nonsense codon. Therefore, the *e1170* allele is presumed to be a genetic null. Much of the literature to date uses *unc-55(e402)*, which was later shown by the Walthall lab to correspond to a Q>Y mutation in the ligand-binding domain of *unc-55*. Interestingly, the phenotypes for *e402* and *e1170* appear indistinguishable, suggesting that *e402* point mutation is in fact a genetic null. However, it is unclear whether this phenotype is the result of inability of the UNC-55 protein to bind its ligand, or if the protein is otherwise inactive due to misfolding.

The *unc-55(gk818)* deletion allele (**Figure 2.1**) was isolated in the Vancouver Gene Knockout Lab, removes the N-terminal region of *unc*-55, as well as a predicted ORF, *F55D12.6*, which is entirely contained within the first intron of the *unc-55* coding region and is predicted to encode a ribosomal protein. Phenotypically, the *gk818* allele appears similar to the *e1170* allele; however, because of the additional knockout of the *F55D12.6* locus, we used the *e1170* allele for further analysis. Additional point mutants have been isolated by the Walthall lab (**Figure 2.1**) in an EMS mutagenesis screen: *jd3* and *jd4,* which each result in the conversion of cysteine to tyrosine in the DNA binding domain. Three alleles, *jd9, jd13,* and *u411*, each contain the same insertion of the Tc1 transposon in the DNA binding domain. In addition, another deletion allele, *tm3355,* was recently isolated by the National BioResource Project-Japan. We have not characterized these additional *unc-55* alleles.

Presynaptic markers SNB-1::GFP and SYD-2::GFP are mislocalized in *unc-55* VD motor neurons

We confirmed the VD output defect in *unc-55* mutants by visualizing GABAergic neuromuscular junctions (NMJs) with the GFP-tagged SNB-1/synaptobrevin marker *juIs1[punc-25::SNB-1::GFP]*, kindly provided by Mike Nonet (**Figure 2.2A-B**) (Hallam and Jin, 1998). As predicted from the model (**Figure 1.9**), dorsal SNB-1::GFP puncta are more abundant in the adult *unc-55* mutant than in wild-type. This phenotype arises from the progressive remodeling of VD motor neurons throughout larval development due to ectopic activation of the UNC-55-regulated remodeling program. In contrast to the brief remodeling period in DD motor neurons (Hallam and Jin, 1998), the number of dorsal GABAergic synapses from VD motor neurons increases from the L2 to the adult (**Figure 2.2C**). Ventral GABAergic synapses are concurrently reduced during this period until the adult stage when few SNB-1::GFP puncta are observed in the ventral nerve cord of *unc-55* animals (**Figure 2.2D**).

To determine if other presynaptic components are similarly relocated, we used the GFP-tagged SYD-2/Liprin-α to mark the VD presynaptic membrane domain (**Figure 2.2E**). At the L2 stage, the number of SYD-2::GFP ventral puncta in *unc-55* animals is comparable to wild-type but progressively decline during later larval stages in a pattern mimicking that of SNB-1::GFP (**Figure 2.2F**). This result is indicative of the relocation of the entire presynaptic apparatus in *unc-55* mutant VD motor neurons. The progressive appearance of a

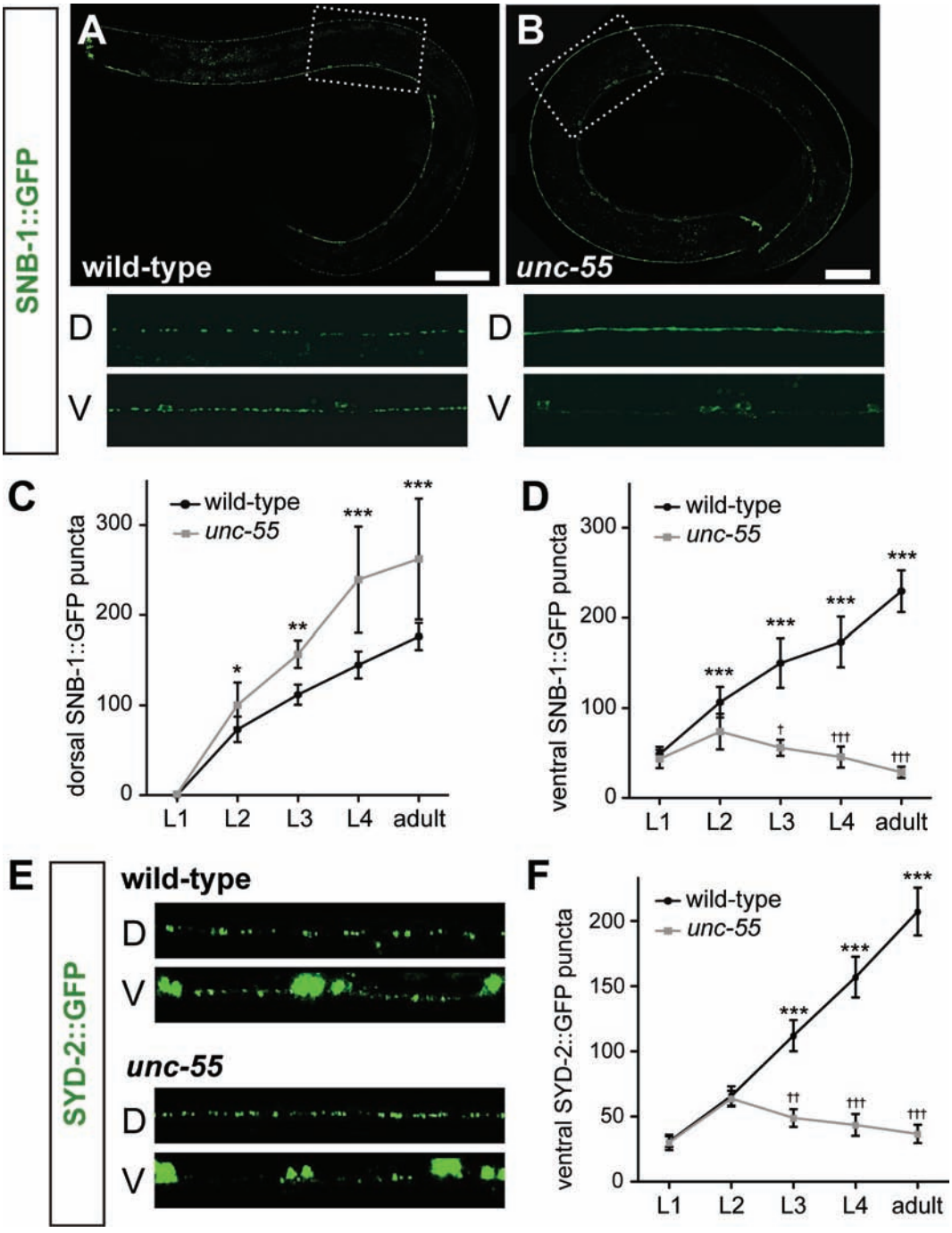
SNB-1::GFP
A
B
wild-type
unc-55
D
V
D
V
C
wild-type
unc-55
dorsal SNB-1::GFP puncta
300
200
100
0
L1
L2
L3
L4
adult
*
**
***
***
D
wild-type
unc-55
ventral SNB-1::GFP puncta
300
200
100
0
L1
L2
L3
L4
adult
***
***
***
***
†
†††
†††
E
SYD-2::GFP
wild-type
D
V
unc-55
D
V
F
wild-type
unc-55
ventral SYD-2::GFP puncta
200
150
100
50
0
L1
L2
L3
L4
adult
***
***
***
***
††
†††
†††

Figure 2.2. Remodeling of presynaptic components SNB-1 and SYD-2 during development of *unc-55* mutants. (**A-D**) The synaptic vesicle marker, SNB-1::GFP, marks GABAergic motor neuron NMJs. Scale bar, 20 μm, inset panels, 50 μm. (**A**) SNB-1::GFP puncta are visible in both dorsal (DD motor neurons) and ventral (VD motor neurons) adult nerve cords. (**B**) In *unc-55* mutants, ventral SNB-1::GFP puncta are depleted whereas the number of dorsal SNB-1::GFP puncta increases. (**C-D**) Quantification of SNB-1::GFP puncta in dorsal and ventral nerve cords throughout development. $N \geq 10$ for each genotype at each stage. Error bars indicate standard deviation. * $p < 0.05$, ** $p < 0.01$, *** $p < 0.001$ for wild-type vs. *unc-55* in 2-way ANOVA with Bonferroni's Multiple Comparison Test. (**C**) Dorsal SNB-1::GFP puncta are more numerous in *unc-55* mutants than wild-type due to ectopic remodeling of VD motor neurons. (**D**) Ventral SNB-1::GFP puncta are more numerous in wild-type than in *unc-55* mutants. Ventral SNB-1::GFP puncta are significantly depleted during development in *unc-55* mutants indicating that VD motor neurons initially establish ventral NMJs in the L2 and then remodel to favor dorsal outputs in the adult. † $p < 0.05$, ††† $p < 0.001$, L2 vs. L3, L4, or YA for 1-way ANOVA with Bonferroni's Multiple Comparison Test. (**E**) The liprin alpha membrane protein, SYD-2::GFP, marks GABAergic motor neuron presynaptic specializations. Panels represent 50 μm length of dorsal (D) or ventral (V) nerve cords. (**F**) Quantification of SYD-2::GFP puncta in the ventral nerve cord throughout development. SYD-2::GFP localization in *unc-55* is indistinguishable from wild-type at the L2 stage, but ventral SYD-2::GFP puncta are depleted as VD motor neurons remodel during development. $N \geq 10$ for each genotype at each stage. Error bars indicate standard deviation. *** $p < 0.001$ for wild-type vs. *unc-55* in 2-way ANOVA with Bonferroni's Multiple Comparison Test, †† $p < 0.01$, ††† $p < 0.001$, L2 vs. L3, L4, or YA for 1-way ANOVA with Bonferroni's Multiple Comparison Test.

movement defect during *unc-55* larval development is also consistent with this model and is described in the following section.

unc-55(e1170) mutants causes a progressive ventral coiling defect

Cholinergic motor neurons form dyadic synapses to excite both muscle and GABAergic motor neurons (Von Stetina et al., 2005), while GABAergic motor neurons form inhibitory NMJs with dorsal and ventral muscle (Driscoll and Kaplan, 1997; Schuske et al., 2004; Von Stetina et al., 2005). This arrangement predicts a cross-inhibitory network (**Figure 2.3A**) in which cholinergic motor neuron stimulation and muscle contraction on one side of the body results in GABA-stimulated relaxation of muscle on the opposite side of the body. This pattern would result in sinusoidal body bends that cause coordinated forward and backward locomotion (**Figure 2.3B**).

Mutations in the *unc-55* locus were originally isolated due to a backward movement phenotype characterized by ventral coiling (**Figure 2.3C)**. This loss of backing ability is due to ectopic remodeling of VD motor neurons, which causes a loss of inhibition on ventral muscle with a concurrent increase of inhibitory GABAergic synapses onto dorsal muscle. As observed in other mutants with genetically ablated GABAergic motor neuron function (*i.e. unc-25, unc-47*), *unc-55* mutants are able to execute forward locomotion. The “foraging” motor circuit in the head likely compensates for the absence of proper GABAergic innervation to body wall muscle during forward locomotion. Thus, the loss of ventral innervation in *unc-55* mutants is more prominent during backward locomotion.

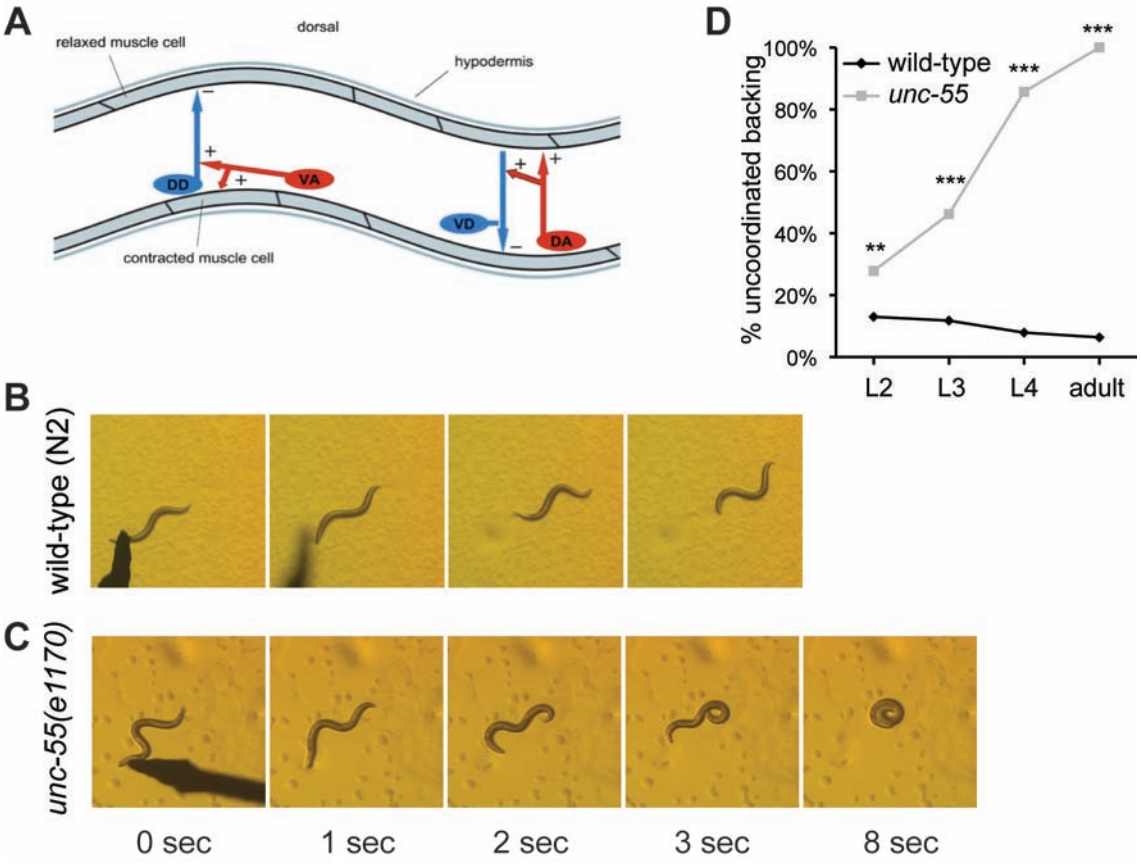

Figure 2.3. Progressive loss of ventral muscle inhibition in *unc-55* mutants leads to ventral coiling. (**A**) Model of cross-inhibition with cholinergic (red) and GABAergic (blue) neurons to innervate body wall muscle (gray). Contralateral stimulation by cholinergic motor neurons and relaxation by GABAergic motor neurons results in coordinated locomotion. This output depends on the prevention of VD synaptic remodeling by UNC-55. Adapted from Schuske et. al., 2004. (**B-C**) Backward locomotion following head tap at t=0 for wild-type (**B**) and *unc-55(e1170)* (**C**) adults. Time is indicated in seconds following head-tap, and panels are oriented with anterior to the left and ventral side down. Note sinusoidal backward locomotion in wild-type and ventral coiling in *unc-55* adult. (**D**) VD motor neurons initially form ventral NMJs in *unc-55* as indicated by movement similar to wild-type at younger stages. A progressive increase in uncoordinated movement as the animal ages is indicative of ongoing VD motor neurons remodeling. ** $p < 0.01$, *** $p < 0.001$ for wild-type vs. *unc-55*, Fisher's Exact Test, $n \geq 100$ for each genotype at each stage.

The initial ventral enrichment and then subsequent elimination of SNB-1::GFP and SYD-2::GFP in the *unc-55* mutant suggests that VD motor neurons establish synapses in L2 larva, but that these ventral NMJs are gradually removed as development proceeds (*e.g.*, 74±20 SNB-1::GFP puncta in *unc-55* L2 vs. 29±6 in *unc-55* adult). Because ventral output from VD motor neurons is required for normal locomotion, this model predicts that coordinated movement should progressively decline as *unc-55* mutants undergo larval development. To test this idea, we quantified the Unc-55 backward movement defect at different larval stages. Although this experiment showed that that a higher proportion of *unc-55* L2 larvae display uncoordinated backward locomotion than wild-type (29% of *unc-55* vs. 13% of wild-type) this disparity is enhanced during larval development until the adult stage when virtually all *unc-55* mutant animals show uncoordinated backward movement vs. only 6% of wild type animals (**Figure 2.3D**). This behavior parallels the progressive depletion of synaptic markers in the ventral nerve cord during *unc-55* development (**Figure 2.2D, F**) and therefore is consistent with the proposal that VD synapses are initially functional but are then are removed as ectopic remodeling ensues.

Ventral muscles retain UNC-49B/GABA-B receptor clusters in *unc-55* mutants

As an additional test of the finding that VD motor neuron initially establish ventral synapses in *unc-55* mutants, we examined the localization of the postsynaptic GABA receptor UNC-49B to ventral muscles, a result that depends

on a synaptic signal from GABAergic motor neurons (Gally and Bessereau, 2003). UNC-49::GFP puncta are initially evident only on the ventral side in early L1 larvae at locations corresponding to DD presynaptic markers. At the L1-L2 transition, UNC-49::GFP puncta in dorsal muscle appear, corresponding to the establishment of dorsal DD synapses. UNC-49 clusters in ventral muscle are apparently maintained by the establishment of nascent VD synapses; in a genetic mutant (*lin-6*) that blocks postembryonic cell divisions that give rise to VD motor neurons, these ventral UNC-49B clusters are removed after the L2 stage. This result indicates that VD input is required to sustain ventral UNC-49 clusters after DD motor neurons remodel (Gally and Bessereau, 2003).

We found that ventral UNC-49::GFP puncta persist in *unc-55* mutant adults (**Figure 2.4A-B**) (62$\pm$22 in wild-type vs. 66$\pm$23 in *unc-55*). This finding is consistent with the conclusion that VD motor neuron synapses are initially established in L2 larvae as suggested by the coincident ventral localization of SNB-1 and SYD-2 presynaptic markers at this stage (**Figure 2.2D, F**). Taken together with the behavioral assay (**Figure 2.3D**), our findings argue that the Unc-55 synaptic defect in VD motor neurons arises from ectopic activation of a remodeling program that effectively dismantles an initial set of signaling competent synapses to reconstitute them on the dorsal side. The establishment of ventral synapses prior to remodeling in *unc-55* VD motor neurons mirrors the synaptic arrangement of DD motor neurons during development. It is likely, therefore, that the components required to remove immature ventral synapses in DD motor neurons are also activated in *unc-55* VD motor neurons.

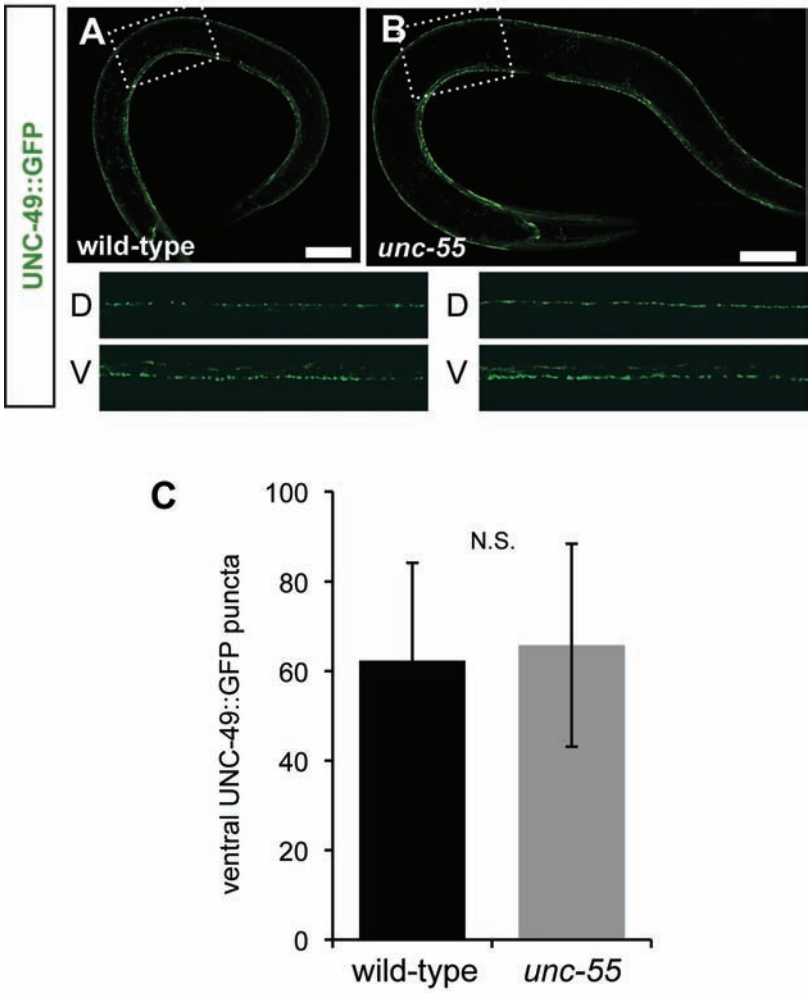

Figure 2.4. UNC-49B remains clustered in ventral muscle in *unc-55* mutants. (**A**) GABA receptors (UNC-49B::GFP) cluster in both dorsal and ventral muscle in wild-type adults to receive input from GABAergic motor neurons. (**B**) GABA receptor localization in body wall muscle is unperturbed in *unc-55* adults, suggesting that L2 *unc-55* VDs initially form functional ventral synapses. Scale bar, 20 μm, inset panels, 50 μm. (**C**) Quantification of UNC-49B::GFP puncta in ventral muscle of wild-type and *unc-55* adults. Receptor localization is unchanged in *unc-55* relative to wild-type, $p > 0.1$, Student's t-test.

UNC-55 expression in DD motor neurons results in a dorsal coiling defect

Our model predicts that UNC-55 blocks the activation of a remodeling program in VD motor neurons that is normally executed in the DD motor neurons. The Walthall laboratory tested this model with a transgenic strain carrying UNC-55 expressed in DD and VD motor neurons with the *unc-30* promoter. They found that ectopic UNC-55 expression in DD motor neurons is sufficient to block remodeling (Shan et al., 2005). We repeated this experiment with the *ttr-39* promoter because of an incompletely penetrant lethal phenotype and other morphological defects observed in the *punc-30::UNC-55* strain, a phenotype which is possibly due to expression from the *unc-30* promoter in other neurons. The *ttr-39* promoter is specific to DD and VD motor neurons, so we used this promoter to express the *unc-55a* cDNA isoform tagged with GFP. This *unc-55* gain-of-function [*unc-55(gf)*] mutant consistently shows bright UNC-55::GFP expression in GABAergic motor neurons. Sporadic expression is also observed in other unrelated cell types (**Figure 2.5A**).

Importantly, we found that ectopic expression of UNC-55 in DD motor neurons induces a characteristic movement defect. When tapped on the head, wild-type worms execute typical sinusoidal backward locomotion. In contrast, *unc-55(gf)* mutant adults show a dorsal coiling phenotype (**Figure 2.5B**). This result is indicative of excess excitatory input to dorsal muscles, an outcome predicted to result from the retention of ventral DD GABAergic synapses in the adult. Thus, the phenotype is consistent with a model in which ectopic UNC-55 expression blocks the DD remodeling program (**Figure 2.5C**). It follows that

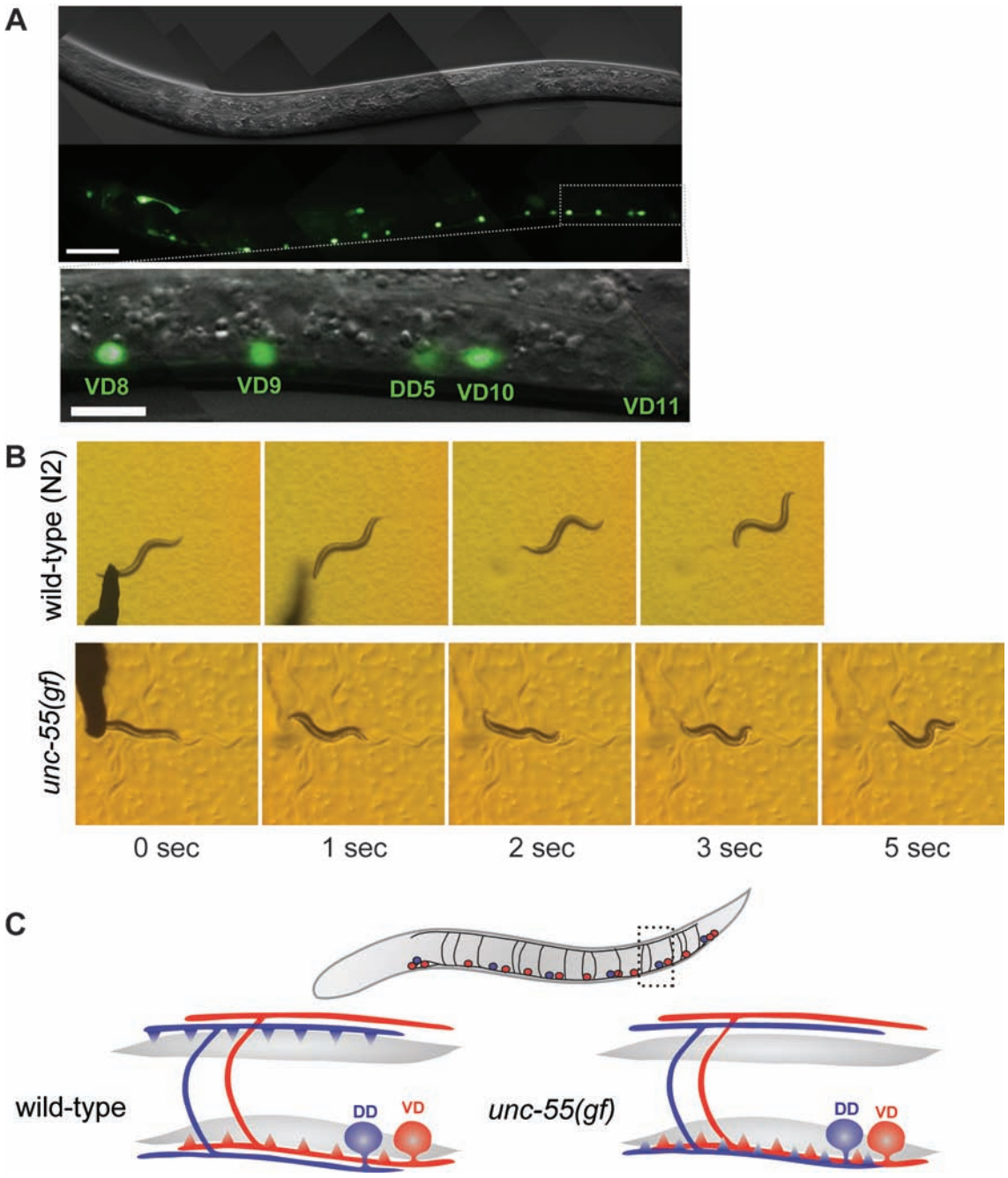

Figure 2.5. Ectopic UNC-55 expression in DD motor neurons induces dorsal coiling. (**A**) L3-stage larvae expressing *pttr-39::UNC-55a::GFP [unc-55(gf)]* with DIC (top) and GFP fluorescence (middle). Scale bar, 20 μm. Enlargement (bottom) shows expression in nuclei of GABAergic motor neurons in the ventral nerve cord. Scale bar, 5 μm. (**B**) Backward locomotion following head tap at t=0 for wild-type and *unc-55(gf)* adults. Time is indicated in seconds following head-tap, and panels are oriented with anterior to the left and ventral side down. Note sinusoidal backward locomotion in wild-type and dorsal coiling in *unc-55(gf)* adult. (**C**) Model of synaptic arrangement in post-L2 wild-type and *unc-55(gf)* GABAergic motor neurons. Note DD motor neurons maintain ventral synapses (triangles) due to ectopic *unc-55* expression.

these *unc-55* targets are also likely to be ectopically expressed in *unc-55* mutant VD motor neurons where they drive the relocation of synapses to the dorsal side.

The GFP translational fusion to the UNC-55 protein in this strain makes it particularly useful for future studies in this project. For instance, targets of UNC-55 may be identified via differential gene expression studies (see **Chapter III**) in wild-type and *unc-55(gf)* GABAergic motor neurons, and anti-GFP antibodies may be used for ChIP experiments to immunopreciptate UNC-55::GFP and its bound DNA sequence to identify target promoter sequences (Niu et al., 2011). The sensitivity of these assays could be enhanced by exploiting this strain to isolate UNC-55::GFP-labeled larval stage GABAergic motor neurons (Zhang et al., 2011) and nuclei (Okada et al., 2011) as starting material.

Dendritic proteins are localized primarily in ventral processes in wild-type and *unc-55* GABA motor neurons

The cross-inhibition model of the motor circuit (**Figure 2.3A**) predicts that DD and VD motor neurons are polarized with neurites reserved exclusively for axonal or dendritic components. In this model, DD motor neurons receive inputs from ventral cholinergic motor neurons, whereas VD motor neurons are innervated by cholinergic synapses on the dorsal side (**Figure 2.6A**). We wanted to test this model by observing the localization of dendritic components in GABAergic motor neurons and then determine if these domains are reorganized in *unc-55*. For this experiment, we expressed fluorescently-tagged proteins that were strong candidates for localization to the postsynaptic (dendritic)

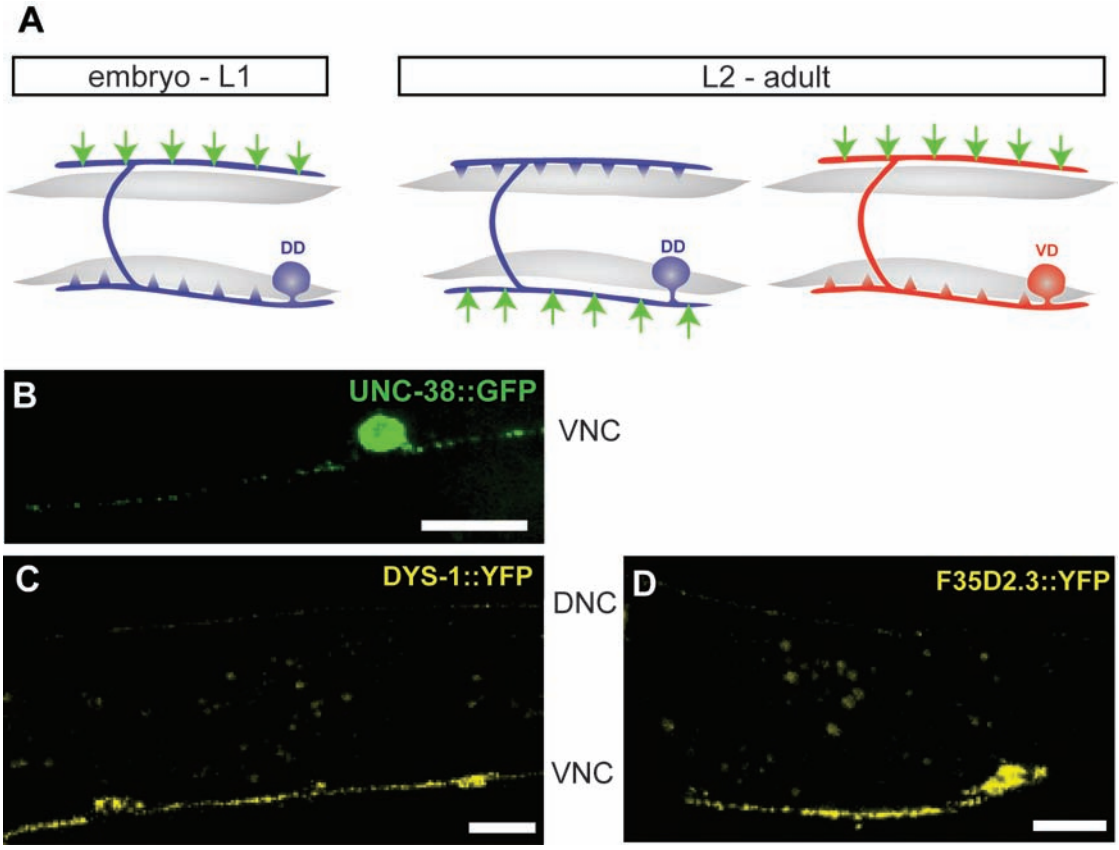

Figure 2.6. UNC-38, DYS-1, and F35D2.3 are primarily localized to the ventral nerve cord of GABAergic motor neurons. (**A**) Model for the location of postsynaptic domains in GABAergic motor neurons throughout development. (**B**) Expression of UNC-38::GFP in an adult VD motor neuron is punctate and restricted to the ventral nerve cord (VNC). UNC-38::GFP was not detected in the dorsal nerve cord. Expression of DYS-1::YFP (**C**) and F35D2.3::YFP (**D**) in adults is punctate and mostly restricted to the ventral nerve cord (VNC). The dorsal nerve cord (DNC) has relatively few, dim, tiny puncta in the animals shown, which represent the highest level of DNC fluorescence observed among all animals assayed. Scale bars, 10 μm.

compartment. The nicotinic acetylcholine receptor (nAChR) subunit UNC-38, the dystrophin homologue DYS-1, and the fibrillin protein encoded by *F35D2.3* were predicted to be localized in the ventral neurite of DD motor neurons and the dorsal neurite of VD motor neurons (Poon et al., 2008; Klassen et al., 2010). Therefore, we expected to see puncta representative of GABAergic dendritic domains in both the ventral and dorsal nerve cord. Surprisingly, we found that UNC-38::GFP puncta were localized exclusively in the ventral nerve cord. To account for the possibility that endogenous UNC-38 protein is competing with transgenic UNC-38::GFP for proper localization, we crossed the UNC-38::GFP transgene into the *unc-38* mutant background. However, UNC-38::GFP localization in *unc-38* mutants is the same as in wild-type, with strong UNC-38::GFP puncta in the ventral nerve cord and none in the dorsal nerve cord (**Figure 2.6B**). We conclude that either UNC-38 does not mark dorsal VD postsynaptic domains, or that the location of VD motor neuron is not in dorsal neurites. Similarly, DYS-1::YFP (**Figure 2.6C**) and F35D2.3::YFP (**Figure 2.6D**) were predominantly expressed in the ventral nerve cord. Few small puncta were rarely observed in the dorsal nerve cord (1-2 animals out of >20 examined). Thus, DYS-1::YFP and F35D2.3::YFP do not reliably mark the proposed dorsal VD dendritic domain.

The data from our panel of candidate postsynaptic markers do not conclusively address the location of dendritic domains of GABAergic motor neurons. The cross-inhibition model of GABAergic function in the motor circuit (**Figure 2.3**) predicts that these proteins would be localized in both the dorsal

and ventral nerve. We instead saw strong punctate localization of these markers in the ventral nerve cord with little to no expression in the dorsal cord. One explanation for this result is that these markers are not representative of the postsynaptic domain in GABAergic motor neurons. It is also possible, however, that the current cross-inhibition model (**Figure 2.3A**) is incorrect. Other acetylcholine receptor subunits (e.g*., acr-9, acr-16*) are expressed in GABAergic motor neurons, and examining the subcellular localization of these proteins in DD and VD motor neurons may help to resolve this question.

Discussion

The COUP-TF homologue *unc-55* functions as a transcriptional switch to block a synaptic remodeling program

unc-55 encodes the single COUP-TF nuclear hormone receptor in *C. elegans* (Zhou and Walthall, 1998). COUP-TF proteins function as transcription factors and adopt multiple roles in neural development including the widely observed function of preventing the adoption of alternative cell fates (Armentano et al., 2007; Tomassy et al., 2010). For example, in *Drosophila*, *seven-up/COUP-TF* preserves the specification of photoreceptors R1, R3, R4, and R6 by blocking the R7 fate (Mlodzik et al., 1990), a role that resembles that of *unc-55* which prevents VD motor neurons from expressing a specific DD motor neuron trait (Walthall and Plunkett, 1995). Similarly, COUP-TFI and COUP-TFII maintain the balance of GABAergic neuron types arising from different regions of the ganglionic eminence in the mammalian forebrain (Lodato et al., 2011). The

conservation from nematodes to mammals of analogous roles for COUP-TFs in establishing GABAergic neuron fates is intriguing and may reflect a primordial genetic program that operates in both contexts (Hammock et al., 2010).

The proposal that *unc-55/COUP-TF* regulates GABAergic neuron remodeling was originally based on the observation of a diagnostic movement defect and the relocation of synaptic varicosities in the *unc-55* mutant animals (Walthall, 1990; Walthall and Plunkett, 1995). Here, this hypothesis is validated by our results demonstrating that both an "early" marker of the presynaptic apparatus, SYD-2, as well as a "late" arriving synaptic vesicle component, SNB-1, are both relocated in VD motor neurons (**Figure 2.2**). Our work also established, for the first time, that VD motor neurons appear to form functional ventral synapses and the reconstitute them in the dorsal nerve cord in *unc-55* mutants (**Figure 2.3**). This temporal order of first ventral, then dorsal synaptic assembly mirrors the remodeling program that is normally executed in DD motor neurons. Moreover, the finding that ectopic expression of UNC-55 can block DD remodeling (**Figure 2.5**) (Shan et al., 2005) is also consistent with the idea that *unc-55*-regulated targets in VD motor neurons are likely to include genes that also drive remodeling in wild-type DD motor neurons.

Open questions regarding postsynaptic domain specification and maintenance in the GABAergic motor circuit

Our results showed that the GABA receptor subunit, UNC-49B, remains clustered in postsynaptic ventral muscle following remodeling of *unc-55* mutant

VD motor neurons (**Figure 2.4**). This finding is consistent with the idea that VD motor neurons initially establish functional ventral synapses. We note that in *lin-6* mutants in which the VDs are genetically ablated, UNC-49B clusters induced by immature DD motor neurons are subsequently removed from ventral muscle after DD remodeling is complete (Gally and Bessereau, 2003). Thus, we argue that the persistent appearance of UNC-49B ventral puncta in *unc-55* mutants must be due to the establishment of VD ventral synapses in the L2 stage prior to remodeling. However, our results showing that the density of UNC-49B::GFP puncta along the length of the ventral nerve cord did not change throughout development (data not shown) must mean that the additional UNC-49B::GFP subunits are assembled on muscle as the animal lengthens. This result is surprising because, as noted above, early maintenance of UNC-49B::GFP clusters depends on a signal from VD motor neuron synapses which are actively removed during larval development in an *unc-55* mutant. Thus, our data suggests that UNC-49B GABA receptor subunits may not require an exogenous cue to promote assembly in later developmental periods. An alternative model suggests that the “presynaptic factor” which promotes GABA receptor clustering is not remodeled along with other synaptic components in VD motor neurons and continues to promote postsynaptic NMJ specification in ventral muscle throughout the life of an *unc-55* mutant animal. Further studies, especially the identification of the VD-derived factor that promotes GABA receptor clustering, are needed to understand the specification of GABA postsynaptic domains in muscle.

We also met with surprising results in our attempts to understand the dendritic domain of the GABA motor neurons. The cross-inhibition model of nematode locomotion (**Figure 2.3**) suggests that GABAergic motor neurons specify separate axonal and dendritic domains on opposite sides of the animal. In this model, adult DD motor neurons provide output to dorsal muscle while receiving input from ventral cholinergic motor neurons in dyadic synapses that also excite ventral muscle. VD motor neurons adopt the opposite polarity, with cholinergic input on the dorsal side and GABAergic output to ventral muscles. This architecture was initially inferred from electron micrograph reconstruction of the ventral nerve cord and was at least partially confirmed by the well-established distribution of presynaptic markers (*e.g.* SNB-1::GFP) to dorsal DD synapses and ventral VD synapses. However, this model also predicts that postsynaptic (*i.e.* dendritic) markers should show the opposite pattern of localization corresponding to ventral DD and dorsal VD inputs. Our experiments with the candidate dendritic markers, UNC-38 (nAChR), DYS-1 (dystrophin), and F35D2.3 (fibrillin) did not show this pattern. We found that these presumptive dendritic proteins localize predominantly to the ventral nerve cord throughout the life of the animal. This must mean that these fluorescently tagged proteins are not dendritic markers, or that the current model of the GABAergic circuit is not correct. Therefore, the actual location of the dendritic domain in DD and VD motor neurons remains an open area of investigation.

The original impetus for marking the dendritic domain of GABAergic motor neurons was to determine if the remodeling program that relocates the axonal

domain also specifies a reciprocal change in the dendritic compartment. Again, we did not observe that the dendritic markers tested in this study were relocated from their initial positions in the L1 ventral nerve cord by the DD remodeling program. We also found no change in the number of UNC-38::GFP puncta in the *unc-55* ventral nerve cord compared to wild-type (data not shown, N=2 for both wild-type and *unc-55*). These data fail to substantiate a model in which the *unc-55*-regulated synaptic remodeling program reverses the signaling polarity of GABAergic motor neurons. This experiment should be revisited in the future when we have a more comprehensive understanding of GABAergic motor neuron dendritic domains.

Conclusions

Despite our difficulties in elucidating postsynaptic specification in GABAergic motor neurons and body wall muscle, it is clear that DD and VD motor neurons have polarized axonal domains, and that *unc-55* VD motor neurons largely mimic the remodeling event observed in wild-type DD motor neurons. Furthermore, remodeling is blocked when UNC-55 protein is ectopically expressed in DD motor neurons. Together, these data support the hypothesis that synaptic remodeling genes are repressed by UNC-55, and therefore that the identification of UNC-55 targets should reveal the downstream effectors that drive synaptic remodeling. We have adapted this approach and report the results of our studies in the following chapters.

CHAPTER III

CELL-SPECIFIC PROFILING OF LARVAL GABAERGIC MOTOR NEURONS TO UNCOVER UNC-55/COUP-TF-REGULATED TRANSCRIPTS

Introduction

The overarching goal of this project was to identify synaptic remodeling genes in GABAergic motor neurons that are normally activated in DD motor neurons. Our strategy for addressing this question is based on the model that remodeling genes are ectopically activated in VD motor neurons lacking the COUP-TF homologue, *unc-55*. Available genetic evidence is consistent with a model in which UNC-55 functions as a transcriptional repressor to prevent expression of synaptic remodeling genes in VD motor neurons; in *unc-55* mutant VD motor neurons, these *unc-55* target genes are de-repressed to activate the DD synaptic remodeling program. The ectopic remodeling of VD motor neurons in *unc-55* mutants causes a backward movement defect that involves excessive ventral coiling (see **Chapter II**) due to the loss of GABAergic inhibition on ventral muscle. Previous attempts to identify *unc-55*-regulated genes via genetic screens have focused on this phenotype; however, no suppressors of Unc-55 were identified using this approach (W. W. Walthall, Y. Jin, personal communication), suggesting redundancy or complexity of the remodeling program.

We therefore decided to utilize the recently developed mRNA-tagging strategy to identify transcripts that are de-repressed in *unc-55* GABAergic motor

neurons. In this method, epitope-tagged poly-A binding protein (3xFLAG::PAB-1) is expressed exclusively in the cell type of interest using a cell-specific promoter. mRNA from this cell type can then be co-immunoprecipitated with epitope (FLAG)-tagged PAB-1 via commercially available anti-FLAG antibodies and subjected to genomic analysis, such as *C. elegans* gene expression microarrays (Von Stetina et al., 2007b). This approach has proven more sensitive than whole-animal expression profiling and has been previously utilized to detect transcription factor targets in another subset of *C. elegans* motor neurons (Von Stetina et al., 2007a).

In this chapter, I describe the generation and validation of the first gene expression profile of larval wild-type GABAergic motor neurons, identification of *unc-55* targets via comparison of wild-type and *unc-55* cell-specific gene expression profiles, attempts to validate the screen via GFP reporters, screens of candidate targets for synaptic remodeling roles via RNAi suppression, and confirmation of a role in GABAergic synaptic patterning for a subset of the *unc-55*-regulated targets identified by this approach.

Author Contributions

All microarray experiments described in this chapter (benchwork and analysis) were a joint effort with a fellow graduate student and subsequent postdoctoral fellow in the lab, Joseph Watson, who is second-author on our *Journal of Neuroscience* paper describing some of these experiments. Joseph and I received additional assistance from other members of the lab, including

postdoctoral fellow Steve Von Stetina and graduate student Clay Spencer. The *wdIs31* transgenic strain was created with the microinjection help of a research assistant in the lab, Kathie Watkins. A former postdoctoral fellow in the lab, Sue Barlow, generated the embryonic GABAergic profiles to which the larval GABAergic profiles are compared. Alyssa Fesmire, an undergraduate in our lab, assisted with the construction and analysis of *cnt-1* strains.

Methods

Strains and genetics: Nematode strains were maintained at 20-25°C with standard culture techniques (Brenner, 1974). The wild-type strain is N2 and all references to *unc-55* mutants used the allele *unc-55(e1170)* (Walthall, 1990).

Strain list:

note: *unc-119*(+) refers to *unc-119*-rescuing minigene from MM051(Maduro and Pilgrim, 1995) (see details of strain construction)

<u>mRNA tagging strains:</u>

NC1412 *dpy-5(e907); wdEx562[pttr-39::3xFLAG::PAB-1 dpy-5(+)]* (prior to integration)

NC1645 *dpy-5(e907); wdIs31[pttr-39::3xFLAG::PAB-1 dpy-5(+)]* IV (integrated strain)

NC1546 *dpy-5(e907) unc-55(e1170); wdIs31[pttr-39::3xFLAG::PAB-1 dpy-5(+)]* IV

GFP reporter strains:

BC11521 *dpy-5(e907); sIs10354[rCesY39D8C.1::GFP + pCeh361]*

NC2080 *dpy-5(e907) unc-55(e1170); sIs10354[rCesY39D8C.1::GFP + pCeh361]*

BC15319 *dpy-5(e907); sEx15319[rCesC54D10.10::GFP + pCeh361]*

NC2085 *dpy-5(e907) unc-55(e1170); sEx15319[rCesC54D10.10::GFP + pCeh361]*

BC13365 *dpy-5(e907); sEx13365[rCesC54D10.10::GFP + pCeh361]*

NC2086 *dpy-5(e907) unc-55(e1170); sEx13365[rCesC54D10.10::GFP + pCeh361]*

BC13447 *dpy-5(e907); sEx13447 [rCesC11E4.1::GFP + pCeh361]*

NC2087 *dpy-5(e907) unc-55(e1170); sEx13447 [rCesC11E4.1::GFP + pCeh361]*

BC12422 *dpy-5(e907); sEx12442 [rCes F23F12.9a::GFP + pCeh361]*

NC2088 *dpy-5(e907) unc-55(e1170); sEx12442 [rCes F23F12.9a::GFP + pCeh361]*

NC2096 *unc-119; wdEx680[pnlp-26::GFP; unc-119+]*

NC2113 *unc-55(e1170); unc-119; wdEx680[pnlp-26::GFP; unc-119+]*

BC13641 *dpy-5; [dpy-5+; pnas-38::GFP]*

BC12934 *dpy-5(e907) I; sIs12169[rCesT19D2.1::GFP + pCeh361]*

NC2128 *dpy-5(e907) unc-55(e1170); sIs12169[rCesT19D2.1::GFP + pCeh361]*

BC15234 *dpy-5(e907) I; sEx15234[rCesT18H9.1::GFP + pCeh361]*

RNAi strains:

NC1613 *eri-1 (mg366) juIs1[punc-25::SNB-1::GFP; lin-15+]*

NC1713 *eri-1; wdIs20[punc-4::SNB-1::GFP]*

NC1852 *unc-55(e1170); eri-1(mg366) juIs1[punc-25::SNB-1::GFP; lin-15+]*

Synaptic analysis strains:

CZ333 *juIs1[punc-25::SNB-1::GFP; lin-15+]*

NC1851 *unc-55(e1170); juIs1[punc-25::SNB-1::GFP; lin-15+]*

NC2100 *arx-5(ok1990)/hT2; juIs1[punc-25::SNB-1::GFP; lin-15+]*

NC1915 *cnt-1(tm2313)* II outcrossed 2x

NC1919 *cnt-1(tm2313); juIs1[punc-25::SNB-1::GFP; lin-15+]*

NC2129 *unc-55(e1170); cnt-1(tm2313); juIs1[punc-25::SNB-1::GFP; lin-15+]*

GABA mRNA-tagging strain: An 861 bp fragment from the promoter region of *ttr-39* was amplified with 5' primer (5' ATT ATT ATT TCT ATC GGC TA 3') and 3' primer (5' ATG ATT TTT TGT TTT AAC AA 3') and inserted into pENTR D-TOPO (Invitrogen) via TOPO TA reaction. *Pttr-39* was then inserted upstream of 3XFLAG::PAB-1 via Gateway LR reaction with pSV41 resulting in the expression vector pSA2. The entire p*ttr-39*::3XFLAG::PAB-1 cassette was then amplified via PCR, and half of the PCR reaction (12 μL) was co-injected with *dpy-5* rescuing plasmid pCes361 (25 ng) into *dpy-5(e907)* animals. Gamma irradiation of the transgenic line yielded NC1645 *dpy-5(e907); wdIs31[Pttr-39:: 3xFLAG::PAB-1 dpy-5(+)]* IV. The integrant was outcrossed five times prior to microarray profiling (Spencer et al., 2011).

Gene expression profiling experiments used the *wdIs31[pttr-39::3xFLAG::PAB-1]* transgene in both wild-type and *unc-55* backgrounds. For *unc-55* profiles, a *dpy-5(e907) unc-55(e1170)* recombinant was generated and crossed into NC1645 to yield NC1546 *dpy-5(e907) unc-55(e1170); wdIs31*. *wdIs31* transgenics were immunostained with monoclonal mouse anti-FLAG antibodies (Sigma) and goat anti-mouse IgG Cy3 (each 1:1000) to detect expression of FLAG-PAB-1.(Finney and Ruvkun, 1990) To identify GABA motor neurons, animals were co-stained with DAPI, mounted on a 2% agarose pad, and imaged on a Zeiss Axioplan compound microscope. DD and VD motor neurons were identified by their stereotyped locations in the ventral nerve cord.

Detection of *unc-55*-regulated transcripts from GABA neuron-specific microarray profiling results: mRNA tagging methods were as described (Von Stetina et al., 2007b). Briefly, anti-FLAG beads were used to isolate GABA-neuron specific RNA from lysates of wild-type and *unc-55* mutant mid-L2 stage larvae expressing the *wdIs31* transgene. ~10 ng of RNA for each sample was amplified with WT-Ovation^{TM} Pico RNA Amplification System (NuGen Technologies) and ~5 μg of labeled target cDNA was hybridized to Affymetrix *C. elegans* GeneChip arrays. Independent data sets were collected from multiple samples and three wild-type (N2) and four unc-55 mutant mRNA tagging samples with high Pearson correlation coefficients ($R^2 \geq 0.8$ minimum, $R^2 \geq 0.91$ actual) were selected for further analysis. Probe intensities were normalized with robust multi-array analysis (RMA). Transcripts were called as “present” or

"absent" based on MAS 5.0 probe intensity, filtering out genes enriched in reference, and adding genes enriched in L2 GABA motor neurons, as previously described (Von Stetina et al., 2007b). Transcripts showing ≥2-fold difference at <1% false discovery rate (FDR) between wild-type vs. *unc-55* mutant data sets were identified with two-class unpaired analysis in Significance Analysis of Microarray (SAM) (Irizarry et al., 2003).

Annotation of expression profiles: Genes were classified based on gene ontology with Perl scripts and hand annotation as previously described (Von Stetina et al., 2007b) Gene ontology was refined using information consolidated at wormbase.org, release WS221, i.e. INTERPRO protein domains, GO terms inferred from mutant phenotype (IMP), and gene descriptions contributed to Wormbase with references. Conservation was based on BLASTP E-values ($<e^{-10}$ to *H. sapiens*) (wormbase.org).

UNC-55 binding site analysis. We generated a text file containing the sequence of 2 kb of the 5' regulatory regions of candidate *unc-55* targets in FASTA format via WormMart (wormbase.org). We then used the EMBOSS application "fuzznuc" at the Galaxy project (main.g2.bx.psu.edu) for a nucleic acid pattern search for putative UNC-55 binding sites TGACCT and TGACCC on either strand of the regulatory region for candidate UNC-55 genes. As a control, we also collected 2 kb of the 5' regulatory regions for all cosmids in WormBase release WS170 and searched for putative UNC-55 binding sites in the regulatory region of all genes.

Data generated by fuzznuc was manually compiled to determine number of genes with and without UNC-55 binding sites in promoter regions.

Microscopy and synapse scoring: SNB-1::GFP assays were performed with the transgene *juIs1[punc-25::SNB-1::GFP; lin-15+]* (Hallam and Jin, 1998), Animals were anesthetized with 0.1% tricaine/tetramisole, mounted on a 2% agarose pad, and imaged with a Zeiss Axiovert microscope using Metamorph software or Leica TCSSP5 confocal microscope with Leica Application Suite Advanced Fluorescence (LAS-AF) software. For linescan intensity studies (*cnt-1, arx-5*), Z-stacks collected at 1.0 μm/step with a 40x objective were collapsed into maximum intensity projections. Linescan intensity values along the ventral nerve cord of each adult animal were collected with Leica Application Suite Advanced Fluorescence (LAS-AF) software. For each animal, the linescan intensity values were scaled such that the minimum intensity value was set to 0 and the maximum intensity value was set to 255 to compensate for differences in background fluorescence. All intensity values for each animal were averaged, and then average intensity per animal was averaged by genotype. Statistical tests were performed comparing the average intensity among all animals in each genotype.

RNAi screening: Hedgehog-like candidate genes were assayed by RNAi in *juIs1*; *eri-1(mg366* (NC1613); the Unc-55 RNAi suppression screen was performed with *unc-55(e1170); juIs1*; *eri-1(mg366)* (Kennedy et al., 2004). In

both cases the RNAi hypersensitive *eri-1* mutation was confirmed by PCR assay (Earls et al., 2010). RNAi knockdown by feeding used bacterial clones from the *C. elegans* RNAi library (Kamath et al., 2003) with plates created as previously described (Earls et al., 2010) with the exception that no EGTA was added to media. Three L4 hermaphrodites were grown on each RNAi plate at 20-23°C for 5 days until F2 progeny reached young adult stage. SNB-1::GFP puncta in the ventral nerve cord were counted for $\geq$5 animals per clone. Negative control RNAi (L4440 containing no genomic insert) was analyzed with each set of clones screened. For the Hedgehog assays, *unc-30* was used as a positive control; for the suppression screen, *irx-1* and *unc-8* were used as positive controls. Counting was performed with the observer blinded to the identity of the RNAi clones until after data collection was completed. In the suppression screen, “hits” were defined as RNAi clones that resulted in a significant increase in ventral SNB-1::GFP puncta according to these criteria: (1) ventral puncta were significantly higher in animals treated with RNAi for a candidate *unc-55* target than empty vector ($p<0.01$, Student’s t-test); (2), this phenotype was detected in at least half the animals scored, *i.e*. a penetrance of greater than 50%. For this criterion, “phenotype” means a number of puncta above the empty vector control upper bound (~40 puncta). All conserved hits were re-screened independently to confirm *unc-55* suppression. For all hits, the RNAi feeding plasmid was purified from library clones via QIAprep Spin Miniprep kit (Qiagen) and sequenced to verify the gene identity.

Results

The GABA profiling strain, *wdIs31*, yields reproducible datasets

We generated multiple strains carrying *pttr-39::3xFLAG::PAB-1* to profile L2-stage GABAergic motor neurons with the mRNA-tagging method (**Figure 3.1A**). Multiple strains were generated via microparticle bombardment and microinjection and showed variable levels of transgenic rescue, ectopic expression of 3xFLAG::PAB-1, and overall health. One of these strains, NC1412, was selected for integration based on bright anti-FLAG immunostaining, limited ectopic transgene expression, and wild-type health of the strain. The transgene was integrated via gamma irradiation (see **Methods**) to yield *wdIs31*. In this strain, immunostaining of 3xFLAG::PAB-1 is restricted to GABAergic motor neurons at all stages (**Figure 3.1B**).

To identify GABAergic transcripts, seven samples of mid-L2-stage GABAergic mRNA were collected and hybridized to *C. elegans* Affymetrix GeneChip arrays. Of these, we selected three datasets (509DMM25, 509DMM44, 509DMM48) that showed high RMA-normalized probe intensity of GABAergic genes as well as high correlation among datasets (n=3, R^2=0.97, **Figure 3.1C**) to use in additional analyses. Using the normalized probe intensity, we identified 10731 unique transcripts that were expressed (expressed genes, EGs) in larval GABAergic neurons based on a “present” call in two of the three datasets. Most EGs are likely to be housekeeping genes with roles in many tissue types, such as ribosomal proteins (*e. g.* 26 40S and 44 60S ribosomal proteins), cytoskeletal proteins (*e. g.* eight alpha-tubulin, three beta-tubulin, and

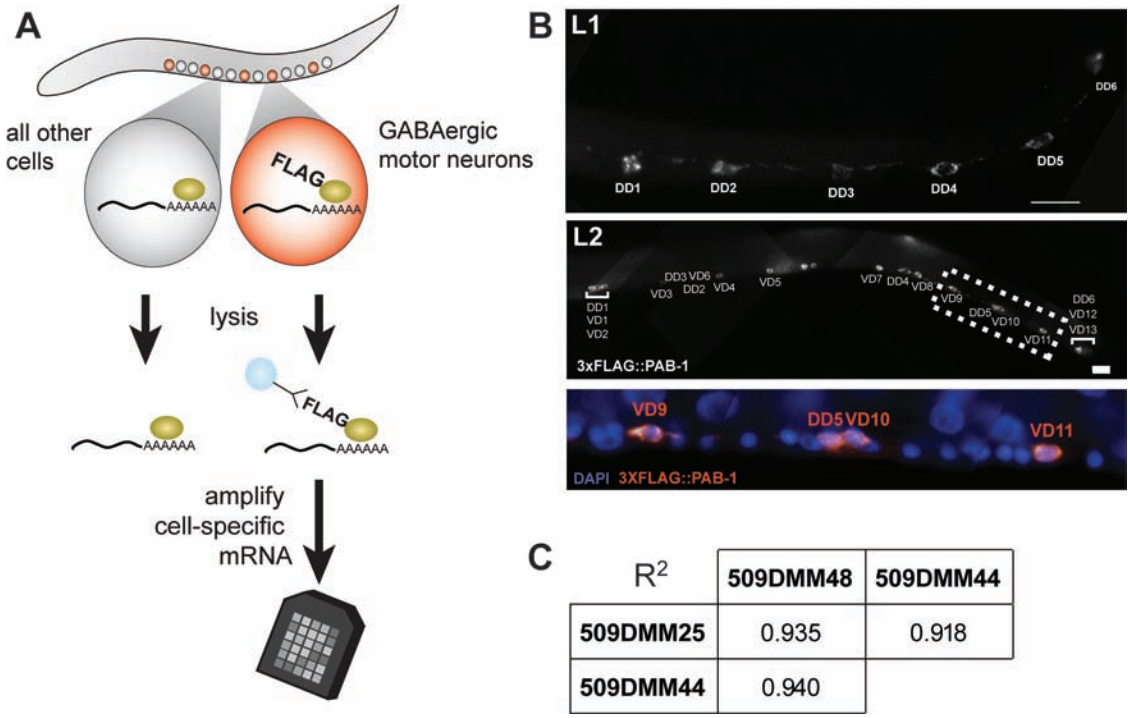

C

R^2	509DMM48	509DMM44
509DMM25	0.935	0.918
509DMM44	0.940	

Figure 3.1. The mRNA tagging method with the larval GABAergic profiling strain, *wdIs31.* (**A**) The mRNA tagging method. Lysates are treated with anti-FLAG-coated beads to capture FLAG-tagged PAB-1 cross-linked to cell-specific mRNA. Immunoprecipitated mRNA is amplified and labeled for hybridization to a *C. elegans* Affymetrix GeneChip array (see Methods). (**B**) Anti-FLAG staining of FLAG-tagged PAB-1 transgenic line, *wdIs31[pttr -39::3xFLAG::PAB-1]* is restricted to GABAergic motor neurons in both L1 (top panel) and L2 (middle panel) larvae; ventral cord motor neuron soma are stained with DAPI (bottom panel). Scale bar, 10 μm. (**C**) Pearson correlation coefficients (R^2) for larval GABAergic datasets 509DMM25, 509DMM44, and 509DMM48 were calculated from normalized probe intensity. Note high values (near 1), which indicate low variability in sample collection.

six Arp2/3 complex components), regulators of protein turnover (*e. g.* more than 30 proteasome components or regulators), and basal polymerases (*e. g.* at least 41 RNA polymerase subunits/factors). In addition, 59% of the 2886 EGs with known expression patterns (as of WormBase Release WS170) were annotated as having neuronal expression. Of these, many have functions in a broad range of neurons, such as axon guidance genes (netrin receptors *unc-5* and *unc-40*, *sax-3/Roundabout*), neurotransmitter receptors (3 dopamine receptors and 24 acetylcholine receptors) and neuropeptides (22 FMRFamide-like and at least 29 in other classes).

Comparison of larval GABAergic gene expression to other cell types

To identify genes with significant and/or selective function in GABAergic motor neurons, we compared the three well-correlated GABAergic replicates to a reference mRNA dataset from all larval cells. This analysis revealed 1476 transcripts enriched >1.5-fold in GABAergic motor neurons with a threshold of 10% False Discovery Rate (FDR). A more stringent dataset of 733 transcripts enriched >1.5-fold with a 5% FDR does not contain *unc-55* which suggests that this treatment may exclude some *bona fide* GABAergic genes; therefore, we opted to use the $\leq$10% FDR threshold for subsequent analysis.

Transcripts encoding proteins predicted to have a wide variety of cellular functions were enriched in GABAergic motor neurons (**Figure 3.2A**). One prominent group of enriched transcripts encode transcription factors, including ten homeobox-family transcription factors (*e. g. Aristaless/ARX* homologue *alr-1*,

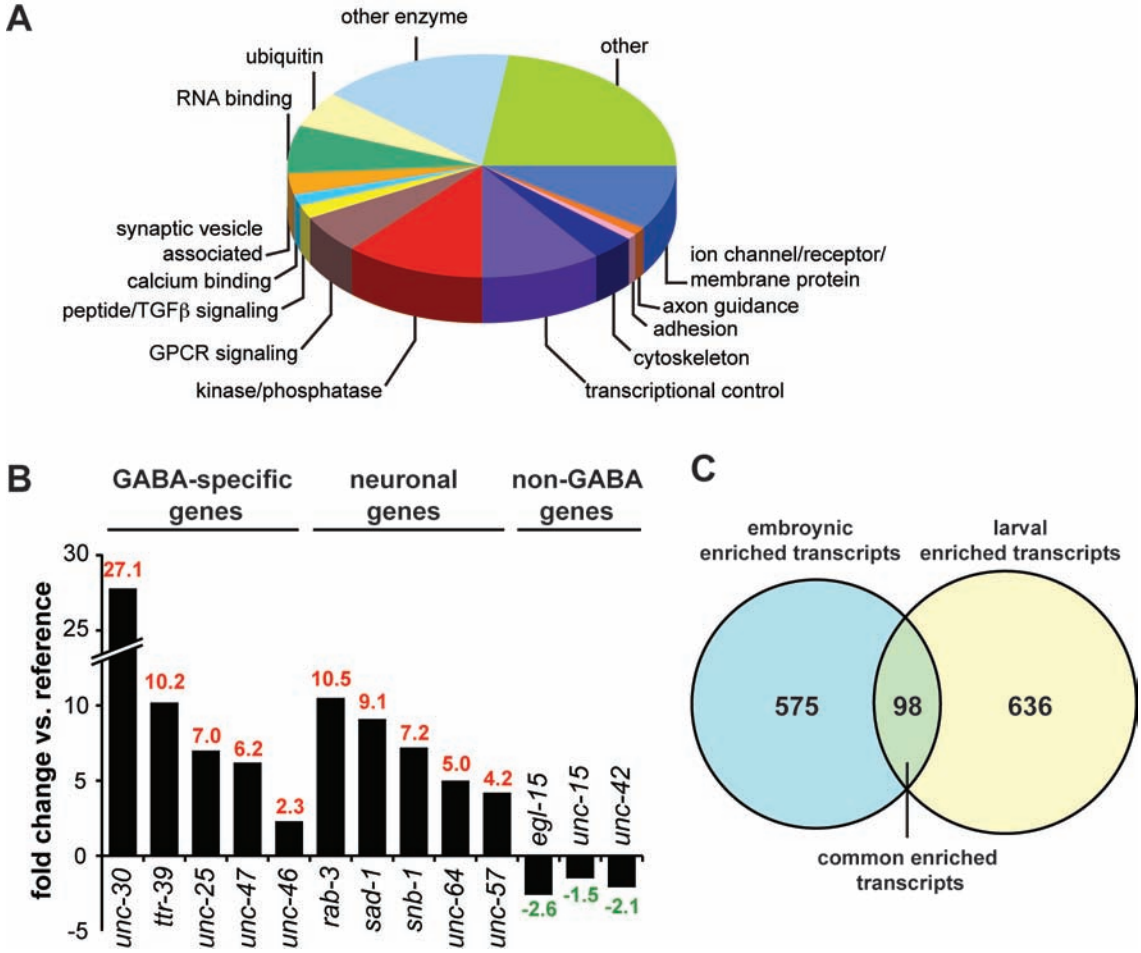

Figure 3.2. Gene expression profiles of GABAergic motor neurons. (**A**) Gene ontology of transcripts enriched ≥1.5-fold in larval (L2) GABAergic motor neurons compared to a mock-immunoprecipitated N2 reference, representative of all cells (10% FDR). Only 1060 transcripts (of 1476) with annotation (*i.e.* GO terms) indicative of gene function are included in the chart; the remaining 416 transcripts are uncharacterized with no predicted function. (**B**) Expression levels of transcripts in larval GABAergic motor neurons relative to reference. Fold change indicated over column; enrichment in GABA motor neurons is denoted in red, and depletion in GABA motor neurons is denoted in green. Fold change calculated by Significance Analysis of Microarrays (SAM). Note GABAergic (*unc-30*, *ttr-39*, *unc-25*, *unc-47*, *unc-46*) and neuronal transcripts (*rab-3*, *sad-1*, *snb-1*, *unc-64*, *unc-57*) are enriched in GABAergic motor neurons but non-neuronal transcripts (*egl-15*, *unc-15*, *unc-42*) are significantly depleted in GABAergic motor neurons (*i.e.* enriched in "all cells" reference). (**C**) Significant overlap of transcripts elevated in embryonic and larval GABAergic expression profiles. For complete list of common transcripts, see **Table 3.1**.

LIM homeodomain-containing *lin-11*, zinc-finger transcription factor *zag-1*, and *Iroquois/IRX* homologue *irx-1*) and thirteen members of the nuclear hormone receptor superfamily (*e. g. COUP-TF* homologue *unc-55*). Some of these transcription factors have established roles in GABAergic neuron development (e.g. *alr-1*, *lin-11, unc-55*), which validates our methodology (Zhou and Walthall, 1998; Melkman and Sengupta, 2005). Many of these transcription factors, however, have known roles in other *C. elegans* neurons or in the neuronal development of other organisms, but no reported functions in GABAergic motor neurons (Sarafi-Reinach et al., 2001; Gomez-Skarmeta and Modolell, 2002; Clark and Chiu, 2003; Smith et al., 2010). The enriched GABAergic motor neuron dataset includes 107 mRNAs predicted to encode regulators of transcription. This finding could be indicative of a complex network of gene regulation that specifies for proper GABAergic motor neuron differentiation and function.

To test the validity of our method, we searched our list of enriched transcripts for genes with known roles in identified transcripts with key roles in GABAergic neuronal development. For instance, the *Pitx* homologue, *unc-30*, which defines GABA neuron fate (Jin et al., 1994), is elevated 27-fold in DDs and VDs versus all cells (**Figure 3.2B**). The GABA-specific genes *unc-25*, *unc-47*, *unc-46*, and *ttr-39*, as well as known neuronal genes (*e.g. rab-3, sad-1, snb-1, unc-64, unc-57*), also showed high levels of enrichment. Furthermore, transcripts known to be expressed in tissues other than GABA neurons, such as those expressed in vulval muscle (*egl-15*), body wall muscle (*unc-15*), and non-GABA interneurons (*unc-42*) were significantly depleted.

For additional validation and to identify dynamically-regulated genes, we compared our larval GABAergic enriched profile to an *unc-25::GFP* embryonic enriched profile generated by Sue Barlow via the MAPCeL approach (Fox et al., 2005). For this comparison, we used the more-stringent 5% FDR larval GABA dataset, which has a comparable number of enriched transcripts (733) to the embryonic profile (673). We see significant overlap ($p < 10^{-30}$) between the larval and embryonic enriched gene lists, despite the significant differences in how the datasets were collected (MAPCeL vs. mRNA-tagging, *unc-25* vs. *ttr-39* promoters, etc.). This result confirms the validity of our approach and allows us to identify 98 key genes common to both profiles (**Figure 3.2C**). These include neuronal genes (*e.g. rab-3*, *unc-57*) and all expected GABAergic (*unc-30, unc-47, unc-46, unc-25, ttr-39*, *oig-1*) genes, as well as transcripts not previously known to be expressed in GABAergic motor neurons (**Table 3.1**) We note, for instance, neuropeptides (*flp-15*, *nlp-13*) and membrane proteins (potassium channel *F14F11.1,* stomatins *sto-2* and *sto-4*) with previously unidentified expression or function in GABAergic motor neurons. Of particular interest is the enrichment of the GABA receptor *unc-49*. To date, *unc-49* expression has been observed only in muscle with transcriptional and translational reporters; however, a cell-autonomous feedback role for GABA receptor in GABAergic motor neurons has been suspected but not confirmed (B. Bamber, personal communication). This idea is substantiated by our finding that the *unc-49* transcript is enriched in both embryonic and larval GABAergic motor neurons.

Table 3.1. Genes enriched in both embryonic and larval GABAergic profiles

Sequence Name	Gene Name	Description	Embryonic Fold Enrichment	Larval Fold Enrichment	Previously ID'd in GABAs?
		Adhesion			
C09E7.3	*oig-1*	Predicted adhesion molecule	49.7	14.8	yes
C33F10.5	*rig-6*	Contactin	5.7	2	
		Calcium Binding			
Y105E8A.7	*lev-10*	Cubilin	4.2	6	
Y64G10A.7		Fibrillin	2.3	10.2	
		Cytoskeleton			
C01G10.11	*unc-76*	Fasiculation/elongation factor zeta	3.1	8.4	yes
		Enzymes			
C34F6.4	*hst-2*	Sulfotransferase	2.1	2.2	
D1022.8	*cah-2*	Carbonic anhydrase	8.8	5.9	
F10G8.6		Predicted ATPase, nucleotide-binding	1.8	2.6	
F53B6.2		ADAM	9.9	6.1	
H15N14.2	*nsf-1*	AAA+type ATPase	2.4	2.6	
R153.1	*pde-4*	Cyclic nucleotide phosphodiesterase	1.9	2	
T05H10.2	*apn-1*	Apurinic/apyrimidinic endonuclease	2.7	5.1	
Y34B4A.7		Predicted spermine/spermidine synthase	1.9	3.5	
Y75B12B.2	*cyn-7*	Cyclophilin A	2.1	2.7	
ZK994.3	*pxn-1*	Peroxidasin	4.1	5.8	
		GPCR signaling			
C09B7.1	*ser-7*	G-protein coupled receptors	2.4	2.4	
C33G8.5	*srab-4*	Sra family integral membrane protein	1.8	4.2	
F15A8.4		7-transmembrane receptor	7.8	4.5	
F53F10.4	*unc-108*	GTPase Rab2	2	2.1	yes
Y87G2A.4	*aex-6*	GTPase Rab27	1.8	2.8	
		Ion channels, receptors, membrane proteins			
C40C9.2	*acr-9*	Acetylcholine receptor	24.7	14.2	yes
C53A5.5		K+ channel subunit	4.2	2	
F10G7.5		Transporter	2.5	2.2	
F14F11.1		K+ channel subunit	2	3	
F32A6.5	*sto-2*	Stomatin	6.3	8.1	
R12H7.1	*unc-9*	Innexin	2.5	5.6	
T21C12.1	*unc-49*	GABA receptor	4.4	3.5	
Y110A7A.3	*unc-63*	Acetylcholine receptor	2.1	2.2	yes
Y48B6A.9	*hot-7*	GPI-linked signaling protein	12.8	5.7	
Y71H9A.3	*sto-4*	Stomatin	4.4	2	

Sequence Name	Gene Name	Description	Embryonic Fold Enrichment	Larval Fold Enrichment	Previously ID'd in GABAs?
		Transcriptional Control			
B0564.10	*unc-30*	Homeobox transcription factor, Pitx family	20.1	69.6	yes
D1037.1		SON DNA binding protei	2	2.2	
F58A4.7	*hlh-11*	Transcription factor, helix-loop-helix	1.7	4.1	
R08B4.2	*alr-1*	Homeobox transcription factor Aristaless	4.1	4.3	yes
Y54F10AM.4	*ceh-44*	Homeobox transcription factor, CUT family	2	3.6	
		Axon Guidance			
K12F2.2	*vab-8*	Kinesin	1.9	3.3	yes
		Kinases/Phophatases			
B0478.1	*jnk-1*	Jun-N-terminal kinase (JNK)	3.7	5.6	yes
C18B12.2		Calcitonin receptor	2.2	10.2	
C50F2.8		MAGUK	2	6.5	
E01H11.1	*pkc-2*	Protein Kinase C	3.5	5.7	
M03C11.1		Ribosomal protein S6 kinase	2.2	4.7	
R90.1		Casein kinase	2.2	2.9	
Y42G9A.4		Mevalonate kinase	2.2	3.3	
Y71H10A.1		Phosphofructokinase	1.7	2.6	
		Neuropeptides			
CC4.2	*nlp-15*	Neuropeptide-like	3.1	2.8	yes
E03D2.1	*nlp-13*	Neuropeptide-like	8	12.8	
ZK1320.10	*nlp-11*	Neuropeptide-like	3.4	4.5	
ZK525.1	*flp-15*	FRMFamide-like	6.5	3.6	
		Other			
C04G2.1	*ttr-39*	Transthyretin-related protein	14.6	10.2	yes
F13G3.9	*mif-3*	Macrophage migration inhibitory factor	2.4	3.8	
K06A5.8		WD repeat protein	2.5	1.9	
R06A4.4	*imb-2*	Nuclear transport receptor Karyopherin-beta2/Transportin	2	2.4	
ZC84.3		CLIP-associating protein	4	3.5	
ZK1073.1		Differentiation-related gene 1 protein	2	4.1	yes
H28G03.1		Nuclear riboprotein	1.9	3.6	
		Novel/Uncharacterized			
C06E7.2			6.2	9.4	
C13A10.2			5.9	17.7	
C16E9.2			4.3	7.6	
C24A3.2			2.5	3.4	
C43H6.1			2.1	1.8	
C54G4.5			8.4	5.1	
C55F2.2			7.0	14.3	

Sequence Name	Gene Name	Description	Embryonic Fold Enrichment	Larval Fold Enrichment	Previously ID'd in GABAs?
F13C5.1			2.0	2.4	
F15G9.1			1.8	3.7	yes
F21C10.3			1.9	2.0	
F28E10.1			4.4	2.9	
F29G6.2			3.5	11.4	
F45E4.3			4.0	1.8	
F53B1.3			2.0	2.2	
F58A3.4			2.6	2.1	
F58H1.7			3.2	2.8	
H14E04.3			7.5	6.5	
M03E7.1			7.7	3.6	
R05D7.3			2.4	8.1	
R07E4.5			2.7	2.4	
T10G3.5	*eea-1*		2.3	2.7	
T24D5.2			2.8	9.5	
T27C4.1			4.3	6.2	
Y49E10.23			3.0	3.7	
Y51H4A.20			2.4	3.5	
Y53F4B.45			2.4	4.8	
Y54G2A.26			2.0	3.4	
Y73B3A.15			4.3	4.6	
ZK287.3			1.7	2.5	

We predict that some of the differentially enriched genes (i.e., enriched in the embryonic but not larval profile, and vice versa) are dynamically regulated in DD motor neurons or expressed in a subset (DD or VD) of GABAergic motor neurons. Therefore, these datasets could be useful in the future for identifying genes with roles specific to DD or VD motor neurons.

GABA-specific expression profiles reveal candidate *unc-55* target genes

Because UNC-55 functions as a transcription factor to repress synaptic remodeling genes, we reasoned that UNC-55-regulated transcripts would be enriched in an *unc-55* GABAergic gene expression profile vs. wild-type (**Figure 3.3A**). To identify these enriched candidate synaptic remodeling genes, we profiled larval animals during the L2 stage in which VD motor neurons initiate remodeling in *unc-55* mutants (see **Chapter II**). Transcripts were isolated from *unc-55* DD and VD motor neurons by co-immunoprecipitation with FLAG::PAB-1 from *wdIs31[pttr-39::3xFLAG::PAB-1]* and hybridized to Affymetrix Gene Chip Arrays. Comparison of highly reproducible *unc-55* datasets (n=4, R^2=0.93, **Figure 3.3B**) to the three wild-type datasets described above yielded 188 significantly enriched transcripts that were 2-fold enriched at $\leq$1% FDR (**Figure 3.3C,** red). This dataset is predicted to include genes that are normally repressed by *unc-55* in wild-type animals and candidates for genes that promote synaptic remodeling. The proposal that UNC-55 functions largely as a transcriptional repressor is consistent with our finding that only 11 transcripts were significantly depleted in the *unc-55* dataset (**Figure 3.3C**, green).

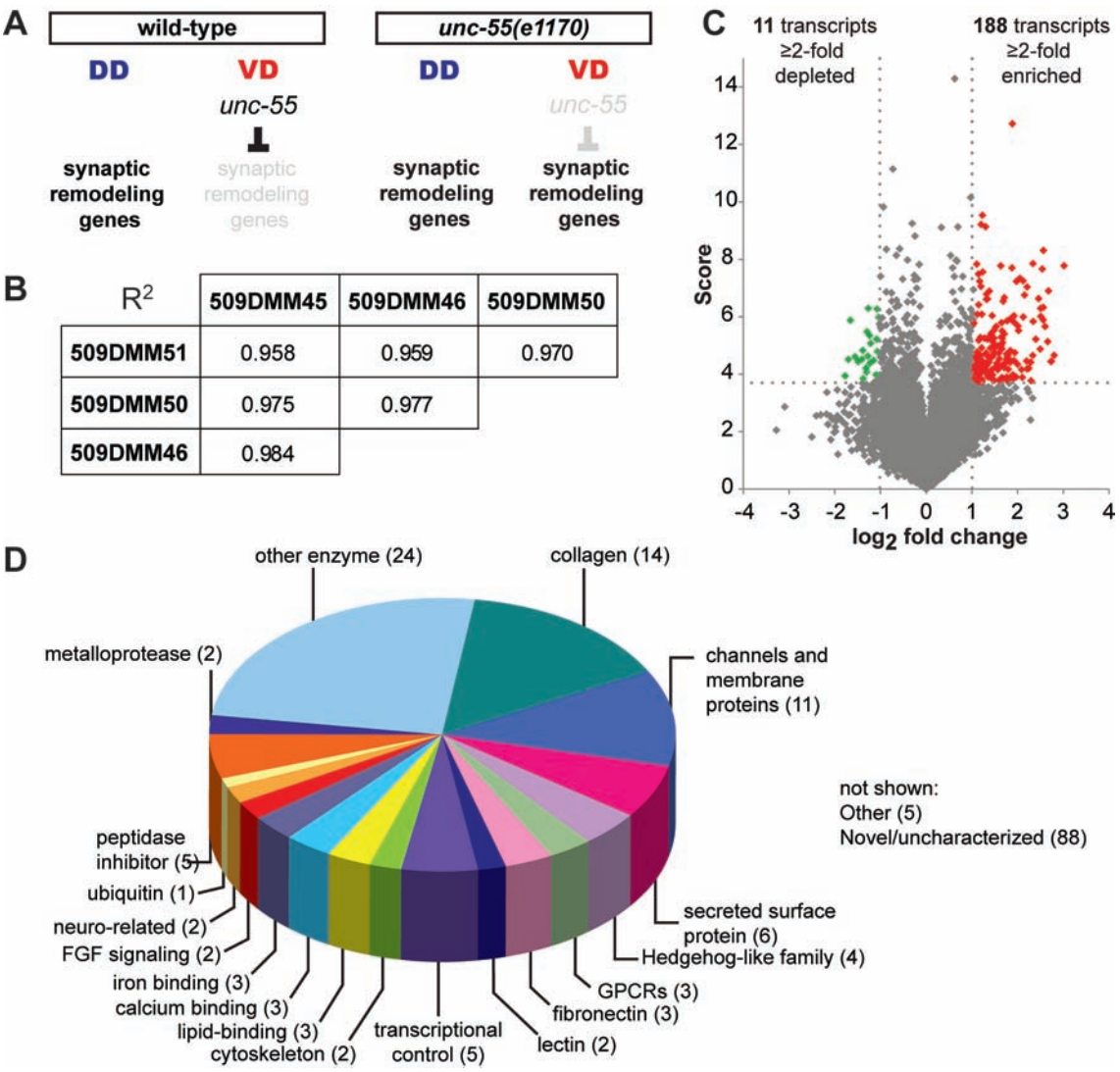

Figure 3.3. Identification of *unc-55* targets via gene expression profiling of GABAergic motor neurons. (**A**) Experimental design: In wild-type L2 larvae, synaptic remodeling genes are expressed in DD motor neurons but not in VD motor neurons; in *unc-55(e1170)* larvae, synaptic remodeling genes are also expressed in VD motor neurons. (**B**) Pearson correlation coefficients (R^2) for *unc-55* GABAergic datasets 509DMM45, 509DMM46, 509DMM50, and 509DMM51 were calculated from normalized probe intensity. (**C**) Volcano plot indicating transcript expression in L2 *unc-55* GABAergic motor neurons relative to wild-type GABAergic motor neurons. A score, which indicates significance of change in normalized probe intensities relative to reference, was calculated with SAM for all transcripts. A high score indicates high significance; the horizontal cut-off line corresponds to a false discovery rate of 1% among the 199 significantly enriched/depleted transcripts. Transcripts significantly enriched at least 2-fold in *unc-55* mutants (188) are indicated in red and transcripts at least 2-fold depleted (11) are indicated in green. Most transcripts were not significantly different from wild-type and are represented in gray. Note right-ward bias of the distribution, indicating that more transcripts are enriched in *unc-55* mutants than depleted as predicted by previous studies indicating that UNC-55 primarily functions as a repressor. (**D**) Gene ontology of transcripts enriched at least 2-fold in *unc-55* L2 GABAergic motor neurons compared to wild-type (1% FDR), *i.e.* candidate *unc-55* targets. Only 95 transcripts (of 188) are included in the chart; five genes in other categories and 88 uncharacterized genes were excluded. For a complete list of transcripts enriched in *unc-55* GABAergic motor neurons, see **Table 3.2**.

Of the 188 candidate *unc-55* targets identified in our analysis, 79 (42%) are conserved in humans (BLAST E-value >10) (**Table 3.2**), and 88 of the 188 candidate remodeling genes (46%) are novel genes with uncharacterized function. The remaining 100 *unc-55* candidate targets were classified into functional groups based on KOGs, BLAST homologue function, or other identifying information using previously published gene classes (**Figure 3.3D**). We found a wide range of cellular functions encoded among these putative synaptic remodeling genes, including ion channels (*e. g.* degenerin-family acid sensing ion channel *unc-8*, aquaporin *aqp-4*), cytoskeletal/trafficking regulators (*e. g.* Arp2/3 complex component *arx-5*, Centaurin β ArfGAP *cnt-1*), and proteins that likely function in remodeling the extracellular matrix (two matrix metalloproteases, fourteen collagens).

UNC-55 may directly regulate some candidate targets identified in the microarray profile

To verify that our microarray dataset represents *unc-55* regulated genes, we looked for enrichment of the COUP-TFII binding site within 2 kb of upstream regulatory regions among our candidate targets. The canonical COUP-TFII binding half-site TGACCT (Pereira et al., 2000) is present at least once in 92/188 candidate *unc-55* targets (49%), which is significantly more frequent than the motif appearing in the 2 kb upstream region of all annotated genes (7142/17,704 or 40%, p=0.02, Fisher's Exact Test). The presence of the non-canonical COUP-TFII binding site TGACCC (Montemayor et al., 2010) is also significantly

Table 3.2. Genes enriched in *unc-55* GABAergic motor neurons

Sequence Name	Gene Name	Description	Fold Enrichment	Human Homologue?
		Channels and Membrane Proteins		
R13A1.4	*unc-8*	ASIC/DEG/ENaC	4.0	yes
C33G3.3	*lgc-21*	ligand-gated ion channel	3.5	
Y58A7A.1		copper transporter	2.4	
ZC13.4	*mab-7*	EGF-domain containing	2.4	
F40F9.9	*aqp-4*	aquaporin	2.4	yes
C25E10.5		predicted transporter	2.4	yes
F53H8.3		permease	2.3	yes
K03B8.9	*deg-3*	acetylcholine receptor	2.2	yes
F21F8.11		permease	2.2	yes
Y39D8C.1	*abt-4*	ABC transporter	2.2	yes
F28H1.4		chemokine-like factor	2.2	yes
		Fibronectins		
F26G1.5		Fibronectin	5.9	
C42D4.3		Fibronectin	5.0	
F35B3.4		Fibronectin	3.5	
		Cytoskeleton		
H06A10.1		spindle matrix formation protein	3.1	
Y37D8A.1	*arx-5*	Arp2/3 subunit	2.1	yes
		Transcription		
F55D12.4	*unc-55*	COUP-TFII	3.2	yes
T14F9.5	*lin-32*	Atonal transcription factor	2.5	yes
C36F7.1	*irx-1*	Iroquois transcription factor	2.5	yes
T22B7.1	*egl-13*	SOX5 transcription factor	2.2	yes
		FGF pathway		
T23B12.5		FGF receptor activating protein	2.7	yes
M176.6	*kin-15*	FGF receptor related	2.1	yes
		G protein signaling		
D1079.1		7-transmembrane receptor	2.6	
Y70D2A.1		7-transmembrane receptor	2.2	
Y17G7B.15	*cnt-1*	centaurin beta ArfGAP	**	yes
		Neuro-related		
Y43F8C.2	*nlp-26*	neuropeptide-like	2.2	yes
F23H12.1	*snb-2*	synaptobrevin-related	2.0	yes
		Calcium binding		
H10E21.4		calmodulin	5.8	yes
Y69H2.3		fibrillin	2.3	yes
F35D2.3		fibrillin	2.2	yes
		Iron binding		
W08E12.3		Iron ion binding	3.0	
W08E12.4		Iron ion binding	2.9	

Sequence Name	Gene Name	Description	Fold Enrichment	Human Homologue?
W08E12.2		Iron ion binding	2.6	yes
		Lectins		
R07C3.12	*clec-44*	C-type lectin	2.8	yes
Y38E10A.5	*clec-4*	C-type lectin	2.4	yes
		Lipid-binding		
C06E8.5		LPS binding protein	4.8	
F10D11.6		lipid-binding glycoprotein	3.1	yes
C06G1.1		LPS binding protein	2.3	
		Ubiquitin		
C28G1.1	*ubc-23*	huntingtin interacting E2 ligase	2.2	yes
		Secreted surface proteins		
F48G7.8		Secreted surface protein	8.1	
T05B4.11	*phat-5*	Secreted surface protein	3.6	
F23B12.4		Secreted surface protein	2.6	
F48G7.5		Secreted surface protein	2.3	
F01D5.5		Secreted surface protein	2.2	
F21A3.3		secreted EGF-domain containing	2.2	
		Hedgehog-related		
T18H9.1	*grd-6*	Groundhog family	6.6	yes
ZC168.5	*grl-21*	hedgehog-like	5.3	
F41E6.2	*grd-5*	Secreted surface protein	3.4	
F42C5.7	*grl-4*	Groundhog-like	3.1	yes
		Collagens		
C50B6.4	*col-161*	collagen type IV/XIII	5.6	yes
F08G5.4	*col-130*	collagen type IV/XIII	5.3	yes
M195.1	*col-77*	collagen type IV/XIII	4.5	yes
F09G8.6	*col-91*	collagen type IV/XIII	3.4	yes
C46A5.3	*col-14*	collagen type IV/XIII	3.4	yes
F38A3.2	*ram-2*	collagen type IV/XIII	3.2	yes
C44C10.1	*col-180*	collagen type IV/XIII	3.1	yes
C09G5.4	*col-39*	collagen type IV/XIII	3.1	yes
F33D11.3	*col-54*	collagen type IV/XIII	2.9	yes
F15H10.2	*col-13*	collagen type IV/XIII	2.8	yes
F15H10.1	*col-12*	collagen type IV/XIII	2.7	yes
B0024.2	*col-150*	collagen	2.3	yes
F57B1.3	*col-159*	collagen type IV/XIII	2.1	yes
T11B7.3	*col-118*	cuticle collagen	2.0	yes
		Peptidase inhibitors		
F45G2.5	*bli-5*	endopeptidase inhibitor	5.3	
K08B4.6	*cpi-1*	cysteine protease inhibitor	4.5	
F35B12.4		endopeptidase inhibitor	4.3	
C54D10.10		endopeptidase inhibitor	3.7	yes
F32D8.7		endopeptidase inhibitor	2.8	

Sequence Name	Gene Name	Description	Fold Enrichment	Human Homologue?
		Metalloproteases		
T19D2.1		predicted ADAM	4.0	yes
F57C12.1	*nas-38*	astascin/BMP-1 related	3.7	yes
		Other Enzymes		
K08E3.1	*tyr-2*	tyrosinase	4.4	yes
W01A8.6		carboxypeptidase	4.2	yes
C11E4.1		glutathione peroxidase	3.7	yes
Y18H1A.9		Zinc carboxypeptidase	3.2	yes
R11A5.7		Zinc carboxypeptidase	3.1	yes
R07G3.2	*lips-17*	Triacylglycerol lipase	3.0	
K01A2.5		predicted hydrolase	3.0	yes
C46H11.2		Flavin-containing monooxygenase	3.0	yes
T09B9.1		predicted esterase	2.6	yes
ZK430.8	*mlt-7*	peroxidase	2.5	yes
T05H4.7		predicted chitinase	2.5	
ZC434.9		predicted carboxypeptidase	2.3	yes
F59B2.3		N-acetyl-glucosamine-6-phosphate deacetylase	2.3	yes
F20G2.1		Predicted short chain-type dehydrogenase	2.3	yes
C26F1.2	*cyp-32A1*	cytochrome p450 family	2.3	yes
T10E9.3		histidine catalysis	2.3	
F36G9.12	*oac-20*	O-acyltransferase	2.2	
C42C1.7	*oac-59*	integral membrane O-acyltransferase	2.2	
F14E5.5	*lips-10*	triacylglycerol lipase	2.2	
K06A4.5	*haao-1*	3-hydroxyanthranilate oxygenase	2.1	yes
F14B6.6		galactosyltransferase	2.1	
M03A8.1	*dhs-28*	17-beta-hydroxysteroid dehydrogenase	2.1	yes
ZC455.10	*fkb-4*	peptidylprolyl isomerase	2.1	yes
T05C3.6		phospholipase	2.0	yes
		Other		
T03F7.7		SEC14-related	2.8	yes
F49H12.3		KCTD-domain containing	2.5	
Y37B11A.2		DNA polymerase	2.2	yes
R02E12.6	*hrg-1*	vacuolar H+-ATPase associated	2.2	
Y92C3B.1	*kbp-4*	kinetochore binding protein	2.1	
Y113G7B.12		reverse transcriptase	2.1	yes
		Novel/uncharacterized		
Y47D7A.15			6.2	
F35C5.10	*nspb-11*		5.8	
F07F6.5	*dct-5*		5.7	
H04M03.2	*nspb-6*		5.4	
F43C11.3			5.2	

Sequence Name	Gene Name	Description	Fold Enrichment	Human Homologue?
K04C2.5			5.2	
ZK970.7			5.0	
F09F7.8	*nspb-12*		4.9	
C49H3.12			4.8	
F35A5.3	*abu-10*		4.5	yes
K10H10.4			4.4	
C38C6.6	*tag-297*		4.4	
T21C9.9			4.4	
ZK1307.2			4.3	
ZK682.5			4.3	yes
C05E7.2			4.3	
Y77E11A.14			4.2	
W01B11.5	*pqn-72*		4.0	yes
ZK662.2			3.9	
R09B5.5	*pqn-54*		3.8	yes
R07B1.9			3.8	
R09F10.7	*pqn-57*		3.8	yes
T01D1.6	*abu-11*		3.8	yes
B0034.1			3.7	
C26F1.1			3.6	
M03E7.2			3.6	
T23F1.6	*pqn-71*		3.5	yes
K01D12.5			3.4	
F39D8.1	*pqn-36*		3.4	yes
F45E4.5			3.4	
Y95B8A.2			3.4	
Y46G5A.20			3.3	yes
D2096.6			3.3	
F20B10.3			3.3	
C02D4.1	*jud-4*		3.2	
F14B8.4			3.2	
M28.8			3.2	
F38A5.10	*nspb-4*		3.1	
C50F7.5			3.1	yes
K02B7.3			3.1	
R07E5.4			2.9	
Y7A9D.1			2.8	
Y40C7B.4			2.8	
F38A5.5	*nspb-3*		2.8	
C55A6.12			2.7	
R13A5.3	*ttr-32*	transthyretin-like domain containing	2.7	
F56B6.6			2.7	
T14A8.2			2.7	

Sequence Name	Gene Name	Description	Fold Enrichment	Human Homologue?
T24C4.4			2.7	
C05E7.1			2.7	
C02E7.7			2.7	
T25G12.3			2.7	
K11H12.4			2.6	
B0310.6			2.6	
Y69A2AR.28			2.6	
F53H4.3			2.6	
F55G11.4			2.6	
T05A7.1			2.6	
W01F3.2			2.6	
C35C5.9			2.5	
F35E12.8			2.5	
W03F8.6			2.4	
T05D4.4	*osm-7*		2.4	
Y66A7A.7			2.4	
C49F5.7			2.4	
F42C5.10			2.4	
C10C5.2			2.4	
Y45F10A.7			2.3	
C08B6.3			2.3	
F14B8.7			2.3	yes
Y45G12C.1			2.3	
F46C8.8			2.3	
T17H7.7			2.2	
F23H11.6			2.2	
Y75B8A.39			2.2	
Y69E1A.5			2.2	yes
F01D5.6			2.1	
F36G3.1			2.1	yes
C04E12.2			2.1	
F35E12.7	*dct-17*		2.1	
F18E9.3			2.1	yes
K04A8.1			2.0	
Y37D8A.16			2.0	
K08D12.4			2.0	
C39H7.4			2.0	
Y97E10AR.3			2.0	
ZK154.1			2.0	
R90.2	*ttr-27*	transthyretin-like domain containing	2.0	

enriched over all 2 kb promoter regions (50/138 or 27% in *unc-55* target promoters vs. 4569/17,704 or 21% in all promoters, $p < 0.05$, Fisher's Exact Test) (**Figure 3.4A**). We predict that these non-canonical binding motifs may be important based on high conservation among distantly related nematode species. For example, three conserved non-canonical half-sites were identified in the upstream regulatory region of a candidate *unc-55* target, the homeodomain-containing protein *irx-1/Iroquois* (see further discussion in **Chapter IV**).

We next asked if we could validate our *unc-55* microarray results via promoter::GFP transgenic strains, reasoning that remodeling genes may be normally expressed in DD motor neurons and de-repressed in *unc-55* mutants. Transcriptional reporters for seven candidate genes containing putative UNC-55 binding sites in the *cis*-regulatory region were obtained from the *C. elegans* Gene Expression Consortium (Hunt-Newbury et al., 2007) (see **Methods** for full strain list); for *nlp-26,* we built a reporter strain with a plasmid kindly provided by the Hart lab (Nathoo et al., 2001). Each of these strains carry a transgenic array that includes the intergenic 5' region of a candidate *unc-55* target fused to the GFP coding sequence. Surprisingly, none of these transgenic strains express GFP in wild-type or *unc-55* GABAergic motor neurons (**Figure 3.4B**), but do show expression in other tissues (data not shown). Although it is possible that some of these genes are in fact not regulated by *unc-55* and are false positives in our microarray screen, it is also possible that at least a subset of these transgenic arrays do not contain the full complement of *cis*-regulatory elements required to recapitulate endogenous gene expression. We have confirmed that this latter

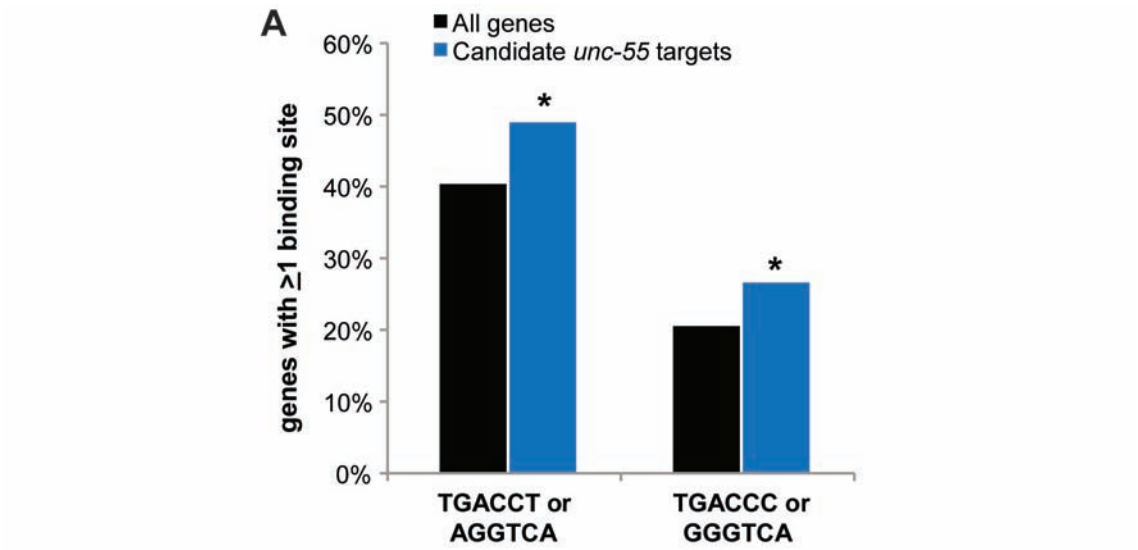

B

Gene Name	Description	Fold Enrichment	UNC-55 binding site 1	UNC-55 binding site 2	Exp. in DDs?	Exp. in *unc-55* VDs?
C11E4.1	glutathione peroxidase	2.79	-44-39		no	no
F23F12.9	leucine zipper TF	2.63	-1674-1669		no	no
nas-38	metalloprotease (BMP-1 rel)	3.78	-1634-1639		no	ND
K01A2.5	hydrolase precursor	3.09	-1899-1894	-1702-1697	no	no
T19D2.1	metalloprotease (ADAM)	4.52	-1325-1330		no	no
nlp-26	neuropeptide	3.44	-1693-1688	-647-642	no	no
C54D10.10	endopeptidase inhibitor	2.18	-1879-1884		no	no
abt-4	ATP binding cassette	2.13	-1443-1438		no	no

Figure 3.4. Analysis of UNC-55 binding sites in candidate target genes. (**A**) Percentage of genes with at least one putative *unc-55* binding site within 2 kb upstream of the transcription start site, among all genes (black) and those in the *unc-55* dataset (blue). The proportion of genes containing UNC-55 binding sites (TGACCT or TGACCC) is significantly higher than chance (i.e. found in all genes). * $p < 0.05$, Fisher's Exact test. (**B**) Candidate *unc-55* targets enriched in our dataset which contain UNC-55 binding sites were surveyed with available promoter::GFP transgenic strains. ND = no data.

explanation is in fact the case for *irx-1*, which does not show expression or regulation in GABAergic motor neurons with an intergenic promoter::GFP transgenic array (data not shown), but does display GFP expression that is largely restricted to remodeling motor neurons (DD and *unc-55* VD) in larval stages when expressed from an *irx-1::GFP* fosmid that includes 40 kb of genomic DNA surrounding the *irx-1* locus (see **Chapter IV**). In any case, we next focused our effort on utilizing a functional screen to identify the subset of *unc-55*-regulated transcripts for roles in synaptic remodeling.

Hedgehog-related proteins have a role in GABA motor neuron synaptic organization

Hedgehog (Hh) signaling has an established role in motor neuron fate determination in the vertebrate spinal cord (Jessell, 2000). In the developing vertebrate spinal cord, Sonic Hedgehog (Shh) is secreted from the ventral notochord and floorplate and functions as a graded morphogen to specify neuron identity in the spinal cord. Ventral V3 interneurons and motor neurons differentiate in the presence of high Hh levels while V1 and V2 interneurons, which are positioned more dorsally, are induced by lower Hh levels (Chiang et al., 1996; Ericson et al., 1996). During spinal cord development, diffusible Hh ligand binds to the Patched (Ptc) receptor on neuroblasts. Hh binding releases Ptc suppression of Smoothened (Smo) activity, which in turn activates Gli-mediated transcription (Stone et al., 1996; Quirk et al., 1997; Pan et al., 2006). Integration of Hh-signaling with other morphogens gradients results in expression

of a combinatorial code of homeodomain transcription factors that specify spinal cord neurons (Jessell, 2000). Although Hh signaling is crucial for development in other invertebrates and vertebrates, *C. elegans* does not appear to have a canonical Hh-signaling pathway due to the absence of a Smo homologue (Zugasti et al., 2005; Burglin and Kuwabara, 2006; Burglin, 2008). However, *C. elegans* Hh-related and Ptc-related proteins are required for key developmental events such as larval molting (Kuwabara et al., 2000; Zugasti et al., 2005; Hao et al., 2006a; Hao et al., 2006b).

We found enrichment of four Groundhog or Ground-like family members in our *unc-55* candidate target list, *grd-5*, *grd-6*, *grl-4*, and *grl-21*. These are predicted to encode Hh-like ligands with conserved C-terminal autocatalytic domains and similar N-terminal signaling sequences (Aspock et al., 1999). Additionally, the Hedgehog modulator Glypican, *gpn-1/dally-like* (Burglin and Kuwabara, 2006), and multiple V0-ATPase (*vha*) genes involved in secretion of Hh-related proteins (Liegeois et al., 2006) are enriched in the wild-type dataset of GABA neurons (**Figure 3.2**) by 1.8-fold. Together, these data suggest a role for Hh-related signaling in GABA neuron synaptogenesis.

These findings suggest that RNAi knockdown of these Hh-related genes may cause synaptic remodeling defects in the DD motor neurons (**Figure 3.5A**). To test this idea, we ablated *grd-5*, *grd-6*, and *grl-4* function by the RNAi feeding method in a hypersensitive line carrying a GFP-labeled synaptic vesicle marker (*eri-1; juIs1[punc-25::SNB-1::GFP]*) (Hallam and Jin, 1998; Timmons et al., 2001; Kennedy et al., 2004). Animals treated with *grd-5*, *grd-6*, or *grl-4* RNAi appear to

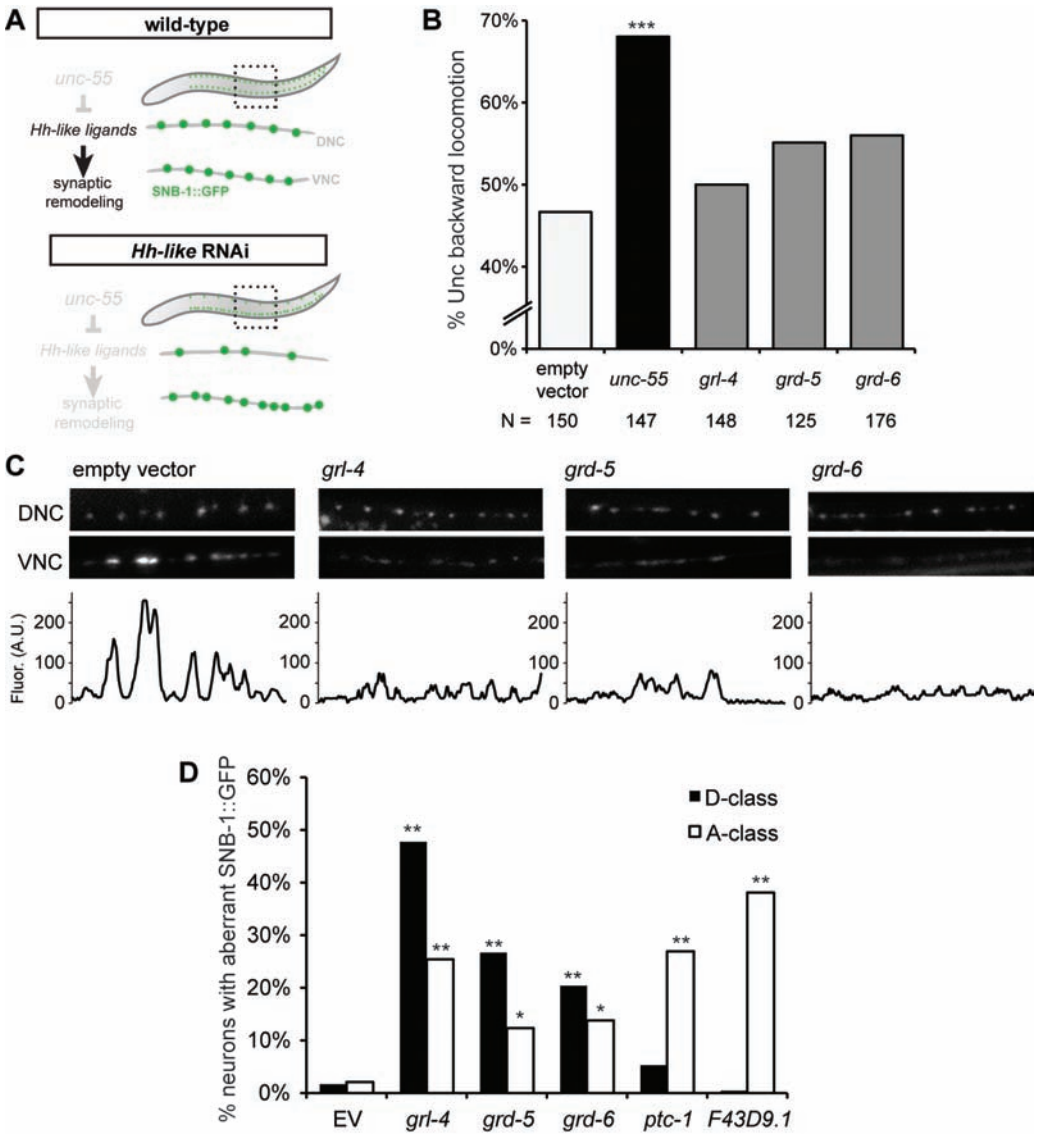

Figure 3.5. Knockdown of Hedgehog-related genes causes defects in both GABAergic and cholinergic motor neurons. (**A**) Predicted function for Hh-like ligands regulated by *unc-55*. Based on their enrichment in *unc-55* VD motor neurons, Hh-like proteins were predicted to promote remodeling in wild-type DD motor neurons and contribute to the localization of SNB-1::GFP puncta (marking GABAergic NMJs) in the dorsal nerve cord (DNC). In animals treated with RNAi against Hh-like proteins *grl-4*, *grd-5*, or *grd-6*, we predicted a loss of dorsal NMJs and concurrent gain in ventral NMJs due to a disruption in the synaptic remodeling program. (**B**) Percentage of L4 animals displaying uncoordinated backward locomotion when treated with RNAi against candidate synaptic remodeling genes. Empty vector served as a negative control; the Unc behavior in these worms is likely caused by the *eri-1* mutation used to sensitize the animals to RNAi. *unc-55* served as a positive control. *** $p < 0.01$, other bars are not significantly different from empty vector. (**C**) Representative views (20 μm) of GABAergic SNB-1::GFP in adult dorsal (DNC) and ventral (VNC) nerve cords. Defective synaptogenesis appears restricted to the ventral nerve cord; linescans (in arbitrary fluorescence units) are of the ventral nerve cord, indicating aberrant synapses. (**D**) Percentage of GABAergic (D-class, in black) and cholinergic (A-class, in white) neurons with ventral synaptic defects (as seen in panel **C**) in animals treated with RNAi against Hh-like ligands *grl-4, grd-5,* and *grd-6* or Patched-related proteins *ptc-1* and *F43D9.1*. * $p < 0.05$, ** $p < 0.01$, Student's t-test vs. control empty vector (EV) for each neuronal type.

have a backward movement defect compared to reference empty-vector treated animals (**Figure 3.5B**). This phenotype included slower backing, pausing, and variable body bend amplitude. Negative control animals (RNAi with empty vector) consistently showed a weak Unc phenotype that can be attributed to the *eri-1* mutation. Positive controls (*unc-55* RNAi) coiled upon backing as predicted. In all cases, RNAi-treated and mutant animals were evaluated in a blind test with controls. Thus, although the movement defect resulting from inactivation of these Hh-related genes is incompletely penetrant and not statistically different from empty-vector control, they are robust.

GABAergic synapses marked with SNB-1::GFP showed aberrant localization in the ventral nerve cord of adult animals after RNAi treatment of Hh-related genes (**Figure 3.5C**, bottom images and linescans). In contrast, GABAergic synapses in the dorsal nerve cord of Ground-RNAi treated animals were unaffected in comparison to the empty vector control (**Figure 3.5C**, top). These results suggest that Hh-related signaling pathways are essential for normal development of VD synapses in the ventral nerve cord but are not required for the creation of DD synapses in the dorsal nerve cord. The absence of a detectable role in DD remodeling is surprising given our results that Ground-family transcripts (*grd-5*, *grd-6*, *grl-4*, and *grl-21*) are de-repressed in *unc-55* mutant neurons. However, the potent effect in the ventral cord provides strong evidence of a previously unknown role for Hh-related protein function in synaptic assembly.

To determine if this effect is specific for GABAergic (D-class) motor neurons, we expanded our analysis to include the synapses of cholinergic (A-class) motor neurons using the synaptic marker *wdIs20[punc-4::SNB-1::GFP]*. When treated with RNAi to knock down Hh-related ligands *grl-4*, *grd-5*, and *grd-6*, both GABAergic and cholinergic synapses displayed partial but significant disorganization relative to control empty-vector treated animals (**Figure 3.5D**). Furthermore, we found that while D-class neurons were more sensitive to perturbations of Hh-related ligands than A-class, cholinergic motor neurons were uniquely affected by knockdown of Ptc-related receptors *ptc-1* and *F43D9.1* (**Figure 3.5D**). These data indicate a broad role for previously uncharacterized Hh-related ligands and receptors, and suggest that their function is not limited to GABAergic motor neuron synaptic remodeling.

These forward-genetic-screen experiments with wild-type animals, while revealing a previously unidentified purpose for Hh-related proteins in *C. elegans*, did not further our understanding of the *unc-55*-regulated synaptic remodeling pathway. Thus, we took a different approach involving a diagnostic RNAi screen with *unc-55* mutants to identify the subset of *unc-55* targets that function in GABAergic synaptic remodeling.

An RNAi screen reveals *unc-55* target genes that function in synaptic remodeling

UNC-55 is proposed to prevent synaptic remodeling by repressing transcription of specific target genes (Shan et al., 2005). This assumption

predicts that genetic ablation of these *unc-55* regulated genes should effectively "suppress" the Unc-55 synaptic phenotype by disabling the ectopic remodeling process. Therefore, we used RNAi (see **Methods**) to screen candidate *unc-55* targets (**Table 1**) for the restoration of GABAergic synapses to the ventral side of *unc-55* mutants (**Figure 3.6A-C**). Bacterial RNAi feeding clones for 138 of the 188 candidate *unc-55* targets available in the Ahringer RNAi library (Kamath et al., 2003) were tested for induction of ventrally localized SNB-1::GFP puncta in RNAi-treated *unc-55* animals vs. an empty vector negative control (see Methods) (**Figure 3.6D-E**). This assay revealed multiple suppressors of the Unc-55 phenotype, including the C-lectin *clec-44*, the Iroquois homeodomain-containing transcription factor *irx-1*, the DEG/ENaC channel subunit *unc-8*, the Arp2/3 subunit *arx-5*, the Hedgehog-related ligand *grl-4*, and the synaptobrevin homologue *snb-2* (**Figure 3.6F**). In total, this screen detected significant RNAi suppression of the Unc-55 synaptic phenotype in 49 candidate *unc-55*-regulated genes for a hit rate of ~40%. We note that 19 of these synaptic remodeling genes are conserved in humans (**Figure 3.6G, Table 3.3**). Genes in our microarray profile that do not show RNAi suppression of the Unc-55 remodeling phenotype could be involved in other *unc-55*-dependent traits.

We have begun to explore the roles of these candidate *unc-55* targets in synaptic remodeling. Below are our preliminary results for the ArfGAP *cnt-1* and the Arp2/3 complex component *arx-5*; in **Chapter IV**, I describe a comprehensive characterization of the homeodomain-containing protein *irx-1/Iroquois* in synaptic remodeling; **Chapter V** presents additional results pointing to a role for the

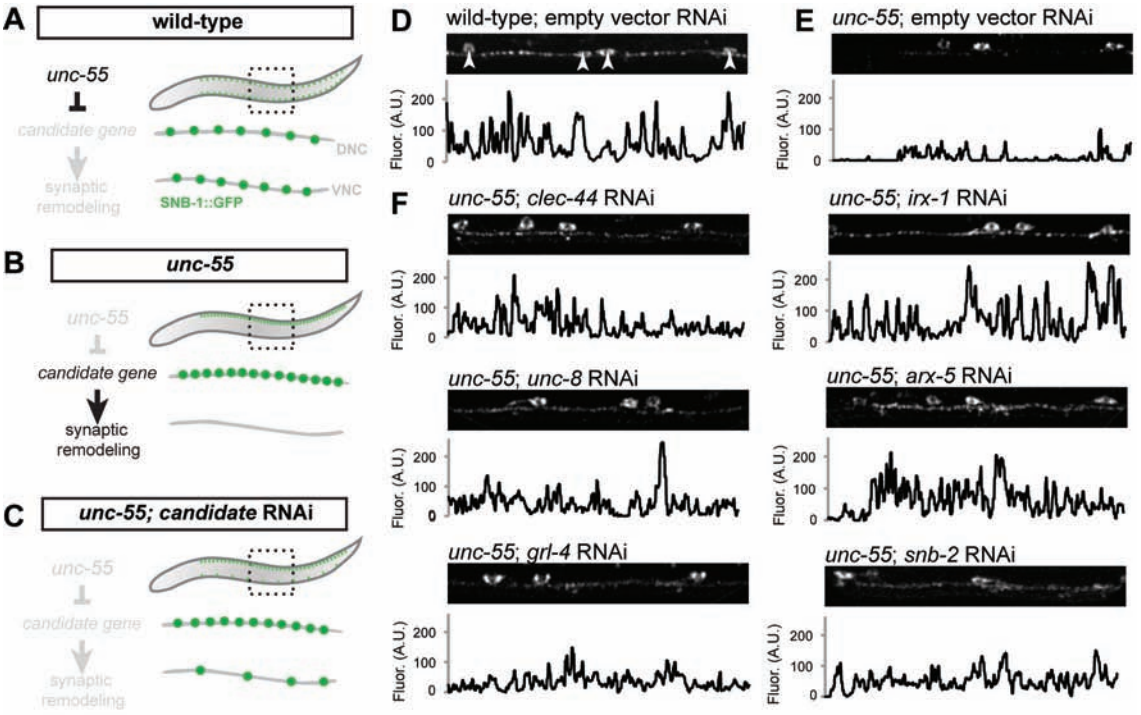

G

RNAi	Gene Description	N	Penetrance	# ventral puncta
empty vector		114		30.1
cnt-1	centaurin beta ArfGAP	21	86%	59.0
clec-44	C-type lectin	19	95%	55.2
C11E4.1	glutathione peroxidase	20	75%	52.9
irx-1	Iroquois transcription factor	27	81%	52.5
unc-8	ASIC/DEG/ENaC	62	81%	51.1
arx-5	Arp2/3 subunit	16	75%	50.1
col-54	collagen type IV/XIII	20	65%	47.8
K01A2.5	predicted hydrolase	19	68%	47.4
col-12	collagen type IV/XIII	19	68%	47.3
F20G2.1	short chain-type dehydrogenase	20	75%	47.3
nas-38	astascin/BMP-1 related	19	68%	46.4
ZC434.9	predicted carboxypeptidase	19	63%	45.9
T19D2.1	predicted ADAM	18	78%	45.6
pqn-36	uncharacterized prion protein	20	80%	44.2
grl-4	hedgehog-like	19	63%	42.8
snb-2	synaptobrevin-related	20	60%	42.6
T23B12.5	FGF receptor activating protein	20	60%	42.6
col-77	collagen type IV/XIII	15	60%	41.2
F28H1.4	chemokine-like factor	14	50%	39.6

Figure 3.6. RNAi of candidate UNC-55 targets identifies genes required for synaptic remodeling. (**A-C**) Experimental design of Unc-55 suppression screen. (**A**) In wild-type animals, SNB-1::GFP puncta (marking GABAergic NMJs) localize to both dorsal and ventral nerve cords. (**B**) In *unc-55* animals, synaptic remodeling genes are de-repressed in VD motor neurons and SNB-1::GFP is depleted from the ventral nerve cord. (**C**) RNAi knockdown of UNC-55 target genes in *unc-55* mutants disrupts synaptic remodeling and restores SNB-1::GFP puncta to the ventral nerve cord. (**D-F**) Representative views (50 μm length) of GABAergic SNB-1::GFP in adult ventral nerve cords. Linescans (in arbitrary fluorescence units) of the ventral nerve cord (excluding DD/VD cell bodies, see arrowheads in panel D). (**D**) SNB-1::GFP puncta are abundant in the ventral nerve cord of wild-type adults (**E**) but largely absent from *unc-55(e1170)* mutant animals treated with control RNAi (empty vector). (**F**) RNAi knockdown of candidate *unc-55* targets (*clec-44, irx-1, unc-8, arx-5, grl-4, snb-2*) in *unc-55* mutants partially restores ventral SNB-1::GFP puncta. (**G**) Conserved hits from Unc-55 RNAi suppression screen. Hits were scored as significantly different from empty vector control ($p < 0.01$, Student's t-test) with restoration of ventral SNB-1::GFP puncta in $\geq$50% of animals scored. N represents all animals scored, combined from at least two separate RNAi treatments (see Methods). Boxes on the box-and-whisker plot span the 25th to 75th percentile and whiskers indicate the minimum/maximum number of ventral puncta observed; the vertical line in each box indicates the 50th percentile. Conserved hits show < e^{-10} vs. human homologues by BLAST.

Table 3.3. *unc-55*-regulated synaptic remodeling genes identified via microarray and RNAi suppression screens

Protein Type	Enriched in microarray[1]	Screened for Unc-55 suppression	Hits[2]	Conserved Hits[3]	Gene Names
channels and membrane proteins	11	9	4	2	*unc-8, F28H1.4*
secreted surface protein	6	4	1	0	
Hedgehog-like family	4	3	1	1	*grl-4*
G-protein signaling	2	3[†]	2	1	*cnt-1*
fibronectin	3	2	0	0	
lectin	2	1	1	1	*clec-44*
transcriptional control	5	4	2	1	*irx-1*
cytoskeleton	2	2	1	1	*arx-5*
lipid binding	3	3	1	0	
calcium binding	3	3	0	0	
iron binding	3	0	0	0	
FGF signaling	2	2	1	1	*T23B12.5*
neuro-related	2	2	1	1	*snb-2*
ubiquitin	1	1	0	0	
peptidase inhibitor	5	5	1	0	
metalloprotease	2	2	2	2	*nas-38, T19D2.1*
other enzyme	24	19	9	4	*C11E4.1, F20G2.1, K01A2.5, ZC434.9*
collagen	14	11	3	3	*col-12, col-54, col-77*
other	6	1	0	0	
novel/uncharacterized	88	61	19	1	*pqn-36*
Total	**188**	**138**	**49**	**19**	

[1] determined by ≥2-fold enrichment, 1% false discovery rate

[2] determined by significant enrichment of ventral SNB-1::GFP puncta and a phenotype observed in at least 50% of animals screened, see **Methods**

[3] determined by BLAST score less than 10^{-10}

[†] ArfGAP *cnt-1* added to candidate target RNAi screen based on its enrichment in a dataset with less stringent SAM parameters (≥1.5x enrichment, 5% false discovery rate)

DEG/ENaC cation channel subunit, UNC-8, in an activity-dependent mechanism of synaptic remodeling.

cnt-1, a Centaurin β ArfGAP homologue, is required for *unc-55* remodeling

The combined approach of microarray and RNAi screening (**Table 3.3**) revealed *cnt-1* as a candidate UNC-55 target necessary for synaptic remodeling. *cnt-1* encodes a protein related to Centaurin β, an ADP-ribosylation factor (Arf) family GTPase activating protein (GAP) which also contains C-terminal ankyrin repeats and a pleckstrin homology (PH) domain predicted to bind phosphoinositides. The ArfGAP domain in Centaurin family proteins regulates the small GTPase Arf, which has defined roles in actin assembly at the plasma membrane as well as in vesicular sorting and trafficking in the Golgi (Randazzo et al., 2007; Myers and Casanova, 2008). At the plasma membrane, Centaurins can link Arf activity with phosphatidylinositol (PI) second-messenger signaling via interaction with the PH domain (Jackson et al., 2000). PI pathway components, such as the lipid kinase PI3K, have been shown to regulate synaptic stabilization in long-term potentiation (Kelly and Lynch, 2000; Kim et al., 2011). Interestingly, GIT (GPCR kinase interacting proteins) proteins also contain ArfGAP domains at their N-termini and associate with Liprin-α (*C. elegans* SYD-2) to organize synaptic active zone assembly (Kim et al., 2003; Hoefen and Berk, 2006). Furthermore, an Arf-like GTPase, ARL-8*,* was recently shown to regulate synaptic vesicle precursor trafficking in *C. elegans* neurons by physically traveling with synaptic components, suggesting that proper activation of Arfs may

be key to regulating synaptic trafficking and/or localization (Klassen et al., 2010). Because of these intriguing connections, we examined *cnt-1* to explore its potential roles in synaptic remodeling.

Based on its close similarity to vertebrate Centaurin β, *C. elegans* CNT-1 is predicted to adopt similar roles, but this possibility has not been previously addressed. To elucidate a potential role for CNT-1 in remodeling, Vanderbilt undergraduate Alyssa Fesmire and I analyzed a *cnt-1* deletion allele (*tm2313*), available from the Mitani Lab and the National Bioresource Project. This *cnt-1* allele removes 341 bp of coding sequence (**Figure 3.7A**), resulting in deletion of part of the ArfGAP domain and part of the PH domain. When we crossed *cnt-1(tm2313)* into *unc-55(e1170)* mutants, we found that SNB-1::GFP was partially restored to the ventral nerve cord and also relatively depleted from the dorsal nerve cord (**Figure 3.7B**). Quantification of SNB-1::GFP fluorescence along the length of *unc-55; cnt-1* dorsal nerve cords revealed a significant reduction in SNB-1::GFP (**Figure 3.7C**). However, Alyssa noticed that expression of the SNB-1::GFP transgene is sometimes diminished in the *cnt-1* background, and it is possible that the reduction in dorsal SNB-1::GFP may be due to transgene silencing. Because of this possibility, Alyssa specifically looked for restoration of SNB-1::GFP in the ventral nerve cord in the "VD anterior region" (i.e. the ventral neurite immediately anterior to each VD soma) of VD motor neurons expressing high SNB-1::GFP in the soma indicating that the transgene is not silenced. We found that SNB-1::GFP is in fact restored to the ventral nerve cord of *unc-55; cnt-1* double mutants (**Figure 3.7D**), confirming our RNAi result. These data suggest

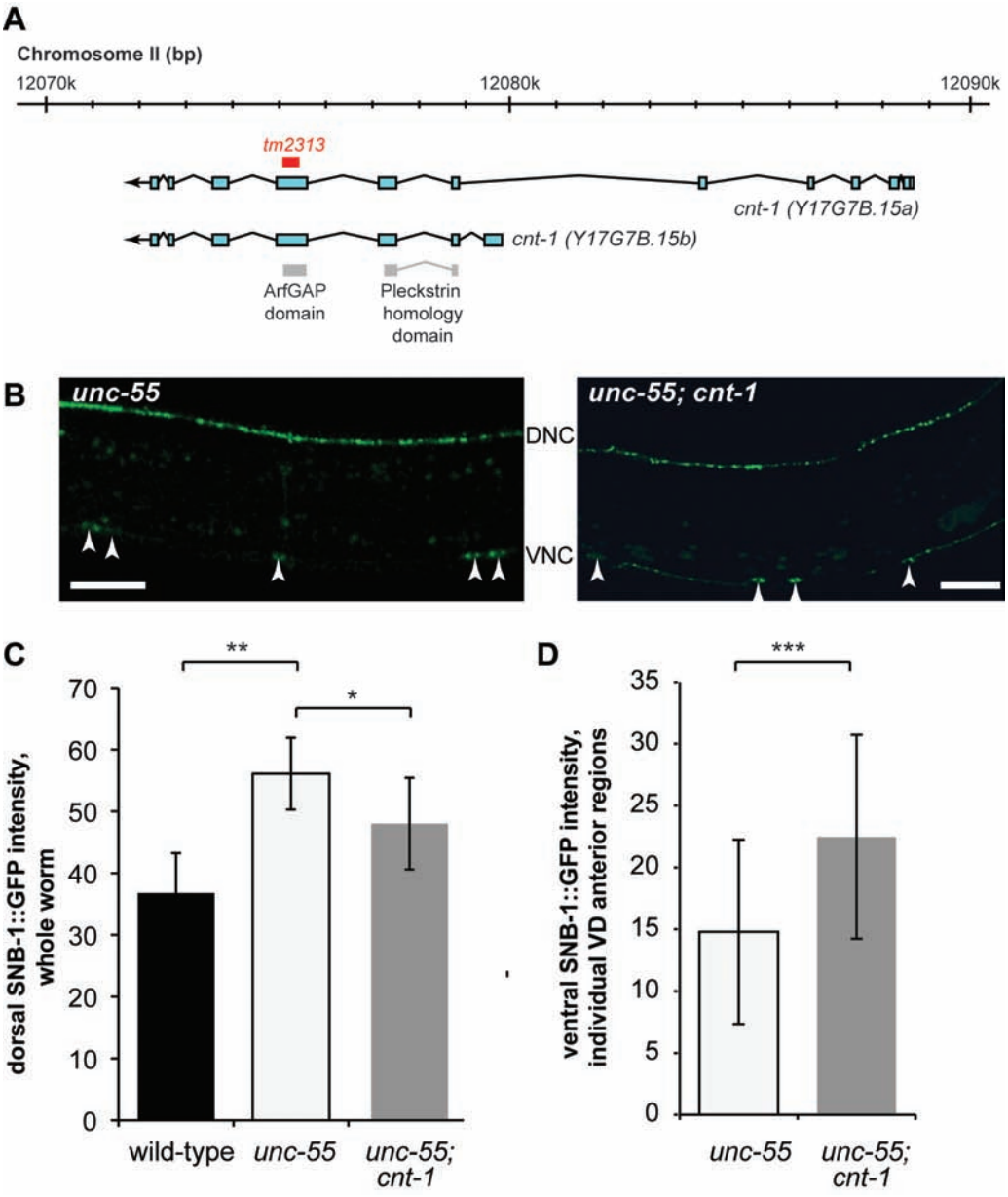

Figure 3.7. *cnt-1(tm2313)* suppresses *unc-55* VD remodeling. (**A**) The exon structure of the *cnt-1* locus on Chromosome II. *cnt-1* has two predicted isoforms; the *tm2313* deletion (red) removes the sequence that encodes the predicted ArfGAP domain (gray) in both isoforms. (**B**) SNB-1::GFP localization in the dorsal (DNC) and ventral (VNC) nerve cords of *unc-55* and *unc-55; cnt-1* adults. Note decreased density of puncta in the dorsal nerve cord of *unc-55; cnt-1* double mutant with increased ventral fluorescence, indicating suppression of the Unc-55 defect. Arrowheads denote GABAergic neuron soma, scale bars indicate 10 μm. (**C**) SNB-1::GFP intensity (in arbitrary units) is increased in the dorsal nerve cord across the length of the animal of *unc-55* mutants due to ectopic VD remodeling but is reduced in *unc-55; cnt-1* mutant adults. * $p < 0.05$, ** $p < 0.01$, Students t-test. Error bars denote standard deviation. (**D**) SNB-1::GFP is increased in the ventral processes of *unc-55; cnt-1* double mutants, as indicated by measuring the fluorescence in the VNC of individual "VD anterior regions" (between adjacent VD cell bodies). Data not collected for wild-type. *** $p < 0.001$, Student's t-test. Error bars denote standard deviation.

that CNT-1 is required for *unc-55* VD synaptic remodeling, perhaps by regulating Arf GTPase activity to mediate vesicular trafficking, for instance (see discussion of *arl-8* in **Chapter I**).

Arp2/3 complex component *arx-5* is required for remodeling but has broader roles in synaptogenesis

arx-5, the p21 subunit of the Arp2/3 complex (ARPC3) (Sawa et al., 2003), is another candidate *unc-55* target gene revealed in our RNAi screen. As noted in **Chapter I**, the enrichment of F-actin in both pre- and post-synaptic domains is well-documented, and Arp2/3 regulation of actin branching appears to govern actin organization at the synapse. (Dillon and Goda, 2005; Lin and Webb, 2009). Due to the enrichment of branched actin at dynamic synapses (*i.e.* dendritic spines) and the finding that F-actin is stabilized via increased synaptic activity (Wegner et al., 2008), we selected *arx-5* as an attractive *unc-55* candidate for elucidating the role of actin dynamics in synaptic remodeling.

To validate our RNAi results, we obtained a deletion allele of *arx-5, ok1990,* from the *C. elegans* Gene Knockout Consortium (**Figure 3.8A**). *ok1990* deletes the C-terminal half of the ARX-5 coding sequence and results in homozygous sterile adults which likely corresponds to the null phenotype. We determined that the *arx-5(ok1990)* mutation partially suppressed the ectopic accumulation of SNB-1::GFP in the dorsal nerve cord of *unc-55* mutant animals (**Figure 3.8B**). This effect is not observed in the *arx-5* single mutant which therefore rules out the possibility that *arx-5* is necessary for completion of DD

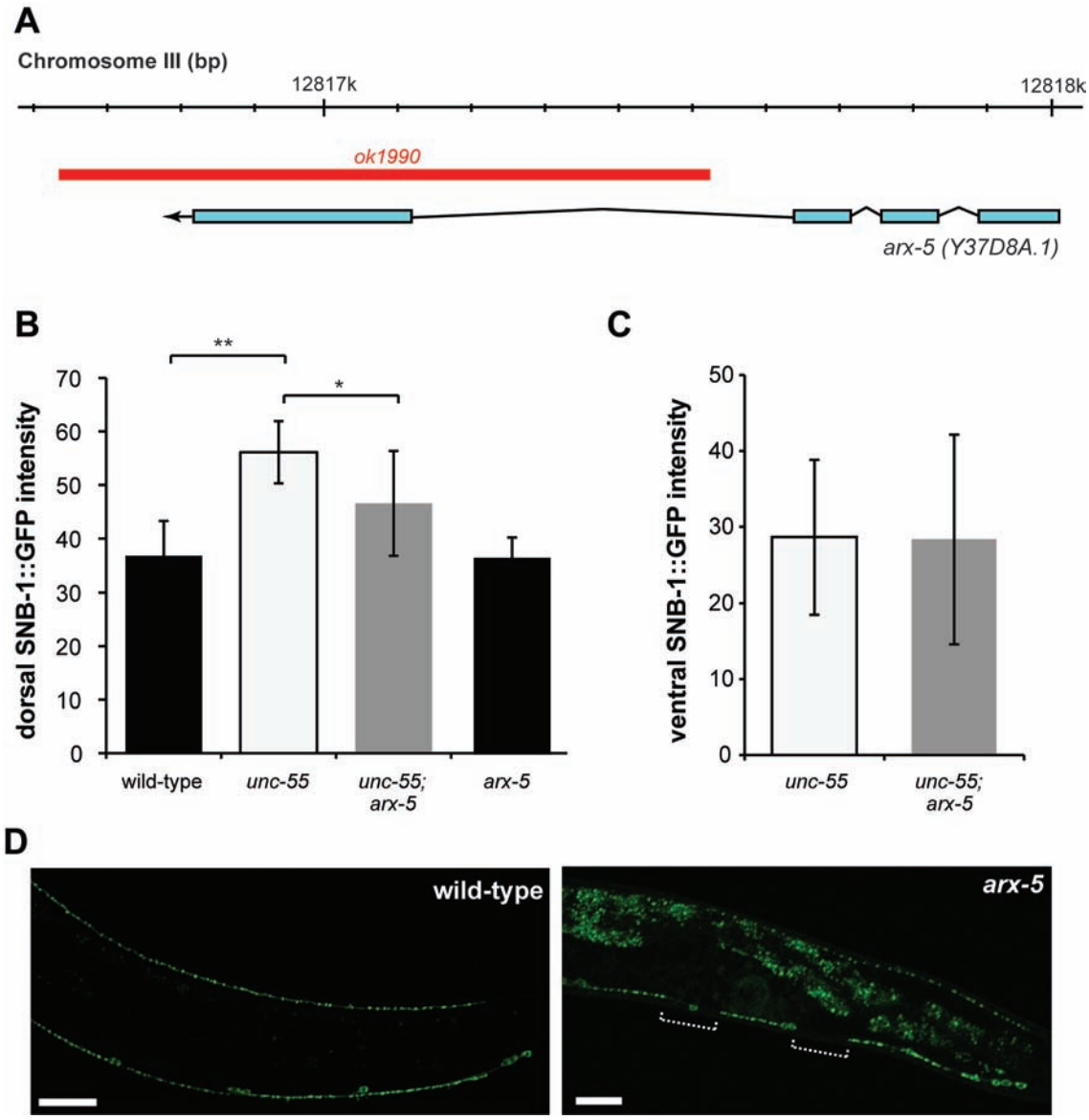

Figure 3.8. ***arx-5(ok1990)* blocks dorsal synaptogenesis in *unc-55* and causes gaps in ventral synaptogenesis.** (**A**) The exon structure of the *arx-5* locus on Chromosome III. The *ok1990* deletion (red) is a predicted null allele. (**B**) SNB-1::GFP intensity (in arbitrary units) is increased in the dorsal nerve cord across the length of the animal of *unc-55* mutants due to ectopic VD remodeling but reduced in *unc-55; arx-5* mutant adults. This reduction is specific to the *unc-55* ectopic remodeling defect; *arx-5* single mutants have dorsal fluorescence comparable to wild-type. * $p < 0.05$, ** $p < 0.01$, Students t-test. Error bars denote standard deviation. (**C**) SNB-1::GFP intensity (in arbitrary units) is unchanged in the ventral nerve cord of *unc-55; arx-5* adults compared to *unc-55.* Error bars denote standard deviation. (**D**) Wild-type SNB-1::GFP puncta are distributed evenly across the ventral nerve cord, whereas *arx-5(ok1990)* mutants show distinct gaps (dashed lines), potentially due to axon extension or synaptic patterning defects in VD motor neurons. Scale bars indicate 10 μm.

synaptic remodeling and, instead, argues for a role in ectopic remodeling in *unc-55* VD motor neurons (**Figure 3.8B**).

However, we did not see a increase in ventral fluorescence in the *unc-55(e1170); arx-5(ok1990)* double mutants at the adult stage (**Figure 3.8C**), as was previously observed with *arx-5* RNAi (**Figure 3.6**). This disparity may be due to a more severe effect of the null allele on *arx-5* function that blocks synaptogenesis in the ventral nerve cord. *arx-5* mutant have large asynaptic gaps in the ventral nerve cord (**Figure 3.8D**) which may be due to defects in patterning, trafficking, or axon extension. However, the dorsal cord appears unperturbed at this stage. This result suggests that *arx-5* must be available at some level for VD synaptogenesis. Further experiments are needed to test whether *arx-5(ok1990)* can block VD remodeling at younger stages, or if the additional defects observed in the mutant result in aberrant synaptogenesis throughout development and thereby prevent suppression of Unc-55.

Discussion

Microarray experiments reveal a gene expression profile of larval wild-type and *unc-55* GABAergic motor neurons

We used the mRNA-tagging technique to produce gene expression profiles for wild-type and *unc-55* larval GABAergic motor neurons (Von Stetina et al., 2007b; Watson et al., 2008; Spencer et al., 2011). Comparison of the wild-type GABAergic dataset to a reference profile (collected from all cells) identified over 1400 genes with potential roles in GABAergic development and function

(**Figure 3.1-2**). These GABAergic mRNA samples were also used in tiling arrays and compared to over thirty other tissue types by a fellow graduate student in the lab, Clay Spencer. This study identifies cohorts of genes that appear to be co-regulated and regulatory elements that may drive this differential gene expression (Spencer et al., 2011). These findings are particularly important because they can lead to future studies to clarify the roles of genes encoding novel or uncharacterized function in the GABAergic dataset.

Our goal was to use the mRNA tagging approach to uncover genes with potential roles in synaptic remodeling. Thus, we used the wild-type GABAergic profile as a reference for *unc-55* larval GABAergic gene expression to identify transcripts regulated by the synaptic remodeling repressor, UNC-55. This analysis revealed 188 transcripts with significant enrichment in *unc-55* mutant GABAergic motor neurons; these transcripts likely encode proteins with roles in executing the synaptic remodeling program in DD and *unc-55* VD motor neurons (**Figure 3.3**). We then used a functional genetic approach to identify which of these 188 genes are required for ectopic remodeling in *unc-55* mutant VD motor neurons.

unc-55 blocks expression of a complex synaptic remodeling program

Our RNAi suppression screen identified at least 50 genes that promote synaptic remodeling (**Table 3.3**). Whether these remodeling genes are also required for the creation of dorsal synapses awaits additional detailed analysis (see **Chapter IV** and **Chapter V** for studies on two of these targets). This in-

depth analysis will be crucial for developing models of how these downstream effectors control remodeling. Nineteen of these genes encode proteins with conserved human homologs and together embody a wide array of potential cellular functions (**Figure 3.6**). This finding parallels profiling results for the transcription factor Mef2 which also identified a diverse spectrum of downstream genes that affect synaptic assembly in the hippocampus (Flavell et al., 2008).

Other downstream effectors of synaptic remodeling revealed by our approach could fulfill additional roles. For example, RNAi knockdown of the DEG/ENaC cation channel subunit protein UNC-8 impedes the removal of ventral GABAergic motor neuron synaptic components in *unc-55* mutants. This finding indicates that wild-type UNC-8 protein functions in a biological process that destabilizes ventral synapses in remodeling VD motor neurons. A potential role for UNC-8 in synaptic plasticity is consistent with findings that members of the closely related ASIC (Acid Sensing Ion Channel) family are synaptically localized and contribute to learning and memory mechanisms that depend on neuronal activity (Coryell et al., 2007; Voglis and Tavernarakis, 2008; Zha et al., 2009). Our evidence suggests the additional possibility that ASIC proteins are also involved in developmentally regulated synaptic plasticity. In this context, we suggest that UNC-8 may fulfill an indirect role in the removal of ventral GABAergic synapses by stabilizing dorsal outputs.

A notable group of UNC-55-regulated genes revealed by our study points to an important role for the extracellular matrix (ECM) in synaptic remodeling. The mammalian neuromuscular junction is bisected by a basal lamina that

courses between presynaptic and postsynaptic membranes (Chiu and Sanes, 1984). This characteristic feature is preserved in *C. elegans* (White et al., 1986) and thus it is reasonable to expect that remodeling of GABAergic synapses could involve specific changes in ECM architecture. One of the ECM-related genes in our list, *clec-44,* encodes a presumptive C-lectin cell surface protein. A likely role for *clec-44* in synaptogenesis is supported by the finding that a related C-lectin, *clec-38*, contributes to the assembly of the presynaptic apparatus in *C. elegans* GABAergic motor neurons (Kulkarni et al., 2008). Potential ECM components regulated by *unc-55* include three collagen genes, *col-12, col-54* and *col-77*. Collagens fulfill multiple roles at the neuromuscular synapse such as anchoring neurotransmitter receptors and promoting synaptic maturation and maintenance (Fox, 2008; Latvanlehto et al., 2010). Recent reports indicate that GABAergic neurons in the mouse hippocampus (Su et al., 2010) and in the *C. elegans* motor circuit (Ackley et al., 2003) secrete specific collagens that promote synaptogenesis. Finally, our study found that two of the conserved synaptic remodeling genes encode the predicted matrix metalloproteases (MMPs), *nas-38* (a nematode astacin homologous to mammalian BMP1) and *T19D2.1* (predicted to function as A Disintegrin And Metalloproteinase, ADAM). Important roles for MMPs in synaptic plasticity are indicated by the findings that injury-induced remodeling and activity-dependent LTP in the hippocampus require MMP activity (Ethell and Ethell, 2007; Wang et al., 2008).

unc-55-regulated genes that function in synaptic remodeling are also crucial for synaptogenesis

In addition to identifying *unc-55*-regulated synaptic remodeling genes, this study also uncovered additional, broader synaptogenic roles for a subset of *unc-55* targets. Knockdown of Hh-related proteins *grl-4*, *grd-5*, and *grd-6*, resulted in defects in NMJ morphology in the ventral nerve cord. Although Hh has well-defined roles in cell differentiation in the spinal cord and other tissues, little is known about how Hh signaling might mediate synaptogenesis or synaptic remodeling. In the *Drosophila* retina, Hh is trafficked to the growth cone of photoreceptor neurons and released from the axon to induce differentiation of the postsynaptic neuron (Kunes, 2000; Chu et al., 2006). This suggests that Hh-like ligands may be expressed and secreted from *C. elegans* motor neurons to promote NMJ formation. Intriguingly, aberrant synaptic morphology from Hh-RNAi treatment was only observed in the ventral nerve cord, not the dorsal nerve cord. This result indicates that these components are necessary for synapses created by VD motor neurons, but are not required for DD synaptogenesis in the dorsal nerve cord. These results suggest the intriguing possibility that these Hh-related genes are expressed at a basal level for homeostatic roles in VD synaptogenesis in the ventral nerve cord, but that UNC-55 blocks higher levels of expression that contribute to a remodeling program that relocates VD synapses to the dorsal nerve cord. Additional studies with reporter genes, perhaps fosmid::GFP transgenes to more closely recapitulate endogenous gene expression, may be used to test this model.

Similarly, the Arp2/3 component, *arx-5*, appears to have roles in VD remodeling as well as normal morphology (**Figure 3.6, 3.8**). The Arp2/3 complex is composed of seven conserved components that function together to nucleate the formation of branched actin networks (Machesky and Gould, 1999). The observation that residual ventral VD synapses are retained with RNAi disruption of *arx-5* function in an *unc-55* mutant (**Figure 3.8**) suggests that reorganization of the actin cytoskeleton is required for their removal. This finding is intriguing because F-actin (filamentous actin) is a known synaptic component and has been shown to promote synaptic assembly and function (Dillon and Goda, 2005). Here, our results are consistent with an alternative model in which actin polymerization leads to disassembly of the presynaptic machinery. We also observed, however, that *arx-5* is required for normal VD morphology, suggesting that basal expression of *arx-5* in VDs promotes synaptogenesis while UNC-55 prevents higher expression that promotes remodeling. We are intrigued by the possibility that a single subunit of the Arp2/3 complex (composed of seven subunits) is transcriptionally regulated to tightly mediate synaptic placement. We predict that *arx-5*-mediated cytoskeletal reorganization could also depend on the *unc-55*-regulated synaptic remodeling gene, *cnt-1*, which encodes a conserved Centaurin-β Arf GTPase activating protein (ArfGAP). Arf family GTPases are key regulators of the actin cytoskeleton and vesicular trafficking in neurons (Myers and Casanova, 2008; Klassen et al., 2010).

Additional studies are now needed to elucidate the role of *cnt-1* in remodeling. Alyssa Fesmire found that *arf-1.1*, which encodes a protein related

to ARF1 in humans, is co-expressed with *cnt-1* in *unc-55* GABAergic motor neurons (1.5-fold enriched in *unc-55* mutants, 5% FDR). Additionally, a related Arf family member, *arf-1.2*, is enriched in the wild-type GABAergic dataset, suggesting differential Arf expression in remodeling vs. non-remodeling neurons. Centaurins are known to preferentially bind particular Arf GTPases (Jackson et al., 2000). Therefore, it would be useful for building a model of CNT-1 function to determine if either of these Arf GTPases is also involved in synaptic remodeling.

Conclusions

The phenomenon of synaptic plasticity is widely observed and crucially important to the development and maintenance of functional nervous systems (Consoulas et al., 2000; Bailey and Kandel, 2008; Barnes and Finnerty, 2010). Our approach has now discovered a large and diverse array of protein types with necessary roles in synaptic remodeling. Future studies will explore the specific functions of these components which offer a powerful opportunity to elucidate the molecular mechanism of this fundamental biological process. We have characterized the synaptic remodeling function of two of these genes, the transcription factor *irx-1/Iroquois,* and a degenerin, acid-sensing ion channel family member, *unc-8*, in subsequent chapters.

CHAPTER IV

IRX-1/IROQUOIS PROMOTES REMODELING OF GABAERGIC SYNAPSES DOWNSTREAM OF UNC-55/COUP-TF

Introduction

As detailed in **Chapter III**, we used candidate *unc-55* targets in an RNAi suppression screen to reveal suppressors of ectopic synaptic remodeling in *unc-55* mutants. Our approach yielded nineteen conserved synaptic remodeling genes. Of these, we selected *irx-1/Iroquois*, which encodes a homeodomain-containing transcription factor, for additional experiments to confirm its role in GABAergic remodeling.

The importance of homeodomain-containing transcription factors in patterning various tissue types has been well-established (De Robertis et al., 1991; Tsuchida et al., 1994; Akam, 1995). Typical homeobox genes contain a homeodomain consisting of 60 amino acids, whereas atypical homeobox genes contain a larger or smaller homeodomain. One subclass of atypical homeobox genes, TALE (Three-Amino acid Loop Extension in the homeodomain), includes the Iroquois family of transcription factors (Bertolino et al., 1995; Burglin, 1997). Iroquois family proteins are defined by the TALE homeodomain as well as a conserved 13-amino acid “IRO box” of unknown function (Burglin, 1997; Gomez-Skarmeta and Modolell, 2002).

Iroquois family transcription factors were first identified as regulators of proneural genes in *Drosophila* and *Xenopus* (Cavodeassi et al., 2001). During *Drosophila* dorsoventral eye patterning, Wnt and Hedgehog signaling in the dorsal eye primordium promote the expression of *iro* transcription factors. The boundary where dorsal Iroquois-expressing cells meet ventral non-expressing cells forms the midline of the compound eye. Misexpression of *iro* genes in the eye primordium results in the formation of an ectopic boundary (Cavodeassi et al., 1999). *Iroquois* family genes also are required for patterning vertebrate brain and spinal cord. In the chick brain, Irx3 defines the posterior half of the forebrain, whereas Irx2 patterns the hindbrain. The *Xenopus* Iroquois homologue, Xiro1, has a similar role in brain patterning (Gomez-Skarmeta and Modolell, 2002; Kobayashi et al., 2002). In the vertebrate spinal cord, Irx3 is activated in response to the Hh-gradient to specify dorsal interneuron fates (Briscoe and Ericson, 1999; Muhr et al., 2001).

Multiple Iroquois-family genes with tissue-specific roles are found in most model organisms (*i.e.* three in *Drosophila,* six in mice and humans). In contrast, *C. elegans* contains a single Iroquois homologue encoded by *irx-1* (Gomez-Skarmeta and Modolell, 2002; Mukherjee and Burglin, 2007). Prior to this study, the role of IRX-1 function in *C. elegans* was unknown. Because of the well-established role of Iroquois in neural development and the potential to identify a synaptic remodeling role for Iroquois, we selected *irx-1* from the list of Unc-55 suppressors for additional experiments. We have found that *irx-1* is indeed a key regulator of *C. elegans* synaptic remodeling, and study of *irx-1* offers an

attractive opportunity to characterize a new and potentially conserved role of *Iroquois* family members in synaptic remodeling.

Author Contributions

The IRX-1::GFP fosmid construct was built by Mihail Sarov, TransgeneOmics Facility at the Max Planck Institute of Molecular Cell Biology and Genetics. All electrophysiological assays were performed by Janet Richmond, University of Illinois at Chicago.

Methods

Strains and genetics: Nematode strains were maintained at 20-25°C with standard culture techniques (Brenner, 1974). The wild-type strain is N2 and all references to *unc-55* mutants used the allele *unc-55(e1170)* (Walthall, 1990). All animals used in this study were hermaphrodites.

Strain list:

note: *unc-119*(+) refers to *unc-119*-rescuing minigene from MM051 (Maduro and Pilgrim, 1995) (see details of strain construction)

<u>General synaptic remodeling analysis strains</u>:

CZ333 *juIs1[punc-25::SNB-1::GFP; lin-15+]*

NC1851 *unc-55(e1170); juIs1[punc-25::SNB-1::GFP; lin-15+]*

NC2296 *unc-119; juIs1[punc-25::SNB-1::GFP; lin-15+]; wdEx658[punc-25::mCherry::unc-54UTR, unc-119(+)]*

NC2319 *unc-55(e1170); unc-119; juIs1[punc-25::SNB-1::GFP; lin-15+]; wdEx658[punc-25::mCherry::unc-54UTR, unc-119(+)]*

ZM54 *hpIs3[punc-25::SYD-2::GFP; lin-15(+)]*

NC1849 *unc-55(e1170); hpIs3[punc-25::SYD-2::GFP; lin-15(+)]*

NC1859 *lin-6(e1466) dpy-5(e61)I/hT2[bli-4(e937) let(q782) qIs48](I;III); juIs1[punc-25::SNB-1::GFP; lin-15+]*

irx-1::GFP strains:

NC2233 *unc-119(ed3); wdIs78[irx-1::GFP; unc-119+ fosmid]*

NC2298 *unc-55; unc-119(ed3); wdIs78[irx-1::GFP; unc-119+ fosmid]*

irx-1(csRNAi) strains:

NC2111 *unc-119(ed3); wdEx686[pttr-39::irx-1::unc-10UTR; unc-119+; punc-25::mCherry::unc-54UTR; pttr-39::irx-1 antisense::unc-10UTR]*

NC2297 *unc-119(ed3); juIs1[punc-25::SNB-1::GFP; lin-15+]; wdEx686[pttr-39::irx-1::unc-10UTR; unc-119+; punc-25::mCherry::unc-54UTR; pttr-39::irx-1 antisense::unc-10UTR]*

NC2169 *unc-55(e1170); unc-119(ed3); juIs1[punc-25::SNB-1::GFP; lin-15+]; wdEx686[pttr-39::irx-1::unc-10UTR; unc-119+; punc-25::mCherry::unc-54UTR; pttr-39::irx-1 antisense::unc-10UTR]*

irx-1 mutant strains:

FX03354 *irx-1(tm3354)/+*

NC2345 *irx-1(tm3354)/unc-55(e1170); juIs1[punc-25::SNB-1::GFP; lin-15+]*

Electrophysiology strains:

EG5025 *oxIs351[punc-47:ChR2::mCherry::unc-54UTR lin-15+ LITMUS 38i]*

NC2211 *unc-55 (e1170); oxIs351[punc-47:ChR2::mCherry::unc-54UTR lin-15+ LITMUS 38i]*

NC2212 *unc-55 (e1170); unc-119(ed3); oxIs351[punc-47:ChR2::mCherry::unc-54UTR lin-15+ LITMUS 38i]; wdEx686[pttr-39::irx-1::unc-10UTR; unc-119+; punc-25::mCherry::unc-54UTR; pttr-39::irx-1 antisense::unc-10UTR]*

irx-1(gf) strain:

NC2347 *unc-119(ed3); juIs1[punc-25::SNB-1::GFP; lin-15+]; wdEx753[pttr-39::IRX-1::GFP; unc-119+]*

Microscopy and synapse scoring: SNB-1::GFP assays were performed with the transgene *juIs1[punc-25::SNB-1::GFP; lin-15+]* (Hallam and Jin, 1998) and SYD-2::GFP assays used *hpIs3[punc-25::SYD-2::GFP; lin-15+]* (Yeh et al., 2005). Animals were anesthetized with 0.1% tricaine/tetramisole, mounted on a 2% agarose pad, and imaged with a Zeiss Axiovert microscope using Metamorph software. Images in Figure 4.1, 4.3, and 4.6, were obtained with a Leica TCSSP5 confocal microscope with Leica Application Suite Advanced Fluorescence (LAS-AF) software and created using maximum intensity projections of Z-stacks collected at 1.0 μm/step with a 40x objective.

For *irx-1(csRNAi)* quantification, individual VD motor neurons expressing mCherry (control or *irx-1(csRNAi)*-labeling) were scored. For each mCherry+ VD, the number of SNB-1::GFP puncta in the anterior interval between the VD and

the next anterior VD were counted in the dorsal and ventral nerve cords. These analyses were considered puncta per “VD anterior region”.

For SYD-2::GFP quantification, Z-stacks collected at 1.0 μm/step with a 40x objective were collapsed into maximum intensity projections. Linescan intensity values along the ventral nerve cord of each adult animal were collected with Leica Application Suite Advanced Fluorescence (LAS-AF) software. For each animal, the linescan intensity values were scaled such that the minimum intensity value was set to 0 and the maximum intensity value was set to 255. All intensity values for each animal were averaged, and then average intensity per animal was averaged by genotype/RNAi treatment. Results in this graph are from >8 adults for each genotype/RNAi treatment.

For *irx-1(gf)* studies, the *wdEx753* transgene was crossed into the *juIs1[punc-25::SNB-1::GFP]* background. In this strain, SNB-1::GFP is normally excluded from the nucleus. We performed mosaic analysis by identifying individual VD motor neurons scoring as “wild-type” (SNB-1::GFP in cell soma, but no IRX-1::GFP in nucleus) or *irx-1(gf)* (IRX-1::GFP localized in nucleus, with SNB-1::GFP in soma). We observed that very high IRX-1::GFP expression sometimes silenced SNB-1::GFP expression. Therefore, the fluorescence in the nucleus (IRX-1::GFP) and soma (SNB-1::GFP) of every neuron scored was quantified using confocal microscopy and Z-stack maximum intensity projections in LAS-AF software. Only neurons with equivalent fluorescent intensity in the nucleus and soma were scored as “*irx-1(gf)*” neurons. Adjacent neurons with high cell soma intensity/low nuclear intensity were scored as “wild-type” neurons.

For each VD, the number of SNB-1::GFP puncta in the anterior interval between the VD and the next anterior VD were counted in the dorsal and ventral nerve cords. These analyses were considered puncta per “VD anterior region”.

Construction of *irx-1::GFP*: GFP and the *unc-119* minigene were inserted into a fosmid containing the *irx-1* locus (Sarov et al., 2006; Zhong et al., 2010). In this construct, GFP is fused within the *irx-1* C-terminus and produces a functional protein capable of rescuing the lethality observed in *irx-1* null mutants (data not shown). The *irx-1::GFP* fosmid was purified using a modified column-less Qiagen miniprep protocol (Warming et al., 2005) and *unc-119* worms were transformed via microparticle bombardment with 8 μg *irx-1::GFP* fosmid coated on gold beads at 1800 psi as previously described (Spencer et al., 2011). Bombardment yielded a spontaneous integrant, *wdIs78*.

Movement assays: For *irx-1* global (*i.e.,* feeding) RNAi movement assays, *unc-55; juIs1* L4 larvae were treated with empty vector and *irx-1* RNAi as described previously (**Chapter III**) with the exception that *eri-1(mg366)* was not used in this assay. Worms were tapped on the head to assess suppression of the Unc-55 backward movement defect and were binned into “severe Unc” (coil ventrally immediately upon tapping), “moderate Unc” (coil ventrally while attempting backward locomotion), and “wild-type” (sustain backward locomotion with at least two body bends) categories.

Construction of *irx-1(csRNAi)*: Whole-worm cDNA was generated by RT-PCR of mixed-stage N2 RNA with poly-dT (Affy 100) primers and Superscript II (Invitrogen). 2 μL of the RT-PCR reaction was used as template to PCR-amplify *irx-1* cDNA (1131 bp). *irx-1 cDNA* was cloned into pCR2.1 via TOPO TA cloning (Invitrogen) resulting in plasmid pSA17. The "*irx-1* sense" construct pSA47 was cloned as follows: The *pttr-39* promoter (composed of 891 bp immediately upstream of *ttr-39*) and *irx-1* cDNA were PCR-amplified and cloned into a derivative of *pitr-1::DYS-1::YFP* (kindly provided by Kang Shen) (Poon et al., 2008) resulting in *irx-1* sense RNA expression in GABA neurons. The *unc-119* minigene (originally from MM051 (Maduro and Pilgrim, 1995)) was cloned into the backbone to produce pSA47. The "*irx-1* antisense" construct pSA49 was cloned as follows: *irx-1* cDNA was PCR-amplified and inserted into pSA47 in the opposite orientation, replacing forward-*irx-1* with reverse *irx-1* sequence. The *unc-119* minigene was replaced with *punc-25::mCherry* from pMLH41 (Earls et al., 2010) to result in pSA49. pSA47 ("*irx-1* sense") and pSA49 ("*irx-1* antisense") were linearized and ligated, then transformed into *unc-119* worms via microparticle bombardment (Praitis et al., 2001). The presence of "*irx-1* sense" was identified by wild-type (*unc-119+)* movement, and the presence of "*irx-1* antisense" was detected as mCherry expression in the GABA motor neurons.

Electrophysiology: Electrophysiology measurements were collected from dissected preparations, as previously described (Richmond and Jorgensen, 1999), with the following modifications to recording media. The extracellular

solution consisted of 150 mM NaCl, 5 mM KCl, 5mM $CaCl_2$, 4 mM $MgCl_2$, 10 mM glucose, 5 mM sucrose, and 15 mM HEPES 15 (pH 7.4, ~340 mOsm). The patch pipette was filled with 120 mM KCl, 20 mM KOH, 4 mM $MgCl_2$, 5 mM *N*-tris[Hydroxymethyl] methyl-2-aminoethane-sulfonic acid, 0.25 mM $CaCl_2$, 4 mM Na^2ATP, 36 mM sucrose, 5 mM EGTA (pH 7.2, ~ 315mOsm). Electrophysiological measurements were carried out in wild-type, *unc-55*, and *unc-55; irx-1(csRNAi)* with the *oxIs351* GABA channelrhodopsin transgene in the background. Recordings of GABAergic activity were collected from body wall muscles, patched in the whole-cell voltage clamp mode at a holding potential of -60mV, in the presence of 10^{-4}M d-tubocurare (dTBC) to block muscle stimulation from acetylcholine receptors.

DD remodeling timecourse: For the DD remodeling timecourse, NC2296 was used as the "wild-type" reference for *irx-1(csRNAi)* to eliminate the possibility of remodeling delays due to *unc-119* rescue or mCherry expression. Separate groups of 100 gravid wild-type (NC2296) and *irx-1(csRNAi)* (NC2297) adults were picked to single 60mm plates and allowed to lay eggs for one hour and then removed from the plate. The mid-point of the hour in which eggs were laid was considered to be t=0. Plates were incubated at 23°C throughout the timecourse. Beginning at 21 hours post-lay and for each hour thereafter, larvae were picked off wild-type and *irx-1(csRNAi)* plates and imaged (as above) on a Zeiss Axiovert microscope. The number of dorsal SNB-1::GFP puncta, number of GFP+ neurons (i.e. GABA neurons), and number of mCherry+ neurons (i.e. wild-type

mCherry or *irx-1(csRNAi)*) were recorded for ≥6 worms for each timepoint. Data were recorded from worms with mCherry in ≥50% of GABA (GFP+) neurons. Results were pooled from three separate timecourse experiments.

Construction and analysis of *irx-1(gf)*: To generate *pttr-39::irx-1::GFP; unc-119+*, the entire GFP-tagged *irx-1* ORF from the *irx-1::GFP* fosmid was PCR-amplified and cloned into pCR2.1 via TOPO-TA cloning to yield pSA64. The *irx-1::GFP* ORF was then cloned into pSA47 (see above) to yield pSA70. This construct was transformed into *unc-119* worms via microparticle bombardment as above. Animals exhibited mosaic *wdEx753[pttr-39::IRX-1::GFP; unc-119+]* expression in DD and VD motor neurons.

Results

irx-1 is expressed in remodeling GABAergic motor neurons

The elevation of *irx-1* transcript in *unc-55* mutants suggests that *irx-1* is negatively regulated by *unc-55*. Moreover, the RNAi results indicate that *irx-1* is required for GABA neuron remodeling. These findings suggest that *irx-1* should be normally expressed in remodeling DDs and de-repressed in *unc-55* VDs. To test this idea, we engineered an *irx-1* reporter gene in which GFP was fused to the *irx-1* coding sequence in a construct that spans the complete *irx-1* gene as well as large flanking regions (see **Methods**). The resultant IRX-1::GFP fusion protein is capable of rescuing the lethal phenotype of an *irx-1* null allele (data not shown). Thus, we reasoned that endogenous *irx-1* gene regulatory sequences

should be preserved in this construct and that the chimeric IRX-1::GFP protein retains native activity. IRX-1::GFP was consistently detected in the nuclei of DD motor neurons from both wild-type and *unc-55* mutant animals (**Figure 4.1A-B,** 73 of 76 wild-type DDs and 77 of 78 of *unc-55* DDs). Moreover, IRX-1::GFP is not expressed in wild-type VD motor neurons (2 of 170) but is de-repressed in *unc-55* VD motor neurons (171 of 176). Weak IRX-1::GFP expression was also observed in hypodermal nuclei and in two unidentified head neurons (data not shown). We found that the Pitx-1 homolog *unc-30,* which is necessary for DD remodeling in the L1*,* is also required for expression of IRX-1::GFP in GABA motor neurons (GFP expression in 0 of 40 DD motor neurons and 0 of 90 VD motor neurons). This result is consistent with the idea that the GABAergic motor neuron synaptic remodeling program is controlled by modulation of the opposing roles of UNC-30 (positive) and UNC-55 (negative) (Shan et al., 2005). Together, these findings support a role for *irx-1* in synaptic remodeling and confirm that the native *irx-1* gene is negatively regulated by *unc-55.*

To predict whether *irx-1* is directly regulated by *unc-55*, we searched the upstream regulatory region of *irx-1* for COUP-TF binding sites. UNC-55 represses expression of the *flp-13* locus in VD motor neurons via a single COUP-TF half-site, TGACCT, which represents the canonical COUP-TF binding site (Shan et al., 2005). In general, COUP-TFs bind imperfect direct or inverted repeats of TGACCT with variable lengths of separation between a pair of half-sties (Park et al., 2003). In the *irx-1* promoter, we found two variants of the canonical binding half-site (Montemayor et al., 2010), TGACCC and TGACCA,

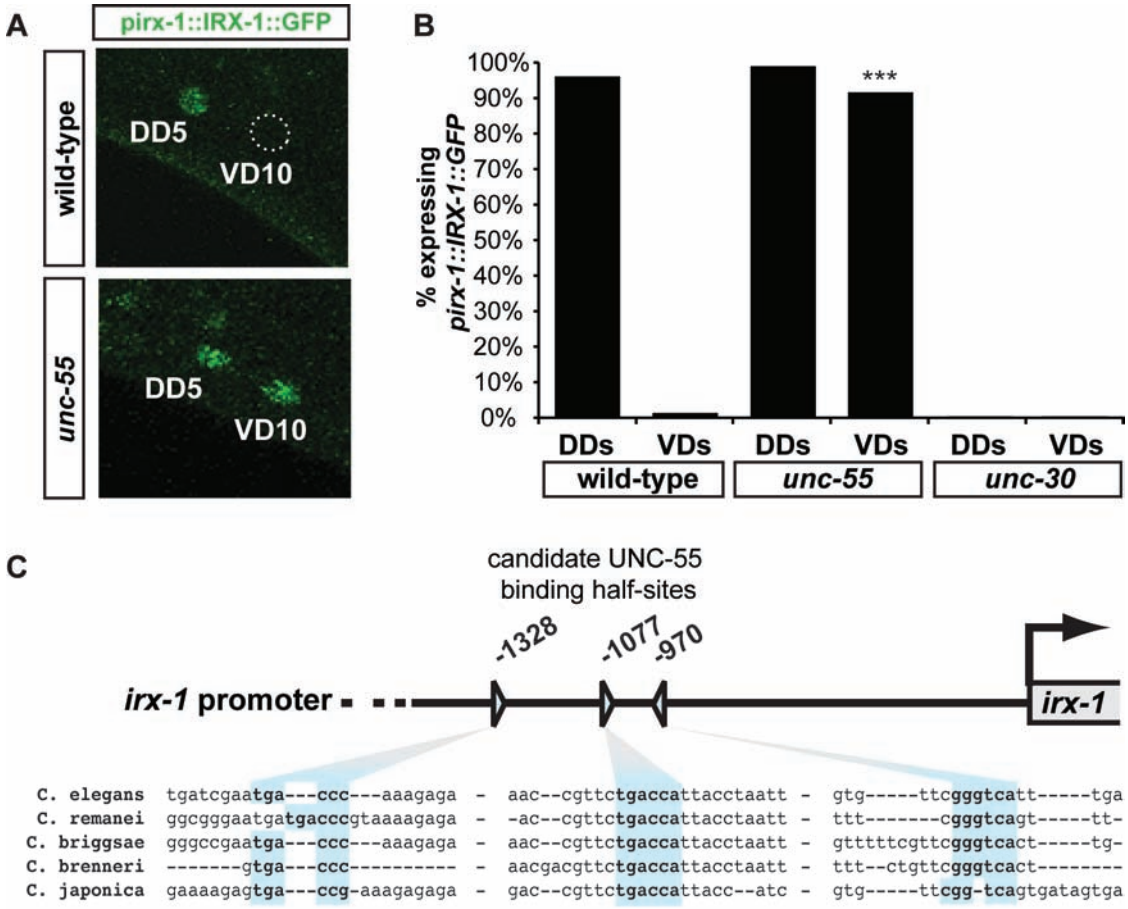

Figure 4.1. *irx-1::*GFP is expressed in remodeling GABAergic motor neurons. (**A**) IRX-1::GFP is restricted to the nucleus of DD motor neurons in wild-type L4 larvae. In *unc-55* mutants, IRX-1::GFP is observed in both DD and VD motor neurons (DD5 and VD10 shown for examples). Similar expression patterns were observed for all DD and VD motor neurons. Scale bar, 5 μm. (**B**) Quantification of IRX-1::GFP expression in GABAergic motor neurons of L2 larvae. Note that IRX-1::GFP is de-repressed in *unc-55* VD motor neurons and not expressed in *unc-30* GABAergic motor neurons. *** $p < 0.0001$, Fisher's Exact 2-tailed Test. (**C**) Location and conservation of predicted COUP-TF binding half-sites in the *irx-1* 5' regulatory region. Distances are indicated in base pairs upstream of the *irx-1* start site.

with high conservation among nematode species (**Figure 4.1C**). It remains an open question whether these sites are physically occupied by UNC-55 to repress *irx-1* expression.

Ectopic *irx-1* function is required for the Unc-55 backward locomotion defect

In *unc-55* mutants, the loss of GABAergic ventral input from VD motor neurons results in ventral coiling during backward locomotion (Walthall and Plunkett, 1995). If *irx-1* function is required for VD synaptic remodeling in an *unc-55* mutant, then the loss of *irx-1* activity should preserve ventral VD inputs and thus restore normal backward movement (*i.e.,* "suppress" the Unc-55 movement defect). Because an *irx-1* null allele results in embryonic and early larval lethality, we used global RNAi to test this model. As expected, *unc-55* animals from control RNAi plates displayed the characteristic backward Unc phenotype (**Figure 4.2A**,). In contrast, a substantial fraction of surviving *unc-55* animals from *irx-1* RNAi feeding plates were capable of sustained backward locomotion (**Figure 4.2B**). We quantified this effect by scoring three distinct categories of movement: severe Unc (coils ventrally with tap on the head), moderate Unc (attempts backward locomotion before coiling ventrally), and wild-type (executes at least 2 body bends of backward locomotion, see **Methods**). All control-treated *unc-55* adults exhibited Unc backward locomotion (39% severe Unc, 61% moderate Unc, N=61); in contrast, most of the *irx-1* RNAi-treated *unc-55* adults showed wild-type backward locomotion (80%, N=50) (**Figure 4.2B**). The small

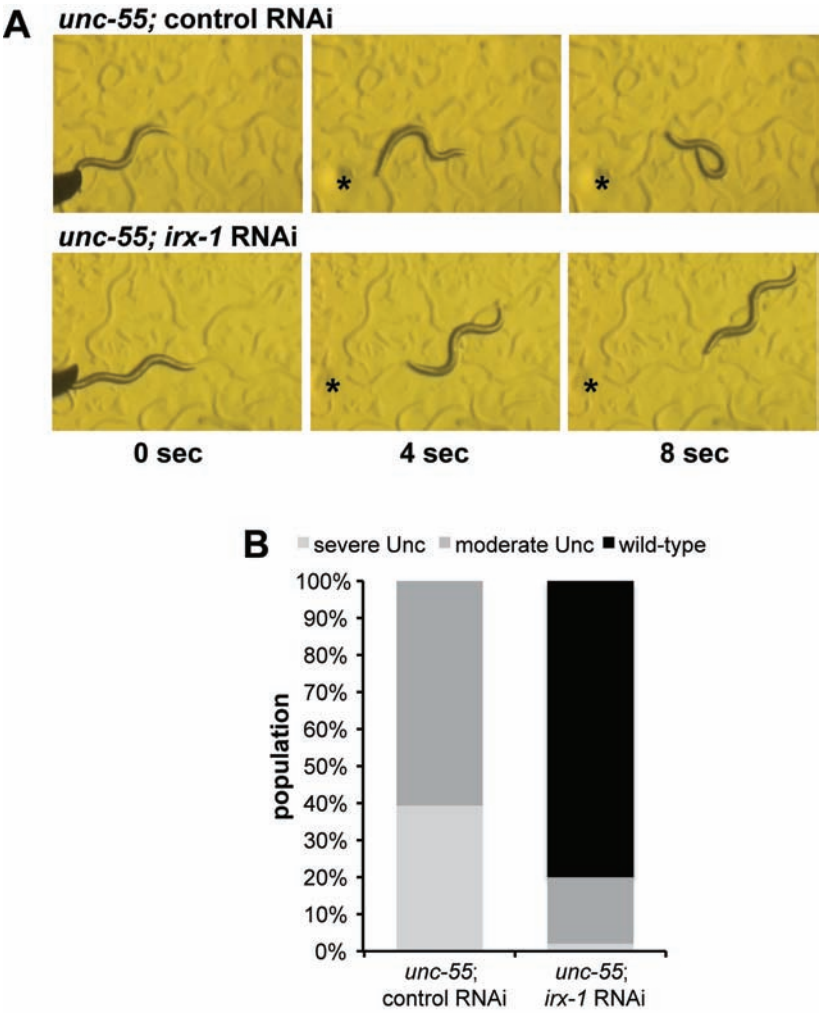

Figure 4.2. *irx-1* knockdown restores backward locomotion in *unc-55* mutants. (**A**) *unc-55* mutants coil ventrally during backward locomotion due to loss of inhibitory GABAergic input to ventral muscles (top panels). Treatment of *unc-55* mutants with *irx-1* RNAi restores backward locomotion (bottom panels). Animals were tapped on the head (asterisk) at t = 0. (**B**) Quantification of *irx-1* suppression of backward movement defect in *unc-55* adults treated with control (empty vector) or with *irx-1* RNAi. Animals were binned in three categories: "severe Unc" which coil ventrally immediately after a head tap, "moderate Unc" which attempt backward locomotion but stop after coiling ventrally (for example, see top panels in A), and "wild-type" which sustain backward locomotion (at least 1 body length, for example, see bottom panels in A). All control-treated animals exhibit uncoordinated backward locomotion (N = 61), whereas most (>80%) *irx-1* treated animals show wild-type backward movement (N = 50).

fraction showing some Unc behavior (18% moderate Unc, 2% severe Unc) may be attributed to the incomplete effect of RNAi knockdown or to necessary remodeling roles for additional *unc-55* regulated genes (**Figure 4.2B**). To confirm that *irx-1* function in this pathway is cell-autonomous, we constructed a transgenic line carrying a heritable GABA-specific *irx-1* RNAi array, *wdEx686[irx-1(csRNAi)]*. The *irx-1(csRNAi)* transgene expresses both sense and antisense *irx-1* RNA strands under control of the GABA-specific *ttr-39* promoter; GABA neurons with the *irx-1(csRNAi)* array are marked by co-expression of GABA::mCherry (see **Methods**). These experiments confirmed that selective ablation of *irx-1* in ventral cord GABA neurons is sufficient to suppress the Unc-55 backward movement defect (data not shown).

irx-1 promotes synaptic remodeling in *unc-55* mutant VD motor neurons

Our finding that cell-specific *irx-1* RNAi restores backward locomotion to an *unc-55* mutant suggests that cell-autonomous knockdown of *irx-1* is also likely to block synaptic remodeling in *unc-55* VD motor neurons. To test this prediction, we scored the distribution of SNB-1::GFP puncta in the dorsal and ventral nerve cords of *unc-55*; *irx-1(csRNAi)* mutant animals. These arrays show mosaic expression and the mCherry marker identifies the subset of GABAergic neurons that actually carry either the *irx-1(csRNAi)* or the *wdEx658* control array (see Methods). We first confirmed that SNB-1::GFP is strongly enriched in the dorsal nerve cord (**Figure 4.3A**) and depleted in the ventral nerve cord (**Figure 4.3C**) of mCherry-marked GABA motor neurons in *unc-55* mutant animals carrying the

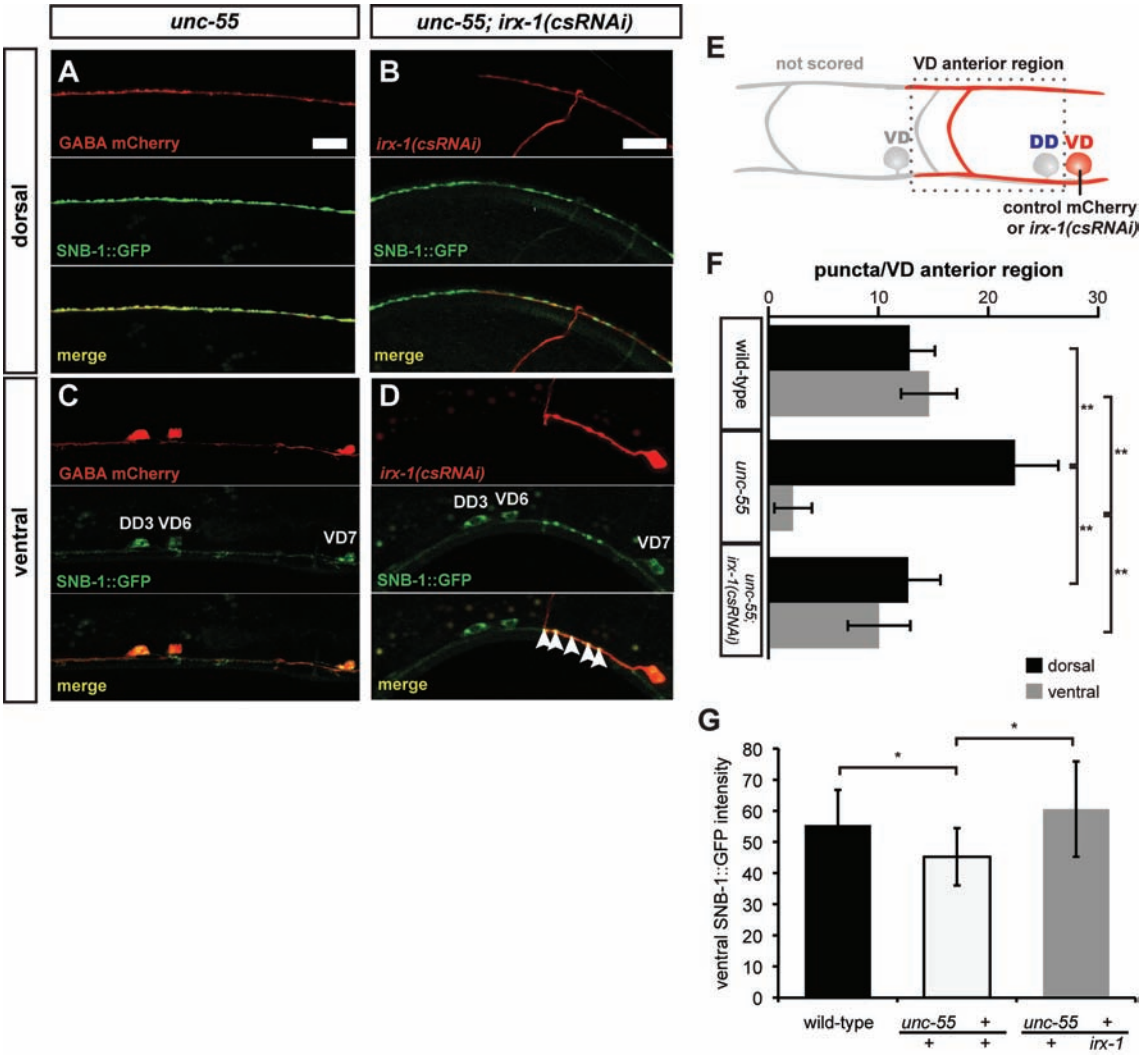

Figure 4.3. Cell-autonomous expression of *irx-1* is required for synaptic remodeling in *unc-55* VD motor neurons. (**A-D**) SNB-1::GFP puncta label GABAergic NMJs. mCherry marks cells expressing the control *wdEx658* transgenic array (panels **A** and **C**) or specific neurons expressing the *irx-1(csRNAi)* transgene, *wdEx686* (panels **B** and **D**) (see Methods). **A-B**, dorsal nerve cord, **C-D**, ventral nerve cord. Common region of single adult animal in panels **A, C** and separate adult in **B, D.** Scale bars = 10 μm. (**A**) Note dense array of SNB-1::GFP puncta in the dorsal nerve cord of *unc-55* adult. (**B**) Fewer SNB-1::GFP puncta are observed in the region corresponding to dorsal arm of *irx-1(csRNAi)* expressing VD motor neuron (marked with mCherry). Note that dorsal SNB-1::GFP puncta from DD3 in this region do not overlap with the VD6 mCherry marker. (**C**) SNB-1::GFP puncta are depleted from the ventral nerve cord of *unc-55* adults. (**D**) Expression of *irx-1(csRNAi)* in VD7 (marked with mCherry) of an *unc-55* mutant restores ventral SNB-1::GFP puncta. SNB-1::GFP puncta are absent from neighboring VD6 motor neuron that does not express *irx-1(csRNAi).* (**E**) Dotted lines denote anterior regions of mCherry-marked VD motor neurons in which SNB-1::GFP puncta were counted (see Methods). (**F**) Quantification of *irx-1(csRNAi)* suppression of the Unc-55 synaptic remodeling defect. ** $p < 0.0001$, 2-way ANOVA with Bonferroni's Multiple Comparison Test. N = 50 VD anterior regions per genotype. (**G**) Average fluorescence intensity of SNB-1::GFP in the ventral nerve cords of *unc-55*, *unc-55/+*, and *unc-55/irx-1* adults. * $p < 0.05$, Student's t-test.

wdEx658 control array. In contrast, *unc-55* mutant VD motor neurons that express *irx-1(csRNAi)* show fewer SNB-1::GFP puncta in the dorsal nerve cord (**Figure 4.3B**) with a concomitant increase in ventral SNB-1::GFP-marked NMJs (**Figure 4.3D**, arrowheads). To quantify this effect, we counted SNB-1::GFP puncta in a region ("VD anterior region") that includes the dorsal and ventral processes of the given mCherry marked VD motor neuron (**Figure 4.3E**). In wild-type animals, the number of ventral NMJs (from VDs) was roughly equivalent to the number of dorsal NMJs (from DDs) in each VD anterior region (**Figure 4.3F**, 12.7$\pm$2.9 ventral puncta, 10.1$\pm$2.8 dorsal puncta, N=50 VD anterior regions). As expected, in *unc-55* mutants, the number of dorsal SNB-1::GFP puncta was significantly increased (22.4$\pm$4.0, $p<0.0001$ vs. wild-type, 2-way ANOVA with Bonferroni's Multiple Comparison Test) with a corresponding depletion of ventral puncta (2.3 $\pm$1.7, $p<0.0001$ vs. wild-type, N=50 VD anterior regions) (**Figure 4.3F**). In comparison to *unc-55* mutant VD motor neurons, *unc-55; irx-1(csRNAi)* VDs had significantly fewer dorsal puncta and more ventral puncta (**Figure 4.3F**, 14.6$\pm$2.5 dorsal puncta, $p<0.0001$ vs. *unc-55*, 12.9$\pm$2.3 ventral puncta, $p<0.0001$ vs. *unc-55*, N=50 VD anterior regions). These results confirm that knockdown of *irx-1* specifically in *unc-55* mutant VDs prevents remodeling and substantiates the proposal that de-repression of *irx-1* in *unc-55* mutants promotes VD remodeling.

We wanted to test whether a null allele of *irx-1* could also suppress the *unc-55* defect to confirm the *irx-1* RNAi results. Because of the technical challenges of building an *unc-55; irx-1* double mutant and the lethality observed

in *irx-1* homozygotes, we analyzed *unc-55/irx-1(tm3354)* heterozygotes. We found that *unc-55/+* displays a partial ectopic remodeling phenotype as indicated by a significant loss of SNB-1::GFP intensity in the ventral nerve cord (**Figure 4.3G**). This subtle but significant ectopic remodeling defect is suppressed in *unc-55/irx-1* (double heterozygotes). This result confirms our RNAi knockdown experiments and demonstrates that loss of *irx-1* prevents remodeling in *unc-55* VD motor neurons.

Cell-specific *irx-1* knockdown restores GABAergic input to ventral muscles in *unc-55* mutants

The restoration of backward locomotion (**Figure 4.2**) as well as ventral GABAergic SNB-1::GFP puncta to *unc-55; irx-1(csRNAi)* animals (**Figure 4.3**) is indicative of functional GABAergic inputs to ventral body wall muscles. To test this idea, we recorded miniature postsynaptic events (mPSCs) in the ventral muscles of wild-type, *unc-55,* and *unc-55; irx-1(csRNAi).* These animals were treated with the cholinergic antagonist, d-tubocurare (dTBC), to insure that all mPSCs are exclusively induced by GABAergic signaling (Richmond and Jorgensen, 1999). Recordings from ventral muscles detected robust mPSCs in wild-type adults (**Figure 4.4A**). In contrast, mPSCs were rarely observed in ventral recordings of *unc-55* mutants (**Figure 4.4A**) as predicted from the observation that VD synapses are largely confined to the dorsal nerve cord in *unc-55* animals (Walthall and Plunkett, 1995). *irx-1(csRNAi)* expression in *unc-55* mutants restores mPSCs to ventral muscle (**Figure 4.4A**) and thus indicates that

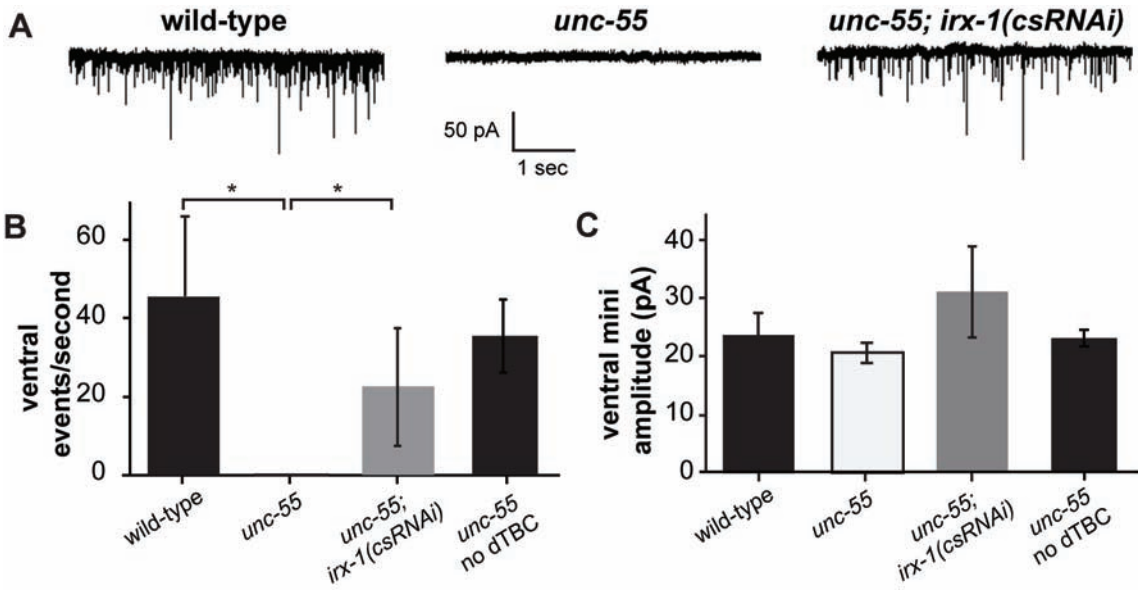

Figure 4.4. *irx-1* knockdown restores ventral GABAergic synaptic output in *unc-55* mutants. (**A**) Miniature post-synaptic currents (mPSCs) are abundant in ventral body muscles of wild-type and *unc-55; irx-1(csRNAi)* animals but are rare in *unc-55* mutants. Animals in panel **A** were treated with d-tubocurare (dTBC) to block cholinergic activity. (**B**) Quantification of results in panel **A** shows restoration of ventral mPSCs to *unc-55* mutants treated with *irx-1(csRNAi)*. As a control, *unc-55* animals were recorded without dTBC. Robust cholinergic mPSCs in *unc-55* animals in the absence of dTBC indicate that the Unc-55 defect is specific to GABAergic synapses. * $p < 0.05$, Mann-Whitney U-test. N = 4-6 for each genotype, error bars indicate standard deviation. (**C**) Average mPSC amplitude is similar for all recordings, indicating that mPSCs are quantal. N = 4-6 for each genotype, error bars indicate standard deviation.

the ventral GABAergic SNB-1::GFP puncta that reappear in this strain (**Figure 4.4D, F**) correspond to functional synapses. These results were confirmed by quantification; mPSCs were virtually absent from *unc-55* ventral muscles (45.8±20.3 events/sec in wild-type, N=5, vs. 0.05±0.06 events/sec in *unc-55*, N=4, $p<0.02$, Mann-Whitney U-test) but were significantly restored in *unc-55; irx-1(csRNAi*) animals (22.6+15.0 events/sec, N=6, $p<0.02$ vs. *unc-55*, $p>0.1$ vs. wild-type, Mann-Whitney U-test). Robust ventral mPSCs were detected in *unc-55* mutants in the absence of dTBC thereby demonstrating that ventral cholinergic inputs are not perturbed by ectopic VD remodeling (**Figure 4.4B**). Similar mPSC event amplitudes were observed for all genotypes ($p<0.01$ in all comparisons, Mann-Whitney U-test), suggesting that quantal neurotransmitter release for the residual mPSCs in *unc-55* mutants and receptor sensitivity are unchanged (**Figure 4.4C**).

We conclude that the sparse occurrence of ventral mPSCs in *unc-55* is due to a loss of ventral GABAergic input and that the restoration of ventral activity by *irx-1(csRNAi)* indicates re-establishment of ventral GABAergic synapses. However, we also found that these synapses were apparently incapable of evoked release (data not shown) when stimulated via a channelrhodopsin excitation system (Liu et al., 2009). This result predicts that *irx-1* knockdown does not restore full functionality to these synapses and that knockdown of other *unc-55*-regulated genes in addition to *irx-1* would be required for evoked release of these VD ventral synapses.

SYD-2 is not enriched at restored *unc-55; irx-1* ventral synapses

The Liprin-α homologue in *C. elegans*, *syd-2*, encodes a membrane protein required for normal synaptogenesis in both immature and remodeled GABAergic motor neurons (Zhen and Jin, 1999). Because of the normal SNB-1::GFP morphology (**Figure 4.3**) but only partially restored function (**Figure 4.4**) of VD ventral synapses in an *unc-55* mutant, we wanted to examine the localization of SYD-2 in *unc-55; irx-1*(*RNAi*)-treated adults.

In *unc-55* mutants, SYD-2 localization mirrors the localization of SNB-1 and is remodeled to dorsal synapses of VD motor neurons with a concurrent depletion of SYD-2 in the ventral nerve cord (see **Chapter II**). Interestingly, whereas *irx-1* knockdown results in ventral SNB-1::GFP-labeled synapses in *unc-55* mutants, SYD-2::GFP is not restored to the ventral nerve cord in *unc-55; irx-1(RNAi)* larvae (**Figure 4.5**). This result suggests that *irx-1* functions to regulate synaptic vesicle trafficking, as indicated by ventral SNB-1::GFP-labeled synaptic vesicles, but does not regulate the localization of the membrane component SYD-2. This absence of SYD-2 at *unc-55; irx-1* restored ventral synapses may explain why these synapses are incapable of evoked release, as discussed in the previous section.

***irx-1* is required for normal DD motor neuron remodeling**

Our results have shown that *irx-1* is required for ectopic remodeling of VD motor neurons in *unc-55* mutants. Because *irx-1* is normally expressed in DD motor neurons, we next asked whether *irx-1* is also necessary for DD

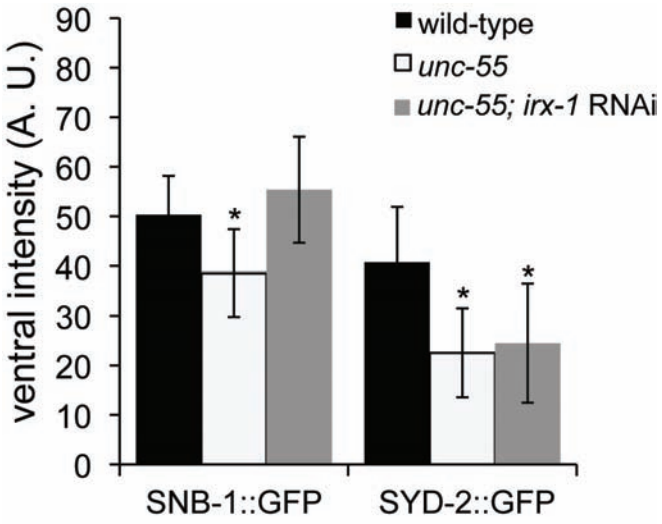

Figure 4.5. SYD-2 does not co-localize with restored ventral synapses in *unc-55; irx-1(RNAi)*-treated adults. Both SNB-1::GFP and SYD-2::GFP are depleted from the ventral nerve cord in *unc-55* mutants (white bars) relative to wild-type (black bars). Only SNB-1::GFP is restored to the ventral nerve cord of *irx-1(RNAi)*-treated *unc-55* animals; SYD-2::GFP localization remains unchanged (gray bars). Values are shown are average normalized arbitrary fluorescence units among >8 adults of each genotype/RNAi-treatment. $p < 0.05$ relative to wild-type, Student's t-test.

remodeling. Dorsal synapses from DDs are established late in the first larval stage (White et al., 1978; Hallam and Jin, 1998). To visualize this remodeling event, we monitored the appearance of dorsal SNB-1::GFP puncta at 1 hour intervals during this period (**Figure 4.6A**). In wild-type larvae, dorsal SNB-1::GFP puncta are initially detected at 22 hours (elapsed time since egg-laying, see **Methods**) and increase in number until reaching a plateau at the onset (~30 hours) of the L2 stage. DD remodeling is significantly slower in L1 larvae carrying the *irx-1(csRNAi)* transgene with an approximate 4-hour delay in the initial detection of dorsal SNB-1::GFP puncta at 26 hours (**Figure 4.6A,** ** $p<0.01$, wild-type vs. *irx-1(csRNAi)*, Student's t-test). This effect is strikingly evident in DD motor neurons with high *irx-1(csRNAi)* expression (indicated by *punc-25::mCherry*, see DD5 in **Figure 4.6C, D**) in which dorsal SNB-1::GFP puncta are small and few in number compared to DDs without cell-specific *irx-1* knockdown (DD6 in **Figure 4.6C, D**).

We note, however, that DD remodeling is not completely blocked by *irx-1(csRNAi)* but appears to reach completion later in larval development (**Figure 4.6A**). To determine if this effect could be due to an overall delay in the GABA neuron developmental program, we monitored the expansion of GABA motor neurons during this period. L1 larvae are born with 6 DD motor neurons; 13 VD motor neurons are added to the ventral cord by the end of the L1 stage (White et al., 1978). We noted no difference in the rate of appearance of GABAergic motor neurons in wild-type vs. *irx-1(csRNAi)* animals and conclude that the timing of this expansion is not perturbed by *irx-1(csRNAi)* (**Figure 4.6B**, all timepoints

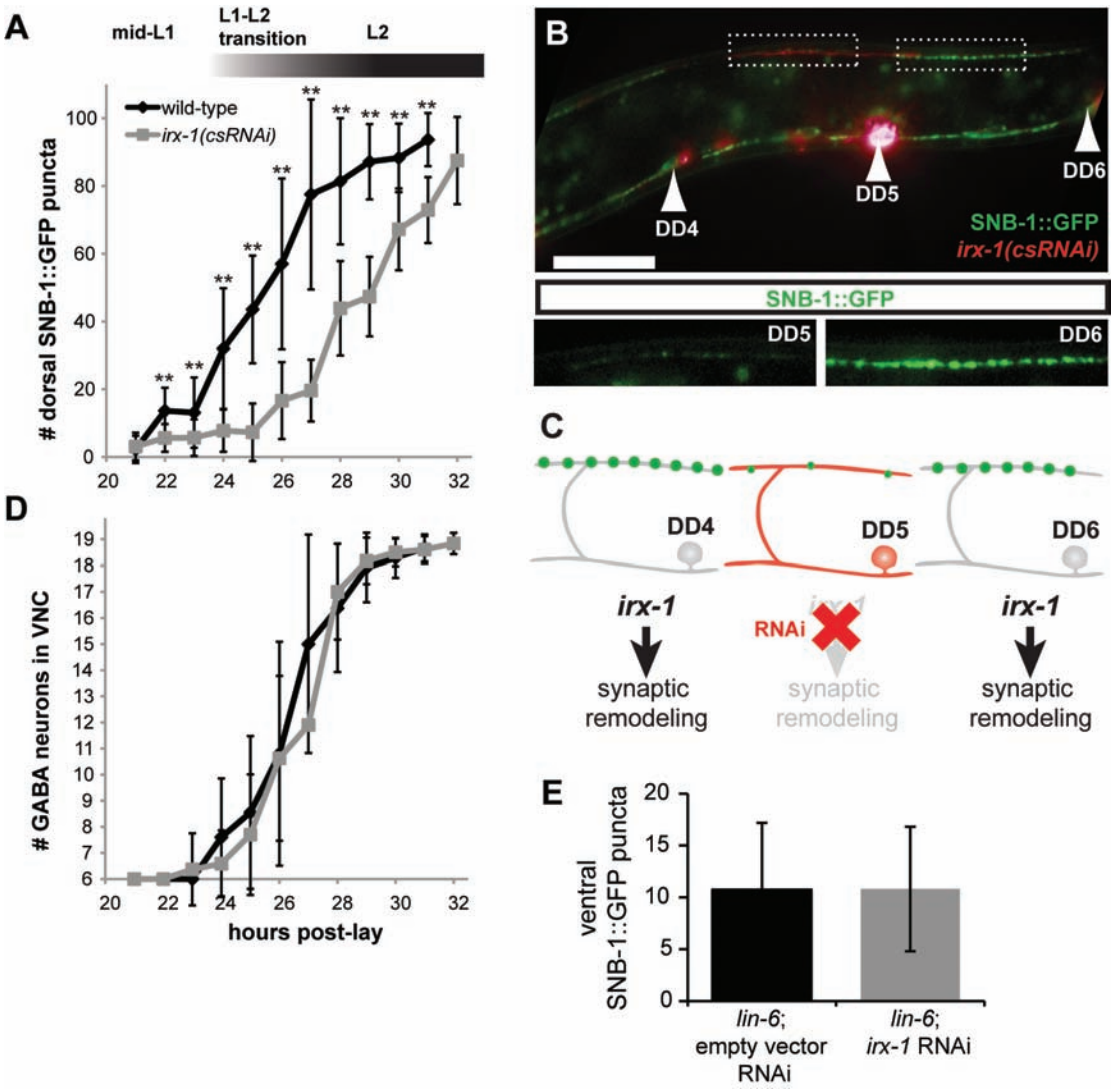

Figure 4.6. *irx-1* function is required for the normal progression of synaptic remodeling in DD motor neurons. (**A-B**) DD synaptic remodeling is delayed in *irx-1(csRNAi)* animals. (**A**) DD remodeling was quantified by counting dorsal SNB-1::GFP puncta during L1-L2 larval stages. In wild-type (*SNB-1::GFP; GABA::mCherry*-expressing) larvae, DD remodeling begins at 22-24 hours (see Methods) in L1 larvae and is completed by the L2 stage. In contrast, remodeling is delayed in *irx-1(csRNAi*) larvae. ** $p < 0.01$, wild-type vs. *irx-1(csRNAi)*, Student's t-test. Error bars indicate standard deviation. N = 6-21 for each genotype at each hour, results pooled from three independent experiments. (**B, C**) *irx-1(csRNAi)* causes cell-autonomous delays in DD motor neuron synaptic remodeling. Image of a mosaic *irx-1(csRNAi)*-expressing larva at 29 hours when DD remodeling is largely complete in wild-type (Top panel). Strong expression of the *irx-1(csRNAi)* transgene, indicated by the mCherry marker, in DD5 but not DD6 (or DD4) is correlated with reduced dorsal SNB-1::GFP puncta in DD5 compared to DD6 (inset panels). (**D**) Generation of GABAergic motor neurons is not disrupted by abrogation of *irx-1* activity. The normal complement of 6 embryonic DD motor neurons was observed in both wild-type and *irx-1(csRNAi)* larvae prior to remodeling (t = 21 hours). The rate of appearance of the 13 post-embryonic VD motor neurons was not delayed in *irx-1(csRNAi)* larvae compared to wild-type. Scale bar, 10 μm. (**E**) SNB-1::GFP is removed from DD ventral processes by late larval stages in *irx-1*-treated animals. *lin-6* was used as a tool to genetically ablate VD motor neurons so as to assess the localization of SNB-1::GFP in DD motor neurons only. There is no significant difference between the number of ventral DD puncta in control versus *irx-1* RNAi.

p>0.05, wild-type vs. *irx-1(csRNAi)*, Student's t-test). We also confirmed that *irx-1* RNAi does not inhibit expression from the *unc-25* promoter and therefore exclude the possibility that this would account for the reduced number of GFP puncta arising from the *punc-25::SNB-1::GFP* reporter (data not shown).

To confirm that DD remodeling reaches completion despite knockdown of *irx-1* expression, we examined the localization of SNB-1::GFP in *lin-6* mutants. In these mutants, VD motor neurons are genetically ablated and thus all SNB-1::GFP puncta are representative of DD NMJs only, rather than both DD and VD NMJs (Hallam and Jin, 1998). In *lin-6* animals treated with *irx-1* RNAi, very few puncta are observed in the ventral nerve cord of late larval-stage animals, comparable to the number of ventral puncta in control RNAi-treated animals (**Figure 4.6E**). This result indicates that that NMJs are completely removed from *irx-1* DD ventral processes by late-larval stages and supports the above conclusion that *irx-1* knockdown does not completely block DD remodeling.

On the basis of these results, we conclude that *irx-1* normally promotes DD remodeling. However, because RNAi knockdown of *irx-1* retards but does not arrest DD remodeling, we conclude that additional genes functioning in parallel to *irx-1* may provide partially redundant function.

irx-1 is sufficient to induce synaptic remodeling in VD motor neurons

The finding that *irx-1* promotes DD remodeling suggested that *irx-1* might also be sufficient to drive synaptic remodeling in wild-type (*i.e.*, *unc-55*+) VD motor neurons. To test this idea, we used the *ttr-39* promoter to drive expression

of IRX-1::GFP in GABAergic motor neurons. *ttr-39* is specific to DD and VD motor neurons (Cinar et al., 2005) and is not regulated by *unc-55* (data not shown). IRX-1::GFP in these animals localizes to the nucleus (**Figure 4.7A,** see also **Figure 4.1A**) of DDs and VDs, unlike the marker SNB-1::GFP which remains in the cytoplasm. We used this difference in GFP localization to distinguish gain-of-function IRX-1::GFP-positive or *irx-1(gf)* VDs (nuclear GFP) from wild-type VDs (cytoplasmic GFP only). Wild-type VD motor neurons in these mosaic animals show SNB-1::GFP puncta in the ventral process of the VD anterior region as expected (**Figure 4.7A-B,** VD5). In contrast, *irx-1(gf)* VD motor neurons exhibit an Unc-55-like phenotype with excess dorsal SNB-1::GFP puncta coupled with a concomitant depletion on the ventral side (**Figure 4.7A-B**, VD6). We quantified this result by counting SNB-1::GFP puncta adjacent to wild-type and *irx-1(gf)* VD motor neurons (**Figure 4.7C**). Comparable numbers of dorsal (from DD motor neurons) and ventral (VD motor neurons) SNB-1::GFP puncta were detected in regions anterior to wild-type VDs (**Figure 4.7C**, 10.2$\pm$2.4 dorsal puncta vs. 11.2$\pm$1.8 ventral puncta, N=20 wild-type VD anterior regions). Ventral puncta were virtually eliminated, however, from *irx-1(gf)* VDs which show a strong Unc-55-like phenotype (17.0$\pm$2.0 dorsal puncta vs. 1.7$\pm$1.7 ventral puncta, N=20 *irx-1(gf)* VD anterior regions, **p<0.01, 2-way ANOVA with Bonferroni's Multiple Comparison Test). The similarity of the cell-specific *irx-1(gf)* phenotype to that of *unc-55* suggests that ectopic *irx-1* is sufficient to induce synaptic remodeling in VD motor neurons and that *irx-1* is a primary downstream effector of the Unc-55 remodeling phenotype (**Figure 4.8**).

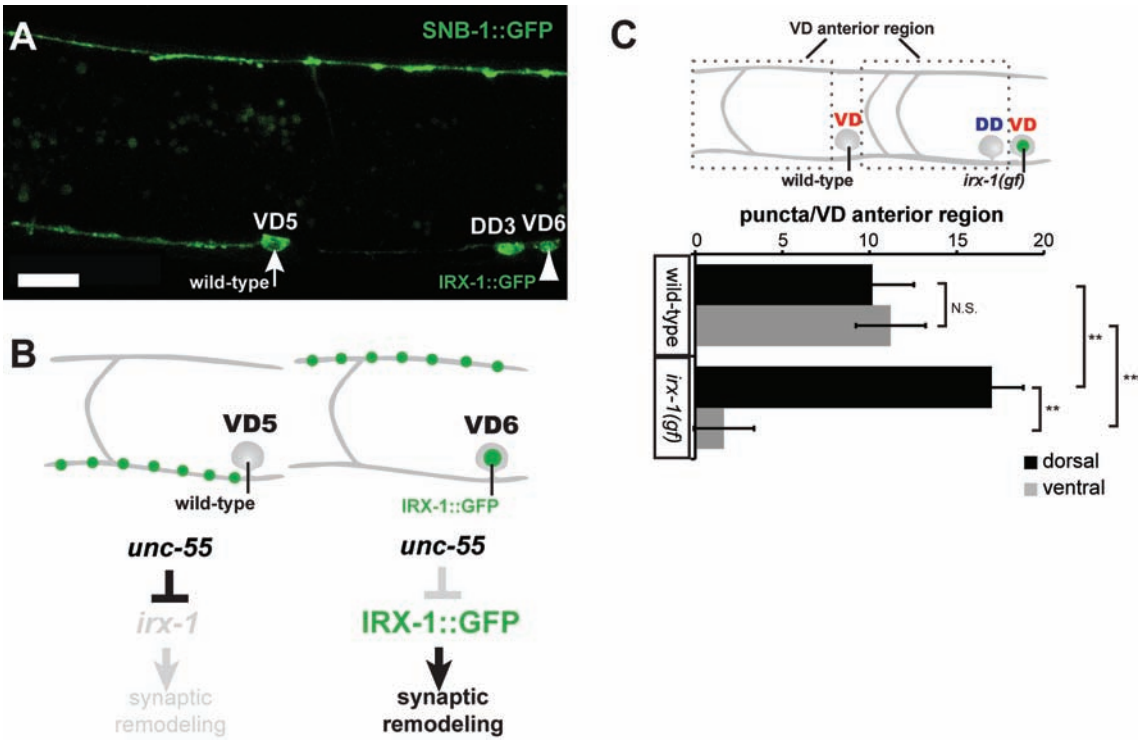

Figure 4.7. Ectopic *irx-1* expression is sufficient to drive remodeling in VD motor neurons. (**A**) Mosaic expression of GFP-labeled IRX-1 (IRX-1::GFP) with the *ttr-39* promoter labels the VD6 nucleus (arrowhead) but not VD5. Residual SNB-1::GFP in the VD5 cell soma is excluded from the nucleus (arrow) (adult stage). Note absence of ventral SNB-1::GFP puncta in the ventral process of VD6 and corresponding enhanced SNB-1::GFP expression in the dorsal VD6 process. Scale bar, 10 μm. (**B**) Schematic diagram of results from panel **A**. In VD6, *unc-55* represses endogenous *irx-1* but does not block IRX-1::GFP expression from the *ttr-39* promoter which drives remodeling. (**C**) Quantification of the *irx-1(gf)* phenotype. SNB-1::GFP puncta were counted in the dorsal and ventral nerve cords within each "VD anterior region" for wild-type vs. IRX-1::GFP-expressing VD neurons as indicated. ** $p < 0.01$, 2-way ANOVA with Bonferroni's Multiple Comparison Test, N.S., not significant.

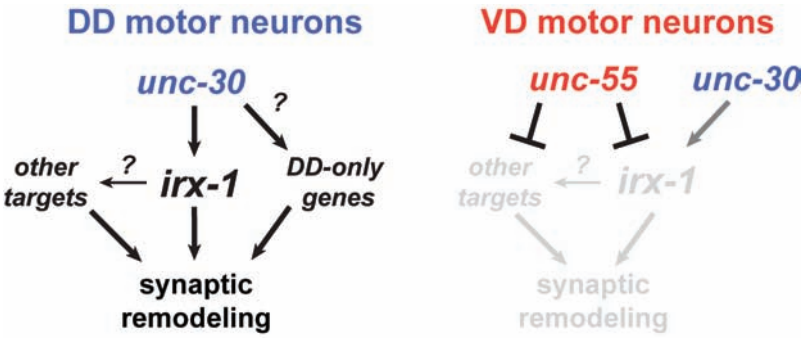

Figure 4.8. Genetic pathways that control synaptic remodeling. *unc-55* prevents expression of *irx-1* and 48 additional factors (18 conserved) to block synaptic remodeling in VD motor neurons. *unc-30* promotes *irx-1* expression. *irx-1* is normally expressed in DD motor neurons where it drives synaptic remodeling in parallel to at least one additional partially redundant pathway.

Discussion

With these experiments, we have defined the role of the conserved homeodomain-containing transcription factor, IRX-1/Iroquois, in synaptic remodeling, thus validating one of our microarray and RNAi screen hits (see **Chapter III**) and establishing experimental methods for systematic analysis of the remaining targets. Our results show that IRX-1 is both necessary and sufficient in VD motor neurons for the Unc-55 remodeling phenotype. We also demonstrated that IRX-1 contributes to developmentally regulated remodeling of DD motor neurons. Thus, these results are consistent with the hypothesis that the ectopic remodeling activated in *unc-55* mutant VD motor neurons includes key components that also drive the re-organization of synaptic output in DD motor neurons.

Our findings indicate that *irx-1* coordinates the overall remodeling scheme by directing the elimination of ventral VD synapses while simultaneously promoting the creation of dorsal VD synapses. This central role for *irx-1* could result from its function as a master regulator that coordinates expression of separate sets of genes with remodeling roles at either dorsal or ventral synaptic locations. Alternatively, remodeling could be orchestrated by a cell biological mechanism in which assembly of dorsal synapses activates a negative feedback loop that destabilizes ventral synapses (Ding et al., 2007; Park et al., 2011). Our results do not distinguish between these possibilities but systematic identification of *irx-1* targets and their sites of action should help to resolve this question.

We note that DD remodeling is delayed but not entirely prevented when *irx-1/Iroquois* function is disabled (**Figure 4.6**) whereas remodeling of *unc-55* mutant VDs is completely blocked (**Figure 4.3**). This finding suggests that additional partially redundant synaptic remodeling genes that function in parallel to *irx-1* may be active in DD motor neurons (**Figure 4.8**). The existence of DD-specific remodeling genes could also explain why our RNAi screen was capable of detecting transcripts with roles in ectopic VD remodeling but did not prevent DD motor neurons from eventually establishing dorsal synapses in the adult (**Chapter III**).

The *irx-1* locus encodes a transcription factor containing a homeodomain and flanking IRO box (Burglin, 1997) with strong homology to human *Iroquois* genes. In other organisms, the *Iroquois* family of transcription factors has been shown to pattern the nervous system by specifying neural ectoderm and later functioning to refine neural architecture (Cavodeassi et al., 2001; Gomez-Skarmeta and Modolell, 2002). Here, we have demonstrated that *irx-1* has an important role in synaptic remodeling during *C. elegans* neurodevelopment. Our results show that *irx-1* is normally expressed in DDs to promote synaptic remodeling but is negatively regulated in nearby VDs by *unc-55* (**Figure 4.1**) to prevent that adoption of the DD pattern of synaptic output (**Figure 4.3**).

Although COUP-TF and Iroquois proteins have been separately observed to perform developmental functions in common neural tissues, such as the vertebrate eye and cerebellum (Matsumoto et al., 2004; Cheng et al., 2005; Kim et al., 2009; Tang et al., 2010), our results identify the first regulatory link

between these two conserved transcription factors. We have identified 18 other conserved *unc-55*-regulated synaptic remodeling genes in our microarray and RNAi screens. There is a strong possibility that these genes may also be regulated by *irx-1* in within this synaptic remodeling transcriptional program. Future experiments will address whether these genes are positively regulated by *irx-1* to promote synaptic remodeling in wild-type DD motor neurons and *unc-55* VD motor neurons.

CHAPTER V

A DEGENERIN-FAMILY ACID SENSING ION CHANNEL, UNC-8, REGULATES SYNAPTIC REMODELING IN GABAERGIC MOTOR NEURONS

Introduction

Non-voltage-gated and acid-sensing ion channels have been implicated in synaptic plasticity in multiple model organisms, but the mechanisms by which they modulate plasticity are unclear (Wemmie et al., 2006; Voglis and Tavernarakis, 2008). In our microarray and RNAi screens for UNC-55 targets, we uncovered the degenerin-family non-voltage gated sodium channel UNC-8 as a potential mediator of GABAergic synaptic remodeling. Based on sequence homology, UNC-8 is predicted to function as an acid-sensing ion channel (ASIC). Because recent studies have placed ASICs as mediators of synapses in both learning and memory in other model organisms, we have pursued UNC-8 as an UNC-55 target with a potential key physiological role in the GABAergic synaptic remodeling program.

UNC-8 was originally described as a putative mechanotransducing channel with a structure similar to that of other ion channel proteins, such MEC-4 and MEC-10, which are also members of the degenerin/epithelial sodium channels (DEG/ENaCs) family. These proteins contain two membrane-spanning domains and a large extracellular loop containing three cysteine-rich domains (Tavernarakis et al., 1997) (**Figure 5.1**). Gain-of-function mutations in *unc-8* are

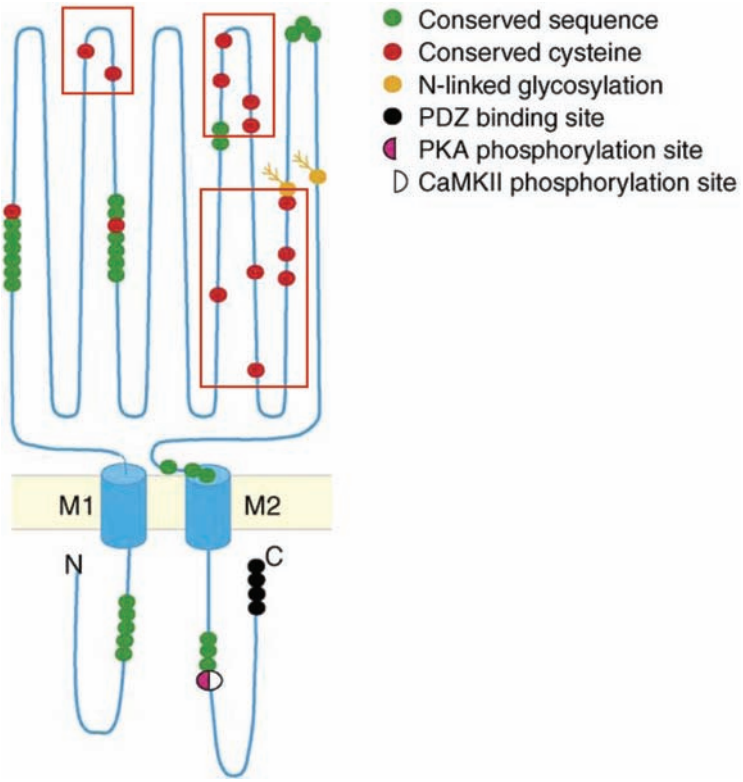

Figure 5.1. Structure and features of acid-sensing ion channel (ASIC) subunits. ASIC subunits contain two membrane-spanning domains (M1 and M2, in blue) and a large extracellular domain for sensing protons and other ligands. Three cysteine-rich domains, which have been identified in UNC-8 by Tavernarakis et. al. (1997), are indicated in red. Figure adapted from Wemmie, et. al., 2006.

dominant and cause neuronal swelling and severe uncoordination (Brenner, 1974). The *unc-8(gf)* swollen neuron defect is reminiscent of a necrotic phenotype caused by misregulated or constitutively open degenerin ion channels (Chalfie and Wolinsky, 1990; Driscoll, 1996). In contrast, recessive loss-of-function alleles of *unc-8* cause a very subtle behavioral phenotype, with slightly reduced amplitude and wavelength of sinusoidal body bends (Tavernarakis et al., 1997). Although *unc-8* has been postulated to function as a stretch receptor, direct evidence of this role is lacking.

Another potential role for *unc-8*, based on its protein structure and role in synaptic re-patterning (see **Chapter III**), is as an ASIC channel that contributes to synaptic function. ASIC proteins are members of the DEG/ENaC superfamily, with similar protein topology and selective sodium ion transport (Wemmie et al., 2006). ASICs are expressed throughout central and peripheral nervous systems of mammals. Channel activity of ASIC proteins is stimulated at low pH (<7.2) (Krishtal and Pidoplichko, 1980; Benson et al., 2002; Wemmie et al., 2006). This acid-sensing function has been proposed to result in a positive feedback loop in which presynaptic ASICs are activated by the acidification of the synaptic cleft that accompanies neurotransmitter release (Miesenbock et al., 1998; Voglis and Tavernarakis, 2008). The large extracellular domain that is characteristic of ASIC family proteins mediates this response to low pH and also can detect other regulatory cues. For instance, ASIC3 can be stimulated by small molecules (*e.g.*, 2-guanidine-4-methylquinazoline) at physiological pH, and neuropeptides can potentiate acid-evoked currents (Askwith et al., 2000; Yu et al., 2010). Thus, the

physiological mechanisms that regulate ASIC activity *in vivo* could involve diverse classes of signals.

In cell culture models, ASICs are enriched at dendritic spines of hippocampal neurons (Wemmie et al., 2006; Zha et al., 2009). Dendritic spines are dynamic sites of activity-dependent synaptic plasticity via long-term potentiation (LTP) and long-term depression (LTD), both of which are mediated by calcium. In the best-understood mechanism of LTP/LTD, glutamatergic receptors facilitate an influx of calcium during periods of high stimulation, which then functions as a second messenger to modify function (Yang et al., 1999; Yashiro and Philpot, 2008). In ASIC1-null mice, LTP is reduced, and the animals manifest deficits in learning and memory, specifically in conditioned fear and pain, while restoration of ASIC1 expression in the amygdala reverses these behaviors (Wemmie et al., 2002; Wemmie et al., 2004; Coryell et al., 2008). ASIC1 is presumed to function at the postsynaptic membrane due to the dendritic enrichment of ASIC1 in cultured cells (Wemmie et al., 2006). In contrast, ASIC-1 in *C. elegans* functions specifically in presynaptic dopaminergic neurons to mediate neurotransmitter release and dopamine-dependent learning behavior (Voglis and Tavernarakis, 2008). In either postsynaptic or presynaptic context, however, these studies suggest that the influx of sodium ions functions to promote synaptic strength. However, the mechanism by which ASICs modulate synaptic function is unclear.

The potential of ASICs to detect synaptic activity by proton-sensing in the synaptic cleft, the ability of ASICs to transduce cations, and the localization of

ASICs at sites of dynamic synaptic formation and elimination all point to a mechanistic role for ASICs in learning and memory. In our microarray and RNAi screens, we identified *unc-8* as a candidate UNC-55-regulated remodeling gene (see **Chapter III**), suggesting that this potential ASIC is involved in developmentally-controlled synaptic plasticity. In this chapter, I describe our studies of *unc-8* in the GABAergic synaptic remodeling program and propose a model for how *unc-8* contributes to the mechanism.

Author Contributions

The recombineering protocols (Zhang et al., 2008; Tursun et al., 2009) to generate *unc-8::GFP* were optimized with the help of fellow graduate students Clay Spencer and Rachel Skelton. The *unc-55; unc-2* experiment described in this chapter was performed by an undergraduate in the lab under my mentorship, Megan Gornet.

Methods

Strains and genetics: Nematode strains were maintained at 20-25°C with standard culture techniques (Brenner, 1974). The wild-type strain is N2 and all references to *unc-55* mutants used the allele *unc-55(e1170)*(Walthall, 1990). All animals used in this study were hermaphrodites.

Construction of *unc-8; juIs1* recombinants strains: Both *unc-8* and *juIs1[punc-25::SNB-1::GFP]* map to chromosome IV. Because the integration site of *juIs1* on chromosome IV is unknown, we used a brute-force screening

approach instead of traditional three-point recombination techniques (Brenner, 1974). For *n491* (Unc phenotype) and *n491n1193* (fainter phenotype), *unc-8/juIs1* F1 heterozygotes were built and allowed to self. F2 progeny with the appropriate Unc-8 movement phenotype were then visually screened for the *juIs1* GFP marker, indicating the presence of a recombinant *unc-8 juIs1* chromosome IV. These F2s were allowed to self and generate homozygous F3s for further analysis.

The deletion alleles *unc-8(tm2071)* and *unc-8(tm5052)* do not show an obvious movement phenotype and presence of the deletion allele must be assessed via single worm PCR. For these alleles, *unc-8/juIs1* F1 heterozygotes were allowed to self. Bright *juIs1*-expressing F2 animals, assumed to be homozygous for *juIs1*, were picked, allowed to self, and then genotyped for the presence of the *unc-8* deletion allele to detect a potential recombinant *unc-8 juIs1* chromosome IV. Animals that bred true for *juIs1* (*i.e.* homozygous *juIs1* among F3s) and contained an *unc-8* deletion allele were presumed to be recombinants. Homozygous *unc-8 juIs1* were isolated via single-worm PCR and kept for further analysis. For both *tm2071* and *tm5052,* >220 homozygous *juIs1* animals were screened to find one F3 containing a recombinant *juIs1 unc-8* chromosome, indicating close linkage of *juIs1* to the *unc-8* locus.

Strain list:

RNAi strains:

NC1613 *eri-1 (mg366) juIs1[punc-25::SNB-1::GFP; lin-15+]*

NC1852 *unc-55(e1170); eri-1(mg366) juIs1[punc-25::SNB-1::GFP; lin-15+]*

unc-8 alleles

MT1085 *unc-8(n491)*

MT2612 *unc-8(n491n1193)*

FX02071 *unc-8(tm2071)*

NC1909 *unc-8(tm2071)* outcrossed 2x

FX05052 *unc-8(tm5052)*

NC2324 *unc-8(tm5052)* outcrossed 2x

FX05074 *unc-8(tm5074)*

FX05145 *unc-8(tm5145)*

Synaptic analysis strains:

CZ333 *juIs1[punc-25::SNB-1::GFP; lin-15+]*

NC1851 *unc-55(e1170); juIs1[punc-25::SNB-1::GFP; lin-15+]*

NC1715 *unc-8(n491n1193) juIs1[punc-25::SNB-1::GFP; lin-15+]*

NC1850 *unc-55(e1170); unc-8(n491n1193) juIs1[punc-25::SNB-1::GFP; lin-15+]*

NC2051 *unc-8(tm2071) juIs1[punc-25::SNB-1::GFP; lin-15+]*

NC2125 *unc-55(e1170); unc-8(tm2071) juIs1[punc-25::SNB-1::GFP; lin-15+]*

NC2387 *unc-8(tm5052) juIs1[punc-25::SNB-1::GFP; lin-15+]*

NC2388 *unc-55(e1170); unc-8(tm5052) juIs1[punc-25::SNB-1::GFP; lin-15+]*

NC2415 *unc-8(n491) juIs1[punc-25::SNB-1::GFP; lin-15+]*

NC2585 *wyIs202[pflp-13::gfp::rab-3, pflp-13::mcherry; podr-1::GFP]*

NC2480 *wyIs202[pflp-13::gfp::rab-3, pflp-13::mcherry podr-1::GFP]; unc-8(tm5052)*

NC2443 *unc-55(e1170); juIs1[punc-25::SNB-1::GFP; lin-15+]; unc-2(e55)*

unc-8(csRNAi) strains

NC2529 *unc-119; wdIs86[pttr-39::unc-8; unc-119+; punc-25::mCherry; pttr-39::unc-8 antisense]*

NC2601 *unc-55(e1170); unc-119; juIs1[punc-25::SNB-1::GFP; lin-15+]; wdIs86[pttr-39::unc-8; unc-119+; punc-25::mCherry; pttr-39::unc-8 antisense]*

unc-8::GFP strains

OH4956 *otIs151[pceh-36::RFP; rol-6(d)]; otEx2876[punc-8::GFP; elt-2::GFP]*

NC2320 *pttr-39::mCherry V; otEx2876[punc-8::GFP; elt-2::GFP]*

NC2321 *unc-55(e1170); pttr-39::mCherry V; otEx2876[punc-8::GFP; elt-2::GFP]*

NC2527 *unc-119; wdEx840[unc-8::GFP + unc-119 recombineered fosmid]*

Microscopy and scoring: SNB-1::GFP assays were performed with the transgene *juIs1[punc-25::SNB-1::GFP; lin-15+]* (Hallam and Jin, 1998) and RAB-3::mCherry assays were performed with the transgene *wyIs202[pflp-13::RAB-3::mCherry; podr-1::GFP]* (Park et al., 2011). Animals were anesthetized with 0.1% tricaine/tetramisole, mounted on a 2% agarose pad, and imaged with a Zeiss Axiovert microscope using Metamorph software. Confocal images were obtained with a Leica TCSSP5 confocal microscope with Leica Application Suite

Advanced Fluorescence (LAS-AF) software and created using maximum intensity projections of Z-stacks collected at 1.0 μm/step with a 40x objective.

To calculate fluorescence intensity for the enhancement graph in **Figure 5.4,** linescan intensity values along the ventral nerve cord of each adult animal were collected with Leica Application Suite Advanced Fluorescence (LAS-AF) software. Mean intensity values for each animal were calculated, and then averaged with independent measurements for the same genotype. Statistical tests were performed comparing the average intensity among all animals in each genotype (N>8 per genotype).

To visualize *punc-8::GFP*, confocal images were collected to exclude the strong *pelt-2::GFP* expression in the intestine. *pttr-39::mCherry* was used to identify GABAergic motor neurons on the confocal microscope in these experiments. *punc-8::GFP* average area intensity was collected from maximum projections for individual DD and VD motor neurons. To normalize VD expression to DD expression in **Figure 5.2D**, average intensity of all VDs in a single worm was divided by the average DD intensity in the same worm. Statistical tests were performed by comparing the average VD/DD intensity among each worm (N>6 per genotype).

For quantifying *unc-8(csRNAi)* results, individual VD motor neurons expressing mCherry (control or *unc-8(csRNAi)*-labeling) were scored. For each mCherry-labeled VD, the number of SNB-1::GFP puncta in the anterior interval between the VD soma and the next anterior VD neuron were counted in the

dorsal and ventral nerve cords. These analyses were considered puncta per “VD anterior region” (Petersen et al., 2011).

Construction of *unc-8* feeding RNAi clone: Primers were designed to amplify 2266bp of the *unc-8* genomic locus, beginning with the 5’ start site and ending in the eighth exon. This ~2.3 kb *unc-8* fragment was amplified and cloned in pCR8 via TOPO-TA reaction (Invitrogen) to generate pSA53. The *unc-8* fragment was then cloned into L4440-Gateway via LR Clonase II Gateway reaction (Invitrogen) to yield pSA54. The L4440-Gateway vector contains symmetric T7 promoters for double-stranded RNA expression in bacteria,. The pSA54 plasmid resulting from the LR reaction was transformed into HT115 *E. coli* for use in RNAi feeding experiments, termed “RNAi - Miller” in *unc-8* RNAi experiments.

Construction of *unc-8(csRNAi)*: The “*unc-8* sense” construct pSA76 was cloned as follows: The ~2.3 kb *unc-8* fragment used in “RNAi - Miller" experiments was amplified with primers containing 5’AscI/3’SacII adaptors and cloned into pCR2.1 via TOPO-TA reaction (Invitrogen) to yield pSA75. The *unc-8* fragment was then subcloned into the existing GABAergic cell-specific RNAi (csRNAi) plasmid pSA47 (see **Methods, Chapter IV**) (Petersen et al., 2011) via AscI/SacII to yield pSA76. The “*unc-8* antisense” construct pSA78 was cloned as follows: the ~2.3 kb *unc-8* fragment used in “RNAi - Miller" experiments was amplified with primers containing 5’SacII/3’AscI adaptors and cloned into pCR2.1 via TOPO-TA reaction (Invitrogen) to yield pSA73. The *unc-8* fragment from

pSA73 was then inserted into existing GABAergic cell-specific RNAi (csRNAi) plasmid pSA47 (see **Methods, Chapter IV**) via AscI/SacII to yield pSA77. The *unc-8*-containing region of pSA77 between ScaI and SacII was then inserted into existing GABAergic csRNAi plasmid pSA49 (replacing the "*irx-1* antisense" cassette) to yield pSA78. pSA76 ("*unc-8* sense") and pSA78 ("*unc-8* antisense") were linearized and ligated, then transformed into *unc-119* worms via microparticle bombardment (Praitis et al., 2001) to yield a spontaneous integrant, as indicated by 100% transmission of rescued (*unc-119*+) movement (indicating "*unc-8* sense") and mCherry expression in all GABAergic motor neurons (indicating "*unc-8* antisense").

DD remodeling timecourses: For all DD remodeling timecourses, separate groups of 100 gravid control and mutant adults were picked to single 60-mm plates and allowed to lay eggs for one hour and then removed from the plate. The mid-point of the hour in which eggs were laid was considered to be t=0. Plates were incubated at 23°C throughout the timecourse. Beginning at 18 hours post-lay and for each hour thereafter, larvae were imaged (as above) on a Zeiss Axiovert microscope. For experiments with *punc-25::SNB-1::GFP*, the number of dorsal SNB-1::GFP puncta and number of GFP+ neurons (*i.e.* GABA neurons) were recorded for >10 larvae for each timepoint. For experiments with *pflp-13::RAB-3::GFP*, only the number of RAB-3::GFP puncta were recorded either in the dorsal or ventral nerve cords; *pflp-13* is not expressed in VD motor neurons so that could not be used as a proxy for GABAergic development.

Recombineering UNC-8::GFP fosmid: We adapted the Hobert lab recombineering protocol to insert GFP at the C-terminal end of a fosmid containing *unc-8* (Tursun et al., 2009). The fosmid WRM0635cA02 was obtained from GeneService and purified via column-less miniprep (NCI protocol available at http://web.ncifcrf.gov/research/brb/protocol/Protocol3_SW102_galK_v2.pdf). 0.5-2 μg fosmid was then transformed into electrocompetent SW105 cells, prepared as directed (Tursun et al., 2009). Presence of the fosmid in SW105 was verified via colony PCR using primers specific to the *unc-8* locus. The GFP-galK recombineering cassette was amplified with 50 kb homology arms (using PAGE-purified primers) from pBALU1 (available from the Hobert Lab, see Tursun, et. al.) and gel purified. 200 ng of GFP-galK PCR product was transformed into electrocompetent, λ Red recombinase-activated, fosmid-containing SW105 cells, prepared as directed in Tursun, et. al. Cells containing fosmid+GFP-galK were first grown for >60 hours at 32°C and then streaked on MacConkey+galactose plates with chloramphenicol to ensure insertion of recombineering cassette. To excise galK from the GFP intron, colonies were incubated with 0.1% arabinose as directed in Tursun et. al. to create an *unc-8::GFP* expression fosmid. This *unc-8::GFP* fosmid was then purified via column-less miniprep (NCI protocol).

We then used the Fisher lab protocol to insert *unc-119* into the *unc-8::GFP* fosmid (Zhang et al., 2008). 2 μg of *unc-8::GFP* fosmid was co-transformed with the “pLoxP unc-119” plasmid (Zhang et al., 2008) into electrocompetent SW106 cells. Following electroporation, cells were recovered in arabinose to insert the pLoxP *unc-119* plasmid into the *unc-8::GFP* fosmid via a

single loxP site Cre recombination. Presence of *unc-119* in the fosmid was confirmed via colony PCR, and the *unc-8::GFP+unc-119* fosmid was purified via column-less miniprep (NCBI protocol) to transform into *unc-119* mutants via microparticle bombardment.

Results

punc-8::GFP is expressed in remodeling GABAergic motor neurons

Based on the >4-fold elevation of *unc-8* transcript in our profile of *unc-55* GABAergic neurons, UNC-55 normally inhibits *unc-8* expression. Furthermore, based on the apparent requirement for *unc-8* function in remodeling of *unc-55* mutant VD motor neurons (see **Chapter III**), we also hypothesized that *unc-8* would be normally expressed in DD motor neurons. To test these predictions, we obtained a strain carrying transgenic GFP driven by 2792 bp of the 5' intergenic region of *unc-8* [kindly provided by the Hobert lab (Etchberger et al., 2007)] (**Figure 5.2A**). Because this strain is co-labeled with a bright intestinal marker (note bright intestinal cells in **Figure 5.2A**, lower panel), we also expressed *pttr-39::mCherry* in this background to mark GABAergic motor neurons. This experiment showed that *punc-8::GFP* is brightly expressed in mCherry-labeled DD motor neurons in both wild-type and *unc-55* mutant animals (**Figure 5.2B**). In contrast, *punc-8::GFP* is weakly detected in wild-type VD motor neurons, but shows a much stronger signal in *unc-55* VD motor neurons (**Figure 5.2B**). To quantify this visual assessment, we measured the fluorescence intensity in wild-type and *unc-55* DD and VD motor neurons (**Figure 5.2C**). This analysis

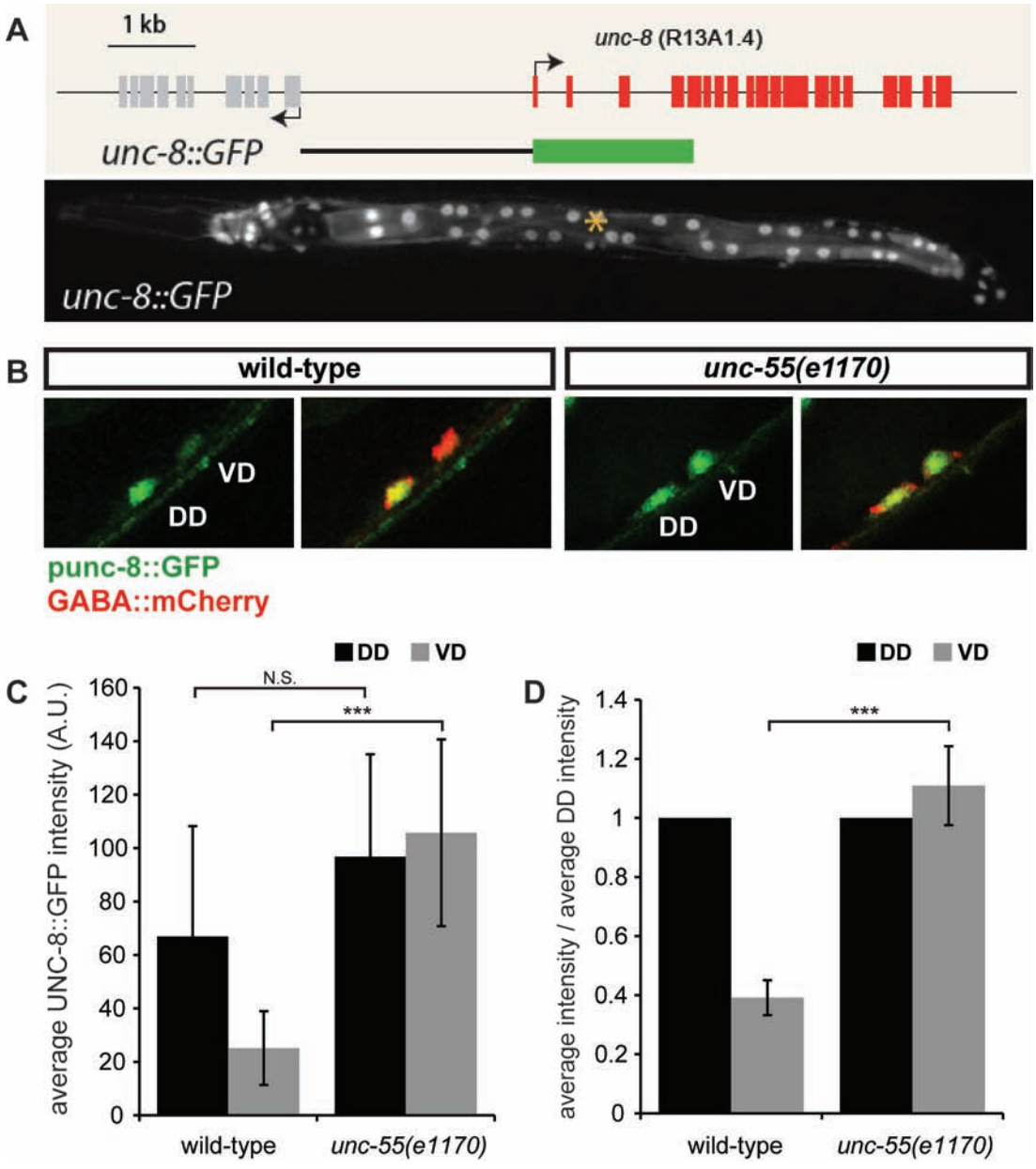

Figure 5.2. *punc-8::GFP* is expressed in remodeling GABAergic motor neurons. (A) The *punc-8* transgene in *otEx2876* contains the intergenic 5' regulatory region of *unc-8* fused to GFP by overlap PCR (top panel). Note bright intestinal marker (indicated by yellow asterisk in bottom panel) which co-injected with *punc-8::GFP.* Figure adapted from Etchberger et. al., 2007. **(B)** *punc-8::GFP* expression is restricted to DD motor neurons in wild-type but observed in both DD and VD motor neurons in *unc-55* mutants. GABAergic motor neurons are indicated with mCherry (via *pttr-39::mCherry*) and DD motor neurons were distinguished from VD motor neurons by their stereotypical location in the ventral nerve cord. **(C-D)** Quantification of *punc-8::GFP* intensity in GABAergic motor neurons. Raw data **(C)** indicates an increase in fluorescence in both DD and VD motor neurons in the *unc-55* mutant (N.S., not significant in DD motor neurons), while normalization to DD fluorescence **(D)** confirms that the *punc-8::GFP* is derepressed in VD motor neurons. *** $p < 0.001$, wild-type vs. *unc-55*, Student's t-test. Error bars indicate standard deviation. N = 24 DDs and 54 VDs per genotype.

revealed that *punc-8::GFP* is significantly elevated in *unc-55* VD motor neurons (**Figure 5.2D**) to a level similar to that in DD motor neurons. These data are consistent with a model in which *unc-8* is strongly expressed in remodeling DD motor neurons, but is not expressed in VD motor neurons due to repression by UNC-55.

unc-8 RNAi inhibits ectopic remodeling of *unc-55* VD motor neurons

We first observed that loss of *unc-8* blocks synaptic remodeling in the RNAi screen of candidate *unc-55* targets (**Figure 3.6**). This screen knocked down expression of *unc-8* via a commercially available RNAi construct (Kamath et al., 2003), which is complementary to approximately 1 kb of the *unc-8* coding region (**Figure 5.3A**, "RNAi-Ahringer", named for the lab in which it was created). We created an additional RNAi clone that spans a larger region of the *unc-8* locus to confirm this result and to limit the possibility of an off-target phenotype (**Figure 5.3A**, "RNAi-Miller"). Knockdown of *unc-8* with either RNAi construct results in similar and significant restoration of SNB-1::GFP to the ventral nerve cord of *unc-55(e1170)* in an RNAi-sensitized (*eri-1*) background (**Figure 5.3B**, 25.2 $\pm$ 7.4 ventral SNB-1::GFP in control RNAi *unc-55* adults vs. 46.7 $\pm$ 10.9 in *unc-55* with *unc-8(RNAi-Ahringer)* and 44.3 $\pm$ 9.0 with *unc-8(RNAi-Miller)*, $p < 0.001$, Student's t-test). Furthermore, these experiments showed that knockdown of *unc-8* in *unc-55* mutants also results in decreased dorsal SNB-1::GFP fluorescence in addition to enhanced ventral SNB-1::GFP (**Figure 5.3C**), as expected for a gene that is specifically required for synaptic remodeling.

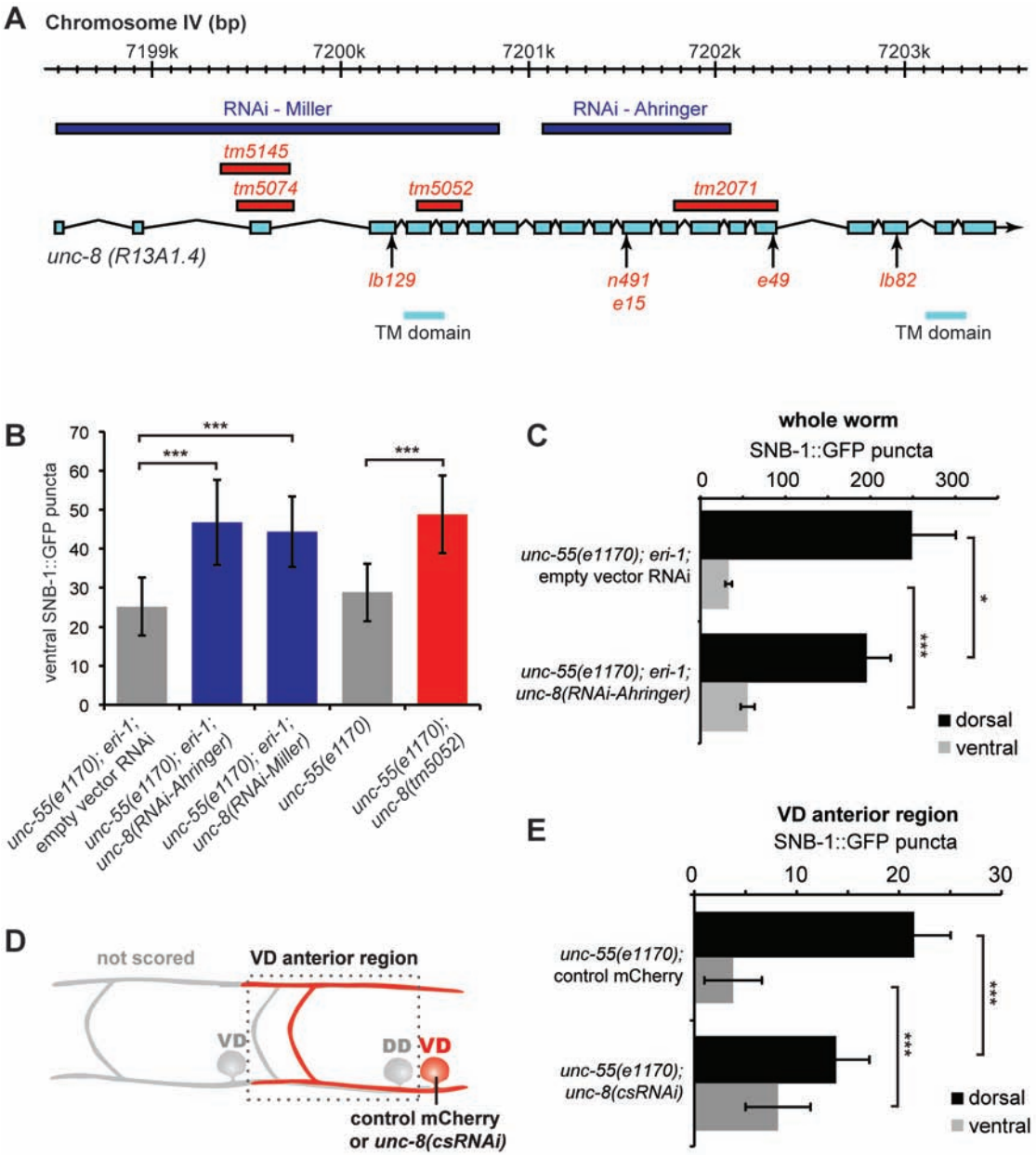

Figure 5.3. *unc-8* is cell-autonomously required for *unc-55* synaptic remodeling. (A) *unc-8* is encoded by *R13A1.4* on Chromosome IV; exons and transmembrane (TM) domains are indicated in light blue. Complementary RNAi sequences (RNAi-Miller, RNAi-Ahringer) are indicated in dark blue and genetic mutations are annotated in red. **(B)** Suppression of *unc-55* via *unc-8* RNAi (blue bars) and *unc-8(tm5052)* (red bar) as indicated by an increase in ventral SNB-1::GFP puncta. *** $p < 0.001$ vs. wild-type, Student's t-test. Error bars indicate standard deviation. N=11-19 worms per genotype. **(C)** The gain in ventral puncta in *unc-55* mutants treated with *unc-8* RNAi is accompanied by a subtle but significant decrease in dorsal SNB-1::GFP puncta. * $p < 0.05$, *** $p < 0.001$ vs. *unc-55*, Student's t-test. Error bars indicate standard deviation. N=7 matched dorsal and ventral nerve cords per RNAi treatment. **(D)** Dotted lines denote anterior regions of mCherry-marked VD motor neurons [carrying either control mCherry or *unc-8(csRNAi)*] in which SNB-1::GFP puncta were counted (see Methods). (**E**) Quantification of *irx-1(csRNAi)* suppression of the Unc-55 synaptic remodeling defect. *** $p < 0.001$, Student's t-test. Error bars indicate standard deviation. N > 50 VD anterior regions per genotype.

unc-8 functions cell-autonomously in VD motor neurons to promote synaptic remodeling

Based on the enrichment of *unc-8* in the GABA-specific *unc-55* profile, we predicted that the function of *unc-8* in remodeling is cell-autonomous. To test this idea, we built a heritable cell-specific RNAi construct, *wdIs86[unc-8(csRNAi)]*, which disrupts *unc-8* expression specifically in GABAergic motor neurons. This *unc-8(csRNAi)* construct expresses both sense and antisense RNA in GABA motor neurons under control of the *ttr-39* promoter. *unc-8(csRNAi)* neurons are marked with mCherry. We scored the SNB-1::GFP pattern in the dorsal and ventral processes of VD motor neurons ("VD anterior regions", **Figure 5.3D**) of *unc-55; GABA::mCherry* control and *unc-55; unc-8(csRNAi*) mutant animals. As a reference, we confirmed that *unc-55; GABA::mCherry* VD motor neurons display strong SNB-1::GFP enrichment in dorsal neurites with a corresponding depletion of ventral NMJs. VD motor neurons with *unc-8(csRNAi),* however, have significantly fewer dorsal puncta (13.8 $\pm$ 3.3 vs. 21.5 $\pm$ 3.6 in *unc-55*, $p < 0.001$) with more ventral puncta (8.2 $\pm$ 3.2 vs. 3.8 $\pm$ 2.8 in *unc-55*, $p < 0.001$) (**Figure 5.3E**). These results are indicative of a cell-autonomous role for UNC-8 in GABAergic motor neuron remodeling.

unc-8(tm5052) suppresses the Unc-55 remodeling defect

We tested loss-of-function *unc-8* alleles to validate the RNAi results. The original mutations identified in the *unc-8* locus (*n491, e15, e49, lb82*) are missense mutations that encode a constitutively open sodium channel and result

in a gain-of-function neuronal swelling phenotype reminiscent of necrotic excitotoxicity (Tavernarakis et al., 1997). We tested a deletion allele generated for this study by the Mitani lab (Tokyo Women's Medical University), *unc-8(tm5052)*, that deletes a portion of the fifth and the entire sixth exon and results in an early stop codon prior to the seventh exon (**Figure 5.3A**). Because this allele removes the first membrane-spanning domain (Tavernarakis et al., 1997), and should block translation of the remainder of the *unc-8* sequence, we predict that *tm5052* corresponds to an *unc-8* null mutation.

We crossed this putative null allele, *unc-8(tm5052),* into the *unc-55(e1170)* background and tested for restoration of ventral SNB-1::GFP. The *unc-55(e1170); unc-8(tm5052)* double mutant showed significant suppression of the Unc-55 defect (**Figure 5.3B**, 28.8 $\pm$ 7.3 ventral puncta in *unc-55* vs. 48.8 $\pm$ 10.0 ventral puncta in *unc-55; unc-8* double mutants, $p < 0.001$, Student's t-test). Interestingly, two other predicted *unc-8* loss-of-function alleles, *n491n1193* or *tm2071* (**Figure 5.3A**, data not shown), did not suppress *unc-55*. *n491n1193* contains the gain-of-function *n491* lesion as well as a second mutation, *n1193*, that reverses the *n491* dominant trait and causes a "fainting" phenotype that is actually a result of a second mutation in the *unc-80* gene (Mei Zhen, personal communication). *tm2071* is a deletion allele that removes a portion of the extracellular loop of *unc-8* and causes a frameshift that is predicted to disrupt the second transmembrane domain (**Figure 5.3A**). *unc-55; unc-8(tm2071)* are indistinguishable from *unc-55* single mutants (data not shown).

Based on our RNAi results and the prediction that *unc-8(tm5052)* encodes a genetic null, we conclude that *unc-8* functions downstream of *unc-55* to promote synaptic remodeling of GABAergic motor neurons. The lack of *unc-55* suppression by *unc-8(tm2071)*, however, is intriguing and suggests that UNC-8 channel function may be dispensable for remodeling. A structure-function analysis with an allelic series of *unc-8* mutations could help to resolve this conundrum. The Mitani lab has already provided two additional alleles (*tm5074, tm5145*, see **Figure 5.3A**) and will continue to collaborate with us to generate additional alleles to address this question.

unc-8 promotes remodeling in parallel to the potent remodeling regulator, *irx-1/Iroquois*

In **Chapter IV**, we demonstrated that the homeodomain-containing transcription factor, IRX-1/Iroquois, is both necessary and sufficient for remodeling GABAergic synapses downstream of *unc-55.* Because IRX-1 functions as a transcription factor, we considered the possibility that *unc-8* expression is positively regulated by IRX-1. Alternatively, UNC-8 and IRX-1 could function in parallel to promote relocation of synapses in *unc-55* VD motor neurons. We designed a set of experiments to distinguish between these two potential models.

First, we tested an *unc-8* mutation for enhancement of the *irx-1* RNAi phenotype. Both *unc-8(tm5052)* and *irx-1*(RNAi) alone result in the restoration of SNB-1::GFP puncta to the ventral nerve cord of *unc-55* mutants (**Figure 5.4A-B**).

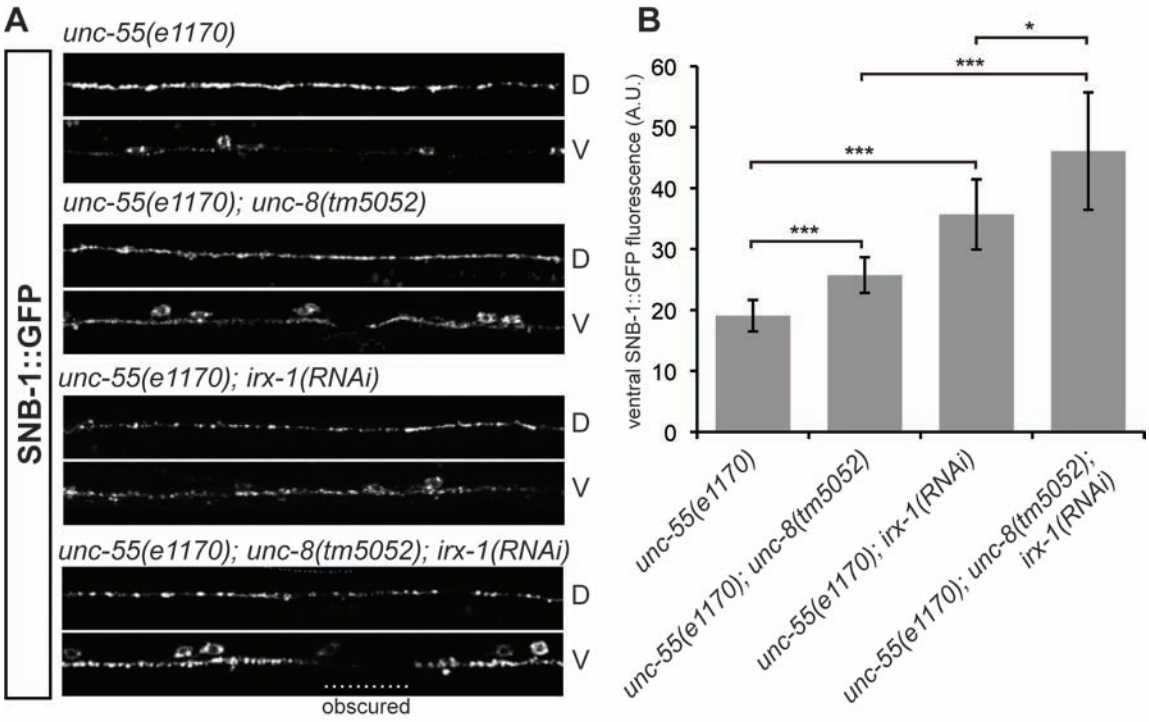

C

	strong unc-8::GFP fluorescence	
	DDs	VDs
wild-type; empty vector RNAi	36/36 (100%)	0/78 (0%)
unc-55(e1170); empty vector RNAi	48/48 (100%)	104/104 (100%)
wild-type; *irx-1* RNAi	30/30 (100%)	3/65 (5%)
unc-55(e1170); *irx-1* RNAi	18/18 (100%)	39/39 (100%)

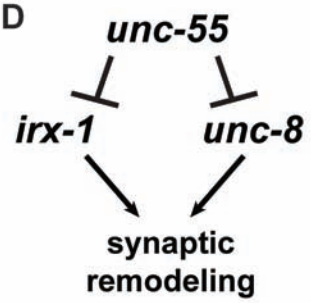

Figure 5.4. *unc-8* functions in parallel to *irx-1/Iroquois* to promote synaptic remodeling. (A) Representative 75-μm lengths of SNB-1::GFP puncta in dorsal (D) and ventral (V) nerve cords of each indicated genotype. Images of each dorsal and ventral nerve cords are from a common region of a single adult. Note that SNB-1::GFP increases in the ventral nerve cord and decreases in the dorsal nerve cord from the top panels (*unc-55)* to bottom panels (*unc-55; unc-8; irx-1*). In *unc-55(e1170); unc-8(tm5052); irx-1(RNAi),* dotted line indicates a region where the ventral nerve cord is obscured by the vulva. **(B)** Quantification of the enhanced suppression observed in panel **(A)**. SNB-1::GFP fluorescence in arbitrary units (A.U.) averaged from ≥6 ventral nerve cords of each genotype. * $p < 0.05$, *** $p < 0.001$, Student's t-test. Error bars indicate standard deviation. **(C)** Expression of *punc-8::GFP* is unaffected by *irx-1* RNAi. **(D)** *irx-1* and *unc-8* both promote synaptic remodeling downstream of *unc-55* in parallel pathways.

We reasoned that if IRX-1 and UNC-8 function in parallel pathways, then *unc-8(tm5052)* should enhance the suppression observed in *unc-55; irx-1* (RNAi-treated) animals. The results of this experiment are consistent with this idea; the *unc-55; unc-8(tm5052)* double mutant treated with *irx-1* RNAi showed brighter and denser puncta compared to either *unc-55; unc-8(tm5052)* or *unc-55; irx-1(RNAi)* (**Figure 5.4A**). We quantified this effect by measuring SNB-1::GFP fluorescence intensity in the ventral nerve cord. SNB-1::GFP fluorescence is significantly more intense in *unc-55; unc-8(tm5052); irx-1(RNAi)* adults [* $p < 0.05$ vs. *unc-55; irx-1(RNAi)*, *** $p < 0.001$ *unc-55; unc-8(tm5052)*] (**Figure 5.4D**).

Because *irx-1* RNAi does not result in a null phenotype, we considered the possibility that *unc-8* could enhance the *unc-55* suppression of *irx-1* RNAi even if both genes function in a common pathway. Thus, we devised additional tests to address this question. First, we noted that *irx-1* RNAi had no effect on expression of the *unc-8::GFP* reporter gene, which argues against *irx-1* regulation of *unc-8* expression (**Figure 5.4C**). In another test, we asked if *unc-8* is required for the ectopic VD remodeling defect shown by *irx-1(gf)* mutant animals (**Figure 4.7**). We reasoned that if *unc-8* functions downstream of *irx-1*, then loss of *unc-8* should suppress ectopic remodeling. Alternatively, if *unc-8* instead functions in a parallel pathway, it should be repressed by wild-type UNC-55 and therefore should have no effect on *irx-1(gf)* remodeling. We observed that the *irx-1(gf)* ectopic remodeling phenotype was not suppressed by *unc-8* RNAi (data not shown, N=5 *irx-1(gf) unc-8*-RNAi animals), though this experiment could be repeated with *unc-8(tm5052)* to validate this result. These results are consistent

with a model in which *irx-1* and *unc-8* function in two separate pathways, both downstream of *unc-55*, to promote synaptic remodeling (**Figure 5.4D**).

unc-8 functions in removal of ventral synapses during synaptic remodeling

We have shown that *unc-8* is necessary for remodeling of VD motor neurons in *unc-55* mutants. Because the remodeling program in VD motor neurons is similar to that in DD motor neurons (*i.e.*, both can be repressed by UNC-55), and because *punc-8::GFP* is expressed in DD motor neurons (**Figure 5.2**), we next examined whether *unc-8* is also required for DD remodeling. To visualize the establishment of DD dorsal synapses at the L1-L2 transition, the appearance of dorsal SNB-1::GFP puncta was noted at hourly intervals in wild-type and *unc-8(tm5052)* mutants. Dorsal SNB-1::GFP puncta are detected in L1 larvae beginning around ~19-20 hours after initiating the experiment (see **Methods**) in both wild-type and *unc-8(tm5052)* mutants (**Figure 5.5A**). Dorsal NMJs continue to form at a similar rate in wild-type and *unc-8(tm5052)* over the next 4-5 hours until remodeling is complete at the onset of the L2 stage (~24 hours). To control for potential differences in developmental timing between wild-type and *unc-8*, we also monitored the appearance of VD motor neurons, which are generated while DD motor neurons are remodeled (**Figure 5.5B**). Again, *unc-8(tm5052)* mutants showed no significant difference in the rate of appearance of VD motor neurons from wild-type, suggesting that neither GABAergic development nor establishment of dorsal DD motor neuron NMJs is delayed due to loss of *unc-8*.

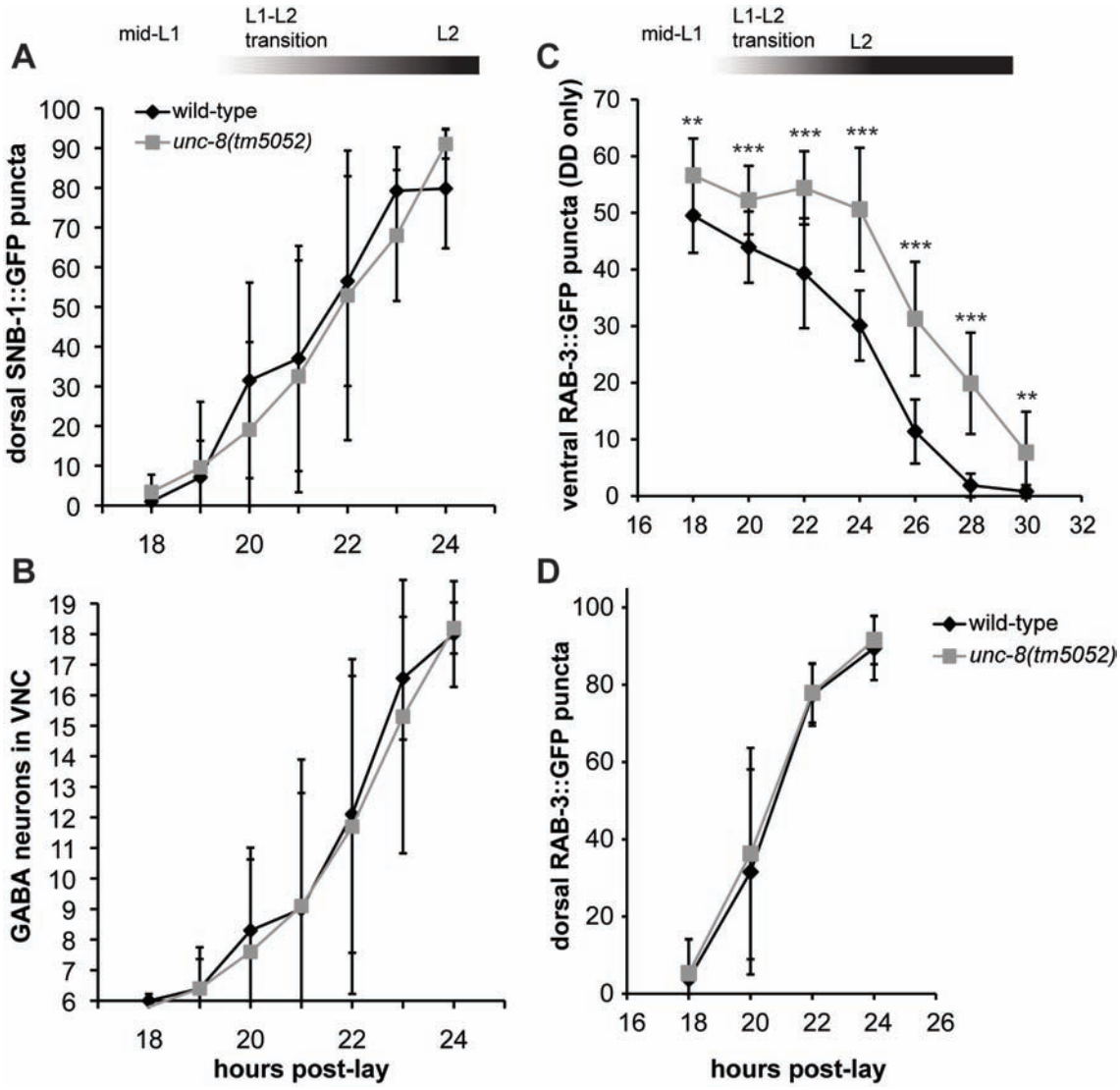

Figure 5.5. *unc-8* functions specifically in removal of ventral NMJs during synaptic remodeling. (A-B) *unc-8(tm5052)* does not delay formation of dorsal NMJs during DD synaptic remodeling. **(A)** DD remodeling was quantified by counting dorsal SNB-1::GFP puncta during L1-L2 larval stages. In both wild-type and *unc-8(tm5052)* larvae, DD remodeling begins at ~19 hours (see Methods) in L1 larvae and is completed by the L2 stage. All timepoints, not significantly different. **(B)** Generation of GABAergic motor neurons, visualized with *juIs1[punc-25::SNB-1::GFP],* is not disrupted by loss of *unc-8*. The normal complement of 6 embryonic DD motor neurons was observed in both wild-type and *unc-8(tm5052)* larvae prior to remodeling (t = 18 hours) and the 13 post-embryonic VD motor neurons appeared at the same rate in wild-type and *unc-8(tm5052)*. **(C-D)** Removal of immature DD ventral synapses is delayed in *unc-8(tm5052)*. **(C)** DD remodeling was quantified by counting ventral GFP::RAB-3 (*wyIs202*) puncta during the L1-L2 transition. In wild-type, removal of ventral synapses begins at ~20 hours and is completed around ~28 hours, occurring at a slower rate than the appearance of dorsal NMJs **(D)**. In *unc-8(tm5052)* mutants, removal of ventral NMJs begins later, ~24 hours, and is not completed by t = 30. However, dorsal NMJ formation appears normal with *wyIs202* **(D)**. ** $p < 0.01$, *** $p < 0.001$, Student's t-test. For all graphs, error bars indicate standard deviation. For **(A-C)**, results are pooled from three independent timecourses, for **(D)**, results from one timecourse are presented.

To test whether removal of DD ventral NMJs is disrupted in *unc-8(tm5052)*, we used the *wyIs202[pflp-13::GFP::RAB-3]* transgene which labels NMJs in DD motor neurons but not VD motor neurons. With this marker, all GFP::RAB-3 puncta in the ventral nerve cord should correspond to DD synapses. In wild-type larvae, ventral synapse removal begins around the same time as dorsal NMJ establishment (~20 hours), but the rate of synapse removal in the ventral nerve cord is slower than the establishment of dorsal NMJs. Whereas the number of dorsal synapses reaches a plateau 4-6 hours after the initiation of DD remodeling, the removal of DD ventral synapses continues for ~10 hours and extends into the L2 period (**Figure 5.5C**, black line).

In *unc-8(tm5052)* mutants, initiation of ventral synapse removal is not initiated until several hours after wild-type, such that persistent ventral synapses are still visible in the L2 stage (**Figure 5.5C**, gray line, ** $p < 0.01$, *** $p < 0.001$). As an internal control for these results, we used *wyIs202[pflp-13::GFP::RAB-3]* to monitor the appearance of dorsal NMJs for remodeling DD motor neurons (**Figure 5.5D**). This experiment confirms the earlier result obtained with the *juIs1[punc-25::SNB-1::GFP]* marker in which dorsal DD NMJs appear at virtually identical rates in wild-type and *unc-8* animals. Therefore, our evidence strongly suggests that *unc-8* is required for the removal of ventral synapses as DD motor neurons remodel but is not necessary for the establishment of DD dorsal NMJs This result suggests that the pathway that drives synaptic assembly in the remodeling program is uncoupled from the mechanism that removes synapses on the ventral side.

GABAergic synaptic remodeling is activity-dependent

In mammals, synapses may be selectively assembled or eliminated via activity-dependent mechanisms that can operate in genetically-regulated developmental programs (Sanes and Lichtman, 1999; Shen and Scheiffele, 2010). Given the role of *unc-8* in GABAergic remodeling, and the evidence that ASICs can mediate activity-dependent plasticity (Zha et al., 2006; Coryell et al., 2008), we wondered if the DD synaptic remodeling program is sensitive to changes in neuronal activity. To explore this possibility, we compared wild-type DD motor neuron remodeling to the rate of remodeling in a *tom-1* mutant. The *tom-1* locus encodes the single nematode homologue of tomosyn, which forms an inhibitory SNARE complex with UNC-64/syntaxin that prevents synaptic vesicle priming and excess neurotransmitter release at NMJs in wild-type animals (McEwen et al., 2006; Gracheva et al., 2007). Thus, *tom-1* mutants exhibit excess synaptic activity. Because *tom-1* L1 larvae develop more slowly than wild-type, the appearance of dorsal SNB-1::GFP puncta are plotted against the number of VD motor neurons in the ventral nerve cord.

A comparison of L1 timepoints revealed that *tom-1* mutants show significantly more dorsal SNB-1::GFP puncta than wild-type. Furthermore, *tom-1* larvae appear to complete remodeling (indicated by a plateau of SNB-1::GFP puncta) prior to the onset of L2 stage, before all postembryonic VD motor neurons are generated [**Figure 5.6A**, * $p < 0.05$, *** $p < 0.001$, wild-type (black line) vs. *tom-1* (blue line), Student's t-test]. These results suggest that DD remodeling program is influenced by synaptic activity.

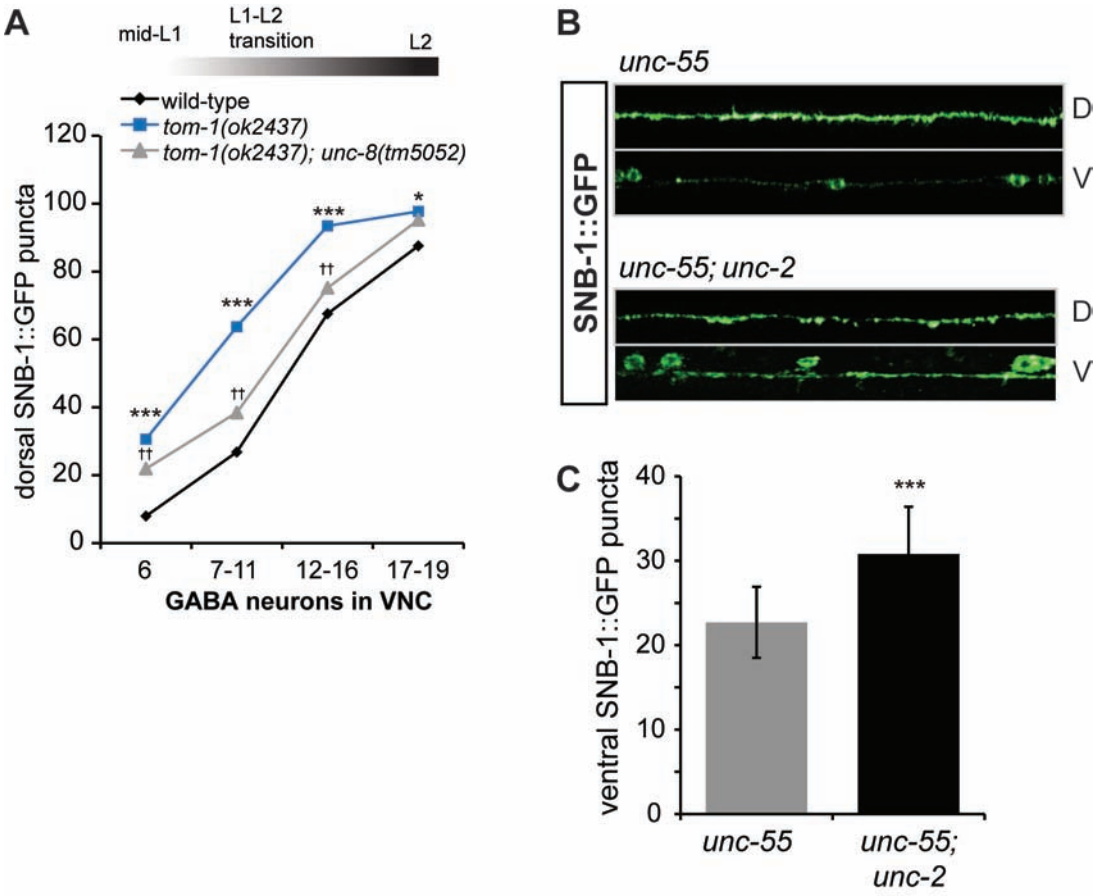

Figure 5.6. Synaptic activity and calcium channels influence GABAergic remodeling. (A) DD remodeling was quantified by counting dorsal SNB-1::GFP (*juIs1*) puncta during L1-L2 larval stages. Because *tom-1* delays normal development, timepoints are binned according to the number of GABAergic motor neurons in the ventral nerve cord (VNC). Thirteen VD motor neurons are added in the late L1 stage to the existing six embryonic DD motor neurons (19 GABAergic motor neurons total). *tom-1* mutants (blue line) exhibit precocious remodeling compared to wild-type (black line). * $p < 0.05$, *** $p < 0.001$, Student's t-test. *unc-8(tm5052)* suppresses ectopic *tom-1* remodeling (gray line). †† $p < 0.01$, Student's t-test. Results are pooled from >3 independent timecourses per genotype. Error bars omitted for clarity. **(B)** Loss of the L-type calcium subunit *unc-2* suppresses *unc-55* VD remodeling. SNB-1::GFP is not detected in the ventral nerve cord (V) of *unc-55* adults but is restored in *unc-55; unc-2* double mutants. Note concurrent reduction of SNB-1::GFP in dorsal nerve cord (D) relative to *unc-55* (not quantified). Representative 50-um lengths of each dorsal and ventral nerve cords are derived from a common region of a single adult. **(C)** Quantification of *unc-2* suppression of *unc-55.* In *unc-55; unc-2* mutants, more SNB-1::GFP puncta are detected in the ventral nerve cord compared to *unc-55* single mutant. *** $p < 0.001$, Student's t-test. Error bars indicate standard deviation. $N \geq 10$ adults per genotype.

Given that excess activity appears to stimulate the precocious appearance of dorsal DD NMJs, we next wondered whether *unc-8* might be required for this remodeling event in the *tom-1*-sensitized background. This experiment showed that the *unc-8(tm5052)* mutation effectively slows the otherwise early dorsal synaptogenesis observed in *tom-1* single mutants [**Figure 5.6A**, †† $p < 0.01$, *tom-1* (blue line) vs. *tom-1; unc-8* (gray line), Student's t-test]. This result indicates that *unc-8* is required for precocious remodeling in *tom-1* mutants and therefore indicates that *unc-8* regulates an activity-dependent mechanism. It is unclear if *tom-1* function is cell-autonomous for DD motor neuron remodeling, or if the enhanced rate of remodeling in *tom-1* is due to excess synaptic vesicle release from other neurons. However, the cell-autonomous role of *unc-8* in VD synaptic remodeling suggests that *unc-8* functions similarly in DD motor neurons. This question can be directly addressed by using the *unc-8(csRNAi)* transgene to knock down *unc-8* function in *tom-1* DD motor neurons.

GABAergic synaptic remodeling is calcium-dependent

We next decided to test whether changes in calcium influx, which is known to mediate activity-dependent plasticity, could also affect the GABAergic synaptic remodeling program. To address this question, we utilized a null mutant of an L-type calcium channel, *unc-2(e55)*. This experiment was performed by undergraduate Megan Gornet. For this assay, Megan tested the role of *unc-2* in remodeling of *unc-55* VD motor neurons. In *unc-55* mutant adults, the ventral nerve cord is largely devoid of SNB-1::GFP puncta (**Figure 5.6B**, top panel).

However, a loss-of-function *unc-2* mutant delays the Unc-55 VD remodeling program (**Figure 5.6B**, bottom panel); in *unc-55; unc-2(e55)* double mutants, SNB-1::GFP puncta were significantly more abundant in the ventral nerve cord than in the *unc-55* control(**Figure 5.6C**, 22.7±4.2 ventral puncta in *unc-55* vs. 30.8±5.6 in *unc-55; unc-2*; *** $p < 0.001$). This result suggests that calcium signaling is required for ectopic VD motor neuron remodeling in *unc-55* mutants, either directly (cell-autonomously) or indirectly, and is again suggestive of an activity-dependent effect on GABAergic plasticity. Whether calcium also modulates DD remodeling, and whether other L-type calcium subunits are also required, remains an open question.

Where is UNC-8 positioned to mediate synaptic removal from the ventral nerve cord?

Based on the expression pattern of other ASICs at synaptic membranes and the isolation of UNC-8 from lipid rafts (Sedensky et al., 2004; Voglis and Tavernarakis, 2008; Zha et al., 2009), we predicted that UNC-8 localizes to GABAergic motor neuron processes to execute its role in the remodeling program. To test this model, we used recombineering to build a GFP-tagged UNC-8 fosmid (Zhang et al., 2008; Tursun et al., 2009). This construct encompasses the *unc-8* genomic region and presumably spans the *cis*-regulatory elements that regulate native UNC-8 expression. In wild-type larvae and adults, UNC-8::GFP is brightly expressed in DD motor neurons and in multiple sensory neurons (not shown), with some dim expression in other neuron

subtypes including some VD motor neurons (DDs indicated with arrows, **Figure 5.7A**, top panel). Importantly, punctate UNC-8::GFP in the ventral nerve cord is likely indicative of localization to DD motor neuron processes (**Figure 5.7A**, bottom panel). Although additional analysis is necessary to confirm this result, this finding suggests that UNC-8 may function locally to remove ventral synapses of remodeling GABAergic motor neurons (**Figure 5.7B**). It follows that the role of UNC-8 in promoting the assembly of dorsal GABAergic synapses (**Figure 5.2, 5.5**) may be indirect.

Discussion

UNC-8 mediates synaptic plasticity in GABAergic motor neurons

The RNAi screen of *unc-55* targets revealed *unc-8* as a potent suppressor of the Unc-55 phenotype (see **Chapter III**). Here, I have presented evidence that UNC-8 is normally expressed in DD motor neurons but is repressed by UNC-55 in VD motor neurons to block the DD synaptic remodeling program (**Figure 5.2**). The RNAi result was confirmed with an *unc-8* null allele which also showed strong suppression of the Unc-55 phenotype. A cell-autonomous role for UNC-8 was established by cell-specific RNAi knockdown of *unc-8* in GABAergic motor neurons (**Figure 5.3**). Although our evidence shows that IRX-1/Iroquois functions as a key regulator of synaptic remodeling, we have also discovered that UNC-8 functions in an independent, parallel remodeling pathway (**Figure 5.4-5**). Based on preliminary evidence with *tom-1* and *unc-2* mutants, we propose that GABAergic motor neuron remodeling is activity dependent. Furthermore,

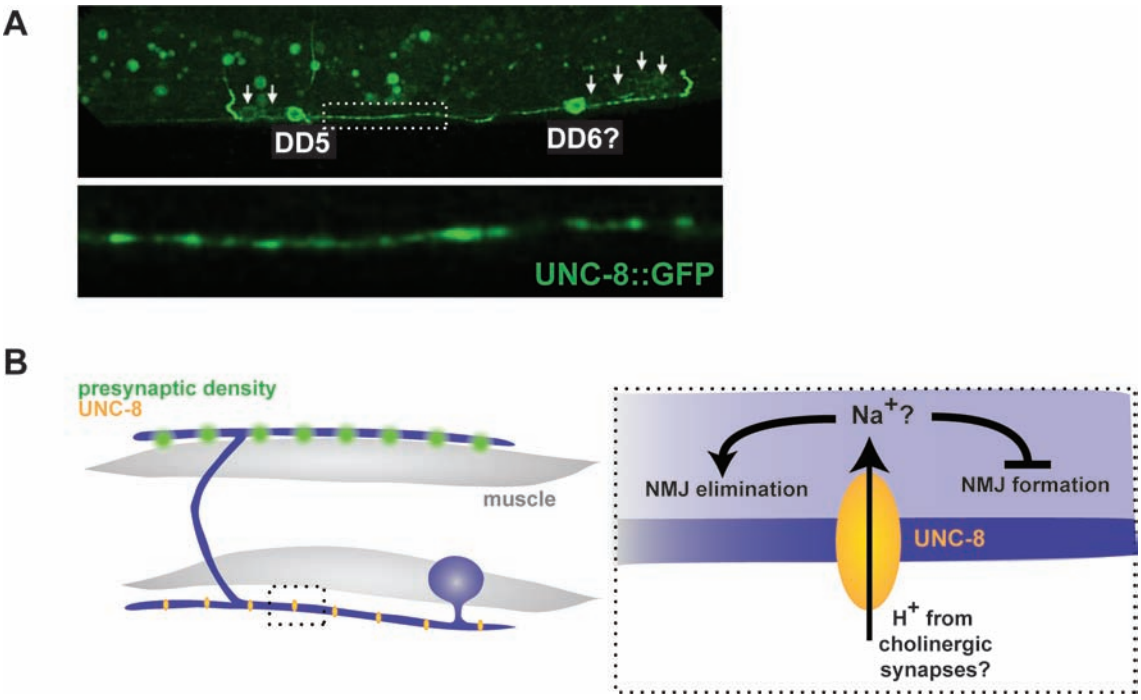

Figure 5.7. Potential role of UNC-8 in the ventral nerve cord of remodeling GABAergic motor neurons. (A) UNC-8::GFP is detected in DD motor neuron soma and in a punctate pattern along the ventral nerve cord. **(B)** Potential mechanism for UNC-8 in GABAergic synaptic remodeling. Left panel depicts a remodeling motor neuron with dorsal NMJs and ventral UNC-8 in a discrete, punctate pattern. Right panel shows an enlargement of the dotted box and demonstrates how UNC-8 might function in the membrane of ventral neurites to promote NMJ elimination.

because UNC-8 is required for precocious remodeling in the *tom-1* mutant, we also propose that UNC-8 participates in an activity-dependent mechanism that drives synaptic remodeling (**Figure 5.6-5.7**).

UNC-8 is a member of the ASIC subfamily of degenerin family non-voltage gated sodium channels (**Figure 5.1**). In other studies, ASICs have been proposed to modulate postsynaptic glutamate receptors and presynaptic neurotransmitter release, either directly through elevating cytoplasmic sodium cations or indirectly by promoting calcium influx through other cation channels (Zha et al., 2006; Voglis and Tavernarakis, 2008). An activity-dependent role for UNC-8 in GABAergic synaptic remodeling is consistent with the observation that the *unc-8(tm5052)* allele, which is predicted to produce a truncated UNC-8 protein consisting of a short N-terminal intracellular domain, suppresses the removal of ventral synapses in *unc-55* mutants (**Figure 5.3**). However, a different deletion allele, *unc-8(tm2071)* that is predicted to introduce a frameshift which disrupts the second transmembrane domain does not suppress the UNC-55 phenotype. This conundrum can be addressed by testing additional *unc-8* mutations but would suggest that UNC-8 channel activity is actually not required for its role in remodeling. Furthermore, we could not show that *unc-8(n491)*, a gain-of-function allele with presumably excess channel activity, affects synaptic remodeling (data not shown). Therefore, it is possible that our results have detected a novel function for ASIC protein function in synaptic plasticity. We will test this model by using the *unc-8(tm2071)* as a negative control in other assays,

such as the delay in elimination of RAB-3::mCherry from the ventral nerve cord during DD remodeling.

unc-8 promotes synaptic elimination during GABAergic remodeling

The finding that *unc-8* is required for synaptic elimination is particularly intriguing in light of the results from the Shen lab (Park et al., 2011). They used photoconvertible Dendra-labeled RAB-3 to demonstrate that ventral NMJ components are dismantled and trafficked to the dorsal nerve cord during DD remodeling (Park et al., 2011). However, the Shen lab did not quantify the rates of synaptic formation and elimination; in our study, we observed that removal of ventral synapses actually occurs at a slower rate than establishment of dorsal synapses even in wild-type DD motor neurons. Therefore, while some ventral synaptic proteins are likely included in remodeled dorsal synapses, we have demonstrated here that removal of ventral synapses is not rate-limiting for dorsal synaptogenesis. Furthermore, we found that the persistence of ventral synapses in an *unc-8* mutant does not affect the timing of dorsal NMJ establishment; in fact, our data indicate that at the onset of L2, DDs in *unc-8* mutants have more synapses overall, including the normal complement of dorsal synapses as well as excess ventral synapses. Thus, we have identified a specific role for *unc-8* in a remodeling program that likely has separately regulated synaptic elimination and formation mechanisms.

How does UNC-8 promote synapse removal?

In addition to structure-function studies based on the allelic series of *unc-8* mutants (**Figure 5.3**), we need additional assays to determine the localization of UNC-8::GFP in GABAergic motor neurons. Because UNC-8::GFP is so brightly expressed in wild-type DD motor neurons, and dimly expressed elsewhere, we predict that the bright UNC-8::GFP puncta in the ventral nerve cord are representative of UNC-8 localization in DD motor neurons (**Figure 5.7A**). However, because the transgenic protein is driven by its own promoter, we cannot exclude the possibility that these puncta are actually representative of expression in another neuronal type. We are therefore currently examining the relative localization of these puncta to other GABAergic markers, *i.e.* testing to see if UNC-8::GFP overlaps with cytosolic GABAergic mCherry or colocalizes with synaptic RAB-3::mCherry in the ventral nerve cord of immature DD motor neurons.

We can nevertheless speculate about UNC-8 function in remodeling based on the hypothesis that it is localized in DD ventral processes. First, if in fact UNC-8 is localized in ventral DD processes, we would therefore predict that UNC-8 has a direct, local role in removal of immature ventral NMJs and/or maintenance to prevent formation of additional ventral NMJs (**Figure 5.7**). The involvement of sodium influx via UNC-8 for this removal remains debatable; our *tm2071* allele suggests that channel activity is not necessary, at least in VD motor neurons, to promote synaptic elimination. However, it is reasonable to suggest that UNC-8 is somehow detecting a signal (protons or other ligands)

from cholinergic motor neurons, which form synapses on the ventral processes of larval and adult DD motor neurons (White et al., 1976).

Activity dependence, calcium, and ASICs in the GABAergic synaptic remodeling program

The precocious remodeling observed in *tom-1* mutants (**Figure 5.6**) strongly suggests that DD remodeling is promoted, either directly or indirectly, by synaptic activity. In this sensitized background, we found that *unc-8(tm5052)* actually slows the formation of dorsal NMJs, which is a phenotype we did not observe in single *unc-8* mutants. One possible explanation is that the slower removal of ventral NMJs in *unc-8* motor neurons impedes the formation of dorsal synapses in *tom-1* mutants by keeping synaptic proteins sequestered in ventral NMJs. While this is not the case in *unc-8* single mutants, *tom-1* mutants may be more sensitive to the delay in synaptic elimination due to the earlier need for trafficking of synaptic proteins to the dorsal side. This idea can be tested with the DD synaptic marker *wyIs202[pflp-13::GFP::RAB-3]* to assess the rate of ventral synaptic elimination in *tom-1* and *tom-1; unc-8* mutants.

Our finding that the L-type calcium channel subunit, *unc-2*, prevents ectopic VD synaptic remodeling, is particularly intriguing. In mammalian neurons, dendritic spines are remodeled by local calcium influx that induces LTP and stabilization of the synapse (Yang et al., 1999). In *C. elegans*, UNC-2 has been shown to localize and function at GABAergic synapses (Saheki and Bargmann, 2009). Therefore, while *unc-8* appears to function in synaptic removal, away from

nascent dorsal synapses, it seems likely that *unc-2* functions to form or maintain remodeled dorsal NMJs. This result is consistent with current experiments performed by Megan Gornet, which places UNC-2::GFP at dorsal NMJs of both wild-type DD motor neurons as well as *unc-55* mutant VD motor neurons (data not shown). Whether this remodeling role is unique to *unc-2*, or is observed with other calcium channels (*cca-1, egl-19*) is a current area of study in this project by Megan as well as graduate student Tyne Miller.

Conclusions

We have discovered that the ASIC subunit UNC-8 functions in GABAergic synaptic remodeling, specifically in removal of immature ventral synapses and perhaps indirectly promoting dorsal synaptogenesis. While we have determined that GABAergic synaptic remodeling is activity-dependent and sensitive to changes in intracellular calcium, how UNC-8 fits into the mechanism of remodeling remains unclear. Further experiments in this study will attempt to understand whether *unc-8* functions as an ASIC, whether its channel activity is required, and whether it signals through influx of sodium or calcium ions to function in synaptic remodeling.

CHAPTER VI

GENERAL DISCUSSION AND FUTURE DIRECTIONS

Key Findings and Discussion

Our work has characterized the molecular features of a synaptic remodeling program in *C. elegans* and identified genetic factors that control this process. Although the developmental plasticity of DD motor neurons was first reported over thirty years ago (White et al., 1978), we are only beginning to create a comprehensive view of the genetic program that drives this event. To understand this process, we have exploited the ectopic remodeling program in *unc-55(e1170)* mutants, in which VD motor neurons remodel to mimic the polarity of DD motor neurons (Walthall, 1990; Shan et al., 2005).

Our results (**Chapter II**) indicate that *unc-55* mutant VD motor neurons initially establish ventral NMJs that are later removed as new synapses emerge on the dorsal side. Our analysis of a locomotory behavior that depends on ventral GABAergic signaling suggests that these transient ventral VD synapses are functional. This possibility is also consistent with the finding that presynaptic active zone markers SYD-2 and SNB-1 are co-localized in ventral VD motor neuron processes during early larval development of *unc-55* mutant animals. Electrophysiological measurements could verify that these transient ventral synapses in *unc-55* mutants are functional; however, these experiments are technically difficult due to the small size of L2 larvae. The idea that UNC-55

negatively regulates a remodeling program similar to the program in DD motor neurons is also supported by our confirmation that ectopic UNC-55 expression in DD motor neurons blocks GABAergic innervation of dorsal muscles. Based on these data, we propose that DD and VD motor neurons are likely remodeled by a common pathway and that UNC-55 normally functions as a transcriptional switch to prevent execution of this program in VD motor neurons.

We used a powerful cell-specific profiling technique, the mRNA tagging method, to identify the transcripts that are upregulated when remodeling is ectopically induced in *unc-55* mutant VD motor neurons (**Chapter III**). A comparison of the wild-type and *unc-55* datasets identified 188 upregulated transcripts, which represent candidate UNC-55 targets. An RNAi screen of these targets identified nineteen conserved genes with necessary roles in ectopic VD remodeling. One of the synaptic remodeling genes uncovered in our screens encodes the Iroquois homeodomain-containing transcription factor, IRX-1 (**Chapter IV**). We used a functional *irx-1::GFP* transgene (provided by Mihail Sarov, Max Planck Institute) to confirm that IRX-1 is selectively expressed in remodeling neurons (*i.e.* DD and *unc-55* VD motor neurons). We confirmed that IRX-1 function is cell autonomous using cell-specific RNAi to show that knockdown of *irx-1* specifically in GABAergic motor neurons suppresses the Unc-55 remodeling phenotype. In collaboration with Janet Richmond (University of Illinois at Chicago), we used electrophysiological measurements to establish, for the first time, that functional ventral GABAergic synapses are absent in *unc-55* mutant adults and that IRX-1 is required for removing these inhibitory inputs to

ventral muscles. In addition to demonstrating that IRX-1 is required for the synaptic remodeling program in *unc-55* VD motor neurons, we also showed that knockdown of *irx-1* perturbs DD remodeling and that ectopic expression of IRX-1 is sufficient to drive VD remodeling. Together, these experiments establish *irx-1* as a key regulator of synaptic remodeling.

It was particularly exciting to discover that the ion channel protein UNC-8, a member of the DEG/ENaC/ASIC family of non-voltage gated ion channels, functions in the GABAergic motor neuron remodeling program (**Chapter V**). Degenerin-family ASICs have been implicated in learning and memory, but the mechanism of this effect is not well understood (Wemmie et al., 2004; Coryell et al., 2008). Our studies with a promoter::GFP transgene indicate that UNC-8 is normally expressed in DD motor neurons but that UNC-8 expression is blocked in the VD motor neurons by UNC-55. We confirmed the cell-autonomous role of UNC-8 that these results suggest by showing that cell-specific RNAi of *unc-8* in the GABAergic motor neurons inhibits remodeling. Interestingly, our results indicate that UNC-8 functions in parallel to IRX-1 and therefore may be directly repressed by UNC-55. The physiological role of UNC-8 in synaptic remodeling is unclear. Our analysis of mutant UNC-8 proteins *in vivo* resulted in the surprising finding that the N-terminal region is required to promote remodeling, but UNC-8 channel activity may not be required. Despite the uncertainty of a role for UNC-8 channel activity in remodeling, our initial assumption that ion channel function might be required led us to perform additional tests for an activity-dependent mechanism. These genetic experiments revealed that an L-type calcium channel,

UNC-2, is necessary for ectopic synaptic remodeling and that excessive neurotransmitter release triggers precocious synaptic remodeling.

Roles for synaptic remodeling genes in broader GABAergic neuron development

Throughout this study, we found evidence that genes identified in our microarray and RNAi screens, originally designed to specifically identify synaptic remodeling genes, are also required for broader developmental roles in GABAergic neurons as well as in other tissues. For instance, despite the strong backward locomotion suppression observed in *unc-55; irx-1(RNAi*) animals (**Figure 4.2**), *irx-1* was not uncovered as a suppressor of Unc-55 backward locomotion in mutagenesis screens (W. Walthall, Y. Jin, personal communication). We attribute this result to the fact that *irx-1* encodes a protein with essential embryonic function. This result in particular demonstrates the utility of our approach in which candidate UNC-55-regulated genes were initially identified with a microarray screen that did not depend on a target gene phenotype. Furthermore, our microarray results were validated with a secondary RNAi test that reduced but did not completely eliminate gene function.

The enrichment of transcripts for *grl-4*, *grd-5*, and *grd-6* in the *unc-55* microarray dataset suggests that these Hh-like ligands are normally expressed in remodeling DD motor neurons but not in VD motor neurons. However, RNAi knockdown of *grl-4*, *grd-5*, and *grd-6* resulted primarily in VD motor neuron defects (**Figure 3.5**). This result may be due to necessary roles for Hh ligands

produced by DD motor neurons to indirectly promote VD synaptogenesis. Interestingly, GRL-4 was also identified as a regulator of synaptic remodeling in our RNAi screen; knockdown of *grl-4* in *unc-55* mutants resulted in GABAergic synapses in the VNC with aberrant morphology. This result suggests that GRL-4 may be required at lower levels for proper VD synaptogenesis and can promote remodeling at higher levels in *unc-55* VD motor neurons.

Validation of our microarray and RNAi screens has been complicated by the pleiotropic function of other genes as well. Preliminary analysis of deletion alleles for the CNT-1/ArfGAP and the Arp2/3 complex component ARX-5 showed that knockout of these genes results in axon guidance defects and reduced synaptogenesis phenotypes that were not detected by RNAi knockdown (**Figure 3.7-8**). These findings are likely indicative of additional roles for these highly conserved proteins in other aspects of neuronal development. For example, GTPase-dependent regulation of the actin cytoskeleton is crucial to multiple events, including the establishment of neuronal polarity, process outgrowth, and synaptogenesis (see **Chapter I**). Thus, it is not surprising to discover that CNT-1/ArfGAP and ARX-5 exercise other roles in GABAergic neuron morphogenesis. One conceivable model is that ARX-5 and CNT-1 are both expressed in low levels in VD motor neurons for proper axonogenesis and synaptogenesis, but that UNC-55 maintains expression below a critical threshold required for synaptic remodeling (**Figure 6.1**). This model is consistent with the finding that *unc-55* heterozygous animals display mild but significant evidence of remodeling (**Figure 4.3**). This result suggests that the remodeling program may be sensitive to

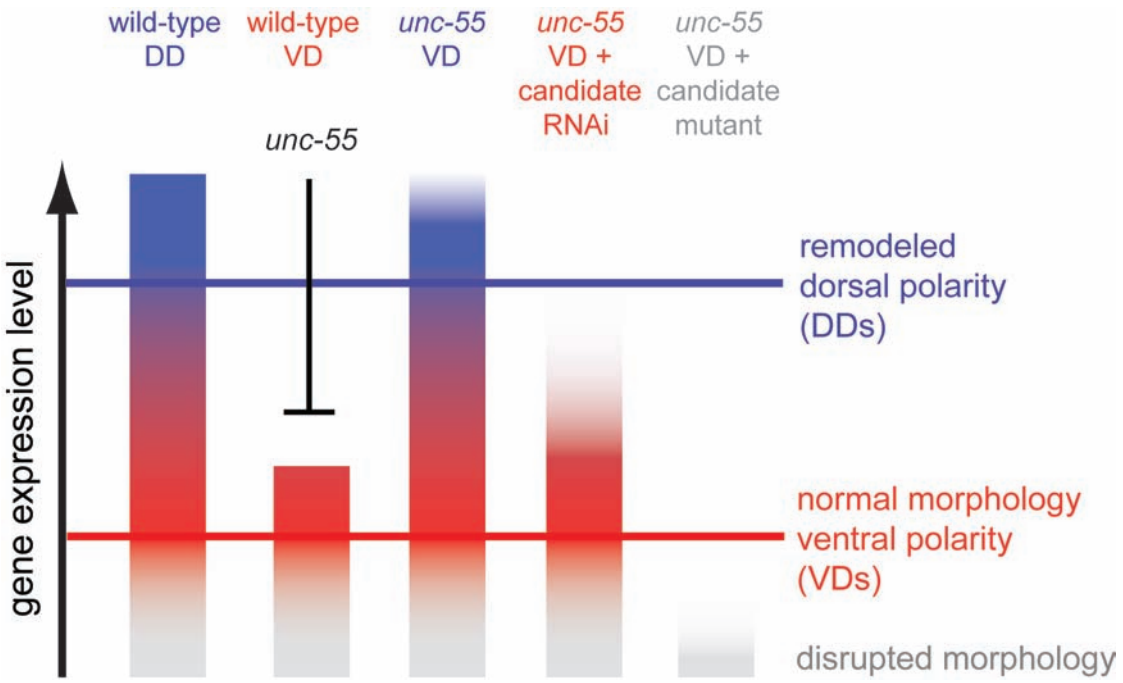

Figure 6.1. Model for UNC-55-regulated targets with essential roles in GABAergic development. In this model, an *unc-55*-regulated transcript may be expressed highly in wild-type DD motor neurons to promote remodeling and at lower levels in VD motor neurons due to repression by UNC-55. In *unc-55* VD motor neurons, the higher level of gene expression promotes remodeling. Knockdown of the gene via RNAi in an *unc-55* background reduces its expression, but does not completely block gene expression and results in a wild-type VD synaptic arrangement. Knockout of the gene via a null mutant, however, completely abrogates gene function and disrupts VD morphology.

relatively minor changes in expression levels and therefore that tight regulation of remodeling gene expression is necessary for proper GABAergic connectivity.

Future Directions

Toward a deeper analysis of the cell biological role of UNC-55 candidate target genes

UNC-55 candidate genes were initially screened with a SNB-1::GFP marker for a necessary role in dismantling ventral synapses (**Figure 3.6**). Our evidence indicates that at least two of these proteins, *irx-1* and *unc-8*, are also necessary for the nascent assembly of new synapses on the dorsal side in remodeling neurons. These dual roles are consistent with other evidence suggesting that these events are coupled by a mechanism that traffics presynaptic components from disassembled ventral synapses to the dorsal side (Park et al., 2011). Our results, however, suggest that this coupling mechanism is not absolute. For example, we observed that assembly of dorsal synapses in remodeling DD motor neurons is complete before ventral synapses are entirely removed. In addition, we showed that UNC-8 is necessary for the removal of ventral synapses in wild-type DD motor neurons but is not required for assembly of dorsal synapses. Thus, it is possible that a subset of UNC-55 targets identified in our microarray dataset may be exclusively involved in assembly of dorsal synapses in remodeling GABAergic motor neurons. These genes would not have been detected by our RNAi assay, which was limited to noting the restoration of SNB-1::GFP to ventral VD synapses.

One way to examine the role of remodeling genes in synaptic assembly and disassembly is time-lapse imaging. The Shen lab has examined the movement of SV precursors labeled with GFP::RAB-3 as they are trafficked in cholinergic neuron commissures (Klassen et al., 2010), and a graduate student in the Miller lab, Cody Smith, has collaborated with Matt Tyska to develop time-lapse imaging techniques that allow observation of protein trafficking within sensory neurons (Smith et al., 2010). This approach could be adapted to observe the dynamic localization of fluorescently-labeled SVs (*e.g.* RAB-3::GFP, SNB-1::GFP) within remodeling GABAergic motor neurons. With this approach, the removal of synapses in the VNC and assembly of synapses in the DNC could be monitored continuously during GABAergic motor neuron remodeling. The movement of GFP-labeled SVs in commissures could also be observed to test the prediction that SV precursors are trafficked in a net ventral-to-dorsal direction during remodeling. Furthermore, this imaging approach could be used to observe the movement of SV precursors in neurons with mutations in Unc-55 suppressor genes to determine which aspect of the remodeling program (*e.g.* disassembly, trafficking, synaptogenesis) is perturbed in the mutant.

Because we wanted to find genes with critical roles in synaptic remodeling, we used the marker SNB-1::GFP which indicates the location of SV pools. The arrival of SVs, however, is one of the final steps in synaptogenesis (Patel et al., 2006) (see **Chapter I** for review). It is possible that use of another marker, such as one that labels the active zone (*i.e.* SYD-2/Liprin-α, UNC-10/RIM), would reveal a different, although perhaps overlapping set of synaptic

remodeling genes. For instance, the Kaplan lab has reported that knockdown of the transcription factor *hbl-1/Hunchback-like* suppresses the Unc-55 defect as marked with fluorescently-labeled endophilin (K. Thompson-Peer, personal communication). However, we have been unable to repeat this result with SNB-1::GFP. Whereas SNB-1 is associated with SVs, endophilin functions in endocytosis during synaptic vesicle recycling (Ringstad et al., 1999; Schuske et al., 2003). Thus, one explanation for these disparate results is that endophilin and SVs are recruited to synapses by different mechanisms, such that knockdown of specific remodeling genes could affect one marker and not the other.

This observation suggests a related question: Do remodeling motor neurons use a different, novel synaptogenic program? Previous work has demonstrated that SYD-1 and SAD-1 are dispensable for dorsal synaptogenesis in remodeled DD motor neurons (Zhen and Jin, 1999; Hallam et al., 2002), Although novel synaptogenic genes could be found in our *unc-55* dataset, they could not be identified by our RNAi suppression screen; our assay looked for restored synapses in the ventral nerve cord, but knockdown of a presumptive synaptic recruitment or scaffolding protein would actually block restored ventral synapses. Thus, identification of these genes would be best accomplished with a forward genetic screen looking for defective dorsal synapses in DD remodeling. Additional gene expression profiling experiments of L1-stage DD motor neurons could also identify candidates for a novel synaptogenic program, particularly when compared to the list of genes enriched in *unc-55* VD motor neurons.

The *irx-1* remodeling pathway

One of the strongest regulators of synaptic remodeling revealed in our screens is the Iroquois homeodomain-containing transcription factor IRX-1. This suggests that many remodeling factors enriched in the *unc-55* microarray screen are positively regulated by IRX-1. Furthermore, *irx-1* is a strong regulator of DD remodeling; when *irx-1* is knocked down, DD remodeling is significantly delayed. This suggests that genes regulated by *irx-1* likely function in dorsal synaptogenesis during GABAergic motor neurons remodeling. By determining which genes function downstream of *irx-1* in VD motor neurons, we can effectively create a “short-list” of candidate genes that normally drive remodeling in DD motor neurons. These *irx-1*-pathway genes can be identified by RNAi or genetic suppression of the *irx-1(gf)* ectopic remodeling phenotype observed in VD motor neurons (**Figure 4.7**). In this epistasis experiment, knockdown of a gene that is required for remodeling downstream of IRX-1 should suppress ectopic *irx-1(gf)* remodeling. In contrast, a knockdown of a gene that functions in parallel or upstream of IRX-1 would not suppress *irx-1(gf)* due to constitutive repression by wild-type. This question is particularly suited for an RNAi screen for downstream *irx-1* targets; thus, I have built an RNAi-sensitized (*eri-1* mutant) strain carrying the SNB-1::GFP transgene and the mosaic *irx-1(gf)* construct. Strong candidates for *irx-1*-pathway genes may be found within our list of Unc-55 suppressors from the RNAi screen (**Figure 3.6**). Therefore, a candidate gene approach to identify *irx-1* targets is favorable to a unbiased screen, particularly because mosaic analysis of *irx-1(gf)* strain is labor-intensive.

For any candidate hits, additional tests for *irx-1* regulation can be performed, such as the *irx-1* enhancement and promoter::GFP experiments with *unc-8* described in **Chapter V**. Generation of promoter::GFP and fosmid::GFP transgenic worms is fairly straightforward (see **Chapter V Methods** for recombineering protocol); these strains can then be analyzed for regulation by *unc-55* and *irx-1*. Remodeling genes downstream of both *unc-55* and *irx-1* should first, show expression in DD motor neurons but not VD motor neurons in wild-type; second, show expression in both DD and VD motor neurons in *unc-55*; and third, exhibit abrogation of expression in *unc-55* DD and VD motor neurons when treated with *irx-1* RNAi. For genes that are not downstream of *irx-1* (*e.g. unc-8*), enhancement of *irx-1* RNAi or *irx-1(csRNAi)* suppression of *unc-55* may be tested in remodeling gene mutants (as in **Figure 5.4**)

Although IRX-1 is an important factor for synaptic remodeling, several of our experiments have demonstrated that other remodeling genes are necessary in parallel to IRX-1. For instance, knockdown of *irx-1* does not completely block DD remodeling (**Figure 4.6**), nor does it restore SYD-2 to ventral VD synapses in an *unc-55* mutant (**Figure 4.5**). Our work has demonstrated that UNC-8 is a key remodeling factor that functions in a parallel pathway to *irx-1*. The experiments described above should parse out genes that function in parallel to *irx-1* and define the major pathways that control GABAergic remodeling.

Does UNC-8 locally break down synapses in the VNC?

We have generated an UNC-8::GFP transgenic strain that is expressed in DD motor neurons and shows distinct GFP puncta along the ventral nerve cord (**Figure 5.7**). This observation, coupled with results demonstrating that UNC-8 is required specifically required for removing ventral DD synapses (**Figure 5.5**), is consistent with the idea that UNC-8 exercises a local function to destabilize ventral synapses. As stated in **Chapter V**, we can test this model by tracking UNC-8::GFP co-localization with NMJs marked with RAB-3::mCherry and testing for loss of RAB-3::mCherry at sites of UNC-8::GFP enrichment. The use of time-lapse imaging, described above, could be particularly informative to address this question.

Our data from *unc-8* deletion mutants (**Figure 5.3**) suggest that the N-terminal region of *unc-8* is required to promote remodeling, but channel activity is not. This prediction is based on the absence of Unc-55 suppression with *unc-8(tm2071)*, an allele which removes a portion of the extracellular loop of the DEG/ENaC/ASIC protein and introduces a frameshift that perturbs the amino acid sequence of the second transmembrane domain. However, it remains to be tested whether the UNC-8 protein encoded by *unc-8(tm2071)* is capable of channel activity; if so, it would predict that UNC-8 channel activity drives remodeling, not the N-terminal region. Furthermore, DEG/ENaC/ASICs have the ability to conduct calcium as well as sodium ions (Bianchi et al., 2004; Wemmie et al., 2006). The potential that UNC-8 might be permeable to calcium is particularly interesting given our finding that the L-type calcium channel subunit

UNC-2 is necessary for remodeling (discussed below). Understanding the channel activity of native UNC-8 as well as UNC-8 mutants will distinguish whether ventral synapse removal is promoted directly by cation influx through UNC-8 or by another novel mechanism.

Activity-dependence in developmental synaptic remodeling

The precocious remodeling phenotype observed in *tom-1* mutants (**Figure 5.6A**) indicates that synaptic vesicle release promotes synaptic remodeling of GABAergic motor neurons. This effect could be driven by synaptic activity within the GABAergic motor neurons or could alternatively result from a non-cell autonomous effect of excess signaling from other motor circuit neurons. These models can be distinguished by RNAi knockdown of *tom-1* specifically in the GABAergic motor neurons, which is predicted to accelerate DD remodeling if TOM-1 function is cell-autonomous. Conversely, we could rescue TOM-1 function specifically in GABAergic motor neurons and look for restoration of wild-type timing of the remodeling program. *tom-1* knockdown in other ventral cord motor neurons could also be evaluated for a non-cell-autonomous effect. Additionally, we can test other components of the synaptic vesicle release pathway (see **Chapter I** for review) for necessary roles in remodeling. For instance, removal of *unc-10/RIM* should prevent synaptic release and could therefore delay synaptic remodeling and potentially suppress *tom-1*-dependent precocious remodeling.

The finding that knockdown of the L-type calcium channel subunit UNC-2 blocks Unc-55 synaptic remodeling is particularly exciting (**Figure 5.6B**), as it links transcriptional regulation to an activity-dependent mechanism of synaptic plasticity. Based on work from the Bargmann lab which demonstrated that UNC-2 functions cell-autonomously at GABAergic synapses to promote synaptic release (Saheki and Bargmann, 2009), we predict that UNC-2-dependent synaptic activity in *unc-55* VD motor neurons could be required for synaptic remodeling. This model can be tested by asking if expression of UNC-2 in GABAergic motor neurons is sufficient to restore ectopic remodeling to *unc-55; unc-2* VD motor neurons. It is also possible that remodeling is driven by calcium-dependent activity from other neurons. Cholinergic motor neurons are obvious candidates because they provide excitatory input to the GABAergic motor neurons in *C. elegans*. A potential role for cholinergic motor neurons in remodeling could be tested by evaluating a genetic mutant of the acetylcholine biosynthetic gene *cha-1* (choline acetyltransferase) (Rand and Russell, 1984). An undergraduate in our lab, Megan Gornet, will be working on this question next semester.

In vertebrate neurons, activity-dependent modulation of synapses depends on the influx of calcium and the protein kinases that transduce this cue (see **Chapter I** for review) (Yang et al., 1999; Flavell and Greenberg, 2008). Because calcium-dependent protein kinases have established roles in *C. elegans* synaptic function (Rongo and Kaplan, 1999; Liu et al., 2007), it is reasonable to predict that some may therefore also have a role in GABAergic remodeling. There are several calcium-dependent serine/threonine protein kinases enriched

in our L2 GABAergic dataset, including *cmk-1/CaMKI* (enriched 5.7-fold), *unc-43/CaMKII* (enriched 2-fold), *unc-51/ULK* (enriched 2.4-fold), and *mnk-1/MAPK-interacting kinase* (enriched 3.1-fold) (**Chapter III**). We can test these for a role in remodeling by treating larvae with feeding RNAi looking for suppression of *unc-55* VD remodeling and a delay in wild-type DD remodeling. If in fact we can identify a calcium-dependent kinase required for remodeling, it would be interesting to test whether it also regulates transcription (i.e. activation of *irx-1* or other *unc-55* targets to drive remodeling) as observed in vertebrate calcium-dependent plasticity (Greer and Greenberg, 2008; Wiegert and Bading, 2011).

Actin dynamics in synaptic remodeling

One of the intriguing hits in our microarray and RNAi screen is the Arp2/3 complex p21 subunit encoded by *arx-5*, named *ARPC4* in mammals. As noted in **Chapter I**, the modulation of actin dynamics is crucial for establishing neuronal polarity and for establishing and modifying synapses. There is some evidence that the seven-subunit complex composed of Arp2, Arp3, and five accessory ARPC subunits mediates branched actin formation in these processes along with the actin nucleating factor, Wiskott-Aldrich syndrome protein (WASP) (Strasser et al., 2004; Wegner et al., 2008). Recently, it was shown that expression of the ARX-5 homologue in mammals, ARPC3, is specifically modulated by a microRNA (*miR-29*) to promote remodeling of dendritic spines (Lippi et al., 2011). This result suggests that, in both *C. elegans* and mammals, ARX-5/ARPC3 is specifically regulated to modify actin dynamics at the synapse in remodeling.

Thus, it follows that other Arp2/3 complex components (ARX-2/Arp2, ARX-1/Arp3, etc.) may also be required for GABAergic motor neuron remodeling. We can test for the requirement of these proteins in DD and *unc-55* VD synaptic remodeling with RNAi knockdown. This will help us understand if the Arp2/3 complex is functioning in remodeling or if some novel role of ARX-5 promotes remodeling.

Structural analysis suggests that mammalian WASP specifically interacts with the p21 ARPC3 subunit (Kreishman-Deitrick et al., 2005). WSP-1/WASP has been shown to prevent excess synaptic release in *C. elegans* motor neurons, perhaps by stabilization of the actin cytoskeleton at the synapse which is predicted by the synaptic localization of WSP-1::GFP (Zhang and Kubiseski, 2010). Thus, given that WSP-1 likely interacts with ARX-5*,* and we have found remodeling defects when synaptic vesicle release is perturbed, the role of WSP-1 and its interaction with ARX-5 seems like a promising avenue to understand how actin dynamics at the synapse modify synaptic activity and ultimately synaptic remodeling. For instance, do *wsp-1* mutants display early DD remodeling (as observed in *tom-1* mutants, which also have excess synaptic vesicle release)? If so, does knockdown of *arx-5* in *wsp-1* mutants suppress this phenotype? This study, as well as testing additional components of the Arp2/3 complex and the cell-autonomy of ARX-5 in synaptic remodeling, is now being pursued by a new graduate student in our lab, Tyne Miller.

REFERENCES

Ackley BD, Crew JR, Elamaa H, Pihlajaniemi T, Kuo CJ, Kramer JM (2001) The NC1/endostatin domain of Caenorhabditis elegans type XVIII collagen affects cell migration and axon guidance. The Journal of cell biology 152:1219-1232.

Ackley BD, Kang SH, Crew JR, Suh C, Jin Y, Kramer JM (2003) The basement membrane components nidogen and type XVIII collagen regulate organization of neuromuscular junctions in Caenorhabditis elegans. J Neurosci 23:3577-3587.

Ackley BD, Harrington RJ, Hudson ML, Williams L, Kenyon CJ, Chisholm AD, Jin Y (2005) The two isoforms of the Caenorhabditis elegans leukocyte-common antigen related receptor tyrosine phosphatase PTP-3 function independently in axon guidance and synapse formation. J Neurosci 25:7517-7528.

Adler CE, Fetter RD, Bargmann CI (2006) UNC-6/Netrin induces neuronal asymmetry and defines the site of axon formation. Nature neuroscience 9:511-518.

Ahmari SE, Buchanan J, Smith SJ (2000) Assembly of presynaptic active zones from cytoplasmic transport packets. Nature neuroscience 3:445-451.

Ajay SM, Bhalla US (2006) Synaptic plasticity in vitro and in silico: insights into an intracellular signaling maze. Physiology (Bethesda) 21:289-296.

Akam M (1995) Hox genes and the evolution of diverse body plans. Philosophical transactions of the Royal Society of London 349:313-319.

Angelo M, Plattner F, Giese KP (2006) Cyclin-dependent kinase 5 in synaptic plasticity, learning and memory. J Neurochem 99:353-370.

Armentano M, Chou SJ, Tomassy GS, Leingartner A, O'Leary DD, Studer M (2007) COUP-TFI regulates the balance of cortical patterning between frontal/motor and sensory areas. Nat Neurosci 10:1277-1286.

Askwith CC, Cheng C, Ikuma M, Benson C, Price MP, Welsh MJ (2000) Neuropeptide FF and FMRFamide potentiate acid-evoked currents from sensory neurons and proton-gated DEG/ENaC channels. Neuron 26:133-141.

Aspock G, Kagoshima H, Niklaus G, Burglin TR (1999) Caenorhabditis elegans has scores of hedgehog-related genes: sequence and expression analysis. Genome research 9:909-923.

Atwood HL (1992) Age-dependent alterations of synaptic performance and plasticity in crustacean motor systems. Exp Gerontol 27:51-61.

Baas PW, Lin S (2011) Hooks and comets: The story of microtubule polarity orientation in the neuron. Dev Neurobiol 71:403-418.

Bacskai BJ, Hochner B, Mahaut-Smith M, Adams SR, Kaang BK, Kandel ER, Tsien RY (1993) Spatially resolved dynamics of cAMP and protein kinase A subunits in Aplysia sensory neurons. Science (New York, NY 260:222-226.

Bading H, Ginty DD, Greenberg ME (1993) Regulation of gene expression in hippocampal neurons by distinct calcium signaling pathways. Science (New York, NY 260:181-186.

Bailey CH, Kandel ER (2008) Synaptic remodeling, synaptic growth and the storage of long-term memory in Aplysia. Prog Brain Res 169:179-198.

Bamber BA, Beg AA, Twyman RE, Jorgensen EM (1999) The Caenorhabditis elegans unc-49 locus encodes multiple subunits of a heteromultimeric GABA receptor. J Neurosci 19:5348-5359.

Banks GB, Fuhrer C, Adams ME, Froehner SC (2003) The postsynaptic submembrane machinery at the neuromuscular junction: requirement for rapsyn and the utrophin/dystrophin-associated complex. J Neurocytol 32:709-726.

Barbosa AC, Kim MS, Ertunc M, Adachi M, Nelson ED, McAnally J, Richardson JA, Kavalali ET, Monteggia LM, Bassel-Duby R, Olson EN (2008) MEF2C, a transcription factor that facilitates learning and memory by negative regulation of synapse numbers and function. Proceedings of the National Academy of Sciences of the United States of America 105:9391-9396.

Barnes AP, Polleux F (2009) Establishment of axon-dendrite polarity in developing neurons. Annual review of neuroscience 32:347-381.

Barnes AP, Lilley BN, Pan YA, Plummer LJ, Powell AW, Raines AN, Sanes JR, Polleux F (2007) LKB1 and SAD kinases define a pathway required for the polarization of cortical neurons. Cell 129:549-563.

Barnes SJ, Finnerty GT (2010) Sensory experience and cortical rewiring. Neuroscientist 16:186-198.

Bartsch D, Casadio A, Karl KA, Serodio P, Kandel ER (1998) CREB1 encodes a nuclear activator, a repressor, and a cytoplasmic modulator that form a regulatory unit critical for long-term facilitation. Cell 95:211-223.

Benson CJ, Xie J, Wemmie JA, Price MP, Henss JM, Welsh MJ, Snyder PM (2002) Heteromultimers of DEG/ENaC subunits form H+-gated channels in mouse sensory neurons. Proceedings of the National Academy of Sciences of the United States of America 99:2338-2343.

Bertolino E, Reimund B, Wildt-Perinic D, Clerc RG (1995) A novel homeobox protein which recognizes a TGT core and functionally interferes with a retinoid-responsive motif. The Journal of biological chemistry 270:31178-31188.

Bianchi L, Gerstbrein B, Frokjaer-Jensen C, Royal DC, Mukherjee G, Royal MA, Xue J, Schafer WR, Driscoll M (2004) The neurotoxic MEC-4(d) DEG/ENaC sodium channel conducts calcium: implications for necrosis initiation. Nature neuroscience 7:1337-1344.

Biernat J, Wu YZ, Timm T, Zheng-Fischhofer Q, Mandelkow E, Meijer L, Mandelkow EM (2002) Protein kinase MARK/PAR-1 is required for neurite outgrowth and establishment of neuronal polarity. Molecular biology of the cell 13:4013-4028.

Bingol B, Sheng M (2011) Deconstruction for reconstruction: the role of proteolysis in neural plasticity and disease. Neuron 69:22-32.

Boulanger A, Clouet-Redt C, Farge M, Flandre A, Guignard T, Fernando C, Juge F, Dura JM (2010) ftz-f1 and Hr39 opposing roles on EcR expression during Drosophila mushroom body neuron remodeling. Nature neuroscience 14:37-44.

Bradke F, Dotti CG (1999) The role of local actin instability in axon formation. Science (New York, NY 283:1931-1934.

Braha O, Edmonds B, Sacktor T, Kandel ER, Klein M (1993) The contributions of protein kinase A and protein kinase C to the actions of 5-HT on the L-type Ca2+ current of the sensory neurons in Aplysia. J Neurosci 13:1839-1851.

Brenner S (1974) The genetics of Caenorhabditis elegans. Genetics 77:71-94.

Briscoe J, Ericson J (1999) The specification of neuronal identity by graded Sonic Hedgehog signalling. Seminars in cell & developmental biology 10:353-362.

Brown HL, Truman JW (2009) Fine-tuning of secondary arbor development: the effects of the ecdysone receptor on the adult neuronal lineages of the Drosophila thoracic CNS. Development (Cambridge, England) 136:3247-3256.

Bruneau EG, Akaaboune M (2010) Dynamics of the rapsyn scaffolding protein at the neuromuscular junction of live mice. J Neurosci 30:614-619.

Bruneau EG, Esteban JA, Akaaboune M (2009) Receptor-associated proteins and synaptic plasticity. FASEB J 23:679-688.

Brunelli M, Castellucci V, Kandel ER (1976) Synaptic facilitation and behavioral sensitization in Aplysia: possible role of serotonin and cyclic AMP. Science (New York, NY 194:1178-1181.

Brunholz S, Sisodia S, Lorenzo A, Deyts C, Kins S, Morfini G (2011) Axonal transport of APP and the spatial regulation of APP cleavage and function in neuronal cells. Exp Brain Res.

Bryant DM, Mostov KE (2008) From cells to organs: building polarized tissue. Nat Rev Mol Cell Biol 9:887-901.

Budnik V, Salinas PC (2011) Wnt signaling during synaptic development and plasticity. Current opinion in neurobiology 21:151-159.

Burglin TR (1997) Analysis of TALE superclass homeobox genes (MEIS, PBC, KNOX, Iroquois, TGIF) reveals a novel domain conserved between plants and animals. Nucleic Acids Res 25:4173-4180.

Burglin TR (2008) Evolution of hedgehog and hedgehog-related genes, their origin from Hog proteins in ancestral eukaryotes and discovery of a novel Hint motif. BMC genomics 9:127.

Burglin TR, Kuwabara PE (2006) Homologs of the Hh signalling network in C. elegans. WormBook:1-14.

Butefisch CM (2004) Plasticity in the human cerebral cortex: lessons from the normal brain and from stroke. Neuroscientist 10:163-173.

Calabrese B, Wilson MS, Halpain S (2006) Development and regulation of dendritic spine synapses. Physiology (Bethesda) 21:38-47.

Cavodeassi F, Modolell J, Gomez-Skarmeta JL (2001) The Iroquois family of genes: from body building to neural patterning. Development (Cambridge, England) 128:2847-2855.

Cavodeassi F, Diez Del Corral R, Campuzano S, Dominguez M (1999) Compartments and organising boundaries in the Drosophila eye: the role of the homeodomain Iroquois proteins. Development (Cambridge, England) 126:4933-4942.

Chalfie M, Wolinsky E (1990) The identification and suppression of inherited neurodegeneration in Caenorhabditis elegans. Nature 345:410-416.

Cheng CW, Chow RL, Lebel M, Sakuma R, Cheung HO, Thanabalasingham V, Zhang X, Bruneau BG, Birch DG, Hui CC, McInnes RR, Cheng SH (2005)

The Iroquois homeobox gene, Irx5, is required for retinal cone bipolar cell development. Developmental biology 287:48-60.

Chetkovich DM, Chen L, Stocker TJ, Nicoll RA, Bredt DS (2002) Phosphorylation of the postsynaptic density-95 (PSD-95)/discs large/zona occludens-1 binding site of stargazin regulates binding to PSD-95 and synaptic targeting of AMPA receptors. J Neurosci 22:5791-5796.

Chiang C, Litingtung Y, Lee E, Young KE, Corden JL, Westphal H, Beachy PA (1996) Cyclopia and defective axial patterning in mice lacking Sonic hedgehog gene function. Nature 383:407-413.

Chiu AY, Sanes JR (1984) Development of basal lamina in synaptic and extrasynaptic portions of embryonic rat muscle. Developmental biology 103:456-467.

Chklovskii DB, Mel BW, Svoboda K (2004) Cortical rewiring and information storage. Nature 431:782-788.

Christensen R, de la Torre-Ubieta L, Bonni A, Colon-Ramos DA (2011) A conserved PTEN/FOXO pathway regulates neuronal morphology during C. elegans development. Development (Cambridge, England) 138:5257-5267.

Chu T, Chiu M, Zhang E, Kunes S (2006) A C-terminal motif targets Hedgehog to axons, coordinating assembly of the Drosophila eye and brain. Developmental cell 10:635-646.

Cinar H, Keles S, Jin Y (2005) Expression profiling of GABAergic motor neurons in Caenorhabditis elegans. Curr Biol 15:340-346.

Clark SG, Chiu C (2003) C. elegans ZAG-1, a Zn-finger-homeodomain protein, regulates axonal development and neuronal differentiation. Development (Cambridge, England) 130:3781-3794.

Conde C, Caceres A (2009) Microtubule assembly, organization and dynamics in axons and dendrites. Nat Rev Neurosci 10:319-332.

Consoulas C, Levine RB, Restifo LL (2005) The steroid hormone-regulated gene Broad Complex is required for dendritic growth of motoneurons during metamorphosis of Drosophila. J Comp Neurol 485:321-337.

Consoulas C, Duch C, Bayline RJ, Levine RB (2000) Behavioral transformations during metamorphosis: remodeling of neural and motor systems. Brain research bulletin 53:571-583.

Coppola T, Magnin-Luthi S, Perret-Menoud V, Gattesco S, Schiavo G, Regazzi R (2001) Direct interaction of the Rab3 effector RIM with Ca2+ channels,

SNAP-25, and synaptotagmin. The Journal of biological chemistry 276:32756-32762.

Coryell MW, Wunsch AM, Haenfler JM, Allen JE, McBride JL, Davidson BL, Wemmie JA (2008) Restoring Acid-sensing ion channel-1a in the amygdala of knock-out mice rescues fear memory but not unconditioned fear responses. J Neurosci 28:13738-13741.

Coryell MW, Ziemann AE, Westmoreland PJ, Haenfler JM, Kurjakovic Z, Zha XM, Price M, Schnizler MK, Wemmie JA (2007) Targeting ASIC1a reduces innate fear and alters neuronal activity in the fear circuit. Biol Psychiatry 62:1140-1148.

Craig AM, Banker G (1994) Neuronal polarity. Annual review of neuroscience 17:267-310.

Crump JG, Zhen M, Jin Y, Bargmann CI (2001) The SAD-1 kinase regulates presynaptic vesicle clustering and axon termination. Neuron 29:115-129.

de la Torre-Ubieta L, Bonni A (2011) Transcriptional regulation of neuronal polarity and morphogenesis in the Mammalian brain. Neuron 72:22-40.

De Robertis EM, Morita EA, Cho KW (1991) Gradient fields and homeobox genes. Development (Cambridge, England) 112:669-678.

Deken SL, Vincent R, Hadwiger G, Liu Q, Wang ZW, Nonet ML (2005) Redundant localization mechanisms of RIM and ELKS in Caenorhabditis elegans. J Neurosci 25:5975-5983.

Derkach VA, Oh MC, Guire ES, Soderling TR (2007) Regulatory mechanisms of AMPA receptors in synaptic plasticity. Nat Rev Neurosci 8:101-113.

Dillon C, Goda Y (2005) The actin cytoskeleton: integrating form and function at the synapse. Annual review of neuroscience 28:25-55.

Ding M, Chao D, Wang G, Shen K (2007) Spatial regulation of an E3 ubiquitin ligase directs selective synapse elimination. Science (New York, NY 317:947-951.

Dotti CG, Banker GA (1987) Experimentally induced alteration in the polarity of developing neurons. Nature 330:254-256.

Dotti CG, Simons K (1990) Polarized sorting of viral glycoproteins to the axon and dendrites of hippocampal neurons in culture. Cell 62:63-72.

Dotti CG, Sullivan CA, Banker GA (1988) The establishment of polarity by hippocampal neurons in culture. J Neurosci 8:1454-1468.

Drever BD, Riedel G, Platt B (2011) The cholinergic system and hippocampal plasticity. Behav Brain Res 221:505-514.

Driscoll M (1996) Cell death in C. elegans: molecular insights into mechanisms conserved between nematodes and mammals. Brain Pathol 6:411-425.

Driscoll M, Kaplan J (1997) Mechanotransduction. In: *C. elegans* II (Riddle TBDA, Meyer BJ, Priess JR, eds), pp 645-677. Cold Spring Harbor, NY: Cold Spring Harbor Press.

Dwyer ND, Adler CE, Crump JG, L'Etoile ND, Bargmann CI (2001) Polarized dendritic transport and the AP-1 mu1 clathrin adaptor UNC-101 localize odorant receptors to olfactory cilia. Neuron 31:277-287.

Earls LR, Hacker ML, Watson JD, Miller DM, 3rd (2010) Coenzyme Q protects Caenorhabditis elegans GABA neurons from calcium-dependent degeneration. Proceedings of the National Academy of Sciences of the United States of America 107:14460-14465.

Eastman C, Horvitz HR, Jin Y (1999) Coordinated transcriptional regulation of the unc-25 glutamic acid decarboxylase and the unc-47 GABA vesicular transporter by the Caenorhabditis elegans UNC-30 homeodomain protein. J Neurosci 19:6225-6234.

Ericson J, Morton S, Kawakami A, Roelink H, Jessell TM (1996) Two critical periods of Sonic Hedgehog signaling required for the specification of motor neuron identity. Cell 87:661-673.

Etchberger JF, Lorch A, Sleumer MC, Zapf R, Jones SJ, Marra MA, Holt RA, Moerman DG, Hobert O (2007) The molecular signature and cis-regulatory architecture of a C. elegans gustatory neuron. Genes & development 21:1653-1674.

Ethell IM, Ethell DW (2007) Matrix metalloproteinases in brain development and remodeling: synaptic functions and targets. J Neurosci Res 85:2813-2823.

Finney M, Ruvkun G (1990) The unc-86 gene product couples cell lineage and cell identity in C. elegans. Cell 63:895-905.

Firestein BL, Rongo C (2001) DLG-1 is a MAGUK similar to SAP97 and is required for adherens junction formation. Molecular biology of the cell 12:3465-3475.

Flavell SW, Greenberg ME (2008) Signaling mechanisms linking neuronal activity to gene expression and plasticity of the nervous system. Annual review of neuroscience 31:563-590.

Flavell SW, Kim TK, Gray JM, Harmin DA, Hemberg M, Hong EJ, Markenscoff-Papadimitriou E, Bear DM, Greenberg ME (2008) Genome-wide analysis of MEF2 transcriptional program reveals synaptic target genes and neuronal activity-dependent polyadenylation site selection. Neuron 60:1022-1038.

Flavell SW, Cowan CW, Kim TK, Greer PL, Lin Y, Paradis S, Griffith EC, Hu LS, Chen C, Greenberg ME (2006) Activity-dependent regulation of MEF2 transcription factors suppresses excitatory synapse number. Science (New York, NY 311:1008-1012.

Fouquet W, Owald D, Wichmann C, Mertel S, Depner H, Dyba M, Hallermann S, Kittel RJ, Eimer S, Sigrist SJ (2009) Maturation of active zone assembly by Drosophila Bruchpilot. The Journal of cell biology 186:129-145.

Fox MA (2008) Novel roles for collagens in wiring the vertebrate nervous system. Curr Opin Cell Biol 20:508-513.

Fox RM, Von Stetina SE, Barlow SJ, Shaffer C, Olszewski KL, Moore JH, Dupuy D, Vidal M, Miller DM, 3rd (2005) A gene expression fingerprint of C. elegans embryonic motor neurons. BMC genomics 6:42.

Fu M, Zuo Y (2011) Experience-dependent structural plasticity in the cortex. Trends in neurosciences 34:177-187.

Fukata Y, Itoh TJ, Kimura T, Menager C, Nishimura T, Shiromizu T, Watanabe H, Inagaki N, Iwamatsu A, Hotani H, Kaibuchi K (2002) CRMP-2 binds to tubulin heterodimers to promote microtubule assembly. Nature cell biology 4:583-591.

Gally C, Bessereau JL (2003) GABA is dispensable for the formation of junctional GABA receptor clusters in Caenorhabditis elegans. J Neurosci 23:2591-2599.

Gally C, Eimer S, Richmond JE, Bessereau JL (2004) A transmembrane protein required for acetylcholine receptor clustering in Caenorhabditis elegans. Nature 431:578-582.

Gao S, Zhen M (2011) Action potentials drive body wall muscle contractions in Caenorhabditis elegans. Proceedings of the National Academy of Sciences of the United States of America 108:2557-2562.

Giagtzoglou N, Ly CV, Bellen HJ (2009) Cell adhesion, the backbone of the synapse: "vertebrate" and "invertebrate" perspectives. Cold Spring Harb Perspect Biol 1:a003079.

Giles AC, Rankin CH (2009) Behavioral and genetic characterization of habituation using Caenorhabditis elegans. Neurobiol Learn Mem 92:139-146.

Ginty DD (1997) Calcium regulation of gene expression: isn't that spatial? Neuron 18:183-186.

Glass DJ, Bowen DC, Stitt TN, Radziejewski C, Bruno J, Ryan TE, Gies DR, Shah S, Mattsson K, Burden SJ, DiStefano PS, Valenzuela DM, DeChiara TM, Yancopoulos GD (1996) Agrin acts via a MuSK receptor complex. Cell 85:513-523.

Gogel S, Wakefield S, Tear G, Klambt C, Gordon-Weeks PR (2006) The Drosophila microtubule associated protein Futsch is phosphorylated by Shaggy/Zeste-white 3 at an homologous GSK3beta phosphorylation site in MAP1B. Mol Cell Neurosci 33:188-199.

Goldstein B, Macara IG (2007) The PAR proteins: fundamental players in animal cell polarization. Developmental cell 13:609-622.

Gomez-Skarmeta JL, Modolell J (2002) Iroquois genes: genomic organization and function in vertebrate neural development. Curr Opin Genet Dev 12:403-408.

Gomis-Ruth S, Wierenga CJ, Bradke F (2008) Plasticity of polarization: changing dendrites into axons in neurons integrated in neuronal circuits. Curr Biol 18:992-1000.

Gracheva EO, Burdina AO, Touroutine D, Berthelot-Grosjean M, Parekh H, Richmond JE (2007) Tomosyn negatively regulates both synaptic transmitter and neuropeptide release at the C. elegans neuromuscular junction. J Physiol 585:705-709.

Greer PL, Greenberg ME (2008) From synapse to nucleus: calcium-dependent gene transcription in the control of synapse development and function. Neuron 59:846-860.

Griffith LC, Budnik V (2006) Plasticity and second messengers during synapse development. Int Rev Neurobiol 75:237-265.

Hall A, Lalli G (2011) Rho and Ras GTPases in axon growth, guidance, and branching. Cold Spring Harb Perspect Biol 2:a001818.

Hall DH, Hedgecock EM (1991) Kinesin-related gene unc-104 is required for axonal transport of synaptic vesicles in C. elegans. Cell 65:837-847.

Hallam SJ, Jin Y (1998) lin-14 regulates the timing of synaptic remodelling in Caenorhabditis elegans. Nature 395:78-82.

Hallam SJ, Goncharov A, McEwen J, Baran R, Jin Y (2002) SYD-1, a presynaptic protein with PDZ, C2 and rhoGAP-like domains, specifies axon identity in C. elegans. Nature neuroscience 5:1137-1146.

Hammock EA, Eagleson KL, Barlow S, Earls LR, Miller DM, 3rd, Levitt P (2010) Homologs of genes expressed in Caenorhabditis elegans GABAergic neurons are also found in the developing mouse forebrain. Neural Dev 5:32.

Han K, Kim E (2008) Synaptic adhesion molecules and PSD-95. Prog Neurobiol 84:263-283.

Hao L, Aspock G, Burglin TR (2006a) The hedgehog-related gene wrt-5 is essential for hypodermal development in Caenorhabditis elegans. Developmental biology 290:323-336.

Hao L, Mukherjee K, Liegeois S, Baillie D, Labouesse M, Burglin TR (2006b) The hedgehog-related gene qua-1 is required for molting in Caenorhabditis elegans. Dev Dyn 235:1469-1481.

Harris TW, Schuske K, Jorgensen EM (2001) Studies of synaptic vesicle endocytosis in the nematode C. elegans. Traffic 2:597-605.

Hawasli AH, Benavides DR, Nguyen C, Kansy JW, Hayashi K, Chambon P, Greengard P, Powell CM, Cooper DC, Bibb JA (2007) Cyclin-dependent kinase 5 governs learning and synaptic plasticity via control of NMDAR degradation. Nature neuroscience 10:880-886.

Hedgecock EM, Culotti JG, Thomson JN, Perkins LA (1985) Axonal guidance mutants of Caenorhabditis elegans identified by filling sensory neurons with fluorescein dyes. Developmental biology 111:158-170.

Hegde AN, Inokuchi K, Pei W, Casadio A, Ghirardi M, Chain DG, Martin KC, Kandel ER, Schwartz JH (1997) Ubiquitin C-terminal hydrolase is an immediate-early gene essential for long-term facilitation in Aplysia. Cell 89:115-126.

Hesser BA, Henschel O, Witzemann V (2006) Synapse disassembly and formation of new synapses in postnatal muscle upon conditional inactivation of MuSK. Mol Cell Neurosci 31:470-480.

Hiromi Y, Mlodzik M, West SR, Rubin GM, Goodman CS (1993) Ectopic expression of seven-up causes cell fate changes during ommatidial assembly. Development (Cambridge, England) 118:1123-1135.

Ho VM, Lee JA, Martin KC (2011) The cell biology of synaptic plasticity. Science (New York, NY 334:623-628.

Hoefen RJ, Berk BC (2006) The multifunctional GIT family of proteins. J Cell Sci 119:1469-1475.

Holtmaat A, Svoboda K (2009) Experience-dependent structural synaptic plasticity in the mammalian brain. Nat Rev Neurosci 10:647-658.

Hrus A, Lau G, Hutter H, Schenk S, Ferralli J, Brown-Luedi M, Chiquet-Ehrismann R, Canevascini S (2007) C. elegans agrin is expressed in pharynx, IL1 neurons and distal tip cells and does not genetically interact with genes involved in synaptogenesis or muscle function. PLoS One 2:e731.

Hummel T, Krukkert K, Roos J, Davis G, Klambt C (2000) Drosophila Futsch/22C10 is a MAP1B-like protein required for dendritic and axonal development. Neuron 26:357-370.

Hung W, Hwang C, Po MD, Zhen M (2007) Neuronal polarity is regulated by a direct interaction between a scaffolding protein, Neurabin, and a presynaptic SAD-1 kinase in Caenorhabditis elegans. Development (Cambridge, England) 134:237-249.

Hunt-Newbury R et al. (2007) High-throughput in vivo analysis of gene expression in Caenorhabditis elegans. PLoS Biol 5:e237.

Hynes RO (2009) The extracellular matrix: not just pretty fibrils. Science (New York, NY 326:1216-1219.

Inagaki N, Chihara K, Arimura N, Menager C, Kawano Y, Matsuo N, Nishimura T, Amano M, Kaibuchi K (2001) CRMP-2 induces axons in cultured hippocampal neurons. Nature neuroscience 4:781-782.

Inoue E, Mochida S, Takagi H, Higa S, Deguchi-Tawarada M, Takao-Rikitsu E, Inoue M, Yao I, Takeuchi K, Kitajima I, Setou M, Ohtsuka T, Takai Y (2006) SAD: a presynaptic kinase associated with synaptic vesicles and the active zone cytomatrix that regulates neurotransmitter release. Neuron 50:261-275.

Irizarry RA, Bolstad BM, Collin F, Cope LM, Hobbs B, Speed TP (2003) Summaries of Affymetrix GeneChip probe level data. Nucleic Acids Res 31:e15.

Jackson TR, Kearns BG, Theibert AB (2000) Cytohesins and centaurins: mediators of PI 3-kinase-regulated Arf signaling. Trends Biochem Sci 25:489-495.

Jaffe AB, Hall A (2005) Rho GTPases: biochemistry and biology. Annu Rev Cell Dev Biol 21:247-269.

Jessell TM (2000) Neuronal specification in the spinal cord: inductive signals and transcriptional codes. Nat Rev Genet 1:20-29.

Jiang H, Guo W, Liang X, Rao Y (2005) Both the establishment and the maintenance of neuronal polarity require active mechanisms: critical roles of GSK-3beta and its upstream regulators. Cell 120:123-135.

Jiang J, Suppiramaniam V, Wooten MW (2006) Posttranslational modifications and receptor-associated proteins in AMPA receptor trafficking and synaptic plasticity. Neurosignals 15:266-282.

Jin Y, Hoskins R, Horvitz HR (1994) Control of type-D GABAergic neuron differentiation by C. elegans UNC-30 homeodomain protein. Nature 372:780-783.

Kaang BK, Kandel ER, Grant SG (1993) Activation of cAMP-responsive genes by stimuli that produce long-term facilitation in Aplysia sensory neurons. Neuron 10:427-435.

Kamath RS, Fraser AG, Dong Y, Poulin G, Durbin R, Gotta M, Kanapin A, Le Bot N, Moreno S, Sohrmann M, Welchman DP, Zipperlen P, Ahringer J (2003) Systematic functional analysis of the Caenorhabditis elegans genome using RNAi. Nature 421:231-237.

Kandel ER (2001) The molecular biology of memory storage: a dialogue between genes and synapses. Science (New York, NY 294:1030-1038.

Kania A, Johnson RL, Jessell TM (2000) Coordinate roles for LIM homeobox genes in directing the dorsoventral trajectory of motor axons in the vertebrate limb. Cell 102:161-173.

Kelly A, Lynch MA (2000) Long-term potentiation in dentate gyrus of the rat is inhibited by the phosphoinositide 3-kinase inhibitor, wortmannin. Neuropharmacology 39:643-651.

Kennedy S, Wang D, Ruvkun G (2004) A conserved siRNA-degrading RNase negatively regulates RNA interference in C. elegans. Nature 427:645-649.

Kim BJ, Takamoto N, Yan J, Tsai SY, Tsai MJ (2009) Chicken Ovalbumin Upstream Promoter-Transcription Factor II (COUP-TFII) regulates growth and patterning of the postnatal mouse cerebellum. Developmental biology 326:378-391.

Kim JI et al. (2011) PI3Kgamma is required for NMDA receptor-dependent long-term depression and behavioral flexibility. Nature neuroscience.

Kim JS, Hung W, Narbonne P, Roy R, Zhen M (2010) C. elegans STRADalpha and SAD cooperatively regulate neuronal polarity and synaptic organization. Development (Cambridge, England) 137:93-102.

Kim S, Ko J, Shin H, Lee JR, Lim C, Han JH, Altrock WD, Garner CC, Gundelfinger ED, Premont RT, Kaang BK, Kim E (2003) The GIT family of proteins forms multimers and associates with the presynaptic cytomatrix protein Piccolo. The Journal of biological chemistry 278:6291-6300.

Kishi M, Pan YA, Crump JG, Sanes JR (2005) Mammalian SAD kinases are required for neuronal polarization. Science (New York, NY 307:929-932.

Klassen MP, Wu YE, Maeder CI, Nakae I, Cueva JG, Lehrman EK, Tada M, Gengyo-Ando K, Wang GJ, Goodman M, Mitani S, Kontani K, Katada T, Shen K (2010) An Arf-like small G protein, ARL-8, promotes the axonal transport of presynaptic cargoes by suppressing vesicle aggregation. Neuron 66:710-723.

Klein M, Kandel ER (1978) Presynaptic modulation of voltage-dependent Ca2+ current: mechanism for behavioral sensitization in Aplysia californica. Proceedings of the National Academy of Sciences of the United States of America 75:3512-3516.

Kobayashi D, Kobayashi M, Matsumoto K, Ogura T, Nakafuku M, Shimamura K (2002) Early subdivisions in the neural plate define distinct competence for inductive signals. Development (Cambridge, England) 129:83-93.

Korey CA, Van Vactor D (2000) From the growth cone surface to the cytoskeleton: one journey, many paths. J Neurobiol 44:184-193.

Kreishman-Deitrick M, Goley ED, Burdine L, Denison C, Egile C, Li R, Murali N, Kodadek TJ, Welch MD, Rosen MK (2005) NMR analyses of the activation of the Arp2/3 complex by neuronal Wiskott-Aldrich syndrome protein. Biochemistry 44:15247-15256.

Krishtal OA, Pidoplichko VI (1980) A receptor for protons in the nerve cell membrane. Neuroscience 5:2325-2327.

Kruse SW, Suino-Powell K, Zhou XE, Kretschman JE, Reynolds R, Vonrhein C, Xu Y, Wang L, Tsai SY, Tsai MJ, Xu HE (2008) Identification of COUP-TFII orphan nuclear receptor as a retinoic acid-activated receptor. PLoS Biol 6:e227.

Kulkarni G, Li H, Wadsworth WG (2008) CLEC-38, a transmembrane protein with C-type lectin-like domains, negatively regulates UNC-40-mediated axon outgrowth and promotes presynaptic development in Caenorhabditis elegans. J Neurosci 28:4541-4550.

Kunes S (2000) Axonal signals in the assembly of neural circuitry. Current opinion in neurobiology 10:58-62.

Kuwabara PE, Lee MH, Schedl T, Jefferis GS (2000) A C. elegans patched gene, ptc-1, functions in germ-line cytokinesis. Genes & development 14:1933-1944.

Lai T, Jabaudon D, Molyneaux BJ, Azim E, Arlotta P, Menezes JR, Macklis JD (2008) SOX5 controls the sequential generation of distinct corticofugal neuron subtypes. Neuron 57:232-247.

Latvanlehto A, Fox MA, Sormunen R, Tu H, Oikarainen T, Koski A, Naumenko N, Shakirzyanova A, Kallio M, Ilves M, Giniatullin R, Sanes JR, Pihlajaniemi T (2010) Muscle-derived collagen XIII regulates maturation of the skeletal neuromuscular junction. J Neurosci 30:12230-12241.

Lee H, Van Vactor D (2003) Neurons take shape. Curr Biol 13:R152-161.

Lee T, Marticke S, Sung C, Robinow S, Luo L (2000) Cell-autonomous requirement of the USP/EcR-B ecdysone receptor for mushroom body neuronal remodeling in Drosophila. Neuron 28:807-818.

Lichtman JW, Colman H (2000) Synapse elimination and indelible memory. Neuron 25:269-278.

Liegeois S, Benedetto A, Garnier JM, Schwab Y, Labouesse M (2006) The V0-ATPase mediates apical secretion of exosomes containing Hedgehog-related proteins in Caenorhabditis elegans. The Journal of cell biology 173:949-961.

Lin WH, Webb DJ (2009) Actin and Actin-Binding Proteins: Masters of Dendritic Spine Formation, Morphology, and Function. Open Neurosci J 3:54-66.

Lin Y, Bloodgood BL, Hauser JL, Lapan AD, Koon AC, Kim TK, Hu LS, Malik AN, Greenberg ME (2008) Activity-dependent regulation of inhibitory synapse development by Npas4. Nature 455:1198-1204.

Lippi G, Steinert JR, Marczylo EL, D'Oro S, Fiore R, Forsythe ID, Schratt G, Zoli M, Nicotera P, Young KW (2011) Targeting of the Arpc3 actin nucleation factor by miR-29a/b regulates dendritic spine morphology. The Journal of cell biology 194:889-904.

Littleton JT, Stern M, Schulze K, Perin M, Bellen HJ (1993) Mutational analysis of Drosophila synaptotagmin demonstrates its essential role in Ca(2+)-activated neurotransmitter release. Cell 74:1125-1134.

Liu Q, Hollopeter G, Jorgensen EM (2009) Graded synaptic transmission at the Caenorhabditis elegans neuromuscular junction. Proceedings of the

National Academy of Sciences of the United States of America 106:10823-10828.

Liu Q, Chen B, Ge Q, Wang ZW (2007) Presynaptic Ca2+/calmodulin-dependent protein kinase II modulates neurotransmitter release by activating BK channels at Caenorhabditis elegans neuromuscular junction. J Neurosci 27:10404-10413.

Llano E, Pendas AM, Aza-Blanc P, Kornberg TB, Lopez-Otin C (2000) Dm1-MMP, a matrix metalloproteinase from Drosophila with a potential role in extracellular matrix remodeling during neural development. The Journal of biological chemistry 275:35978-35985.

Lledo PM, Vernier P, Vincent JD, Mason WT, Zorec R (1993) Inhibition of Rab3B expression attenuates Ca(2+)-dependent exocytosis in rat anterior pituitary cells. Nature 364:540-544.

Lodato S, Tomassy GS, De Leonibus E, Uzcategui YG, Andolfi G, Armentano M, Touzot A, Gaztelu JM, Arlotta P, Menendez de la Prida L, Studer M (2011) Loss of COUP-TFI alters the balance between caudal ganglionic eminence- and medial ganglionic eminence-derived cortical interneurons and results in resistance to epilepsy. J Neurosci 31:4650-4662.

Low LK, Liu XB, Faulkner RL, Coble J, Cheng HJ (2008) Plexin signaling selectively regulates the stereotyped pruning of corticospinal axons from visual cortex. Proceedings of the National Academy of Sciences of the United States of America 105:8136-8141.

Lowery LA, Van Vactor D (2009) The trip of the tip: understanding the growth cone machinery. Nat Rev Mol Cell Biol 10:332-343.

Luo L, O'Leary DD (2005) Axon retraction and degeneration in development and disease. Annual review of neuroscience 28:127-156.

Macara IG (2004) Par proteins: partners in polarization. Curr Biol 14:R160-162.

Machesky LM, Gould KL (1999) The Arp2/3 complex: a multifunctional actin organizer. Curr Opin Cell Biol 11:117-121.

Maduro M, Pilgrim D (1995) Identification and cloning of unc-119, a gene expressed in the Caenorhabditis elegans nervous system. Genetics 141:977-988.

Magill-Solc C, McMahan UJ (1988) Motor neurons contain agrin-like molecules. The Journal of cell biology 107:1825-1833.

Malenka RC, Bear MF (2004) LTP and LTD: an embarrassment of riches. Neuron 44:5-21.

Margeta MA, Wang GJ, Shen K (2009) Clathrin adaptor AP-1 complex excludes multiple postsynaptic receptors from axons in C. elegans. Proceedings of the National Academy of Sciences of the United States of America 106:1632-1637.

Martin DM, Skidmore JM, Fox SE, Gage PJ, Camper SA (2002) Pitx2 distinguishes subtypes of terminally differentiated neurons in the developing mouse neuroepithelium. Developmental biology 252:84-99.

Martin KC, Michael D, Rose JC, Barad M, Casadio A, Zhu H, Kandel ER (1997) MAP kinase translocates into the nucleus of the presynaptic cell and is required for long-term facilitation in Aplysia. Neuron 18:899-912.

Matsumoto K, Nishihara S, Kamimura M, Shiraishi T, Otoguro T, Uehara M, Maeda Y, Ogura K, Lumsden A, Ogura T (2004) The prepattern transcription factor Irx2, a target of the FGF8/MAP kinase cascade, is involved in cerebellum formation. Nature neuroscience 7:605-612.

McEwen JM, Madison JM, Dybbs M, Kaplan JM (2006) Antagonistic regulation of synaptic vesicle priming by Tomosyn and UNC-13. Neuron 51:303-315.

McIntire SL, Jorgensen E, Kaplan J, Horvitz HR (1993) The GABAergic nervous system of Caenorhabditis elegans. Nature 364:337-341.

Melkman T, Sengupta P (2005) Regulation of chemosensory and GABAergic motor neuron development by the C. elegans Aristaless/Arx homolog alr-1. Development (Cambridge, England) 132:1935-1949.

Mellman I (1996) Endocytosis and molecular sorting. Annu Rev Cell Dev Biol 12:575-625.

Mellman I, Nelson WJ (2008) Coordinated protein sorting, targeting and distribution in polarized cells. Nat Rev Mol Cell Biol 9:833-845.

Meyer F, Moussian B (2009) Drosophila multiplexin (Dmp) modulates motor axon pathfinding accuracy. Dev Growth Differ 51:483-498.

Miesenbock G, De Angelis DA, Rothman JE (1998) Visualizing secretion and synaptic transmission with pH-sensitive green fluorescent proteins. Nature 394:192-195.

Miller DM (2007) Neuroscience. Synapses here and not everywhere. Science (New York, NY 317:907-908.

Mlodzik M, Hiromi Y, Weber U, Goodman CS, Rubin GM (1990) The Drosophila seven-up gene, a member of the steroid receptor gene superfamily, controls photoreceptor cell fates. Cell 60:211-224.

Montemayor C, Montemayor OA, Ridgeway A, Lin F, Wheeler DA, Pletcher SD, Pereira FA (2010) Genome-wide analysis of binding sites and direct target genes of the orphan nuclear receptor NR2F1/COUP-TFI. PLoS One 5:e8910.

Morgan TE, Lockerbie RO, Minamide LS, Browning MD, Bamburg JR (1993) Isolation and characterization of a regulated form of actin depolymerizing factor. The Journal of cell biology 122:623-633.

Muhr J, Andersson E, Persson M, Jessell TM, Ericson J (2001) Groucho-mediated transcriptional repression establishes progenitor cell pattern and neuronal fate in the ventral neural tube. Cell 104:861-873.

Mukherjee K, Burglin TR (2007) Comprehensive analysis of animal TALE homeobox genes: new conserved motifs and cases of accelerated evolution. J Mol Evol 65:137-153.

Murthy VN, Stevens CF (1999) Reversal of synaptic vesicle docking at central synapses. Nature neuroscience 2:503-507.

Murthy VN, De Camilli P (2003) Cell biology of the presynaptic terminal. Annual review of neuroscience 26:701-728.

Myers JP, Santiago-Medina M, Gomez TM (2011) Regulation of axonal outgrowth and pathfinding by integrin-ecm interactions. Dev Neurobiol 71:901-923.

Myers KR, Casanova JE (2008) Regulation of actin cytoskeleton dynamics by Arf-family GTPases. Trends Cell Biol 18:184-192.

Naka H, Nakamura S, Shimazaki T, Okano H (2008) Requirement for COUP-TFI and II in the temporal specification of neural stem cells in CNS development. Nature neuroscience 11:1014-1023.

Nam S, Min K, Hwang H, Lee HO, Lee JH, Yoon J, Lee H, Park S, Lee J (2009) Control of rapsyn stability by the CUL-3-containing E3 ligase complex. The Journal of biological chemistry 284:8195-8206.

Nathoo AN, Moeller RA, Westlund BA, Hart AC (2001) Identification of neuropeptide-like protein gene families in Caenorhabditiselegans and other species. Proceedings of the National Academy of Sciences of the United States of America 98:14000-14005.

Newpher TM, Ehlers MD (2008) Glutamate receptor dynamics in dendritic microdomains. Neuron 58:472-497.

Nie Z, Randazzo PA (2006) Arf GAPs and membrane traffic. J Cell Sci 119:1203-1211.

Nishimura T, Fukata Y, Kato K, Yamaguchi T, Matsuura Y, Kamiguchi H, Kaibuchi K (2003) CRMP-2 regulates polarized Numb-mediated endocytosis for axon growth. Nature cell biology 5:819-826.

Niu W, Lu ZJ, Zhong M, Sarov M, Murray JI, Brdlik CM, Janette J, Chen C, Alves P, Preston E, Slightham C, Jiang L, Hyman AA, Kim SK, Waterston RH, Gerstein M, Snyder M, Reinke V (2011) Diverse transcription factor binding features revealed by genome-wide ChIP-seq in C. elegans. Genome research 21:245-254.

Nonet ML, Grundahl K, Meyer BJ, Rand JB (1993) Synaptic function is impaired but not eliminated in C. elegans mutants lacking synaptotagmin. Cell 73:1291-1305.

Okada S, Saiwai H, Kumamaru H, Kubota K, Harada A, Yamaguchi M, Iwamoto Y, Ohkawa Y (2011) Flow cytometric sorting of neuronal and glial nuclei from central nervous system tissue. Journal of cellular physiology 226:552-558.

Okamoto K, Nagai T, Miyawaki A, Hayashi Y (2004) Rapid and persistent modulation of actin dynamics regulates postsynaptic reorganization underlying bidirectional plasticity. Nature neuroscience 7:1104-1112.

Ou CY, Poon VY, Maeder CI, Watanabe S, Lehrman EK, Fu AK, Park M, Fu WY, Jorgensen EM, Ip NY, Shen K (2010) Two cyclin-dependent kinase pathways are essential for polarized trafficking of presynaptic components. Cell 141:846-858.

Owald D, Fouquet W, Schmidt M, Wichmann C, Mertel S, Depner H, Christiansen F, Zube C, Quentin C, Korner J, Urlaub H, Mechtler K, Sigrist SJ (2010) A Syd-1 homologue regulates pre- and postsynaptic maturation in Drosophila. The Journal of cell biology 188:565-579.

Pan Y, Bai CB, Joyner AL, Wang B (2006) Sonic hedgehog signaling regulates Gli2 transcriptional activity by suppressing its processing and degradation. Mol Cell Biol 26:3365-3377.

Park JI, Tsai SY, Tsai MJ (2003) Molecular mechanism of chicken ovalbumin upstream promoter-transcription factor (COUP-TF) actions. Keio J Med 52:174-181.

Park M, Watanabe S, Poon VY, Ou CY, Jorgensen EM, Shen K (2011) CYY-1/Cyclin Y and CDK-5 Differentially Regulate Synapse Elimination and Formation for Rewiring Neural Circuits. Neuron 70:742-757.

Patel MR, Lehrman EK, Poon VY, Crump JG, Zhen M, Bargmann CI, Shen K (2006) Hierarchical assembly of presynaptic components in defined C. elegans synapses. Nature neuroscience 9:1488-1498.

Pedrotti B, Islam K (1995) Purification of microtubule associated protein MAP1B from bovine brain: MAP1B binds to microtubules but not to microfilaments. Cell Motil Cytoskeleton 30:301-309.

Pereira FA, Tsai MJ, Tsai SY (2000) COUP-TF orphan nuclear receptors in development and differentiation. Cell Mol Life Sci 57:1388-1398.

Petersen SC, Watson JD, Richmond JE, Sarov M, Walthall WW, Miller DM, 3rd (2011) A Transcriptional Program Promotes Remodeling of GABAergic Synapses in Caenorhabditis elegans. J Neurosci 31:15362-15375.

Pfeffer S, Aivazian D (2004) Targeting Rab GTPases to distinct membrane compartments. Nat Rev Mol Cell Biol 5:886-896.

Polleux F, Ince-Dunn G, Ghosh A (2007) Transcriptional regulation of vertebrate axon guidance and synapse formation. Nat Rev Neurosci 8:331-340.

Poon VY, Klassen MP, Shen K (2008) UNC-6/netrin and its receptor UNC-5 locally exclude presynaptic components from dendrites. Nature 455:669-673.

Portera-Cailliau C, Pan DT, Yuste R (2003) Activity-regulated dynamic behavior of early dendritic protrusions: evidence for different types of dendritic filopodia. J Neurosci 23:7129-7142.

Praitis V, Casey E, Collar D, Austin J (2001) Creation of low-copy integrated transgenic lines in Caenorhabditis elegans. Genetics 157:1217-1226.

Quirk J, van den Heuvel M, Henrique D, Marigo V, Jones TA, Tabin C, Ingham PW (1997) The smoothened gene and hedgehog signal transduction in Drosophila and vertebrate development. Cold Spring Harb Symp Quant Biol 62:217-226.

Ramachandran P, Barria R, Ashley J, Budnik V (2009) A critical step for postsynaptic F-actin organization: regulation of Baz/Par-3 localization by aPKC and PTEN. Dev Neurobiol 69:583-602.

Rand JB, Russell RL (1984) Choline acetyltransferase-deficient mutants of the nematode Caenorhabditis elegans. Genetics 106:227-248.

Randazzo PA, Inoue H, Bharti S (2007) Arf GAPs as regulators of the actin cytoskeleton. Biol Cell 99:583-600.

Renaud JP, Moras D (2000) Structural studies on nuclear receptors. Cell Mol Life Sci 57:1748-1769.

Richmond JE, Jorgensen EM (1999) One GABA and two acetylcholine receptors function at the C. elegans neuromuscular junction. Nature neuroscience 2:791-797.

Richmond JE, Weimer RM, Jorgensen EM (2001) An open form of syntaxin bypasses the requirement for UNC-13 in vesicle priming. Nature 412:338-341.

Riederer BM (2007) Microtubule-associated protein 1B, a growth-associated and phosphorylated scaffold protein. Brain research bulletin 71:541-558.

Ringstad N, Gad H, Low P, Di Paolo G, Brodin L, Shupliakov O, De Camilli P (1999) Endophilin/SH3p4 is required for the transition from early to late stages in clathrin-mediated synaptic vesicle endocytosis. Neuron 24:143-154.

Rongo C, Kaplan JM (1999) CaMKII regulates the density of central glutamatergic synapses in vivo. Nature 402:195-199.

Roos J, Hummel T, Ng N, Klambt C, Davis GW (2000) Drosophila Futsch regulates synaptic microtubule organization and is necessary for synaptic growth. Neuron 26:371-382.

Rowland AM, Richmond JE, Olsen JG, Hall DH, Bamber BA (2006) Presynaptic terminals independently regulate synaptic clustering and autophagy of GABAA receptors in Caenorhabditis elegans. J Neurosci 26:1711-1720.

Ruiz-Canada C, Ashley J, Moeckel-Cole S, Drier E, Yin J, Budnik V (2004) New synaptic bouton formation is disrupted by misregulation of microtubule stability in aPKC mutants. Neuron 42:567-580.

Rutter AR, Stephenson FA (2000) Coexpression of postsynaptic density-95 protein with NMDA receptors results in enhanced receptor expression together with a decreased sensitivity to L-glutamate. J Neurochem 75:2501-2510.

Saheki Y, Bargmann CI (2009) Presynaptic CaV2 calcium channel traffic requires CALF-1 and the alpha(2)delta subunit UNC-36. Nature neuroscience 12:1257-1265.

Sanes JR, Lichtman JW (1999) Development of the vertebrate neuromuscular junction. Annual review of neuroscience 22:389-442.

Sarafi-Reinach TR, Melkman T, Hobert O, Sengupta P (2001) The lin-11 LIM homeobox gene specifies olfactory and chemosensory neuron fates in C. elegans. Development (Cambridge, England) 128:3269-3281.

Sarov M, Schneider S, Pozniakovski A, Roguev A, Ernst S, Zhang Y, Hyman AA, Stewart AF (2006) A recombineering pipeline for functional genomics applied to Caenorhabditis elegans. Nat Methods 3:839-844.

Sawa M, Suetsugu S, Sugimoto A, Miki H, Yamamoto M, Takenawa T (2003) Essential role of the C. elegans Arp2/3 complex in cell migration during ventral enclosure. J Cell Sci 116:1505-1518.

Schafer WR, Sanchez BM, Kenyon CJ (1996) Genes affecting sensitivity to serotonin in Caenorhabditis elegans. Genetics 143:1219-1230.

Schlager MA, Hoogenraad CC (2009) Basic mechanisms for recognition and transport of synaptic cargos. Mol Brain 2:25.

Schluter OM, Schmitz F, Jahn R, Rosenmund C, Sudhof TC (2004) A complete genetic analysis of neuronal Rab3 function. J Neurosci 24:6629-6637.

Schneider VA, Granato M (2006) The myotomal diwanka (lh3) glycosyltransferase and type XVIII collagen are critical for motor growth cone migration. Neuron 50:683-695.

Schuske K, Beg AA, Jorgensen EM (2004) The GABA nervous system in C. elegans. Trends in neurosciences 27:407-414.

Schuske KR, Richmond JE, Matthies DS, Davis WS, Runz S, Rube DA, van der Bliek AM, Jorgensen EM (2003) Endophilin is required for synaptic vesicle endocytosis by localizing synaptojanin. Neuron 40:749-762.

Sedensky MM, Siefker JM, Koh JY, Miller DM, 3rd, Morgan PG (2004) A stomatin and a degenerin interact in lipid rafts of the nervous system of Caenorhabditis elegans. Am J Physiol Cell Physiol 287:C468-474.

Shamloo M, Soriano L, von Schack D, Rickhag M, Chin DJ, Gonzalez-Zulueta M, Gido G, Urfer R, Wieloch T, Nikolich K (2006) Npas4, a novel helix-loop-helix PAS domain protein, is regulated in response to cerebral ischemia. The European journal of neuroscience 24:2705-2720.

Shan G, Kim K, Li C, Walthall WW (2005) Convergent genetic programs regulate similarities and differences between related motor neuron classes in Caenorhabditis elegans. Dev Biol 280:494-503.

Shapira M, Zhai RG, Dresbach T, Bresler T, Torres VI, Gundelfinger ED, Ziv NE, Garner CC (2003) Unitary assembly of presynaptic active zones from Piccolo-Bassoon transport vesicles. Neuron 38:237-252.

Shen K, Scheiffele P (2010) Genetics and cell biology of building specific synaptic connectivity. Annual review of neuroscience 33:473-507.

Shen K, Fetter RD, Bargmann CI (2004) Synaptic specificity is generated by the synaptic guidepost protein SYG-2 and its receptor, SYG-1. Cell 116:869-881.

Shepherd JD, Huganir RL (2007) The cell biology of synaptic plasticity: AMPA receptor trafficking. Annu Rev Cell Dev Biol 23:613-643.

Shepherd JD, Bear MF (2011) New views of Arc, a master regulator of synaptic plasticity. Nature neuroscience 14:279-284.

Shi SH, Jan LY, Jan YN (2003) Hippocampal neuronal polarity specified by spatially localized mPar3/mPar6 and PI 3-kinase activity. Cell 112:63-75.

Silverman MA, Kaech S, Jareb M, Burack MA, Vogt L, Sonderegger P, Banker G (2001) Sorting and directed transport of membrane proteins during development of hippocampal neurons in culture. Proceedings of the National Academy of Sciences of the United States of America 98:7051-7057.

Smith CJ, Watson JD, Spencer WC, O'Brien T, Cha B, Albeg A, Treinin M, Miller DM, 3rd (2010) Time-lapse imaging and cell-specific expression profiling reveal dynamic branching and molecular determinants of a multi-dendritic nociceptor in C. elegans. Developmental biology 345:18-33.

Spencer WC, Zeller G, Watson JD, Henz SR, Watkins KL, McWhirter RD, Petersen SC, Sreedharan VT, Widmer C, Jo J, Reinke V, Petrella L, Strome S, Von Stetina S, Katz M, Shaham S, Raetsch G, Miller DM (2011) A Spatial and Temporal Map of C. elegans Gene Expression. Genome research.

Star EN, Kwiatkowski DJ, Murthy VN (2002) Rapid turnover of actin in dendritic spines and its regulation by activity. Nature neuroscience 5:239-246.

Steward O (1997) mRNA localization in neurons: a multipurpose mechanism? Neuron 18:9-12.

Stiess M, Bradke F (2011) Neuronal polarization: the cytoskeleton leads the way. Dev Neurobiol 71:430-444.

Stone DM, Hynes M, Armanini M, Swanson TA, Gu Q, Johnson RL, Scott MP, Pennica D, Goddard A, Phillips H, Noll M, Hooper JE, de Sauvage F, Rosenthal A (1996) The tumour-suppressor gene patched encodes a candidate receptor for Sonic hedgehog. Nature 384:129-134.

Strasser GA, Rahim NA, VanderWaal KE, Gertler FB, Lanier LM (2004) Arp2/3 is a negative regulator of growth cone translocation. Neuron 43:81-94.

Stricker NL, Huganir RL (2003) The PDZ domains of mLin-10 regulate its trans-Golgi network targeting and the surface expression of AMPA receptors. Neuropharmacology 45:837-848.

Stryker E, Johnson KG (2007) LAR, liprin alpha and the regulation of active zone morphogenesis. J Cell Sci 120:3723-3728.

Su J, Gorse K, Ramirez F, Fox MA (2010) Collagen XIX is expressed by interneurons and contributes to the formation of hippocampal synapses. J Comp Neurol 518:229-253.

Sudhof TC (2004) The synaptic vesicle cycle. Annual review of neuroscience 27:509-547.

Svitkina T, Lin WH, Webb DJ, Yasuda R, Wayman GA, Van Aelst L, Soderling SH (2011) Regulation of the postsynaptic cytoskeleton: roles in development, plasticity, and disorders. J Neurosci 30:14937-14942.

Tang K, Xie X, Park JI, Jamrich M, Tsai S, Tsai MJ (2010) COUP-TFs regulate eye development by controlling factors essential for optic vesicle morphogenesis. Development (Cambridge, England) 137:725-734.

Tavernarakis N, Shreffler W, Wang S, Driscoll M (1997) unc-8, a DEG/ENaC family member, encodes a subunit of a candidate mechanically gated channel that modulates C. elegans locomotion. Neuron 18:107-119.

Technau G, Heisenberg M (1982) Neural reorganization during metamorphosis of the corpora pedunculata in Drosophila melanogaster. Nature 295:405-407.

Teichmann HM, Shen K (2010) UNC-6 and UNC-40 promote dendritic growth through PAR-4 in Caenorhabditis elegans neurons. Nature neuroscience 14:165-172.

Tian X, Kai L, Hockberger PE, Wokosin DL, Surmeier DJ (2010) MEF-2 regulates activity-dependent spine loss in striatopallidal medium spiny neurons. Mol Cell Neurosci 44:94-108.

Timmons L, Court DL, Fire A (2001) Ingestion of bacterially expressed dsRNAs can produce specific and potent genetic interference in Caenorhabditis elegans. Gene 263:103-112.

Tissot M, Stocker RF (2000) Metamorphosis in drosophila and other insects: the fate of neurons throughout the stages. Prog Neurobiol 62:89-111.

Tomassy GS, De Leonibus E, Jabaudon D, Lodato S, Alfano C, Mele A, Macklis JD, Studer M (2010) Area-specific temporal control of corticospinal motor

neuron differentiation by COUP-TFI. Proc Natl Acad Sci U S A 107:3576-3581.

Trachtenberg JT, Chen BE, Knott GW, Feng G, Sanes JR, Welker E, Svoboda K (2002) Long-term in vivo imaging of experience-dependent synaptic plasticity in adult cortex. Nature 420:788-794.

Tripodi M, Filosa A, Armentano M, Studer M (2004) The COUP-TF nuclear receptors regulate cell migration in the mammalian basal forebrain. Development (Cambridge, England) 131:6119-6129.

Tsetsenis T, Younts TJ, Chiu CQ, Kaeser PS, Castillo PE, Sudhof TC (2011) Rab3B protein is required for long-term depression of hippocampal inhibitory synapses and for normal reversal learning. Proceedings of the National Academy of Sciences of the United States of America 108:14300-14305.

Tsuboi D, Hikita T, Qadota H, Amano M, Kaibuchi K (2005) Regulatory machinery of UNC-33 Ce-CRMP localization in neurites during neuronal development in Caenorhabditis elegans. J Neurochem 95:1629-1641.

Tsuchida T, Ensini M, Morton SB, Baldassare M, Edlund T, Jessell TM, Pfaff SL (1994) Topographic organization of embryonic motor neurons defined by expression of LIM homeobox genes. Cell 79:957-970.

Tsui HT, Lankford KL, Ris H, Klein WL (1984) Novel organization of microtubules in cultured central nervous system neurons: formation of hairpin loops at ends of maturing neurites. J Neurosci 4:3002-3013.

Tursun B, Cochella L, Carrera I, Hobert O (2009) A toolkit and robust pipeline for the generation of fosmid-based reporter genes in C. elegans. PLoS One 4:e4625.

van Diepen MT, Eickholt BJ (2008) Function of PTEN during the formation and maintenance of neuronal circuits in the brain. Dev Neurosci 30:59-64.

VanSaun MN, Matrisian LM (2006) Matrix metalloproteinases and cellular motility in development and disease. Birth Defects Res C Embryo Today 78:69-79.

Vazquez LE, Chen HJ, Sokolova I, Knuesel I, Kennedy MB (2004) SynGAP regulates spine formation. J Neurosci 24:8862-8872.

Voglis G, Tavernarakis N (2008) A synaptic DEG/ENaC ion channel mediates learning in C. elegans by facilitating dopamine signalling. The EMBO journal 27:3288-3299.

Von Stetina S, Treinin M, Miller DM, 3rd (2005) The Motor Circuit. Int Rev Neurobiol 69:125-167.

Von Stetina SE, Fox RM, Watkins KL, Starich TA, Shaw JE, Miller DM, 3rd (2007a) UNC-4 represses CEH-12/HB9 to specify synaptic inputs to VA motor neurons in C. elegans. Genes & development 21:332-346.

Von Stetina SE, Watson JD, Fox RM, Olszewski KL, Spencer WC, Roy PJ, Miller DM, 3rd (2007b) Cell-specific microarray profiling experiments reveal a comprehensive picture of gene expression in the C. elegans nervous system. Genome biology 8:R135.

Walthall WW (1990) Metamorphic-like changes in the nervous system of the nematode Caenorhabditis elegans. J Neurobiol 21:1085-1091.

Walthall WW, Plunkett JA (1995) Genetic transformation of the synaptic pattern of a motoneuron class in Caenorhabditis elegans. J Neurosci 15:1035-1043.

Wang XB, Bozdagi O, Nikitczuk JS, Zhai ZW, Zhou Q, Huntley GW (2008) Extracellular proteolysis by matrix metalloproteinase-9 drives dendritic spine enlargement and long-term potentiation coordinately. Proc Natl Acad Sci U S A 105:19520-19525.

Warming S, Costantino N, Court DL, Jenkins NA, Copeland NG (2005) Simple and highly efficient BAC recombineering using galK selection. Nucleic Acids Res 33:e36.

Watson JD, Wang S, Von Stetina SE, Spencer WC, Levy S, Dexheimer PJ, Kurn N, Heath JD, Miller DM, 3rd (2008) Complementary RNA amplification methods enhance microarray identification of transcripts expressed in the C. elegans nervous system. BMC genomics 9:84.

Webber CA, Hocking JC, Yong VW, Stange CL, McFarlane S (2002) Metalloproteases and guidance of retinal axons in the developing visual system. J Neurosci 22:8091-8100.

Wegner AM, Nebhan CA, Hu L, Majumdar D, Meier KM, Weaver AM, Webb DJ (2008) N-wasp and the arp2/3 complex are critical regulators of actin in the development of dendritic spines and synapses. The Journal of biological chemistry 283:15912-15920.

Wemmie JA, Price MP, Welsh MJ (2006) Acid-sensing ion channels: advances, questions and therapeutic opportunities. Trends in neurosciences 29:578-586.

Wemmie JA, Coryell MW, Askwith CC, Lamani E, Leonard AS, Sigmund CD, Welsh MJ (2004) Overexpression of acid-sensing ion channel 1a in

transgenic mice increases acquired fear-related behavior. Proceedings of the National Academy of Sciences of the United States of America 101:3621-3626.

Wemmie JA, Chen J, Askwith CC, Hruska-Hageman AM, Price MP, Nolan BC, Yoder PG, Lamani E, Hoshi T, Freeman JH, Jr., Welsh MJ (2002) The acid-activated ion channel ASIC contributes to synaptic plasticity, learning, and memory. Neuron 34:463-477.

Werle MJ, VanSaun M (2003) Activity dependent removal of agrin from synaptic basal lamina by matrix metalloproteinase 3. J Neurocytol 32:905-913.

Westmoreland JJ, McEwen J, Moore BA, Jin Y, Condie BG (2001) Conserved function of Caenorhabditis elegans UNC-30 and mouse Pitx2 in controlling GABAergic neuron differentiation. J Neurosci 21:6810-6819.

White JG, Albertson DG, Anness MA (1978) Connectivity changes in a class of motoneurone during the development of a nematode. Nature 271:764-766.

White JG, Southgate E, Thomson JN, Brenner S (1976) The structure of the ventral nerve cord of Caenorhabditis elegans. Philosophical transactions of the Royal Society of London 275:327-348.

White JG, Southgate E, Thomson JN, Brenner S (1986) The structure of the nervous system of the nematode *Caenorhabditis elegans*. Philosophical Transactions of the Royal Society of London B314:1-340.

Wiegert JS, Bading H (2011) Activity-dependent calcium signaling and ERK-MAP kinases in neurons: a link to structural plasticity of the nucleus and gene transcription regulation. Cell Calcium 49:296-305.

Williams DW, Truman JW (2005) Cellular mechanisms of dendrite pruning in Drosophila: insights from in vivo time-lapse of remodeling dendritic arborizing sensory neurons. Development (Cambridge, England) 132:3631-3642.

Winckler B, Mellman I (1999) Neuronal polarity: controlling the sorting and diffusion of membrane components. Neuron 23:637-640.

Xu W (2011) PSD-95-like membrane associated guanylate kinases (PSD-MAGUKs) and synaptic plasticity. Current opinion in neurobiology 21:306-312.

Yang SN, Tang YG, Zucker RS (1999) Selective induction of LTP and LTD by postsynaptic [Ca2+]i elevation. J Neurophysiol 81:781-787.

Yaron A, Huang PH, Cheng HJ, Tessier-Lavigne M (2005) Differential requirement for Plexin-A3 and -A4 in mediating responses of sensory and sympathetic neurons to distinct class 3 Semaphorins. Neuron 45:513-523.

Yashiro K, Philpot BD (2008) Regulation of NMDA receptor subunit expression and its implications for LTD, LTP, and metaplasticity. Neuropharmacology 55:1081-1094.

Yeh E, Kawano T, Weimer RM, Bessereau JL, Zhen M (2005) Identification of genes involved in synaptogenesis using a fluorescent active zone marker in Caenorhabditis elegans. J Neurosci 25:3833-3841.

Yeh E, Ng S, Zhang M, Bouhours M, Wang Y, Wang M, Hung W, Aoyagi K, Melnik-Martinez K, Li M, Liu F, Schafer WR, Zhen M (2008) A putative cation channel, NCA-1, and a novel protein, UNC-80, transmit neuronal activity in C. elegans. PLoS Biol 6:e55.

Yoshimura T, Arimura N, Kaibuchi K (2006) Signaling networks in neuronal polarization. J Neurosci 26:10626-10630.

Yoshimura T, Kawano Y, Arimura N, Kawabata S, Kikuchi A, Kaibuchi K (2005) GSK-3beta regulates phosphorylation of CRMP-2 and neuronal polarity. Cell 120:137-149.

Yu X, Zuo Y (2011) Spine plasticity in the motor cortex. Current opinion in neurobiology 21:169-174.

Yu Y, Chen Z, Li WG, Cao H, Feng EG, Yu F, Liu H, Jiang H, Xu TL (2010) A nonproton ligand sensor in the acid-sensing ion channel. Neuron 68:61-72.

Zha XM, Wemmie JA, Green SH, Welsh MJ (2006) Acid-sensing ion channel 1a is a postsynaptic proton receptor that affects the density of dendritic spines. Proceedings of the National Academy of Sciences of the United States of America 103:16556-16561.

Zha XM, Costa V, Harding AM, Reznikov L, Benson CJ, Welsh MJ (2009) ASIC2 subunits target acid-sensing ion channels to the synapse via an association with PSD-95. J Neurosci 29:8438-8446.

Zhang H, Macara IG (2006) The polarity protein PAR-3 and TIAM1 cooperate in dendritic spine morphogenesis. Nature cell biology 8:227-237.

Zhang H, Macara IG (2008) The PAR-6 polarity protein regulates dendritic spine morphogenesis through p190 RhoGAP and the Rho GTPase. Developmental cell 14:216-226.

Zhang S, Banerjee D, Kuhn JR (2011) Isolation and culture of larval cells from C. elegans. PLoS One 6:e19505.

Zhang Y, Kubiseski TJ (2010) Caenorhabditis elegans wsp-1 regulation of synaptic function at the neuromuscular junction. The Journal of biological chemistry 285:23040-23046.

Zhang Y, Nash L, Fisher AL (2008) A simplified, robust, and streamlined procedure for the production of C. elegans transgenes via recombineering. BMC Dev Biol 8:119.

Zhen M, Jin Y (1999) The liprin protein SYD-2 regulates the differentiation of presynaptic termini in C. elegans. Nature 401:371-375.

Zhong M et al. (2010) Genome-wide identification of binding sites defines distinct functions for Caenorhabditis elegans PHA-4/FOXA in development and environmental response. PLoS Genet 6:e1000848.

Zhou C, Qiu Y, Pereira FA, Crair MC, Tsai SY, Tsai MJ (1999) The nuclear orphan receptor COUP-TFI is required for differentiation of subplate neurons and guidance of thalamocortical axons. Neuron 24:847-859.

Zhou HM, Walthall WW (1998) UNC-55, an orphan nuclear hormone receptor, orchestrates synaptic specificity among two classes of motor neurons in Caenorhabditis elegans. J Neurosci 18:10438-10444.

Zugasti O, Rajan J, Kuwabara PE (2005) The function and expansion of the Patched- and Hedgehog-related homologs in C. elegans. Genome research 15:1402-1410.